220

Topics in Current Chemistry

Springer

Berlin
Heidelberg
New York
Barcelona
Hong Kong
London
Milan
Paris
Tokyo

New Aspects in Phosphorus Chemistry I

Volume Editor: Jean-Pierre Majoral

With contributions by
G. Bertrand, D. Bourissou, J.-M. Brunel,
G. Buono, V. Cadierno, D. Carmichael, H. Dorn,
M. Ehses, P. Guga, A. Igau, B. A. Kashemirov,
J.-P. Majoral, I. Manners, F. Mathey, C. E. McKenna,
A. R. McWilliams, A. Okruszek, M. Peruzzini,
A. Romerosa, W. J. Stec, M. Zablocka

Springer

The series *Topics in Current Chemistry* presents critical reviews of the present and future trends in modern chemical research. The scope of coverage includes all areas of chemical science including the interfaces with related disciplines such as biology, medicine and materials science. The goal of each thematic volume is to give the non-specialist reader, whether at the university or in industry, a comprehensive overview of an area where new insights are emerging that are of interest to a larger scientific audience.

As a rule, contributions are specially commissioned. The editors and publishers will, however, always be pleased to receive suggestions and supplementary information. Papers are accepted for *Topics in Current Chemistry* in English.

In references *Topics in Current Chemistry* is abbreviated Top. Curr. Chem. and is cited as a journal.

Springer WWW home page: http://www.springer.de
Visit the TCC home page at http:/link.springer.de/series/tcc/
or http://link.springer-ny.com/series/tcc/

ISSN 0340-1022
ISBN 3-540-42246-3
Springer-Verlag Berlin Heidelberg New York

Library of Congress Catalog Card Number 74-644622

Springer-Verlag Berlin Heidelberg New York
a member of BertelsmannSpringer Science+Business Media GmbH

http://www.springer.de

Printed in Germany

Cover design: Friedhelm Steinen-Broo, Barcelona; MEDIO, Berlin
Typesetting: Fotosatz-Service Köhler GmbH, 97084 Würzburg

SPIN: 10779774 02/3020 ra – 5 4 3 2 1 0 – Printed on acid-free paper

Volume Editor

Dr. Jean-Pierre Majoral
Directeur de Recherche
Laboratoire de Chimie de Coordination du CNRS
205, route de Narbonne
31077 Toulouse, Cedex 4, France
E-mail: majoral@lcc-toulouse.fr

Editorial Board

Prof. Dr. Armin de Meijere
Institut für Organische Chemie
der Georg-August-Universität
Tammannstraße 2
37077 Göttingen, Germany
E-mail: ameijer1@uni-goettingen.de

Prof. Dr. Horst Kessler
Institut für Organische Chemie
TU München
Lichtenbergstraße 4
85747 Garching, Germany
E-mail: kessler@ch.tum.de

Prof. Steven V. Ley
University Chemical Laboratory
Lensfield Road
Cambridge CB2 1EW, Great Britain
E-mail: svl1000@cus.cam.ac.uk

Prof. Dr. Joachim Thiem
Institut für Organische Chemie
Universität Hamburg
Martin-Luther-King-Platz 6
20146 Hamburg, Germany
E-mail: thiem@chemie.uni-hamburg.de

Prof. Dr. Fritz Vögtle
Kekulé-Institut für Organische Chemie
und Biochemie der Universität Bonn
Gerhard-Domagk-Straße 1
53121 Bonn, Germany
E-mail: voegtle@uni-bonn.de

Prof. K.N. Houk
Department of Chemistry and Biochemistry
University of California
405 Hilgard Avenue
Los Angeles, CA 90024-1589, USA
E-mail: houk@chem.ucla.edu

Prof. Jean-Marie Lehn
Institut de Chimie
Université de Strasbourg
1 rue Blaise Pascal, B.P.Z 296/R8
67008 Strasbourg Cedex, France
E-mail: lehn@chimie.u-strasbg.fr

Prof. Stuart L. Schreiber
Chemical Laboratories
Harvard University
12 Oxford Street
Cambridge, MA 02138-2902, USA
E-mail: sls@slsiris.harvard.edu

Prof. Barry M. Trost
Department of Chemistry
Stanford University
Stanford, CA 94305-5080, USA
E-mail: bmtrost@leland.stanford.edu

Prof. Hisashi Yamamoto
School of Engineering
Nagoya University
Chikusa, Nagoya 464-01, Japan
E-mail: j45988a@nucc.cc.nagoya-u.ac.jp

Topics in Current Chemistry
Now Also Available Electronically

For all customers with a standing order for Topics in Current Chemistry we offer the electronic form via LINK free of charge. Please contact your librarian who can receive a password for free access to the full articles by registration at:

http://link.springer.de/orders/index.htm

If you do not have a standing order you can nevertheless browse through the table of contents of the volumes and the abstracts of each article at:

http://link.springer.de/series/tcc
http://link.springer-ny.com/series/tcc

There you will also find information about the

- Editorial Board
- Aims and Scope
- Instructions for Authors

Preface

Undoubtedly the chemistry of phosphorus appears more and more attractive in the sense that phosphorus presents an extraordinary versatile behaviour that allows the synthesis of a large number of different phosphorus reagents usable for applications in different fields, from biology to material science without forgetting key applications in catalysis. The full maturity of this topic of research can be explained by all the acquired knowledge over these twenty last years. Organic and inorganic chemistries of P_{III}, P_{IV} and P_V species have been the subject of thousands of publications while the chemistry of low coordinated phosphorus derivatives experienced its hour of glory from the 1970s to the early 1990s. In parallel, interactions between phosphorus compounds and transition metals afforded many complexes, a lot of which present fascinating properties as catalysts.

The interest in all these themes really is not decreasing, indeed some fascinating areas of research are emerging or are the subject of many investigations: the medicinal chemistry of bisphosphonates, the role of phosphorus in biology, phosphorus ligands in radiopharmaceutical chemistry, phosphorus in material science, new polymers and dendrimers incorporating phosphorus, and asymmetric catalysis to name but a few.

Indeed researchers, benefitting from their background in basic phosphorus chemistry are developing many new fields of research.

Therefore it appeared opportune not only to give an overview of the state of the art of the new aspects in phosphorus chemistry but also to try to draw what might be of interest for development in the future using phosphorus.

This *Topics in Current Chemistry* volume starts with a comparison of carbon, nitrogen and phosphorus chemistry concerning the preparation and the properties of three-membered rings as neutral cationic or radical species (G. Bertrand et al.). The specificity of phosphorus is clearly shown. The following contribution by F. Mathey et al. reports new trends in phosphametallocene chemistry with emphasis on the applications of transition-metal phospholyl complexes in homogenous catalysis. How is it possible to take advantage of the properties of a given element to develop the chemistry of another one? This is what is shown in the contribution of J.-P. Majoral et al. describing the use of benzyne zirconocene reagents as tools in phosphorus chemistry.

The use of phosphorus in catalysis is a topic impossible to circumvent. The review by G. Buono et al. highlights the role of new chiral organophosphorus catalysts in asymmetric synthesis.

One of the sources of phosphorus reagents is white phosphorus. All efforts to transform this bulk material are of great interest. M. Peruzzini et al. presents a critical survey of the coordination chemistry of white phosphorus, metal mediating the degradation and reaggregation of P_4.

A survey of the chemistry and the role of phosphorus would not be complete without entering the world of material science and bioscience. Again, phosphorus has proved useful in these areas of research. Synthesis and properties of new inorganic polymers containing phosphorus and more specially poly(thionylphosphazenes), hybrids of "classical" polyphosphazenes and poly(oxothiazenes) are discussed among the preparation of a variety of novel polymeric materials by I. Manners et al. Synthetic methods leading to P-chiral oligonucleotides for which broad applications might be expected in biochemistry and molecular biology are presented in the contribution by W. Stec et al. Special emphasis has been put on the oxathiaphospholane methodology for the stereocontrolled synthesis of P-chiral biophosphate analogues.

Recent advances in carbonylphosphonate chemistry are reported by C. E. McKenna et al. with emphasis on the synthesis, chemical properties and synthetic utility of this versatile class of organophosphorus compounds.

In conclusion the present volume, the first of a series of volumes, gives a general and at the same time rather detailed review on the main research developments in phosphorus chemistry. There is still more to come, such a chemistry being so fascinating and so diversified.

Toulouse, November 2001 Jean-Pierre Majoral

Contents

Contents of Volume 216

Stereoselective Heterocyclic Synthesis III

Volume Editor: P. Metz

ISBN 3-540-41763-X

Diphosphorus-Containing Unsaturated Three-Membered Rings: Comparison of Carbon, Nitrogen, and Phosphorus Chemistry

D. Bourissou, G. Bertrand

Laboratoire d'Hétérochimie Fondamentale et Appliquée, Université Paul Sabatier, 118,
route de Narbonne, 31062 Toulouse Cédex 04, France
E-mail: gbertran@chimie.ups-tlse.fr

Three-membered rings as neutral, cationic, or radical species give a good opportunity to compare the chemistry of phosphorus, nitrogen, and carbon. Due to its specific properties, phosphorus has allowed for the isolation of original compounds which have so far few or even no counterparts in nitrogen and carbon chemistry: the diphosphorus analogue of the cyclopropenyl radical does not dimerize through σ(C–C) coupling but via π^*–π^* interaction leading to phosphorus-phosphorus one-electron bonds, while the phosphorus version of the amidinium salts adopts a cyclic form featuring some carbanionic character!

Keywords. Three-membered rings, Phosphorus heterocycles, Cations, Radicals, Valence isomers

1
Introduction

Phosphorus is a heavier analogue of nitrogen and accordingly numerous phosphorus compounds (such as phosphines) can be related to their nitrogen counterparts (amines). However, this so-called vertical analogy is not so efficient for the low-coordinate phosphorus compounds, which are more strongly related to

Topics in Current Chemistry, Vol. 220

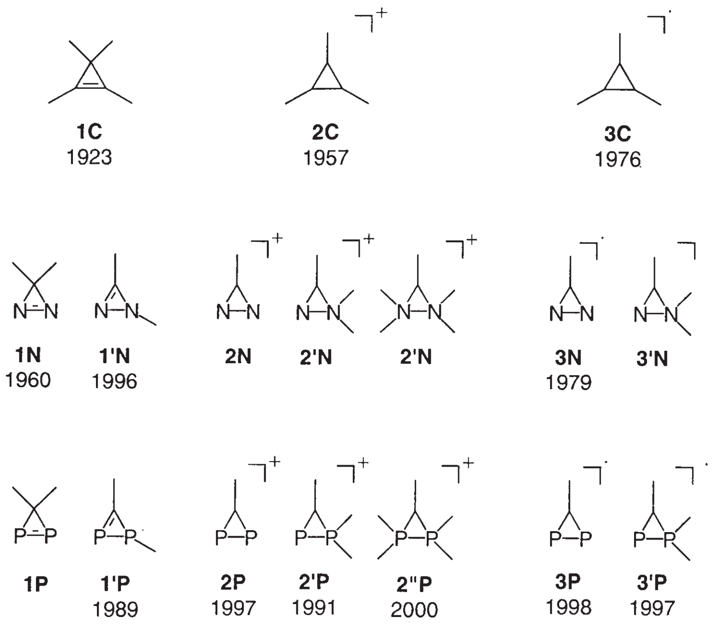

Fig. 1. Cyclopropenes, cyclopropenium salts, cyclopropenyl radicals, and their dinitrogen- and diphosphorus-containing analogues

their carbon analogues [1a]. The diagonal phosphorus-carbon analogy stresses the electronegativity of the elements (P 2.1 vs C 2.5 and N 3.0) which governs, in part, the reactivity of these species.

Due to its specific properties, phosphorus has allowed for the isolation of unsaturated neutral three-membered heterocycles such as **1′P**, which are hardly available in the nitrogen series. Even more striking, cationic three-membered rings **2P**, **2′P**, and **2″P** have, so far, no counterparts in nitrogen chemistry [1b], and the transient diphosphirenyl radical **3P** behaves totally differently from both its carbon and nitrogen counterparts (Fig. 1). This review presents the synthesis, structure and reactivity of diphosphorus-containing unsaturated three-membered heterocycles **1**–**3** [2], and gives a good opportunity to compare the chemistry of phosphorus with those of nitrogen and carbon.

2

Synthesis and Ligand Properties of Diphosphirenes 1P and 1′P

Free as well as coordinated 1*H*-phosphirenes **A** [3] and **B** [4], respectively, can be prepared by trapping of transient phosphinidenes [5] with alkynes. By extension of this synthetic route, Niecke et al. prepared the first 1*H*-diphosphirene **1′Pa** [6] by reaction of the chloro(silyl)phosphine **1** with the phosphaalkyne **2** (Scheme 1). Some years later, Mathey et al. [7a] and Streubel et al. [7b] independently reported analogous reactions in the coordination sphere of transition

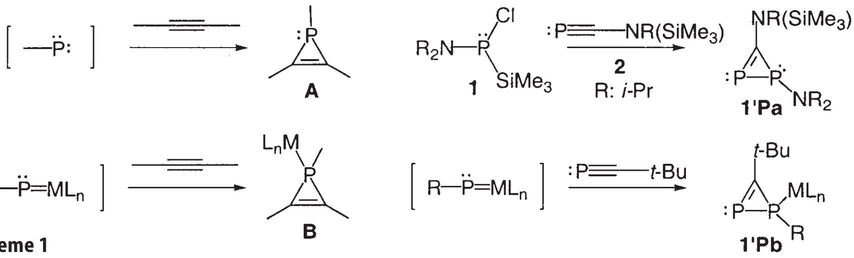

Scheme 1

metals, preparing the first complexes **1′Pb** featuring 1*H*-diphosphirenes as η^1-ligands.

More recently, starting from the readily available *P*-hydrogenophosphaalkene **3**, we reported a simpler synthetic route [8] to free and coordinated 1*H*-diphosphirenes, which is reminiscent of the Neber synthesis [9] of 2*H*-azirines and the Graham synthesis [10] of 3-halogeno-3*H*-diazirines (Scheme 2). To induce the necessary 1,3-elimination reaction, a thf solution of **3** was treated at room temperature with a catalytic amount (5%) of $BF_3.OEt_2$. After work-up, the 1*H*-diphosphirene **1′Pc** was obtained as a light yellow oil in 65% yield. Since this synthesis can be performed on multiplegram scale, the ligand properties of **1′Pc** could be studied [8, 11].

The 1*H*-diphosphirene tungsten complex **1′Pd** [8] is easily obtained by treatment of **1′Pc** with $W(CO)_5(thf)$ (42% yield from **1′Pc**), or alternatively by addition of one equivalent of $W(CO)_5(thf)$ to phosphaalkene **3** (80% yield). Monitoring the latter reaction by ^{31}P NMR spectroscopy at 0 °C showed the primary formation of complex **4** as a single isomer in an *E* configuration, where the metal is η^1-bonded to the σ^2-phosphorus atom. The transformation of **4** into **1′Pd** involved both the 1,3-elimination of diisopropylamine and the migration of the metal fragment. The former process is probably induced by a catalytic amount of $W(CO)_5(thf)$ which acts as a Lewis acid; the metal shift is governed by the higher thermodynamic stability of **1′Pd** compared to the isomeric complex **1′Pe** featuring the metal fragment at the σ^2-phosphorus atom [12] (Scheme 2).

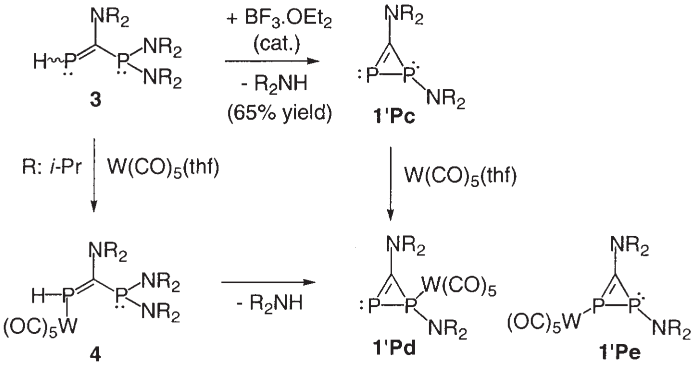

Scheme 2

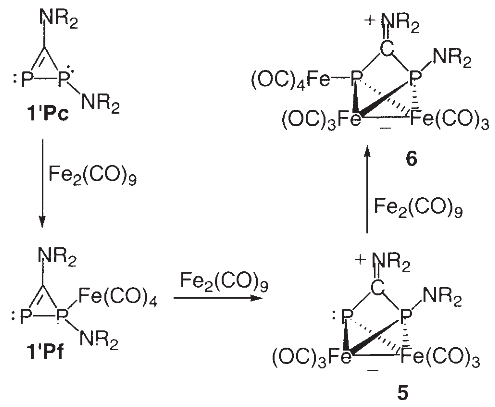

Scheme 3

Similarly, the η^1-iron tetracarbonyl complex **1′Pf** was obtained in 85% yield by treatment of **6** with one equivalent of $Fe_2(CO)_9$ [11] (Scheme 3). Addition of a second equivalent of $Fe_2(CO)_9$ induces the cleavage of the P–P bond and leads to the binuclear complex **5**, in which a 1,3-diphosphorus open chain bridges a metal-metal bonded $Fe_2(CO)_6$ fragment. One of the phosphorus centers of the latter complex can coordinate a further $Fe(CO)_4$ unit affording the trinuclear complex **6**.

3

Structure of Diphosphirenes 1P and 1′P

At first glance, the stability of the potentially anti-aromatic 1*H*-diphosphirenes **1′P** may be surprising. The X-ray analysis performed on **1′Pa** [6] reveals that the σ^3-phosphorus center is in a strongly pyramidalized environment and, since the inversion barrier of phosphorus is rather high (146 kJ/mol), the destabilizing four-π-electron interaction between the phosphorus lone pair and the P=C π-bond is only marginal [13]. Accordingly, 1*H*-diphosphirenes **1′P** can be classified as non-anti-aromatic species and this certainly explains why only these cyclopropene diphosphorus analogues have been isolated so far. Indeed, no isomeric 3*H*-diphosphirenes **1P**, which feature a weak P=P bond [14], have been characterized. However, it is worth mentioning that attempted synthesis of **1Pa** led to the formation of its dimer **7** [15] (Scheme 4).

Due to the low inversion barrier of nitrogen (25 kJ/mol), an opposite situation is observed for the diazirines. The chemistry of 3*H*-diazirines **1N**, which are good precursors for transient carbenes, has been extensively explored [16],

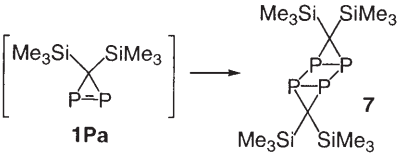

Scheme 4

while only one anti-aromatic 1*H*-diazirine **1′N** has been spectroscopically characterized [17].

4
Synthesis of Diphosphorus-Containing Salts 2P, 2′P, and 2″P

By analogy with the synthetic method used to prepare the first phosphirenium salts **C** [18], we initially tried to prepare a diphosphirenium salt of type **2′P** by [2+1]-cycloaddition reactions of various phosphenium salts to *tert*-butylphosphaalkyne. However, all our attempts failed (Scheme 5).

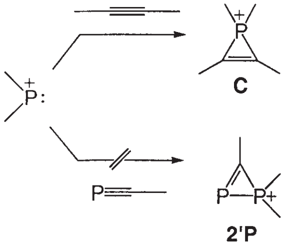

Scheme 5

As a result, we turned our attention towards a totally different synthetic strategy. It is known that, due to their high electrophilicity, dicoordinate [19a] and monocoordinate [19b,c] phosphorus cations react with phosphines giving the corresponding 1,1-adducts, **D** and **E**, respectively. Therefore, $1\sigma^1,3\sigma^3$-diphosphaallyl cations **F**, which might conceivably be available through heterolytic cleavage of the P-X bond of *C*-phosphino-phosphaalkenes **G**, appeared to be potential precursors for the desired diphosphirenium salt **2′P** (Scheme 6).

Since both amino and bulky substituents are known to stabilize cyclopropenium salts [20], we chose to investigate the Lewis-acid induced P-N bond cleavage of the phosphaalkene **9**, which is readily synthesized from the corresponding bis(phosphino)diazomethane **8** [21]. Indeed, treatment of **9** with two equivalents of $BF_3.Et_2NH$ complex at room temperature afforded diphosphirenium salt **2′Pa** as non-air sensitive pale-yellow crystals (mp 118 °C) in 60% yield [22a] (Scheme 6). Subsequently, we found that using $BF_3.Et_2O$ in the place of

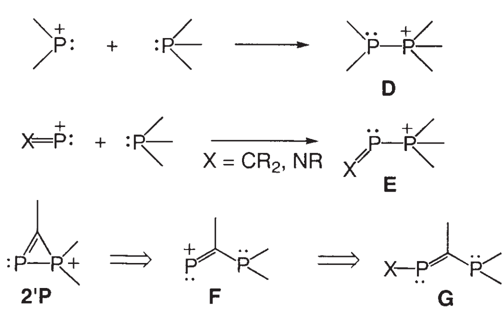

Scheme 6

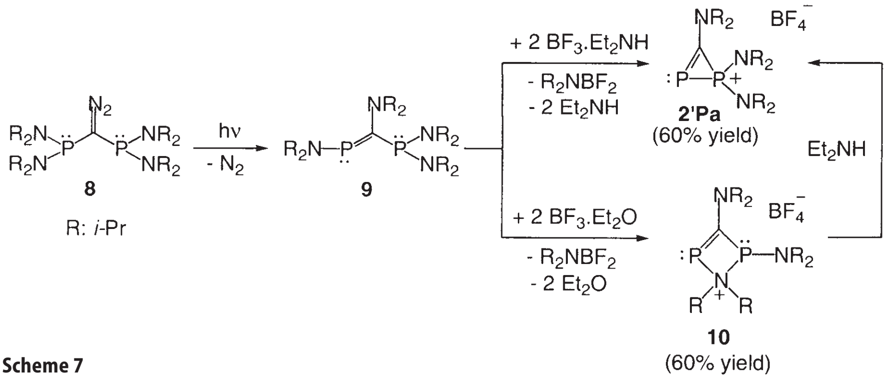

Scheme 7

$BF_3.Et_2NH$ brought about the formation of the four-membered heterocycle **10** (60% yield) rather than **2′Pa** [22b]. We quickly realized that the different outcome of the latter reaction could be attributed to the lack of the base, which induced the transformation of **10** into **2′Pa** (Scheme 7).

Then we demonstrated the complete mechanism for the reaction leading to the diphosphirenium salt **2′Pa** from phosphaalkene **9**. Treating **9** with trifluoromethanesulfonic acid allowed the spectroscopic characterization of the $1\sigma^2,3\sigma^4$-diphosphaallyl cation **11**, which clearly demonstrated that the acid reacted at the σ^3-phosphorus atom of **9** [22b]. By varying the nature of the amino groups, we then proved that a 1,1-elimination occurred at the σ^4-phosphorus atom leading to the transient $1\sigma^2,3\sigma^2$-diphosphaallyl cation **12**, which was isolated as the donor-acceptor complex **10**. In other words, in contrast to our intended synthetic strategy, the reaction does not proceed through the $1\sigma^1,3\sigma^3$-diphosphaallyl cation **14**! Subsequently, we showed that anionic nucleophiles reacted at the σ^2-phosphorus of **10** or **2′Pa** to afford the corresponding *C*-phosphino phosphaalkenes **15** [22b]. In the presence of neutral nucleophiles such as diethylamine, **10** gives the diphosphirenium salt **2′Pa** probably via the transient intermolecular donor-acceptor complexes **13** of the desired $1\sigma^1,3\sigma^3$-diphosphaallyl cation **14** (Scheme 8). Although our retrosynthetic strategy was not perfect, the desired diphosphirenium salt **2′Pa** was obtained!

Having in hand the diphosphirenium salt **2′Pa**, we investigated the possibility of synthesizing a diphosphirenylium salt of type **2P**. However, we had to keep in mind that, in contrast with the phosphirenium salts **C**, which are known to be stable [18, 23], the phosphirenylium salts **H** have only been observed spectroscopically in SO_2 solutions at −78 °C [24a,b], or isolated when complexed in an η^3-fashion to an electron-rich Ni^0 center [24c]. The difficulty in isolating species such as **H** is essentially due to the very high electrophilicity of the phosphorus atom. In addition, the desired diphosphirenylium **2P** suffers from the presence of either a weak P=P or P=C double bond [14] (Fig. 2).

Since obtaining a stable free diphosphirenylium salt **2P** was quite unlikely, we chose to prepare this type of compound in the coordination sphere of a transition metal via the Lewis-acid induced P-N bond cleavage of the 1,3-diaminodiphosphirene complex **1′Pd**. Treatment of **1′Pd** at –78 °C with two equivalents

Scheme 8

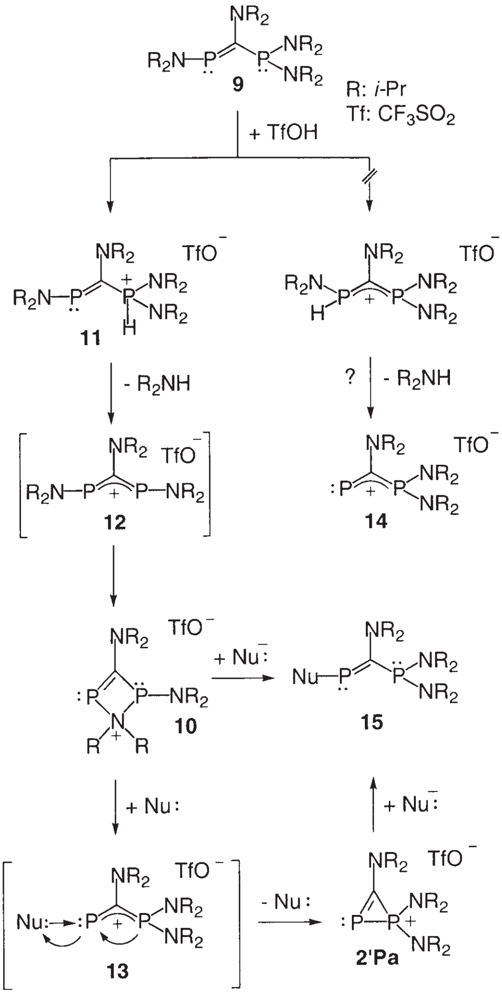

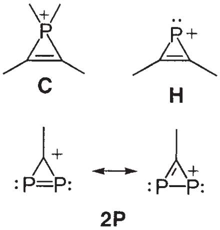

Fig. 2. Phosphirenium salt **C**, phosphirenylium salt **H**, and resonance forms of the diphosphirenylium salt **2P**

of trifluoromethanesulfonic acid gave the desired diphosphirenylium salt **2Pa** as a highly air- and water-sensitive red oil, stable for days in solution at room temperature [25]. The ionic nature of the complex **2Pa** was demonstrated by the preparation of the corresponding tetrachloroaluminate and gallate salts **2Pb** and **2Pc**, which present identical ^{31}P, ^{1}H, and ^{13}C NMR data. Salts **2Pb** and **2Pc** were also obtained in two steps from **1Pd** by treatment with two equivalents of hydrogen chloride in pentane, which gives the 1-chloro-1*H*-phosphirene **1′Pg**, followed by addition of a slight excess of aluminum or gallium trichloride (Scheme 9). The η^2-coordination mode of the heterocycle in **2Pa,b,c** (via the P=P bond) was deduced from the spectroscopic data: the ^{31}P NMR spectrum showed only one singlet at – 157.4 ppm in the range expected for a three-membered phosphorus heterocycle [26], with the axial and equatorial carbonyl groups appearing as two triplets in the ^{13}C NMR spectrum.

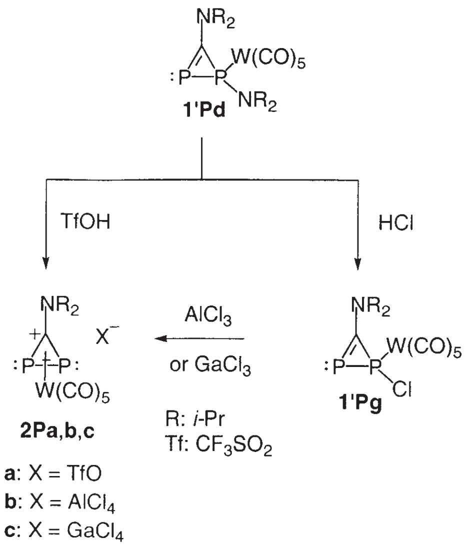

Scheme 9

Since diphosphirenylium salts **2P** can potentially act as 2-, 4-, and 6-electron ligands, we have then studied the possibility of adding further metal fragment to the complex **2Pa.** The reaction of **2Pa** with W(CO)$_5$(thf) in dichloromethane solution was monitored by ^{31}P NMR spectroscopy. On addition of one equivalent of W(CO)$_5$(thf), the sharp singlet corresponding to **2Pa** (δ^{31}P – 157.4) disappears to give a broad signal centered at –130 ppm. Addition of an excess of W(CO)$_5$(thf) subsequently converts the broad signal into a sharp singlet at – 74.1 ppm [8b]. This chemical shift, in the range expected for a three-membered phosphorus heterocycle [26], and the presence of three different J_{PW} coupling constants (176, 61, and 45 Hz) [27] strongly support the trinuclear structure **2Pe** (Scheme 10). In addition, the ^{13}C NMR spectrum for **2Pe** reveals the presence of two types of W(CO)$_5$ fragment [193.6 (t, J_{CP} < 1 Hz, $^{1}J_{CW}$ = 127 Hz, CO$_e$), 194.5 (s, CO$_a$) and 213.6 (s, CO$_e$), 214.7 (s, CO$_a$)]. By comparison with those observed for

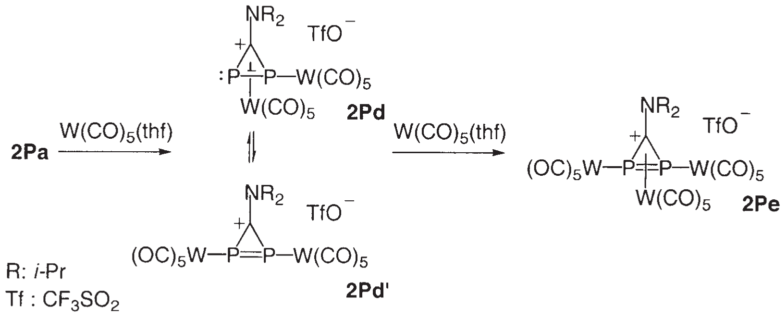

Scheme 10

2Pa [189.3 (t, $J_{CP} = 4$ Hz, $^1J_{CW} = 122$ Hz, CO_e), 194.4 (t, $J_{CP} < 1$ Hz, CO_a)], the signals at 193.6 and 194.5 ppm can be assigned to the η^2-$PW(CO)_5$ moiety while the deshielding of the other two signals ($\Delta\delta = 20$ ppm) can be classically [28] attributed to the η^1-coordination mode of the corresponding $W(CO)_5$ fragments. Taking into account the trinuclear structure of **2Pe**, the intermediate broad signal detected in ^{31}P NMR spectroscopy was certainly due to the binuclear tungsten complex for which an equilibrium between the structures **2Pd** and **2Pd′** is likely to occur. Indeed, calculations have clearly evidenced a small difference in energy between η^1- and η^2-coordination modes for model compounds [8b]. The formation of the mono-, bi-, and trinuclear diphosphirenylium complexes **2Pa**, **2Pd**, and **2Pe**, respectively, shows that the coordination chemistry of diphosphirenylium salts **2P** features some resemblance with that of diphosphenes RP=PR [29], and suggested that the positive charge is shifted toward the nitrogen substituent.

Analogously, treatment of the iron mononuclear complex **1′Pf** with two equivalents of trifluoromethanesulfonic acid leads to the dinuclear diphosphirenylium complex **2Pf** [11] (Scheme 11). The presence of the $Fe_2(CO)_6$ fragment in **2Pf** was evident from the mass spectrum, and the cationic three-membered ring structure was established by comparing the spectroscopic data of **2Pf** (^{31}P NMR: s, δ −139.8 ppm, ^{13}C NMR: t, δ 218.2 ppm J_{PC} 93 Hz) with those of the tungsten complex **2Pa**. Although the mechanism of the reaction of **1′Pf** with triflic acid remains obscure, it is quite clear that the formation of the binuclear complex involves a disproportionation process. To achieve the 18-electron configuration for each iron atom in **2Pf**, the three-membered ring must act as a six-

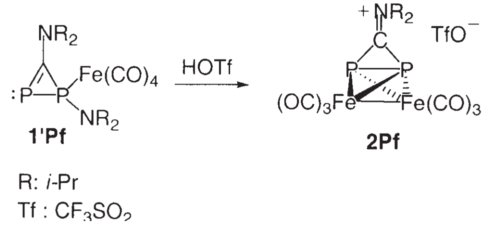

Scheme 11

Scheme 12

electron ligand (via the P=P bond and the lone pair of both phosphorus atoms). This coordination mode is similar to that observed in the dinuclear diphosphene complex [*cis*-P_2(*tert*-Bu)$_2$].[$Fe_2(CO)_6$] [29b].

To prepare a salt of type **2″P** featuring two σ^4-phosphorus centers, a totally different strategy was used, based on the fact that such systems are cyclic valence isomers of the diphosphino-substituted carbocations **I** [30] (Scheme 12).

We had previously demonstrated that the stable (phosphino)(silyl)carbene **16** [31] reacts with trimethylsilyl trifluoromethanesulfonate to give the phosphino-substituted carbocation **17** [32], one of the very few stable phosphorus analogues of iminium salts [33]. The same synthetic strategy was adopted to prepare the diphosphino carbocation **17** or its valence isomer **2″Pa.** A dichloromethane solution of bis(diisopropylamino)phosphenium triflate was added at 0 °C to a pentane solution of the carbene **16.** The adduct **2″Pa** [34] was isolated in 66% yield as extremely air sensitive white crystals (melting point 89–90 °C) by recrystallization from tetrahydrofuran at –5 °C (Scheme 13). The symmetrical three-membered ring structure was evident from the spectroscopic data (^{31}P NMR: s, δ +7.3 ppm, ^{13}C NMR: t, δ 49.6 ppm, J_{PC} 7.3 Hz, ^{29}Si NMR: t, δ –10.7 ppm J_{PSi} 10 Hz).

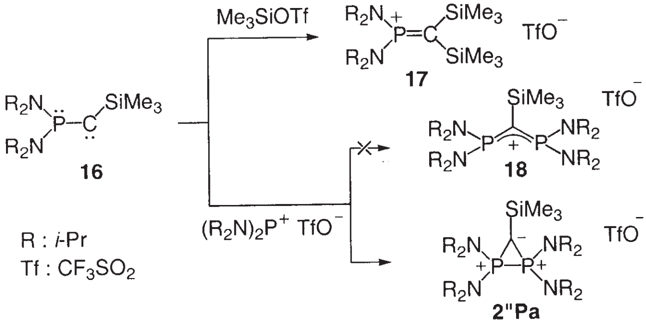

Scheme 13

5
Structure of the Diphosphorus-Containing Salts 2P, 2′P, and 2″P

Cyclopropenium salts **2C** are the prototype of 2-π-electron Hückel aromatic systems [35]. Due to the higher electronegativity of nitrogen compared to carbon, the π-system of diazirinium salts **2N** is strongly polarized towards nitrogen and therefore these compounds are calculated to be less aromatic than the corresponding cyclopropenium salts **2C** [36]. Diazirinium salts **2N** have yet to be characterized, even spectroscopically. Their postulated involvement [37] in the exchange reaction of nucleophiles with halogeno-3*H*-diazirines, a reaction of crucial importance for the synthesis of functionalized diazirines and therefore of carbenes, has been refuted [38]. As far as **2′N** is concerned, nothing is known.

According to calculations [8b, 39], the PP and PC bond distances in diphosphirenylium salts **2P** are halfway between those of single and double bonds, but the positive charge is essentially distributed over the two phosphorus centers. In other words, although the electronegativity of phosphorus is very close to that of carbon, the electronic delocalization becomes less important with increasing phosphorus substitution in the ring system. This is due to the fact that P(3p)-C(2p) and P(3p)-P(3p) interactions are usually weak (π-bond strengths: C=C 293 kJ/mol; P=C 201 kJ/mol; P=P 142 kJ/mol) [14]. For example, the electron delocalization in phosphirenylium salts **H** has been estimated to be only 70% of that of the cyclopropenium salts **2C** [40].

Structural data available from experimental [22a] as well as theoretical [22c, 41] studies demonstrate that diphosphirenium salts **2′P** also benefit from a certain amount of aromatic stabilization. However, the resonance energy of σ^4-phosphorus-containing systems is smaller. From a quantitative point of view, the electron delocalization in phosphirenium salts **C** has been calculated to be half that of the corresponding phosphirenylium salts **H** [42].

This striking difference between the σ^2- and σ^4-phosphorus-containing systems can be explained by considering the nature of the orbitals, which are involved in the delocalization of the two-π-electrons over the ring. In diphosphirenylium salts **2P** (which feature two dicoordinate phosphorus centers) these are one 2p(C) and two 3p(P) orbitals; in contrast, one should consider one 2p(C), one 3p(P), and one σ^*_{PX}-type orbitals for diphosphirenium salts **2′P** (which feature a tetracoordinate phosphorus center) (Fig. 3). It is thus clear that the Hückel-type three-orbital two-electron interaction characteristic of the cyclopropenium cations **2C** is more favored in diphosphirenylium salts **2P** than in the corresponding diphosphirenium salts **2′P**.

Compounds of type **2″P**, featuring two σ^4-phosphorus centers probably benefit from an even weaker aromatic character, but this is not the most interesting point concerning their structure. Ab initio calculations have been performed on the model compound **2″Pb** [34]. The calculated geometric parameters [P-P: 2.102; P-C: 1.726 and 1.727 Å] compare well with those found experimentally for the sterically encumbered derivative **2″Pa** [34] (Fig. 4). The analysis of the electron densities of **2″Pb** is of particular interest. Each diaminophosphenium unit carries approximately +1 charge, whereas the carbon bears −1.6 charge [−1.2 in the σ-space and −0.4 in the (formal) p-orbital]

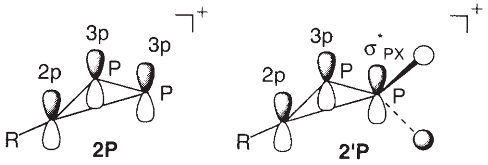

Fig. 3. Orbitals involved in the electronic delocalization of the diphosphirenylium **2P** and diphosphirenium salts **2′P**

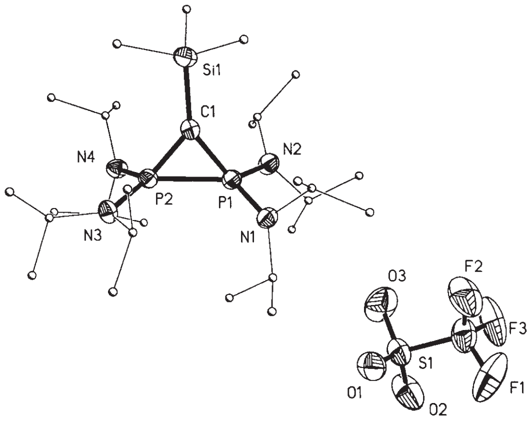

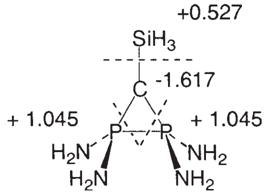

2"Pb

Fig. 4. Molecular view of **2″Pa** in the solid state (thermal ellipsoids at the 50% probability level). Isopropyl and methyl groups are simplified for clarity. Selected bond lengths (in angstroms) are as follows: C(1)-P(1) 1.731(3), C(1)-P(2) 1.710(3), C(1)-Si(1) 1.859(3), P(1)-P(2) 2.1195(11), P(1)-N(1) 1.651(3), P(1)-N(2) 1.659(3), P(2)-N(3) 1.651(2), P(2)-N(4) 1.642(2). Selected bond angles (in degrees) are as follows: P(1)-C(1)-P(2) 76.04(13), P(1)-C(1)-Si(1) 146.00(18), P(2)-C(1)-Si(1) 137.79(18), C(1)-P(1)-P(2) 51.53(10), and C(1)-P(2)-P(1) 52.42(10). Charges of fragments for the model compound **2″Pb**

(Fig. 5). At first glance, this large value seems rather surprising, but if one subtracts –0.5 charge, which is provided by the silyl unit, it leaves –1.1 charge at the carbon. There is a simple explanation for this observation. The angular compression at the carbon makes it extremely electronegative. It therefore withdraws considerable electron density from the neighboring electropositive phosphorus and silyl groups.

Further investigation of **2″Pb** via analysis of the Laplacian of the electron density and the electron localization function (ELF) [34] reveals a strong "banana" P-P-bond with large p-character (the bond ellipticity is 0.45) in the plane of the ring, and partial double bond character (Wiberg bond indices = 1.2) for the PC-bonds (Fig. 5).

The calculations found that the open planar form (C_{2v} symmetry) of type **18′** is not a minimum on the potential energy surface [34] (Fig. 6). However, pyramidalization at one of the phosphorus atoms leads to **18″**, which is not only an energy minimum but also lower in energy by 24 kJ/mol than the cyclic form

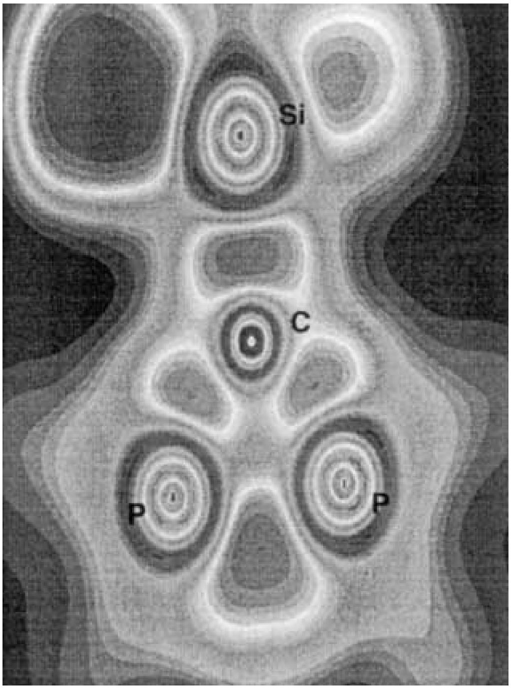

Fig. 5. Electron Localization Function analysis for the model compound **2″Pa** (ring bonds in plane of paper)

2″Pb. The experimental observation of **2″Pa** was explained by the presence of bulky diisopropylamino groups since the steric demand in the linear form is larger than in the cyclic system. This hypothesis has been confirmed by further calculations: the cyclic isomer **2″Pa** is predicted to be 25 kJ/mol lower in energy than the open form **18** [43].

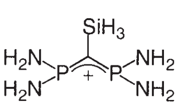
18'

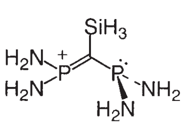
18"

Fig. 6. Open forms **18** and **18′** of the model diphosphino-substituted carbocation

Derivative **2″Pa** can be considered as resulting from a “cascade stabilization” of the electron deficient carbocation center (Fig. 7). As in the case of monophosphinocarbenium ions such as **17**, the first phosphorus atom gives electrons to the carbocationic center and becomes positively charged and, therefore, highly electrophilic [44]. The second phosphorus atom then acts as a Lewis base towards the first and the carbon atom finally bears a negative charge!

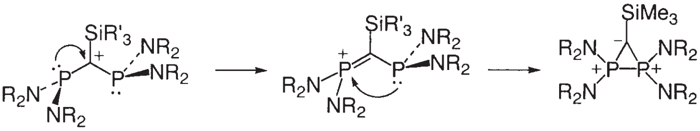

Fig. 7. Cascade stabilization in diphosphino-substituted carbocations

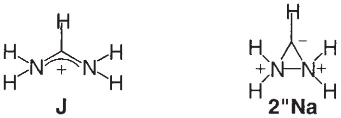

Fig. 8. Structure of the parent diamino-substituted carbocation (amidinium salt) **J** and of its cyclic valence isomer **2″Na**

This type of transformation of a cationic center into an anionic center is unlikely to be unique and shows once again that the electronic properties of phosphorus allow for the preparation of structural moieties that are difficult or impossible to access in the carbon and nitrogen series. For comparison, the related nitrogen systems are the long-known synthetically and biologically important aminidium salts, which adopt open allylic structures. Quantum chemical calculations at the B3LYP/6–31g* level with additional zero-point vibrational energy correction predict the parent amidinium salt **J** to be 541 kJ/mol more stable than its unknown cyclic valence isomer **2″Na** (Fig. 8) [34]! Several factors may explain the striking difference between the nitrogen- and phosphorus-containing systems: (i) the much smaller inversion barrier at nitrogen than at phosphorus favors the three-center 4π-system **J**; (ii) the weakness of the phosphorus-carbon π-bonds (P=C: 188 kJ/mol; N=C: 272 kJ/mol) [14] disfavors the allylic structure in **I**; (iii) phosphorus-carbon bonds are longer than nitrogen-carbon bonds (P-C: 1.89 Å; N-C: 1.47 Å), and thus the ring strain energy is smaller in phosphorus rings.

6
Reactivity of the Diphosphorus-Containing Salts 2P, 2′P, and 2′′P

Since compounds **2Pa**, **2′Pa**, and **2″Pa** have only been recently discovered, little is known about their reactivity. However, some interesting features are emerging, which corroborate the fact that the diphosphirenylium salts **2P** are more closely related to cyclopropenium salt **2C** than diphosphirenium **2′P** and of course **2″P**.

Nucleophiles react with cyclopropenium **2C** and diphosphirenylium salts **2Pa** affording the corresponding cyclopropenes **1C** and 1*H*-diphosphirenes **1′Px** (Scheme 14), respectively. Nucleophiles such as lithium salts also react at the dicoordinate phosphorus atom of the diphosphirenium salt **2′Pa** [22b, 45], but in this case ring opening reactions occur affording the phosphaalkenes **15** rather than the thermodynamically unfavored cyclic 4π-electron ylides **19**. Cleavage of

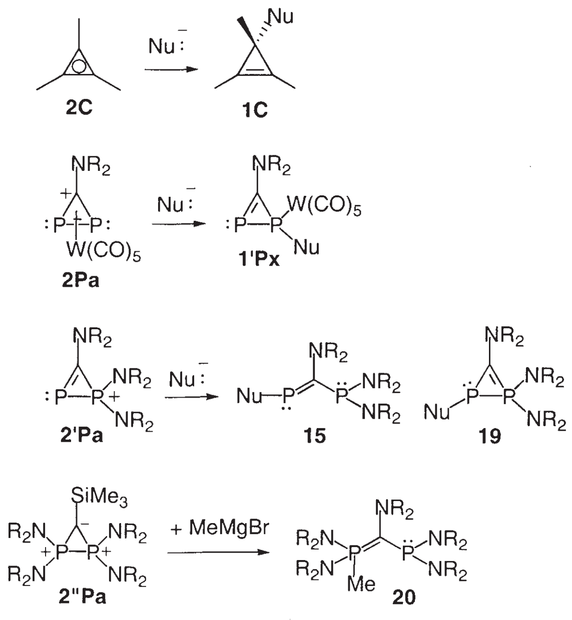

Scheme 14 R : *i*-Pr

the P-P bond is also observed with **2″Pa** by reaction with methylmagnesium bromide: the *P*-methyl phosphorus ylide **20** is obtained in near quantitative yield [34]. Note that the latter result is in perfect agreement with the electronic distribution in **2″Pa**: the carbon center which bears a negative charge has no more electrophilic character.

While diphosphirenium **2′Pa** and also cyclopropenium **2C** exist as borate salts, attempts to abstract chloride from diphosphirene **1′Pg** with sodium tetraphenylborate led to the phenyl-substituted 1*H*-diphosphirene **1′Ph** [25] (Scheme 15). These results clearly demonstrate that diphosphirenylium **2P** are much more electrophilic than either diphosphirenium **2′P** or the cyclopropenium salts **2C**.

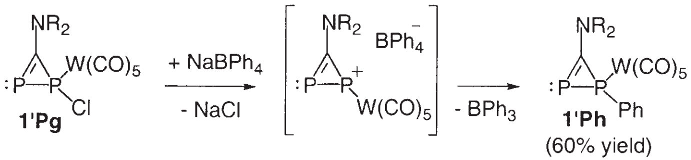

Scheme 15 R: *i*-Pr

It is well documented that carbenium ions undergo nucleophilic attack by the carbon atom of isocyanides [46]. Significantly, diphosphirenium **2′Pa** reacts at −50 °C with *tert*-butyl isocyanide in a similar manner to give the transient nitrilium salt **21**, which undergoes a ring expansion reaction affording **22** [45] (Scheme 16). Note that **22** is one of the very rare four-membered heterocycles featuring a phosphaalkene moieties [47].

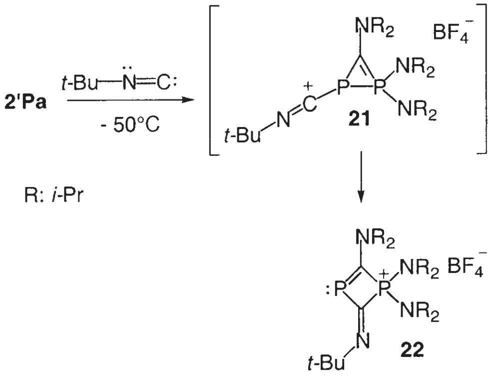

Scheme 16

The interaction of transition metal complexes with cyclopropenium cations **2C** has been widely studied [48–50]. Besides the expected η^3 (an example of η^3 ligation has also been observed by Nixon et al. with phosphirenylium **H** [24c]) and η^1 ligations [48, 49], the η^2 coordination mode with various extents of intrusion of the metal into the CC bond have also been observed [50]. The latter types of complexes represent points on the potential energy surface calculated for the conversion of a metallatetrahedrane (η^3-cyclopropenyl) to a metallacyclobutadiene complex (complete insertion of the metal into the CC bond) [51], a process which has been recognized to play an important role in alkyne metathesis [52]. The complex **23a** [53] obtained by treatment of diphosphirenium **2′Pa** with one equivalent of palladium tetrakis(triphenylphosphine) at –40 °C fits into this category (Scheme 17). The cleavage of the PP bond was suggested by the large deshielding of the σ^2-P ^{31}P NMR signal compared to that of the diphosphirenium salt **2′Pa** ($\Delta\delta = 195$ ppm) and was confirmed by a single crystal X-ray diffraction study of the complex **23b**. Indeed, the PP distance of 2.655 Å is longer than a normal P-P single bond, which is about 2.20–2.35 Å [54] and is also longer than that observed in the related 1,3-diphospha-2,4-disilabicyclo[1.1.0]butane (2.34 Å) [55]. However, the correlation between bond length and bond order is not always simple; yet, as the ring carbon lies only 0.19 Å out of the P-Pd-P plane, a bicyclic structure can be ruled out. The palladium atom has a slightly distorted square-planar geometry, probably due to the strain in the four-membered ring, and can be considered as Pd(II). Since the σ^2-PC bond length [1.745(3) Å] falls in the range observed for *C*-amino substituted phosphaalkenes [56], complexes **23** have to be considered as the first examples of diphosphametallacyclobutene.

Very surprisingly, when a dichloromethane solution of the complex **23a** was refluxed overnight in the presence of the three-membered heterocycle **2′Pa** (0.5 equivalent), a new complex **24a** [57] was obtained in 25% yield (Scheme 17). A single crystal X-ray diffraction study of derivative **24b** revealed that the CN bond length [1.325(10) Å] is in the range expected for a double bond, which implies that the positive charge is more or less localized at nitrogen. The palladium atoms have a slightly distorted square-planar geometry and can be considered as Pd(II). At first glance, these compounds can be regarded either

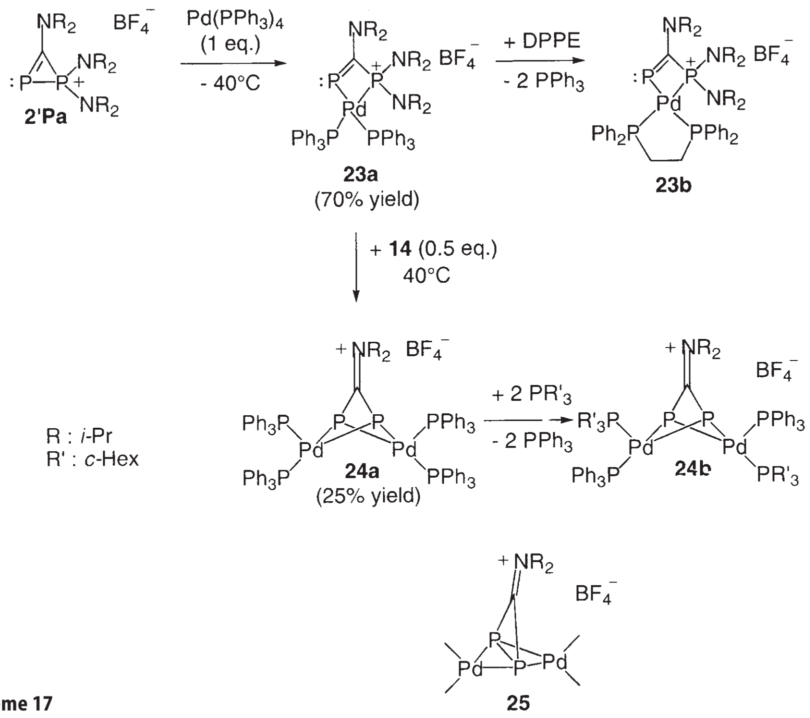

Scheme 17

as [1.1.1]propellanes **25** [58], which possess bridgehead phosphorus atoms having an inverted tetrahedral geometry, or alternatively as tricyclo[1.1.1]pentanes (asteranes) **24** in which the P-P bond is broken. The σ^3-P…σ^3-P distance [2.681(3) Å] in **24b** is much shorter than that observed in the 1,3-diphospha-2,4-disila-5-platinabicyclo[1.1.1]pentane (3.063 Å) [55] and related P_2B_3, P_2B_2Si, and P_2B_2Ge derivatives (2.86–3.07 Å) [59], but longer than normal P-P single bond lengths [54]. The P-C-P bond angle [96.4(4)°] is quite comparable to that observed in the four-membered ring **23b** (96.2°), but much larger than in the three-membered ring **2′Pa** (73.9°). Therefore, complexes **24** can be regarded as having an asterane structure with two strongly pyramidalized bridgehead phosphorus atoms (Σ angles = 254.0 and 251.7°). Although the stoichiometry of the reaction, the cleavage of the diisopropylamino groups, and the mechanism as a whole for the reaction leading to **24a** are still obscure, this type of complex is unique in several respects. Of particular interest – it features two pyramidalized μ^2-phosphinidene units [60] (unknown before this work), and is the first asterane possessing a trigonal carbon atom.

Note that complex **23a** formally results from the insertion of one $Pd(PPh_3)_2$ fragment into the PP bond of the diphosphirenium salt **2′Pa** [61], while derivative **24a** formally results from the insertion of two $Pd(PPh_3)_2$ fragments into the PP bond of a diphosphirenylium salt **2P**.

7
Synthesis, Structure, and Dimerization of Diphosphorus-Containing Radicals 3P and 3′P

It is well known that reduction of cyclopropenium salts **2C** leads to the corresponding cyclopropenyl radicals **3C** [62]. In contrast, under the same conditions the diphosphirenium salt **2′Pa** undergoes a ring opening reaction [63]. After migration of an amino group, a surprisingly [64] stable 1σ^2,3σ^2-diphosphaallyl radical **26** was obtained in 60% yield (mp 95–96°C). The mass spectrum of **26** revealed that no fragmentation reaction occurred during the reduction of **2′Pa**, while the splitting pattern of the ESR signal demonstrated the symmetrical structure of the radical obtained. According to calculations for the parent compounds (R=H), the cyclic radical **3′Pa** is not an energy minimum, while the unsymmetrical allyl radical **27** is 26 kJ/mol higher in energy than the symmetrical allyl radical **26.** Interestingly, oxidation of both radicals **3C** and **26** regenerates the starting cations **2C** and **2′Pa** (Scheme 18).

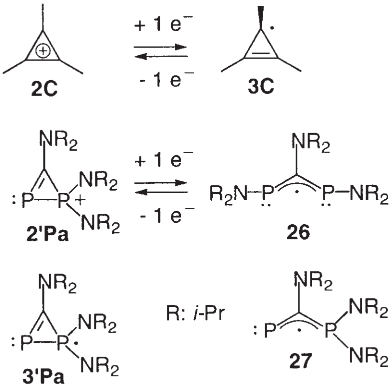

Scheme 18

So far, no free diphosphirenylium salt **2P** is available but one can easily predict that a reduction should lead to a diphosphirenyl radical **3P** [65]. In fact, we have recently postulated the formation of the radical **3Pa** in the homolytic cleavage of the P-N bond of the 1*H*-diphosphirene **1′Pc** [66]. Treatment of **1′Pc** with catalytic amounts of BF_3 (5%) and Et_3 N (5%) in tetrahydrofuran at 50 °C for 2 h led to a diamagnetic red solution. After evaporation of the solvent and extraction with pentane, the compound $[\mathbf{3Pa}]_2$ was isolated in 45% yield as red crystals (melting point: 140°C) (Scheme 19).

The molecular weight obtained by mass spectrometry corresponded to a dimer of the diphosphirenyl radical **3Pa.** The ^{31}P NMR spectrum showed only a singlet at – 164.5 ppm, suggesting the presence of a three-membered ring framework [26]. The high symmetry of the structure was confirmed by the ^{1}H and ^{13}C NMR spectra. Additionally, a single crystal X-ray diffraction study of $[\mathbf{3Pa}]_2$ was performed. In the solid state (Fig. 9), the molecule is organized around an inversion center located at the center of a rectangular P_4 framework, which is almost

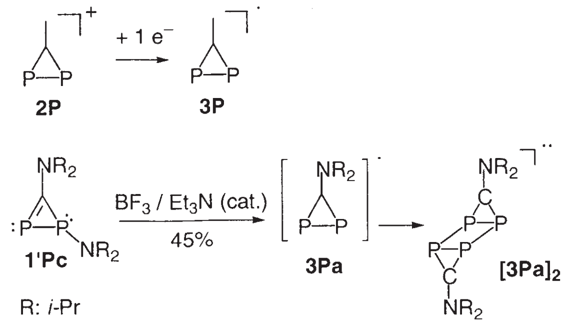

Scheme 19

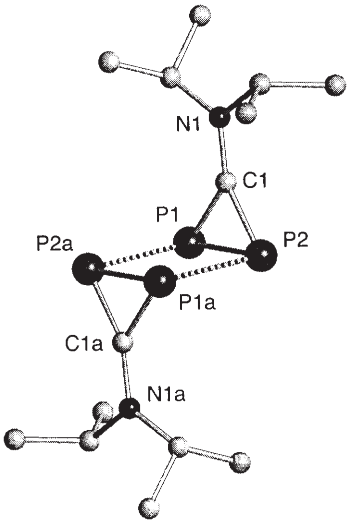

Fig. 9. Molecular view of $[\mathbf{3Pa}]_2$ in the solid state. Selected bond lengths (in angstroms) are as follows: C(1)-P(1) 1.743(6), C(1)-P(2) 1.738(6), C(1)-N(1) 1.336(7), P(1)-P(2) 2.205(3), P(1)-P(2a) 2.634(3). Selected bond angles (in degrees) are as follows: P(1)-C(1)-P(2) 78.6(3), P(1)-C(1)-N(1) 141.4(4), P(2)-C(1)-N(1) 138.8(4), C(1)-P(1)-P(2) 50.6(2), C(1)-P(2)-P(1) 50.8(2), C(1)-P(1)-P(2a) 94.9(2), P(2)-P(1)-P(2a) 89.1(1), P(1)-P(2)-P(1a) 90.9(1)

perpendicular to two three-membered rings (P_4/P_2C: 97°); the NR_2 groups are slightly tilted out of the PPC plans (0.164 Å). The PC and PP bond lengths in the three-membered rings are within the range expected for single bonds; the CN bond lengths are short, indicating a strong double bond character, which is confirmed by the planarity of the nitrogen atoms. Interestingly, the PP bonds between the two three-membered rings [2.634(3) Å] are by far the longest PP bonds ever reported [54, 67], but are clearly less than twice the phosphorus van der Waals radii (3.8 Å).

To gain a better understanding of the nature of $[\mathbf{3Pa}]_2$ and its formation from **3Pa**, ab initio calculations were performed [66]. For the model radical **3Pb**, the calculations predicted a $^2A_2$ ground state (Fig. 10). The spin density is equally

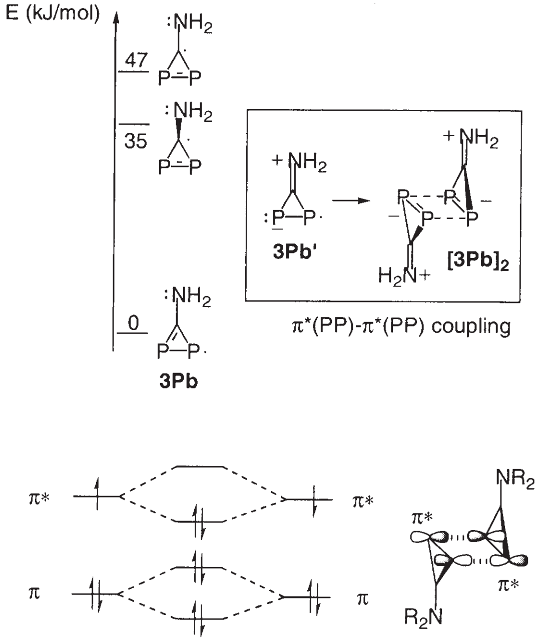

Fig. 10. Relative energies for the different states of the model diphosphirenyl radical **3Pb**, structure of the ensuing π^*-π^* dimer [**3Pb**]$_2$, and orbital diagram for the dimerization of the diphosphirenyl radical **3Pb** into the π^*-π^* dimer [**3Pb**]$_2$ (SOMO-SOMO interaction)

distributed over the two phosphorus atoms and the Single Occupied Molecular Orbital (SOMO) is the π^* orbital of the P=P double bond. Due to the higher strength of the NC π-bond (272 kJ/mol) compared with that of the PC π-bond (188 kJ/mol) [14], derivative **3Pb** is best described by the zwitterionic structure **3Pb′**. The dimerization of the diphosphirenyl radical **3Pb** is exothermic (–163 kJ/mol) and occurs via a π^*-π^* interaction [68], giving rise to the formation of [**3Pb**]$_2$. A six-π-electron four-center bonding system [69] best describes the P_4 framework; each phosphorus-phosphorus bond between the two three-membered rings is formally a one-electron bond [70], which rationalizes the very long PP bond distance. The most accurate, if any, Lewis-like representation of dimers [**3P**]$_2$ is the zwitterionic structure given in Fig. 10.

It is of interest to compare these results with those reported for the analogous carbon- and nitrogen-containing series. All the experimental [71] (EPR parameters) and theoretical [36, 66] studies suggest that the diazirinyl radicals **3N** present a somewhat similar π^*-structure. However, based on the formation of nitriles and dinitrogen, Maeda and Ingold [71] postulated that the bimolecular self-reaction of diazirinyl radicals **3N** proceeds via an N-N σ-dimer of type **28**; the isolation of such compounds, which suffer from the anti-aromaticity of the two 1*H*-diazirine moieties of type **1′N**, is unlikely (Fig. 11). There is no mention in the literature of radicals of type **3′N**.

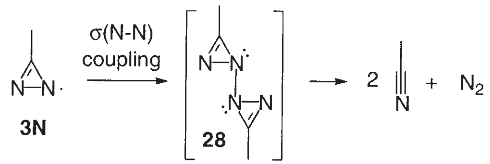

Fig. 11. Diazirinyl radicals **3N** and the ensuing σ(N-N) dimer **28**

As deduced from low temperature ESR characterization [72], as well as theoretical studies [73], cyclopropenyl radicals **3C** adopt a totally different σ-radical structure. The spin density is located at one of the carbon centers, which is in a strongly pyramidal environment. Accordingly, dimerization of such radicals proceeds by σ(C-C) coupling to give bis(cyclopropenyl) derivatives **29** [74] (Fig. 12).

Derivatives $[\mathbf{3P}]_2$ are valence isomers of tetraphosphabenzenes, derivatives which are so far unknown. It is interesting to compare the relative stability of these two types of valence isomers in the carbon, nitrogen and phosphorus chemistry (Fig. 13). The *anti*-tricyclohexylene, the carbon analogue of $[\mathbf{3P}]_2$, has only been postulated as a transition state in the Cope rearrangement of bicycloprop-2-enyl derivatives [75]. According to calculations, it is a minimum on the potential energy surface, which lies 618 kJ/mol above the benzene. In the nitrogen series, the dimer is also an energy minimum and is 405 kJ/mol higher in energy than tetrazine [34]. In marked contrast $[\mathbf{3P}]_2$, is only 33 kJ/mol above the tetraphosphabenzene! This again demonstrates the enormous difference between carbon, nitrogen, and phosphorus chemistry.

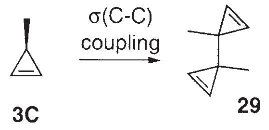

Fig. 12. Cyclopropenyl radicals **3C** and the ensuing σ(C-C) dimer **29**

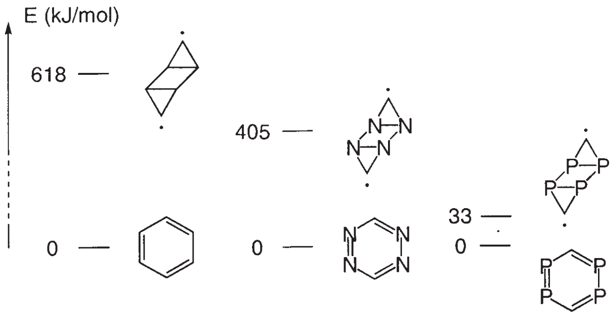

Fig. 13. Calculated relative energies (kJ/mol) for the anti-tricyclohexylene and benzene, and for their tetra-nitrogen- and -phosphorus-containing analogues

8
Conclusions and Perspectives

Due to its specific properties, phosphorus has allowed for the isolation of original three-membered rings which have so far no counterparts in nitrogen and carbon chemistry.

The diphosphorus-containing analogues of cyclopropenes, namely diphosphirenes, have only been isolated in their thermodynamically favored 1*H*-form whereas the corresponding diazirines are almost exclusively known in their 3*H*-form. This dramatic difference results from (i) the high inversion barrier of phosphorus compared to that of nitrogen, which prevents the planarization of the phosphorus and therefore the anti-aromatic character of the 1*H*-diphosphirene and (ii) the weakness of the π-bonds involving phosphorus compared to those involving nitrogen.

No dinitrogen-containing cyclopropenium analogues have been spectroscopically characterized, and even the postulated transient formation of diazirinium salts has been refuted. In contrast, all of the possible diphosphorus-containing cyclopropenium analogues **2P**, **2′P**, and **2″P** have been isolated. Although these phosphorus heterocycles are only weakly aromatic, they benefit from the electropositivity of phosphorus and from a relatively weak ring strain (PC and PP bonds are longer than CC, NC, and NN bonds). The environment of the phosphorus (σ^2 or σ^4) also play an important role. In particular, derivatives **2″P** featuring two σ^4-phosphorus centers must be considered as valence isomers of the diphosphino-substituted carbocations. In other words, the phosphorus analogues of the well-known diamino-substituted carbocations (amidinium salts) exist in a cyclic form featuring a negatively charge carbon center! Such a polarity inversion (transformation of a cationic center into an anionic center) is unlikely to be unique and should be of important synthetic utility.

Both cyclopropenyl and diazirinyl radicals have been characterized by ESR at low temperature. So far the transient formation of a diphosphorus-containing analogue, namely a diphosphirenyl radical, has only been postulated and calculations predict that due to the weakness of the PP π-bonds such a species should adopt a π^*-structure. In fact, an original dimerization process via π^*-π^* interaction occurred and a tetraphospha-benzene valence isomer featuring one-electron phosphorus-phosphorus bonds has been isolated. This result opens brand new research areas, not only in carbon chemistry (the corresponding π^*-π^* dimer of the cyclopropenyl radicals so far postulated as a transition state is in fact an energy minimum that might be observed), but also in phosphorus chemistry (other types of π^*-π^* dimers featuring phosphorus-phosphorus half bonds can be envisaged).

Acknowledgement. Thanks are due to the CNRS for financial support of this work. Special gratitude is expressed to all the research associates whose names appear in the reference list.

9
References

1. a) Dillon KB, Mathey F, Nixon JF (1998) Phosphorus: the carbon copy. Wiley, Chichester New York Weinheim Brisbane Singapore Toronto; b) Grützmacher H (2000) Science 289:737
2. For reviews on related topics, see: a) Bourissou D, Bertrand G (1999) Acc Chem Res 32:561; b) Canac Y, Bourissou D, Gornitzka H, Schoeller WW, Baceiredo A, Bertrand G (1999) Phosphorus Sulfur Silicon 144–146:37; c) Etemad-Moghadam E, Koenig M (1996) Three-membered rings with two heteroatoms including phosphorus to bismuth. In: Katritzky AR, Rees CW, Scriven EFV (eds) Comprehensive heterocyclic chemistry II. Pergamon, Oxford, vol 1a, p 469
3. Li X, Lei D, Chiang MY, Gaspar PP (1992) J Am Chem Soc 114:8526
4. a) Marinetti A, Mathey F, Fischer J, Mitschler A (1982) J Am Chem Soc 104:4484; b) Marinetti A, Charrier C, Mathey F, Fischer J (1985) Organometallics 4:2134; c) Mercier F, Mathey F (1986) Tetrahedron Lett 27:1323
5. a) Mathey F (1987) Angew Chem Int Ed Engl 26:275; b) Mathey F (1990) Phosphinidenes. In: Regitz M, Scherer OJ (eds) Multiple bonds and low coordination in phosphorus chemistry. Georg Thieme, Stuttgart New York, p 33; c) Cowley AH (1997) Acc Chem Res 30:445
6. Niecke E, Streubel R, Nieger M, Stalke D (1989) Angew Chem Int Ed Engl 28:1673
7. a) Mercier F, Ricard L, Mathey F, Regitz M (1991) J Chem Soc Chem Commun 1305; b) Streubel R, Ernst L, Jeske J, Jones PG (1995) J Chem Soc Chem Commun 2113
8. a) Bourissou D, Canac Y, Collado MI, Baceiredo A, Bertrand G (1997) J Chem Soc Chem Commun 2399; b) Bourissou D, Canac Y, Gornitzka H, Marsden CJ, Baceiredo A, Bertrand G (1999) Eur J Inorg Chem 1479
9. a) Neber PW, Burgard A (1932) Liebigs Ann Chem 493:281; b) Nair V (1968) J Org Chem 33:2121; c) Corkins HG, Storace L, Osgood E (1980) J Org Chem 45:3146
10. a) Graham WH (1965) J Am Chem Soc 87:4396; b) Moss RA, Wlostowska J, Guo W, Fedorynski M, Springer JP, Hirshfield JM (1981) J Org Chem 46:5048; c) Creary X (1992) Acc Chem Res 25:31
11. Bourissou D, Canac Y, Gornitzka H, Baceiredo A, Bertrand G (1999) J Chem Soc Chem Commun 1535
12. Gonbeau D, Pfister-Guillouzo G, Marinetti A, Mathey F (1985) Calculations predict that complexation of the σ^3-phosphorus atom strongly stabilizes 1*H*-phosphirenes. Inorg Chem 24:4133
13. A similar situation is found in the 1*H*-phosphirenes: a) Marinetti A, Mathey F, Fischer J, Mitschler A (1984) J Chem Soc Chem Commun 45; b) Wagner O, Ehle M, Birkel M, Hoffmann J, Regitz M (1991) Chem Ber 124:1207
14. Schoeller WW (1990) Bonding properties of low coordinated phosphorus compounds. In: Regitz M, Scherer OJ (eds) Multiple bonds and low coordination in phosphorus chemistry. Georg Thieme, Stuttgart New York, p 5
15. a) The transient formation of a 3*H*-diphosphirene has been postulated: Niecke E, Streubel R, Nieger M (1991) Angew Chem Int Ed Engl 30:90; b) The relative stabilities of 1*H*- and 3*H*-diphosphirenes have been theoretically investigated: Fitzpatrick NJ, Brougham DF, Groarke PJ, Nguyen MT (1994) Chem Ber 127:969
16. a) Liu MTH (1982) Chem Soc Rev 11:127; b) Liu MTH (1987) Chemistry of diazirines, vols I and II. CRC Press, Boca Raton
17. Dubau-Assibat N, Baceiredo A, Bertrand G (1996) J Am Chem Soc 118:5216
18. a) Fongers KS, Hogeveen H, Kingma RF (1983) Tetrahedron Lett 24:643; b) Breslow R, Deuring LA (1984) Tetrahedron Lett 25:1345; c) Vural JM, Weissman SA, Baxter SG, Cowley AH, Nunn CM (1988) J Chem Soc Chem Commun 462
19. a) Schultz CW, Parry RW (1976) Inorg Chem 15:3046; b) David G, Niecke E, Nieger M, Radseck J (1994) J Am Chem Soc 116:2191; c) Romanenko VD, Rudzevich VL, Rusanov EB, Chernega AN, Senio A, Sotiropoulos JM, Pfister-Guillouzo G, Sanchez M (1995) J Chem Soc Chem Commun 1383

20. a) Ciabattoni J, Nathan EC III (1969) J Am Chem Soc 91:4766; b) Yoshida Z (1973) Top Curr Chem 40:47
21. Baceiredo A, Igau A, Bertrand G, Menu MJ, Dartiguenave Y, Bonnet JJ (1986) J Am Chem Soc 108:7868
22. a) Castan F, Baceiredo A, Fischer J, De Cian A, Commenges G, Bertrand G (1991) J Am Chem Soc 113:8160; b) Soleilhavoup M, Canac Y, Polozov AM, Baceiredo A, Bertrand G (1994) J Am Chem Soc 116:6149; c) Soleilhavoup M (1993) PhD Thesis, University of Toulouse
23. a) Heydt H, Hoffmann J, Göller A, Clark T, Regitz M (1998) Synthesis 175; b) Hockless DCR, McDonald MA, Pabel M, Wild SB (1997) J Organomet Chem 529:189
24. a) Laali KK, Geissler B, Wagner O, Hoffmann J, Armbrust R, Eisfeld W, Regitz M (1994) J Am Chem Soc 116:9407; b) Simon J, Bertgsträsser U, Regitz M, Laali KK (1999) Organometallics 18:817; c) Avent AG, Cloke FGN, Folwe FR, Hitchcock PB, Nixon JF, Vickers DM (1994) Angew Chem Int Ed Engl 33:2330
25. Bourissou D, Canac Y, Collado MI, Baceiredo A, Bertrand G (1997) J Am Chem Soc 119:9923
26. a) Mathey F (1990) Chem Rev 90:997; b) Mathey F, Regitz M (1996) Phosphiranes, phosphirenes and heavier analogues. In: Katritzky AR, Rees CW, Scriven EFV (eds) Comprehensive heterocyclic chemistry II. Pergamon, Oxford, vol 1a, p 277
27. Three *J*(P,W) coupling constants with similar values (138, 103, and 30 Hz) have been observed for the trinuclear diphosphene complex (PhP=PPh).$[W(CO)_5]_3$: Mathey F, private communication
28. Such a phenomenon has already been observed for iron phosphaalkene complexes: Appel R, Casser C, Knoch F (1985) J Organomet Chem 293:213
29. a) Weber L (1992) Chem Rev 92:X1839; b) Vahrenkamp H, Wolters D (1983) Angew Chem Int Ed Engl 22:154
30. Grützmacher H, Marchand CM (1997) Coord Chem Rev 163:287
31. a) Igau A, Grützmacher H, Baceiredo A, Bertrand G (1988) J Am Chem Soc 110:6463; b) Kato T, Gornitzka H, Baceiredo A, Savin A, Bertrand G (2000) J Am Chem Soc 122:998; c) Bourissou D, Guerret O, Gabbaï FP, Bertrand G (2000) Chem Rev 100:39
32. Igau A, Baceiredo A, Grützmacher H, Pritzkow H, Bertrand G (1989) J Am Chem Soc 111:6853
33. Guerret O, Bertrand G (1997) Acc Chem Res 30:486
34. Kato T, Gornitzka H, Baceiredo A, Schoeller WW, Bertrand G (2000) Science 289:754
35. a) Breslow R, Yuan C (1958) J Am Chem Soc 80:5991; b) Breslow R, Groves JT (1970) J Am Chem Soc 92:984
36. Byun YG, Saebo S, Pittman CU Jr (1991) J Am Chem Soc 113:3689
37. a) Krogh-Jespersen K, Young CM, Moss RA, Wostowski M (1982) Tetrahedron Lett 23:2339; b) Moss RA, Terpinski J, Cox DP, Denney DZ, Krogh-Jespersen K (1985) J Am Chem Soc 107:2743; c) Liu MTH, Paike N (1987) Tetrahedron Lett 28:3763; d) Liu MTH, Doyle MP, Loh KL, Anand SM (1987) J Org Chem 52:323; e) Moss RA (1989) Acc Chem Res 22:15
38. a) Dailey WP (1987) Tetrahedron Lett 28:5801; b) Bainbridge KE, Dailey WP (1989) Tetrahedron Lett 30:4901; c) Creary X, Sky AF (1990) J Am Chem Soc 112:368
39. Schoeller WW, Tubbesing U (1995) J Mol Struct (THEOCHEM) 343:49
40. Eisfeld W, Regitz M (1998) J Org Chem 63:2814
41. Schoeller WW, Strutwolf (1994) J Mol Struct (THEOCHEM) 305:127
42. Göller A, Heydt H, Clark T (1996) J Org Chem 61:5840
43. Kato T, Gornitzka H, Baceiredo A, Schoeller WW, Bertrand G (results to be published)
44. By contrast with nitrogen, phosphorus is more electropositive than carbon and therefore, calculations predict that the R_2N and R_2P fragments of iminium $(R_2N{=}C<)^+$ and methylenephosphonium $(R_2P{=}\ C<)^+$ ions bear a negative and positive charge, respectively
45. Soleilhavoup M, Baceiredo A, Dahan F, Bertrand G (1994) J Chem Soc Chem Commun 337
46. Bishop R (1991). In: Trost BM (ed), Comprehensive organic chemistry. Pergamon, New York, vol 6, p 293
47. Appel R, Barth V, Knoch F (1983) Chem Ber 116:938
48. Gowling EW, Kettle SFA (1964) Inorg Chem 3:604

49. Gompper R, Bartmann E (1978) Angew Chem Int Ed Engl 17:456
50. Tuggle RM, Weaver DL (1972) Inorg Chem 11:2237
51. a) Jemmins ED, Hoffmann R (1980) J Am Chem Soc 102:2570; b) Lin Z, Hall MB (1994) Organometallics 13:2878
52. Schrock RR (1986) Acc Chem Res 19:342
53. Canac Y, Soleilhavoup M, Ricard L, Baceiredo A, Bertrand G (1995) Organometallics 14:3614
54. Lide DR (1992) CRC handbook of chemistry and physics. CRC, Boca Raton, FL, S 9–1
55. a) Driess M, Fanta AD, Powell DR, West R (1989) Angew Chem Int Ed Engl 28:1038; b) Fanta AD, Driess M, Powell DR, West R (1991) J Am Chem Soc 113:7806
56. Markovski LN, Romanenko VD, Ruban AV (1988). In: Kirsanov AV (ed) The chemistry of acyclic derivatives of two-coodinated phosphorus. Naukova Dumka, Kiev
57. Canac Y, Baceiredo A, Gornitzka H, Stalke D, Bertrand G (1995) Angew Chem Int Ed Engl 34:2677
58. For the preparation of the first [1.1.1]propellane, see: Wiberg KB, Walker FH (1982) J Am Chem Soc 104:5239
59. Paine RT, Nöth H (1995) Chem Rev 95:343
60. Burt JC, Schmid G (1978) J Chem Soc Dalton Trans 1385
61. Insertions of ML_n fragments (M=Ni, Pd, Pt) in the PC bonds of 1*H*-phosphirenes have already been observed: Al-Juaid SS, Carmichael D, Hitchcock PB, Lochschmidt S, Marinetti A, Mathey F, Nixon JF (1988) J Chem Soc Chem Commun 1156
62. Wasielewski MR, Breslow R (1976) J Am Chem Soc 98:4222
63. Canac Y, Baceiredo A, Schoeller WW, Gigmes D, Bertrand G (1997) J Am Chem Soc 119:7579
64. The transient formation of 1,3-diphosphaallyl radicals was postulated based on spin-trapping products: Gouygou M, Tachon C, Koenig M, Dubourg A, Declercq JP, Jaud J, Etemad-Moghadam G (1990) J Org Chem 55:5750
65. A trigermanium-containing cyclopropenyl radical analog has been isolated: Olmstead JF, Pu L, Simons RS, Power PP (1997) J Chem Soc Chem Commun 1595
66. Canac Y, Bourissou D, Baceiredo A, Gornitzka H, Schoeller WW, Bertrand G (1998) Science 279:2080
67. a) Cowley AH (1965) Chem Rev 65:617; b) Durig JR, Carreira LA, Odom JD (1974) J Am Chem Soc 96:2688
68. Note that π^*-π^* interactions have been found in numerous inorganic molecules [Klapötke T, Passmore J (1989) Acc Chem Res 22:234; Beck J (1997) Coord Chem Rev 163:55; Drews T, Koch W, Seppelt K (1999) J Am Chem Soc 121:4379], including in the solid state structure of NO [Dulmage WJ, Meyers EA, Lipscomb WN (1953) Acta Cryst 6:760; Kukolich SG (1982) J Am Chem Soc 104:4715] but so far no example directly involving phosphorus atoms have been reported. For example, $S_2I_4^{2+}$ is a π^*-π^* dimer [Passmore J, Sutherland G, Whidden T, White PS (1980) J Chem Soc Chem Commun 289], but not the isoelectronic P_2I_4 [Leung YC, Waser J (1956) J Phys Chem 60:539]
69. Gleiter R, Bartetzko R, Hofmann P (1980) Z Naturforsch 35b:1166
70. For an intramolecular boron-boron one-electron σ-bond, see: Hoefelmeyer JD, Gabbaï FP (2000) J Am Chem Soc 122:9054
71. Maeda Y, Ingold KU (1979) J Am Chem Soc 101:837
72. a) Schreiner K, Ahrens W, Berndt A (1975) Angew Chem Int Ed Engl 14:550; b) Schreiner K, Berndt A (1976) Angew Chem Int Ed Engl 15:698; c) Closs GL, Evanochko WT, Norris JR (1982) J Am Chem Soc 104:350; d) Sutcliffe R, Lindsay DA, Griller D, Walton JC, Ingold KU (1982) J Am Chem Soc 104:4674; e) Closs GL, Gordon S, Mulac WA (1982) J Org Chem 47:5415; f) Closs GL, Redwine OD (1986) J Am Chem Soc 108:506; g) Cano M, Quintana J, Julia L, Camps F, Joglar J (1999) J Org Chem 64:5096
73. a) Baird NC (1975) J Org Chem 40:624; b) Chipman DM, Miller KE (1984) J Am Chem Soc 106:6236
74. a) Breslow R, Gal P (1959) J Am Chem Soc 81:4747; b) Breslow R, Gal P, Chang HW, Altman LJ (1965) J Am Chem Soc 87:5139
75. Weiss R, Kölbl H (1975) J Am Chem Soc 97:3224

New Trends in Phosphametallocene Chemistry

Duncan Carmichael, François Mathey

"Hétéroéléments et Coordination" UMR CNRS 7653, DCPH, Ecole Polytechnique,
91128 Palaiseau Cedex, France
E-mail: duncanc@mars.polytechnique.fr; E-mail: francois.mathey@polytechnique.fr

The increasing general awareness of phospholyl ligands within the chemical community rests upon two properties: they can replace cyclopentadienyls in metal complexes and their η^5-transition metal complexes can act as π-acceptor ligands for coordination chemistry. In this review three interrelated areas exploiting these characteristics are presented. They comprise new structures and reagents based upon main-group phospholyl complexes, the incorporation of phospholyl ligands into transition metal paramagnetic metallocenes, and the application of transition-metal phospholyl complexes in homogeneous catalysis.

Keywords. Phosphole, Phospholyl, Phosphametallocene, Planar chirality, Paramagnetic complexes

Topics in Current Chemistry, Vol. 220

1
Introduction

Under the generic name “phosphametallocene”, we consider structures incorporating η^5-phospholyl-metal subunits. This definition includes both the genuine phosphametallocenes **1** and **2** and the half-sandwich structures **3**.

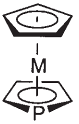
1

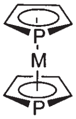
2


3

For comparative purposes we mention paramagnetic η^5-polyphospholyl complexes of the transition metals $[\eta^5\text{-}(C_nR_nP_{5-n})_2]M$ (n = 0 – 3), but make no attempt to treat the chemistry of these rings fully. Benzo-annelated compounds are also excluded. Whilst the chemistry of phosphametallocenes has already been reviewed many times [1–4], several new trends have emerged which justify a concise update. Among the new developments are the synthesis and characterization of main group derivatives, of 16-, 17-, 19-, and 20-electron species and, above all, some promising applications in homogeneous catalysis. This account will concentrate on these new topics.

1.1
Phospholide Ions: General Data

In many respects there is a continuum between the synthesis and chemistry of phospholide ions and of phosphametallocenes. Additionally, most syntheses of phosphametallocenes start from phospholide ions, so a quick glance at their chemistry is desirable.

The first and still most widely employed synthesis of phospholides rests on the cleavage of the exocyclic P-Ph bond of 1-phenylphospholes by alkali metals (Eq. 1) [5]:

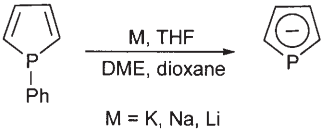

(1)

The reaction is driven by the large gain in aromaticity which occurs upon converting the phosphole into the phospholide. The mechanism of this cleavage involves a single electron transfer from the alkali metal to the phosphole. The phosphole radical anion thus produced collapses with release of a phenyl radical [6]. According to this mechanism, only one equivalent of alkali metal is needed to perform a complete conversion of the phosphole into the phospholide ion. To avoid the formation of phenyl-containing by-products, it is possible to replace cleavage of P-Ph by the cleavage of P-P or P-CH_2CH_2-P bonds. Pure phospholide ions can then be obtained [7]. 1-Halophospholes, when stable, are also convenient starting products [8].

Alternatively, strong bases are able to cleave selectively activated P-alkyl bonds as shown in (Eq. 2) [9]:

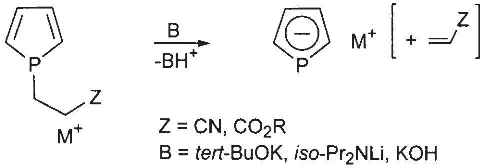

$Z = CN, CO_2R$
$B =$ *tert*-BuOK, *iso*-Pr_2NLi, KOH

(2)

The mechanism involves a proton abstraction from the carbon atom bearing the electron-withdrawing group Z.

A third approach takes advantage of [1,5]-sigmatropic shifts of sp- or sp^2-hybridized carbon substituents from phosphorus to the α-carbons of the ring. These occur upon heating. The transient 2*H*-phosphole products can be deprotonated by a base (Eq. 3) [10]:

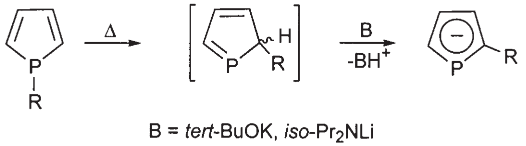

$B =$ *tert*-BuOK, *iso*-Pr_2NLi

(3)

These three approaches all start from a preformed phosphole ring. Recently, a fourth route has been reported in which the phospholide ring is built directly by combination of an anionic P-unit and a 1,3-diyne (Eq. 4) [11]:

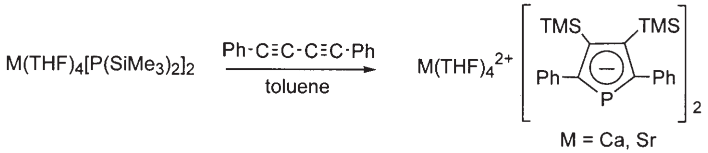

M = Ca, Sr

(4)

From a spectroscopic standpoint, these phospholides are all characterized by a ^{31}P resonance at low fields – at present, the range lies between +55 and +141 ppm [7, 10] – and by a large $^1J_{C-P}$ coupling, typically ca. 45–50 Hz [7]. The ^{31}P deshielding is thought to result from a weak coupling between the in-plane lone pair and the ring, leading to a large paramagnetic downfield shift [12]. Lithium 2,3,4,5-tetramethylphospholide [8] shows a planar ring with equalized CC bonds: C-C 1.424 Å, C=C 1.396 Å, and short P-C bonds at 1.751 Å. The aromatic stabilization energy of 29 kcal mol^{-1} for the parent species [13] is close to that of $[C_5H_5]^-$.

All known reactions of phospholide ions with electrophiles (R^+, H^+...) take place at phosphorus, probably as a result of the high concentration of negative charge at the heteroatom. With transition metal electrophiles (typically metal halides), three reaction pathways can lead either to the desired η^5-complexes (Eq. 5), to η^1-complexes (Eq. 6) or to 1,1′-biphospholes (Eq. 7):

(5)

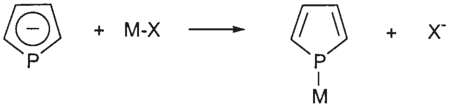

(6)

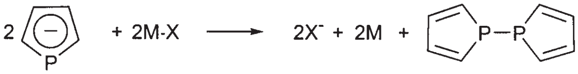

(7)

The formation of the η^1-complexes (Eq. 6) is disfavored by the introduction of bulky substituents at the α-positions of the phosphole ring. For example, η^5-phospholyl-cobalt-dicarbonyls can be synthesized only with α-substituents such as phenyl [14] or *tert*-butyl [15]. In order to avoid redox reactions (Eq. 7), it may be necessary to replace the phospholide ions by tin [16] or lead derivatives [17] (Eqs. 8, 9):

(8)

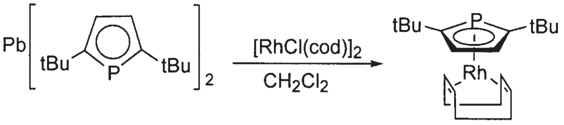

(9)

Applications of these techniques will be detailed in the next sections.

2

Structurally Characterized Main Group Complexes Containing η^5-Phospholyl Ligands

2.1

Introduction

At present, the impetus behind main group phospholyl chemistry lies in its potential applications in two areas: the use of volatile main-group-containing materials as precursors for electronic materials and the preparation of tailored reagents for applications in synthesis. Exchange of phospholides with main group metal halides has sometimes been used to generate reagents in situ, but the small spectroscopic changes occurring upon coordination of phospholides to main group elements means that the nature of such species is poorly defined. Here, we cover crystallographically characterized η^5-complexes and close relatives only.

2.2
Group 1

Most group 1 phospholides have been prepared through alkali metal cleavage of a phosphole P-Ph bond and, after destruction of phenyl-derived byproducts (with *tert*-BuCl $AlCl_3$, etc.), used in situ [3]. However, this convenient method is poorly adapted to sensitive chemistry and effort has been devoted to isolating pure alkali metal phospholides. When not substituted by chromophores, these are colorless, and sometimes pyrophoric materials.

Theopold et al. reported the first structural characterization of a phospholide. It was obtained through lithium cleavage of a P-chlorophosphole (prepared in turn by transmetallation of a Fagan-Nugent zirconium complex with PCl_3) and crystallized from TMEDA-ether as $[LiTMEDA(PC_4Me_4)]$ **4** (Eq. 10) [8]:

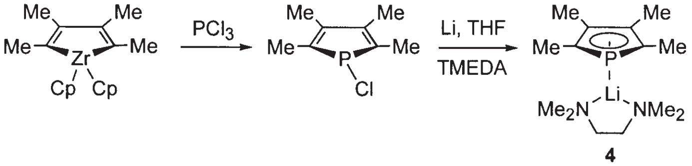

(10)

The chlorophosphole is rather labile but the lithium phospholide is stable indefinitely in the absence of air and moisture. Its structure, showing a planar ring, very similar C_α-C_β and C_β-C_β bond lengths (1.396 and 1.424 Å respectively) and a mean P-C distance (1.751 Å) lying half way between the values for classical P-C and P=C bonds [18], unequivocally confirmed the long-assumed aromaticity of phospholides. The lithium is displaced towards the phosphorus, in accord with the high charge and HOMO localization at P. Cleavage of the chlorophosphole with potassium and 18C6 in THF gave $[K18C6(PC_4Me_4)]$ whilst lithium in TMEDA-free THF gave the desirable solvent-free $[Li(PC_4Me_4)]$[8].

A second paper [19] deals with more elaborate alkali metal monophospholides which are obtained through cleavage of an easily accessible tetraphosphole [20] with lithium, sodium, or potassium. The system equilibrates rapidly and the nature of the product is controlled simply by varying the metal stoichiometry. Sodium cleavage to the tetramer dianion in DME gives a complex **5** where sodium shows η^1-η^5-coordination to phospholides and η^1-coordination to a phosphole and DME. Potassium cleavage to the dimeric dianion in THF-18C6 gives a 'kalocene'-type anionic sandwich **6** (Scheme 1).

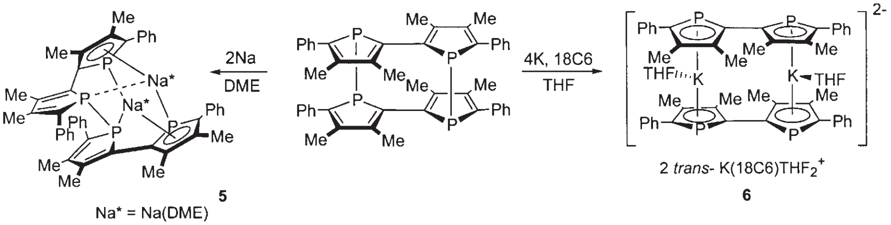

Scheme 1. Synthesis of alkali metal phospholides by cleavage of a tetraphosphole [20]. Products identified by X-ray crystallography

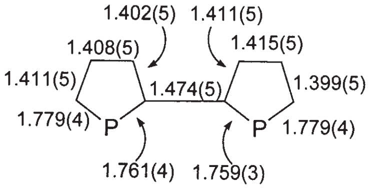

Fig. 1. Bond lengths in the kalocene 'ate' complex anion **6** [20]

Each potassium atom in the 'ate' complex is further coordinated to THF. The bond lengths in **6** show the CPh ring carbon atoms apparently slightly decoupled from the ring delocalization and rather short bonds about the P-C-C-P bridge (Fig. 1).

In a much more complex reaction, interaction of [K(PC_4Me_4)] with $SmCl_3$ in toluene gives a complex supramolecular structure **7** built from two similar but crystallographically distinct eight-membered subunits linked through η^5-potassium-phospholide bonds (Scheme 2) [21].

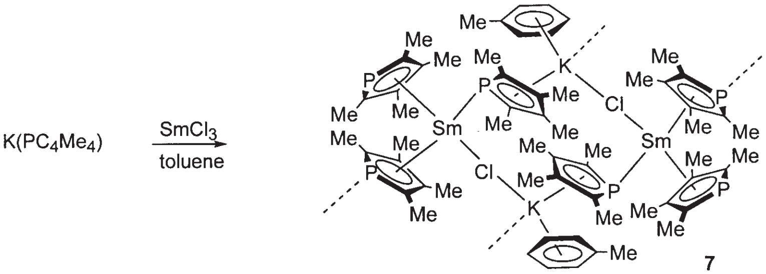

7

Scheme 2. The eight-membered ring forming the basis of the polymeric structure obtained upon reaction of potassium tetramethylphospholide with $SmCl_3$. Product identified by X-ray crystallography

Attempts to produce the potassium-free complex [Sm(PC_4Me_4)$_3$] failed. The toluene is much less strongly bound to the potassium center than the η^5-coordinated phospholide, which also shows η^1-coordination to a samarium center. A degree of oligomerization seems to persist in solution.

2.3
Group 2

Westerhausen et al. have reported detailed studies of the interactions between 1,4-diphenylbuta-1,3-diyne with the THF adducts of group 2 metal bis(trimethylsilyl)phosphides (Scheme 3).

Magnesium gives an alkenylphosphine-complex **8** [22], calcium and strontium produce β,β'-bis(trimethylsilyl)phospholides **9** and **10** [11], and barium gives a dissymmetric phospholide bearing an enyne group **11** [22]. In every case

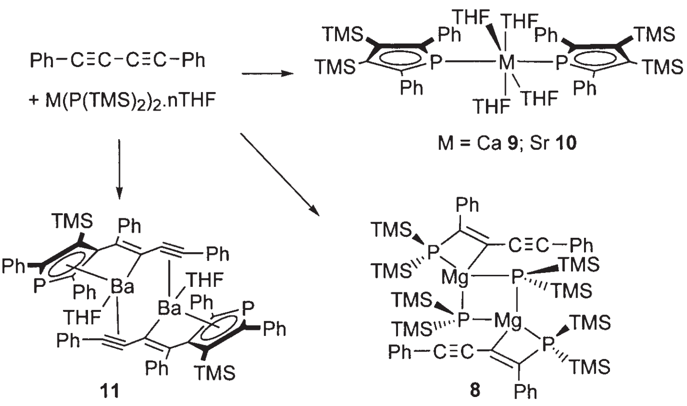

Scheme 3. Reaction of diphenylbuta-1,3-diyne with M[P(TMS)$_2$]$_2$.nTHF (M=Mg, Ca, Sr, Ba) in toluene [11, 22]. All products identified by X-ray crystallography

the authors propose the initial formation of a complexed ynenylphosphane structure of the type found for M=Mg. With magnesium, this product is stable to refluxing toluene even in the presence of excess diphenylbutadiyne. For Ca and Sr, a formal trimethylsilyl shift produces 2,5-diphenyl-3,4-bis(trimethylsilyl)phospholide anions. These adopt η^1-coordination modes having long P-M bonds (Ca: 3.068, Sr: 3.143 Å) because of repulsions with the strongly coordinated THF ligands. The softer Ba ion desolvates more easily, allowing coordination of diphenylbutadiyne prior to its incorporation into a heavily functionalized η^5-phospholide product [11].

Comparison of the reactions in Scheme 2 with the base-catalyzed addition of $PhPH_2$ to PhC_4Ph [5] shows that the phospholides are formed with strikingly high yields and selectivities (Ca, 82; Sr, 76; Ba, 87%). These presumably reflect the thermodynamic well resulting from aromatic $6\pi e$ configurations [23] and imply that the high degree of phospholyl C-C bond localization in **9** (C_α-C_β 1.405; C_β-C_β 1.451) and **10** (C_α-C_β 1.408; C_β-C_β 1.457 Å) may reflect steric repulsions between the $SiMe_3$ groups (see for example [Li(12C4)$_2$($C_5H_2TMS_3$)] [24]) rather than significantly diminished aromaticity. The literature shows that 3-functionalized phospholides are quite difficult to prepare (for a typical example, see [9]), so the simplicity of these syntheses outweighs the difficulties inherent in the preparation of the $P(SiMe_3)_3$ starting material [25].

A more classical cleavage of an inseparable mixture of 1-cyclopentadienyl- and 1-chloro-2,5-bis(trimethylsilyl)-3,4-dimethylphospholes with distilled calcium gave a complex structure **12** containing four calcium atoms. Reaction of calcium with the corresponding pure chloroarsole gave the dicalcium dimer **12a** (Scheme 4) [26].

In this light, the tetrameric phospholyl-containing structure **12** can be viewed as the result of the double insertion of the mixed monophosphacalcocene [CaCp($PC_4TMS_2Me_2$)] into the dicalcium core. The terminal calcium atoms appear to be more hindered in **12a** than **12** but it is unclear whether the combination of bridging Cp and terminal phospholyl ligands results from sterical fac-

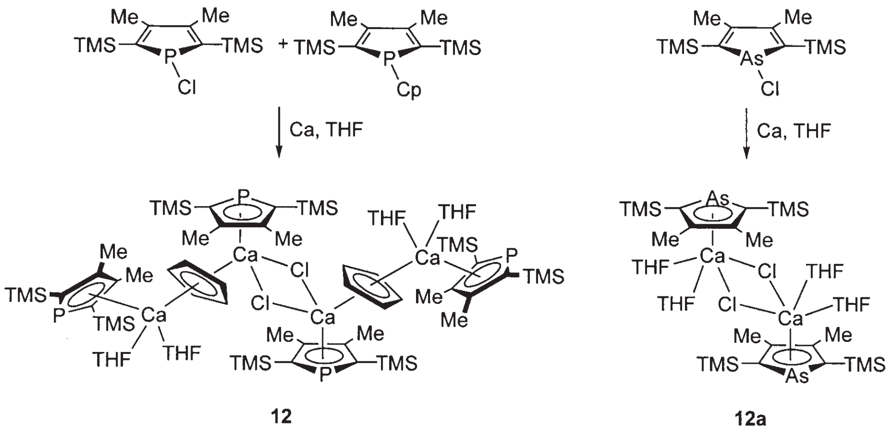

Scheme 4. Reaction of distilled calcium with chloroheteroles [26]. Products identified by X-ray crystallography

tors alone. NMR indicates that this structure is probably not maintained in solution [26].

The variety of products observed in these studies suggests interesting work to come.

2.4
Group 3

Interaction of [K18C6(PC_4Me_4)] with InCl in toluene was studied by Theopold et al. [27] as part of a program directed towards the preparation of single source CVD precursors for group III/V electronic materials. It gave a disappointing tetrahedral bis-η^1-'ate' complex **13** in 24% yield (Eq. 11). Reaction of toluene solutions of InCl with the solvent-free [Li(PC_4Me_4)] produced a yellow insoluble polymer, formulated as [$(InPC_4Me_4)_n$] **14**, which decomposed to indium metal and octamethylbiphosphole upon sublimation or dissolution in THF (Eq. 12) [27]:

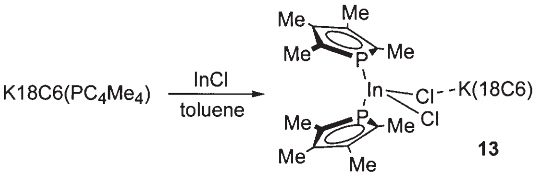

(11)

$$Li(PC_4Me_4) \xrightarrow[\text{toluene}]{\text{InCl}} \underset{\mathbf{14}}{\left[InPC_4Me_4\right]} \xrightarrow{\text{THF}} Me_4C_4P{-}PC_4Me_4 \tag{12}$$

More promising results have been obtained when reacting metastable GaBr solutions with [Li$(THF)_2(PC_4H_2tBu_2)$] (Eq. 13) [28]. The bulky groups on the phospholide inhibit oligomerization and the yellow oily product **15** is quite volatile:

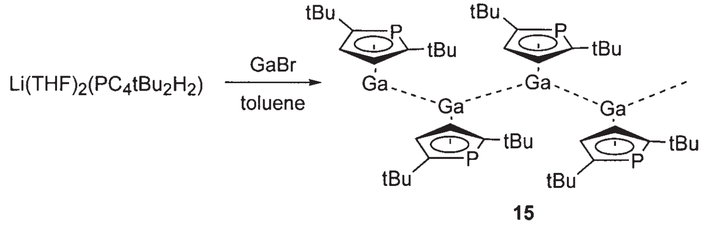

(13)

A combined ^{69}Ga NMR – DFT study indicates the presence of [Ga($PC_4H_2\mathit{t}Bu_2$)] monomers in benzene solution ($\delta Ga_{exp} = -653$; $\delta Ga_{calc} = -655$ ppm) [28]. This form is also maintained in the solid state. Sublimation of [Ga($PC_4H_2\mathit{t}Bu_2$)] prior to cooling below –26 °C produced slightly disordered crystals showing a previously unknown arrangement of Ga(I) monomers bound weakly into a zigzag chain (Ga-Ga = 3.66 Å) [29]. The shielding conferred by the *tert*-butyl groups is clearly shown upon interaction of **15** with [Cr(CO)$_5$(cyclooctene)], where the chromium center binds to gallium rather than phosphorus to give a simple binuclear product **16** (Eq. 14) [28]:

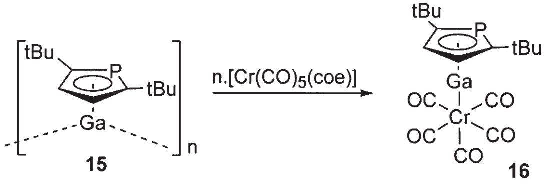

(14)

2.5 Group 4

Two phosphastannocenes **17** and **18** have been obtained by metathesis of tin (II) chloride with anionic phospholide sources (Scheme 5) [11, 17].

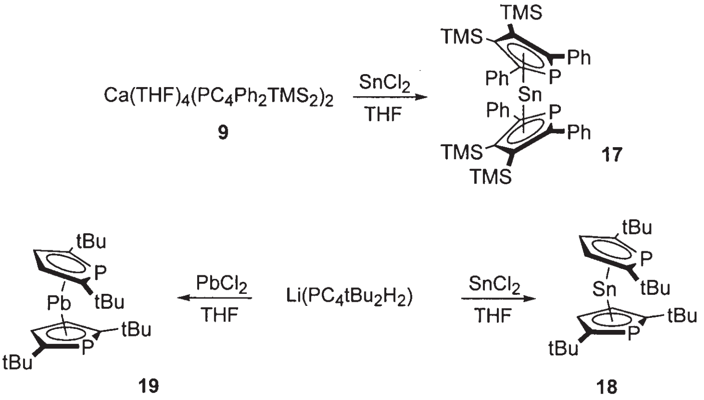

Scheme 5. Preparation of phosphastannocenes and a phosphaplumbocene [11, 17]. Products identified by X-ray crystallography

Compound **18** is soluble without decomposition in hexane and CH_2Cl_2 and shows sharp tin satellites in its ^{31}P and ^{13}C nmr solution spectra, thus suggesting a nondissociating covalent formulation [17]. Structurally, the two compounds differ and their hapticity is controversial. The bulk in **17** is localized on the β carbons so the phospholyl ligands are tilted and the tin binds much more strongly to phosphorus than carbon (mean Sn-P=2.760, Sn-$C_{(min)}$ 2.718, Sn-$C_{(max)}$ 2.988 Å). The bonds within the ring (C_α-C_β 1.412; C_β-C_β 1.465 Å) are longer but only slightly more localized than in the corresponding Ca and Sr analogs **9** and **10** [11]. The more symmetrically encumbered 2,5-di(*tert*-butyl)phospholyl derivative **18** better resembles classical hindered stannocenes [30]. It has a small mean ring interplane angle (19.2°) and tin-phosphorus radii lying towards the high end of the tin-carbon range (mean Sn-P 2.813, Sn-$C_{(min)}$ 2.688, Sn$C_{(max)}$ 2.878 Å) [17]. Nonetheless, the Sn-C distances remain very long (mean Sn-C 2.7955 Å; compare 2.704 Å in octa(iso-propyl)stannocene [31]) and the Sn-P linkage appears to dominate the structure. It is clear that the potential surface controlling the phosphastannocene coordination geometry is fairly flat, but the nature of the bonding continuum between classical η^5-ligation and a more localized η^3- or η^1-coordination to P and the C_α atoms requires clarification.

In a related reaction, $[Li(THF)_2(PC_4H_2tBu_2)]$ interacts with $PbCl_2$ to produce the corresponding bright yellow 1,1′-diphosphaplumbocene **19** (Scheme 5) [17]. Compound **19** resembles **18** in being stable in hydrocarbon and dichloromethane media and showing classical covalent behavior. X-ray analysis of **19** shows intermeshed *tert*-butyl groups which impose a reasonably long P-P separation (4.8 Å) and presumably protect against reductive elimination of the phospholyl ligands. Nonetheless thermolysis to metallic lead and 2,2′5,5′-tetra(*tert*-butyl)-1,1-biphosphole occurs in toluene at around 80 °C (Eq. 15). Consistently, attempted synthesis of 1,1′-diphospha-3,3′4,4′-tetramethylplumbocene in THF gives rapid precipitation of lead metal (Eq. 16) [32]:

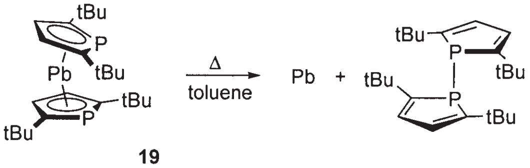

(15)

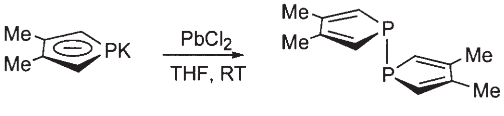

(16)

2.6 Conclusion

The paucity of well-characterized main-group phospholyl-containing complexes is perhaps the most striking aspect of this area. Nonetheless, the variety of elements already incorporated into these structures suggests that many more complexes should be accessible. In addition to any uses for materials, the possibility of modulating solubility, solvent compatibility, nucleophilicity, and redox resistance upon changing metal center should make them useful reagents; furthermore, their reactions with halide-containing materials will often give highly insoluble metal salts which are easily removed from reaction media. A number of such applications appear in the next section.

3
Paramagnetic Complexes Containing Phospholyl Ligands

3.1
Introduction

The first attempts to prepare paramagnetic phosphametallocenes involved oxidation of mono- and 1,1′-diphosphaferrocenes [32–36], and were inspired by potential applications as electronic materials. The phosphaferricinium ion products proved rather unstable and the first definitive characterization of a paramagnetic metallocene incorporating ring phosphorus atoms was made in 1988 by Nixon et al., through a low yield crystallographically-verified synthesis of 3,3′5,5′-tetra(*tert*-butyl)hexaphosphachromocene [37]. Further spectacular complexes [$\mathrm{MC_x}t\mathrm{Bu_xP_{10-x}}$] (x=4–6) M=Sc [38], Ti [39, 40], V [41] reported by Cloke et al. were later supplemented by Zenneck and coworkers' syntheses of [$\mathrm{Mn(C_2}t\mathrm{Bu_2P_3)_2}$] [42] and [$\mathrm{CoCp(C_2}t\mathrm{Bu_2P_3)}$] (Fig. 2) [43]. Only the 20 VE nickel sandwich is missing from the first row of transition metal polyphosphametallocenes.

The mono-and polyphospholyl series seem to be complementary and parallel research into monophospholyl ligand-based metallocene chemistry has been driven by a number of factors. First, whilst monophospholyl ligands resemble the corresponding cyclopentadienyls quite closely, polyphospholyls have rather different electronic properties (Green et al. draw a comparison between $\mathrm{P_3C_2tBu_2^-}$ and $\mathrm{C_7H_7^+}$ on the basis of PES studies of [$\mathrm{Ti(P_3C_2tBu_2)_2}$] [40]). Additionally, organic chemistry allowing the functionalization of phospholes is quite well developed, so it should be possible to 'tune' the behavior of a phosphametallocene by variation of the phospholyl substitution pattern [44]. Finally, only one phosphorus atom is present in each ring, so its behavior can be relatively easily understood and manipulated.

The four transition metal triads which currently include paramagnetic monophospholyl-ring sandwiches are reviewed below. Electronic applications

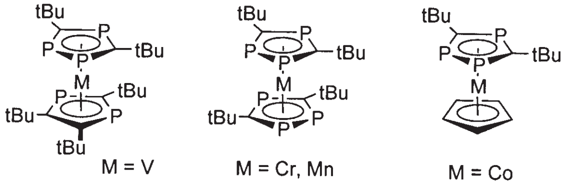

Fig. 2. Examples of paramagnetic polyphosphametallocene transition metal sandwich compounds [37, 41–43]

remain a major motivation for research in this area, so most studies have been oriented towards a physicochemical understanding of the complexes.

3.2
Group 6

Köhler et al. have described the preparation of octamethyl-1,1′-diphosphachromocene **20** in 87% yield as air-sensitive red crystals through metathesis of potassium tetramethylphospholide with $CrCl_2$ in THF (Eq. 17) [45]:

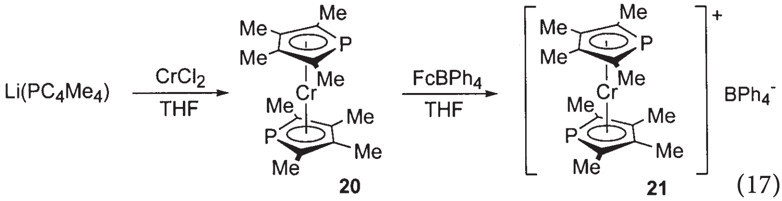

(17)

In the solid state, the complex shows C_{2h} symmetry and a long metal-ligand centroid distance of 1.76 Å indicative of the 16e electron count (compare phosphaferrocenes at ≅1.63 Å [46]). The replacement of the CH group in a cyclopentadienide by a phosphorus atom lifts the degeneracy of the π bonding combinations involved in the metallocene frontier orbitals (Fig. 3). NMR studies indicating that the reduced ligand paramagnetic shifts are essentially temperature invariant imply that the energy gap separating the $\pi_{(s)}$ and $\pi_{(as)}$ orbitals is significantly higher than in more conventionally ring-substituted chromocenes and that one phospholyl π orbital determines the electron spin distribution. The combination of a high-frequency shifted ^{31}P nmr resonance and assumed negative ligand spin density indicate that this orbital is $\pi_{(as)}$ [45].

Cyclic voltammetry of **20** shows reversible one-electron oxidation (0.56 V) and reduction waves (–1.07) and an irreversible two-electron oxidation (2.23 V vs $[Cp_2Co]$ in EtCN). Chemical oxidation with $[Fc^+BPh_4]$ in THF produces a 65% yield of the red air- and THF-sensitive chromocinium salt **21** which shows epr (electron paramagnetic resonance) data consistent with an $I = 3/2$ metallocinium ion having a small zero field splitting and an almost isotropic g factor. Unlike the neutral diphosphachromocene, variable temperature ^{1}H nmr studies imply the involvement of both $\pi_{(s)}$ and $\pi_{(as)}$ in determining the ligand spin density [45].

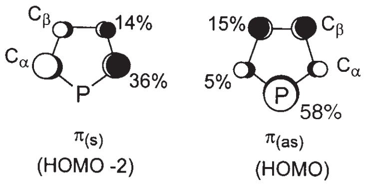

Fig. 3. Non-degenerate π orbitals of the phospholide anion showing their molecular orbital coefficients; after [47]; ($\Delta E\pi_{(as)}$-$\pi_{(s)}$ ca. 1 eV)

3.3
Group 8

The phosphaferrocenes are the oldest class of phosphametallocenes. Fenske-Hall analysis [47] of mono- and diphosphaferrocenes suggest that the HOMO of the parent diphosphaferrocene is a $3d_{z2}$ orbital having greater than 90% metal character whilst the LUMO is a hybrid involving the metal d_{xz} and ligand $\pi_{(s)}$ orbitals; a more recent unpublished DFT B3LYP calculation at the 6–31G* level gives a $3d_{xy}$ HOMO lying less than 0.6 eV above $3d_{x2\text{-}y2}$ and $3d_{z2}$ in both C_{2h} and C_{2v} conformers [48]. Thus, the high-lying filled levels comprise the classical cluster of essentially pure metal d orbitals whilst the LUMO has appreciable ligand character.

Most data pertaining to phosphaferricinium cations have come from electrochemistry. Cyclic voltammetry in apolar solvents shows a first, diffusion-controlled, reversible 1-electron oxidation occurring by an EC mechanism at potentials lying between + 0.4 and + 0.8 V (SCE) (Fig. 4) [33–35, 48, 49].

The formal replacement of a CH group in a ferrocene by an sp^2 phosphorus atom is associated with an anodic oxidation potential shift of about 185 mV. This value is essentially independent of the substitution pattern of the metallocene [33]. This electronic destabilization of the ferricinium cation upon incorporation of the phosphorus atom probably reflects the high π electronegativity of 2-coordinate sp^2 hybridized phosphorus which has been observed in MCD stud-

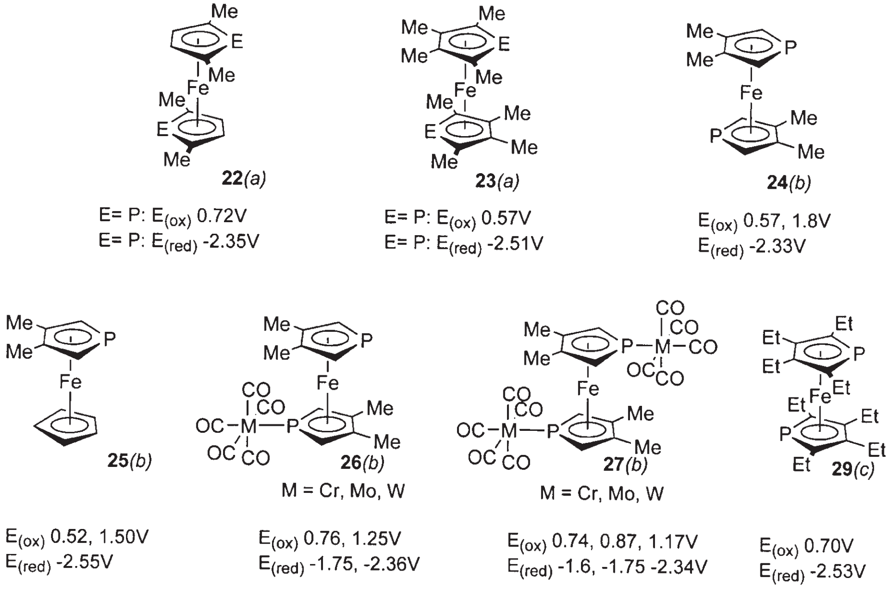

Fig. 4a–c. Selected electrochemical data for phosphaferrocenes. Conditions: **a** DME 0.1 mol/l NBu_4ClO_4 glassy carbon electrode –40 °C [49]; **b** propylene carbonate, 0.1 mol/l NEt_4ClO_4 oxidation: rotating Pt disc; reduction: dropping mercury [33, 34]; **c** THF 3.0 mol/l NBu_4BF_4 electrode: Pt, 25 °C [48]

ies of phosphinines [50]. The replacement of a phosphaferrocene CH by CMe provokes a smaller cathodic shift (40.5 mV) than in ferrocenes (47.0 mV) [49]. A further linear correlation of electrochemical oxidation potential against heteroatom ionization potential has been found for two families of group 15 heteroferrocenes **22** and **23** (E = P, As, Sb, Bi):

$$E_{1/2}(0/+) = 0.219\,(IP_E) - 1.758\ \text{V for } \mathbf{22} \tag{18}$$

$$E_{1/2}(0/+) = 0.192\,(IP_E) - 1.519\ \text{V for } \mathbf{23} \tag{19}$$

These simple first-order relationships confirm that the heteroferricinium SOMO has little interaction with the metallocene ligands [49].

The stability of phosphaferricinium ions in solution is low; cyclic voltammetry reveals that it decreases as the polarity of the medium rises or the degree of ring substitution falls [33]. The parent diphosphaferrocene evolves chemically under electrochemical oxidation in CH_2Cl_2, MeCN, and DMSO and is only stable in solvents such as propylene carbonate [33]. Compounds **24** and **25** are reversibly oxidized in dichloromethane but decompose in DMF, probably to the corresponding 1,1′-biphosphole (Eq. 20) [33]:

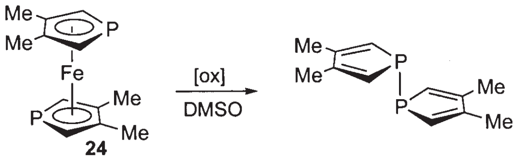

(20)

Coordination of electron-accepting groups such as group 6 metal pentacarbonyl fragments to the phosphaferrocene lone pair in **26** and **27** provokes the anticipated rise in oxidation potential but also further diminishes chemical stability: the first oxidation (for example + 0.74 V for **26c** attributed to the phosphaferrocene center) is not reversible even in non-donor solvents such as dichloromethane [34].

Further irreversible oxidations of the group 6 metals also occur at more positive potentials. A second poorly defined two-electron oxidation of non-coordinated phosphaferrocenes also results in decomposition to unknown products [34].

Reduction reactions of phosphaferrocenes have also been studied electrochemically. The first phosphaferrocene reduction is an irreversible process occurring between –2.1 and –2.6 V [33, 34, 48, 49]. The much greater influence upon the reduction potential (anodic shift of 390 mV) than upon oxidation (anodic: 185 mV) when replacing a CH group by P reflects the substantial ligand contribution found in the phosphaferrocene LUMO [49]. This low stability makes it likely that phosphaferrocenide anions will only be isolable with difficulty. The complexes **26** and **27** are reduced at the $M(CO)_5$ groups and then dissociate: controlled potential electrolysis at –1.8 V gives the decomplexed phosphaferrocene **24** (Eq. 21) [34].

If the electrochemistry of mono- and diphosphaferricinium cations is well defined, their chemistry and characteristics are less perfectly understood. The stability of phosphaferricinium ions appears to be highly medium-dependent and the sometimes conflicting data must be interpreted with care. The first attempted chemical syntheses involved controlled potential electrolysis of **24**

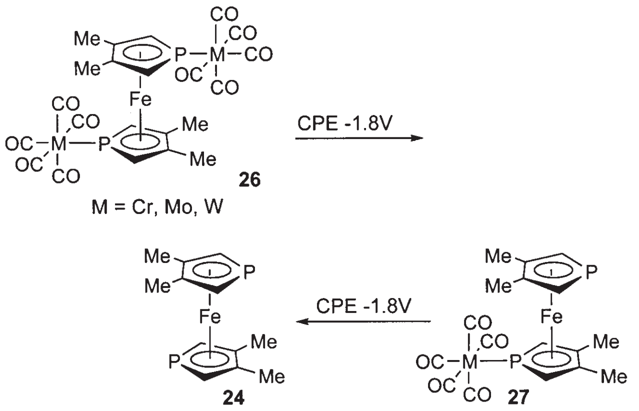

(21)

(+1 V, platinum electrode, dichloroethane, 0.1 M TBAP) and gave orange solutions showing $g_{\parallel} = 2.72$, $g_{\perp} = 1.99$ and no hyperfine coupling to phosphorus [33] (the ferricinium ion is now accepted to give $g_{\parallel} = 4.35$, $g_{\perp} = 1.26$ [51]). In subsequent work also including arsaferrocenes, chemical treatment of **23a** with silver tetrafluoroborate was found to give violet dichloroethane solutions which, whilst epr-silent at room temperature, gave comparable data at 100 K ($g_{\parallel}$ 2.79 and $g_{\perp}$ 1.98). The marked difference from the values found for ferricinium ions was interpreted in terms of a $3d_{z2}$ SOMO and the change in ground state symmetry from $^2E_{2g}$ to $^2A_1$ [49]. The interpretation of these data is complicated by Sava [48], Cowley et al. [52], and Roberts et al. [53] who report deep purple coordination complexes of Ag^+ with phosphaferrocenes, under only slightly different conditions. Roberts et al. have also reported some Mössbauer evidence for the oxidation of phosphaferrocenes by TCNE in aqueous acetone: the data, again from purple solutions, are very different from those for ferricinium (for example **24**: isomer shift 0.48 quadrupole splitting 1.87; [**24**$^+$TCNE$^-$]: IS 0.49; QS 1.81 [36]; Fc$^+$: IS 0.80–0.84; QS ≅ 0 mm s^{-1} vs Fe foil [54]).

Very recently, Sava and Le Floch [49] have succeeded in isolating mono- and diphosphaferricinium salts through oxidation of the parent phosphaferrocenes with iodine (Eqs. 22, 23):

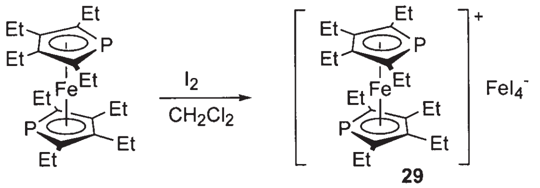

(22)

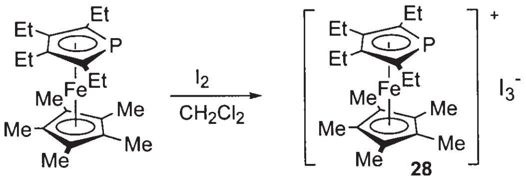

(23)

At present, only X-ray measurements and cyclic voltammetry data have been used to characterize these deep violet compounds but they conclusively demonstrate the existence and stability of isolable phosphaferricinium sandwiches. Very slight alternations in phospholyl intracyclic bond lengths (for example C_α-C_β= 1.415(4), C_β-C_β' = 1.430(5) Å for **28**; C_α-C_β = 1.417(4), C_β-C_β' = 1.34(5) Å for **29**) again accord with the formulation of the SOMO as an essentially unmodified metal 3d orbital.

A full analysis of these compounds would be timely.

3.4
Group 9

Phosphacobaltocenes may be prepared through the direct attack of appropriately substituted lithium phospholides upon CoX_2 precursors (X=Cl, acac) or by reduction of the corresponding phosphacobalticinium salts **30**. In turn, these are available straightforwardly through metathesis of $[CoCp^*I_2]_2$ with a main group phospholyl complex such as the phosphaplumbocene **19** or phosphastannocene **18** described above (Eq. 24) [55]:

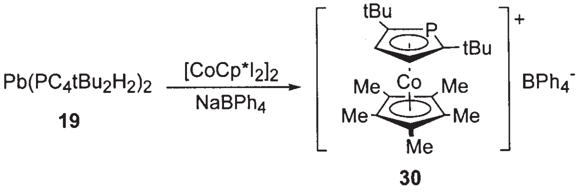

(24)

Electrochemical studies upon the colorless and air-stable 2,5-di(*tert*-butyl) phosphacobalticinium complex **30** show a reversible reduction wave at –0.73 V (compare [CoCpCp*], –1.17 V SCE, DMF [56]; [$CoCp^*_2$] –1.48 V THF [57]) and an irreversible second reduction at –1.85 V (THF). Chemical reduction of **30** can be achieved efficiently by stirring with magnesium; pentane extraction and vacuum sublimation (70 °C, 10^{-3} mmHg) give the purple air sensitive phosphacobaltocene **31** in yields of up to 75% (Eq. 25) [32]:

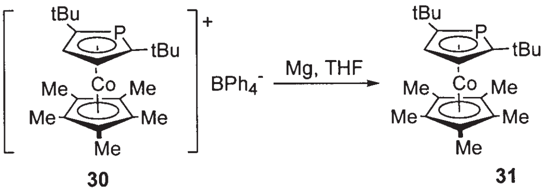

(25)

The solution magnetic moment of 1.69(10) BM at 298 K for **31** compares well with the values found in typical cobaltocenes [58] and the combination of high frequency Cp* with low-frequency phospholyl CH resonances in the ^1H nmr spectrum (δ Cp* = 42 ppm, CH –16 ppm, THF-D_8, 300 K) implies classical positive spin density on the ligands [59]. Two further observations, a reasonably sharp ^{31}P nmr signal (δ= –122 ppm, $\Delta\nu_{1/2}$ = 670 Hz [300 K, THF, H_3PO_4]) and a pronounced localization of the ring C-C bonds (C_α-C_β= 1.409(2), C_β-C_β'=

1.436(2) Å), suggest a SOMO node at phosphorus and a bonding C_α-C_β interaction. Thus, the unpaired electron probably resides in a hybrid incorporating the phospholyl $\pi_{(s)}$ orbital [32].

The alternative approach to phosphacobaltocenes employs the simple attack of a lithium phospholide upon a cobalt(II) precursor. This process is unlikely to work in the general case, but no redox chemistry or product evolution occurs for 2,5-di(*tert*-butyl)phospholides. Use of two phospholide equivalents gives a 1,1′-diphosphacobaltocene **32** which may be isolated by careful sublimation in high vacuum (Eq. 27). Room temperature ^1H nmr data indicate a structure where an intermeshing of the *t*-Bu groups provides a configurational lock, thus implying mixing of the $\pi_{(s)}$ and $\pi_{(as)}$ orbitals in the Co-ring bonds (^1H δ *t*-Bu = 5.5, 4.0 ppm, CH –23, –42 ppm, C_6D_6, 300 K). No ^{31}P nmr signal is observed at 300 K:

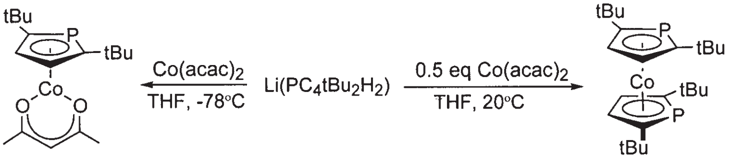

33 **32** (26)

Finally, the interaction of one equivalent of phospholide anion with [Co(acac)$_2$] at low temperature provides the orange air-sensitive paramagnetic half-sandwich complex [Co(acac)(PC$_4$*t*Bu$_2$H$_2$)] **33** (Eq. 27) [32]. This complex may be an important precursor for the [Co(PC$_4$tBu$_2$H$_2$)]$^+$ fragment.

Neutral rhodocenes are notoriously reactive and the first room-temperature stable example, octaphenylrhodocene, only appeared in 1995 [60]. Phospharhodicinium salts (e.g., **34**) are readily available, either through fragmentation of a triple decker complex [61] or more simply by metathesis of [RhCp*Cl$_2$]$_2$ with a suitable main group reagent such as plumbocene **19** (Eq. 27) [55]:

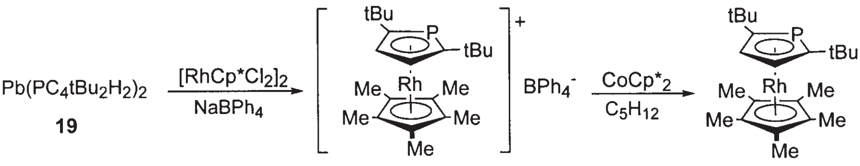

34 **35**

(27)

[RhCp*(PC$_4$*t*Bu$_2$H$_2$)]BPh$_4$ undergoes a reversible electrochemical reduction at –1.29 V (THF, SCE) and chemical reduction upon treatment with decamethylcobaltocene in pentane (Eq. 27). Sublimation (40 °C, 10^{-3} mmHg) and characterization by EI mass spectrometry and ^1H nmr spectroscopy (δ^1H Cp* = 81 ppm, CH = –49 ppm, THF-D_8, 300 K) confirm the formation of the olive green rhodocene **35** [62]. To date, no data concerning the reduction of phosphairidicinium cations [55] is available.

3.5
Group 10

Phosphanickelocenes proved the most elusive of the first-row transition metal phospholyl sandwiches and ring slippage to 18 VE compounds such as **36** and **37** has been observed in several studies [63–65].

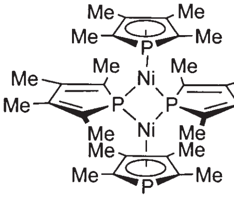

36

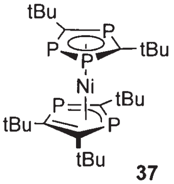

37

The first paramagnetic example was prepared only recently [32]. Deep green air-sensitive monophosphanickelocene **38** is obtained in yields of up to 80% through reaction of [Ni(acac)Cp*] [66] with [Li(THF)$_2$(PC$_4$tBu$_2$H$_2$)] in THF at –78 °C (Eq. 28):

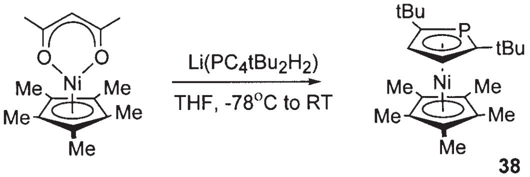

38

(28)

Solution magnetic susceptibility measurements (μ_{eff} = 2.78(10) BM, toluene 298 K) accord with the 20 VE formulation [58] and nmr data show resonances whose shifts imply positive ligand spin density (δ^1H Cp* = 263 ppm, CH = –181 ppm, THF-D$_8$, 300 K) [58]. As expected, given the presence of two SOMOs, no detectable ^{31}P nmr resonance is observed between ± 3000 ppm. A structural analysis shows no significant bond length alternation within the carbon backbone of the phospholyl ligand (C$_\alpha$-C$_\beta$=1.419(3); C$_\beta$-C$_\beta'$ = 1.419(4) Å) [32].

Electrochemically, oxidation of **38** occurs reversibly at 0.03 V (THF, SCE) and chemical oxidation with silver fluoroborate gives the corresponding orange air-sensitive 19 VE nickelocenium cation **39** (Eq. 29) [32]:

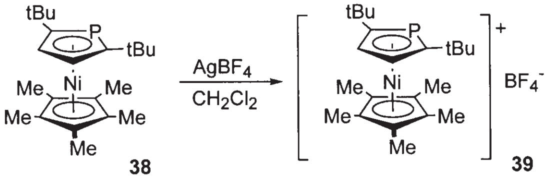

38 **39**

(29)

Spectroscopic (δ^1H Cp* = 109 ppm, CH –50 ppm, C$_6$D$_6$, 300 K) and structural data for **39** suggest strong similarities with the isoelectronic phosphacobaltocene **30**, with **39** showing a marked C-C bond length alternation in the solid state (C$_\alpha$-C$_\beta$ = 1.395(2), C$_\beta$-C$_\beta'$ = 1.443(2) Å) and a clearly discernable ^{31}P nmr resonance ($\delta = -188$ ppm, $\Delta\nu_{1/2} = 960$ Hz, 300 K, THF vs H_3PO_4). Again, these suggest a $\pi_{(s)}$ phospholyl contribution to the SOMO [32].

3.6
Conclusion

Whilst reliable data for paramagnetic phosphametallocenes have been available for a relatively short time, it already seems likely that a continuum of electronic properties may be conferred upon sandwich complexes by introducing phosphorus atoms into the ligands, prior to subsequent fine-tuning using the C-substituents. Green et al. have pointed out that the HOMO to LUMO energy gap decreases as the number of phosphorus atoms in the five-membered ring rises; this permits greater metal-to-ligand backbonding and favors, for instance, singlet spin states over triplets [40]. Unusual electronic configurations have already been found in $[Ti(P_3C_2tBu_2)_2]$ [40] and $[Mn(P_3C_2tBu_2)_2]$ [42] and this kind of carbon-to-phosphorus transposition may provide a means for modulating the electronic state existing at the metal center. The balance between 18 and 20 VE structures in phosphanickelocenes **37** and **38** seems to provide another example of this effect. Given the suggestion that the phosphorus lone pairs may also affect crystal packing within metallocene stacks [46], the intrinsic interest of paramagnetic phosphametallocenes seems to be obvious. The finer details concerning the precise role played by the bulky groups in some of these molecules, the means of manipulating the phospholyl molecular orbitals to allow spin to be placed either into $\pi_{(s)}$ or $\pi_{(as)}$, and the possibility of further coordination to the lone pair electrons, remain to be clarified.

4
Phosphametallocenes in Homogeneous Catalysis

Phosphametallocenes, e.g., phosphaferrocenes, have been known to give σ-complexes through their in-plane lone pairs almost since their discovery [66]. As discussed above, the phosphaferrocenes display three high-lying occupied MOs, mainly centered on the metal, and the P-lone pair only appears as HOMO-3 [47]. As a result, the lone pair is relatively unreactive and phosphaferrocenes behave as relatively weak σ-donors. The low-lying LUMO appears to be mainly localized at P and Fe. As P-ligands, phosphaferrocenes thus behave as good π-acceptors and more resemble phosphites than phosphines.

Three preliminary reports describe their use in non-enantioselective catalysis. Garrett and Fu have shown [67] that the monophosphaferrocene **40** is a good catalyst for the opening of epoxides by Me_3SiCl (Eq. 30):

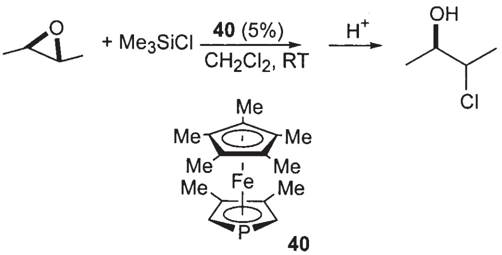

40

(30)

The proposed mechanism involves an adduct between **40** and Me_3SiCl. No ring opening is observed in the absence of catalyst. Complex **40** is less active but more regioselective with non-symmetrical epoxides than either PPh_3 or Bu_4NCl.

More recently, it has been demonstrated that octaethyl-1,1′-diphosphaferrocene **41** is able to give a stable bis-complex [Pd(**41**)$_2$] whose structure has been established by X-ray analysis [68]. In this complex, the two parallel lone pairs of one diphosphaferrocene are side-on coordinated to the tetrahedral Pd(0). The bis-chelate 18-electron [PdP_4] structure can probably equilibrate with the 14-electron [PdP_2] species in which one phosphorus atom of each diphosphaferrocene is axially coordinated to palladium and the other is free. Whatever, [Pd(**41**)$_2$] is a very robust catalyst for the Suzuki cross-coupling reaction. For example, $PhB(OH)_2$ and 4-bromoacetophenone are coupled at 110 °C by [Pd(**41**)$_2$] with a TON of 980,000.

Finally, BASF has issued a very recent patent describing, without detail, the potential use of phosphaferrocenes in the rhodium(I)-catalyzed hydroformylation of olefins [69].

In a different vein, Ganter introduced the concept that 2-functionalized phosphaferrocenes display a planar chirality which can be used beneficially in asymmetric catalysis [70]. A key step of his research program has been the chromatographic resolution of the two enantiomers of the 2-formyl derivative **42** via the corresponding aminals **43** [71]. On that basis, a series of enantiopure 3,4-dimethyl-1-phosphaferrocenes with chelating side-arms at the 2-position has been prepared [72, 73]. Side-arms are of the type $-(CH_2)_n$-Z with n = 1, 2 and Z = PR_2 and 2-pyridyl **44**. The 2-pyridyl derivatives give stable cationic chelates with Pd(II) [73]. Unfortunately, these catalysts give low ees (11–19%) for the reaction of 1,3-diphenylallyl acetate with sodium malonate.

Independently, Qiao and Fu have investigated the use of similar 2-functional 1-phosphaferrocenes with the more bulky (η^5-C_5Me_5)Fe subunit [74]. The higher steric hindrance leads to much better ees. The resolution was carried out by chiral HPLC of the intermediate alcohol **46.** In a first series of experiments, the Rh(I)-catalyzed enantioselective hydrogenation of dehydroaminoacid methyl esters was performed in ethanol at RT in the presence of enantiopure **45.** The ees fall in the range between 79 and 96% [74].

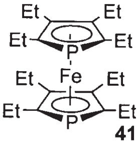

41

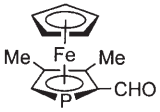

42

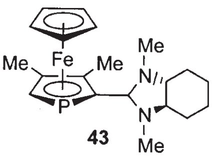

43

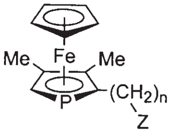

44

Z = PR_2, 2-pyridyl

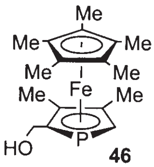

46

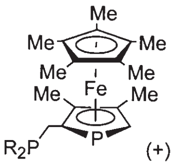

(+)-**45**

Even more significantly, Fu has recently designed the first effective asymmetric isomerization of non-protected allylic alcohols in 55 to 91% yields (Eq. 31) [75]:

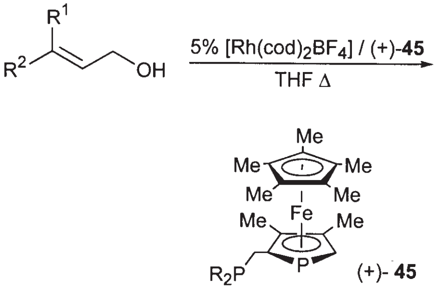

(31)

The observed ees are in the range 64–86%. *Z*-allylic alcohols isomerize with higher ees than the *E*-allylic counterparts. This process has been applied to the synthesis of two naturally-occurring sesquiterpenes. It is interesting to note here that the highest ee previously reported for such an isomerization (53%) employed an Rh$^+$/BINAP catalyst where a modest yield (47%) was also observed [76].

Subsequently, better ligands than **44** have been designed for the asymmetric palladium-catalyzed reaction of 1,3-diphenylallyl acetate with sodium malonate. Both the bis-(phosphaferrocene) **48** synthesized as shown in Eq. (32) [77] and the phosphaferrocene-oxazolines **49** [78] perform this condensation with much higher ees (79% in the first case and up to 82% in the second case). In the second case, the stereochemical outcome of the reaction is determined by the planar chirality at the phosphaferrocene, rather than the chirality of the oxazoline [78]:

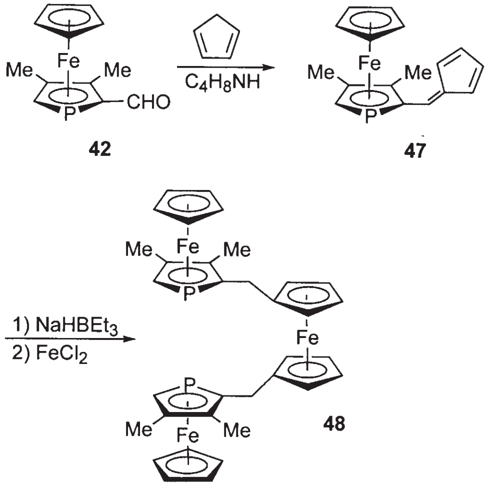

(32)

Instead of being viewed as P-ligands, phosphametallocenes can also be considered as modified metallocenes. It has been experimentally proven in a detailed

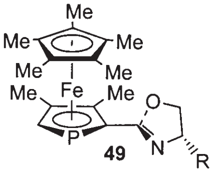

49

IR-Raman study of phosphacymantrenes that the phospholyl ring is an intrinsically poorer π-donor than cyclopentadienyl towards the manganese [79]. The prototype metallocene catalyst for the polymerization of olefins is a cationic species such as $[Cp_2ZrMe]^+$. It is generally formed by reaction of $[Cp_2ZrCl_2]$ with an alkylating agent. Replacing Cp by phospholyl tends to increase the electrophilicity of the metal and, hence, the activity of the catalyst. For this reason, η^5-phospholyl complexes of titanium and zirconium have attracted much interest as potential polymerization catalysts. However, these complexes have one drawback. In most cases, polymeric $[MeAlO]_n$ (MAO) serves as the cocatalyst. This Lewis acid, when in huge excess, tends to coordinate to the P-lone pairs of phosphazirconocene and titanocene derivatives, thus deactivating the metal center by steric hindrance. This effect has been well documented [80, 81]. Consequently, the best catalysts in the phosphametallocene family all have substituents at the α-positions in order to preclude the complexation of the P-lone pairs. Two representative catalyst precursors are the zirconium **50** [82] and the titanium **51** [83] derivatives.

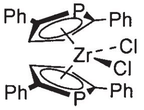

50

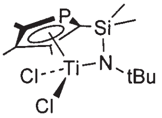

51

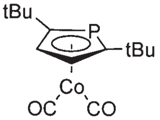

52

The diphosphazirconocene **50**+MAO system is a good catalyst for the polymerization of propene. With 10 µmol of Zr and 5 mmol of MAO at 45 °C under 600 kPa, an activity of 170 kg of polypropylene per gram of Zr per hour and an M_n of 20,000 have been observed [82].

The synthesis of complex **51** is described in Eq. (33) [83]:

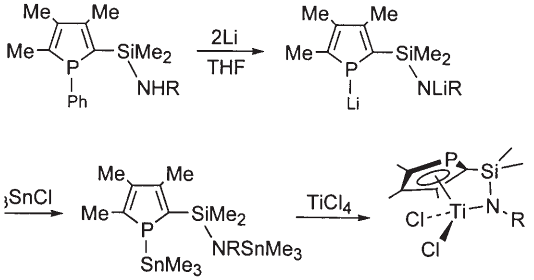

(33)

The system **51**+MAO polymerizes ethylene at 160 °C. It displays the same activity as its all-carbon analogue, but the final M_w of polyethylene is lower for the phosphametallocene catalyst: 50×10^3 vs 126×10^3.

Numerous patents have been issued on the use of phosphametallocenes in polymerization catalysis; for lists, see [82, 84]. In a different vein, it has been briefly stated that the η^5-phospholyl-cobalt complex **52** catalyzes the cyclotrimerization of EtC≡CEt to C_6Et_6 [15].

It is unclear at the moment whether the use of phospholyl in lieu of cyclopentadienyl in metallocene-based catalysts will bring advantages significant enough to justify the corresponding additional complexity and cost. On the contrary, it seems already quite clear that phosphametallocenes have a bright future in asymmetric catalysis.

Acknowledgements. Much of the unpublished work discussed here has been performed with great skill by Ms K Forissier and Ms S Wendicke. We also thank Dr L Ricard for crystal structure analyses and Drs P Le Floch and X Sava for discussions of unpublished data. Our work in this area is supported principally by CNRS and Ecole polytechnique, to whom we also express our thanks.

5
References

1. Mathey F, Fischer J, Nelson JH (1983) Struct Bond 55:153
2. Mathey F (1987) Nouv J Chim 11:585
3. Mathey F (1994) Coord Chem Rev 137:1
4. Dillon KB, Mathey F, Nixon JF (1998) Phosphorus: the carbon copy. Wiley, Chichester, p 294
5. Braye EH, Caplier I, Saussez R (1971) Tetrahedron 27:5523
6. Kilcast D, Thomson C (1971) Tetrahedron 27:5705
7. Charrier C, Mathey F (1987) Tetrahedron Lett 28:5025
8. Douglas T, Theopold KH (1989) Angew Chem Int Ed Engl 28:1367
9. Espinosa-Ferao A, Deschamps B, Mathey F (1993) Bull Soc Chim Fr 130:695
10. Holand S, Jeanjean M, Mathey F (1997) Angew Chem Int Ed Engl 36:98
11. Westerhausen M, Digeser MH, Nöth H, Ponikwar W, Seifert T, Polborn K (1999) Inorg Chem 38:3207
12. Chesnut DB, Quin LD (1994) J Am Chem Soc 116:9638
13. Goldfuss B, Schleyer PR, Hampel F (1996) Organometallics 15:1755
14. Charrier C, Bonnard H, Mathey F, Neibecker D (1982) J Organomet Chem 231:361
15. Caffyn AJM, Carmichael D, Mathey F, Ricard L (1997) Organometallics 16:2049
16. Nief F, Mathey F (1988) Chem Commun 770
17. Forissier K, Ricard L, Carmichael D, Mathey F (1999) Chem Commun 1273
18. Appel R (1990) Phosphaalkenes, phosphacarbaoligoenes and phosphaallenes. In: Scherer OJ, Regitz M (eds) Multiple bonds and low coordination in phosphorus chemistry. Thieme Verlag, Stuttgart New York
19. Paul F, Carmichael D, Ricard L, Mathey F (1996) Angew Chem Int Ed Engl 35:1125
20. Laporte F, Mercier F, Ricard L, Mathey F (1994) J Am Chem Soc 116:3306
21. Gosink H-J, Nief F, Ricard, Mathey F (1995) Inorg Chem 34:1306
22. Westerhausen M, Digeser MH, Nöth H, Seifert T, Pfitzner A (1998) J Am Chem Soc 120:6722
23. Dransfeld A, Nyulászi L, Schleyer PR (1999) Inorg Chem 37:4413
24. Jutzi P (1990) J Organomet Chem 400:1
25. Becker G, Schmidt H, Uhl G, Uhl W (1990) Inorg Synth 27:243
26. Westerhausen M, Digeser MH, Gückel C, Nöth H, Knizek J, Ponikwar W (1999) Organometallics 18:2491
27. Douglas T, Theopold KH, Haggerty BS, Rheingold AL (1990) Polyhedron 9:329

28. Schnepf A, Stößer G, Carmichael D, Mathey F, Schnöckel H 1999 Angew Chem Int Ed Engl 38:1646
29. Chojnacki J, Baum E, Krossing I, Carmichael D, Mathey F, Schnöckel H (2001) Z Anorg Allg Chem 627:1209
30. Jutzi P, Burford N (1999) Chem Rev 99:969 and references cited therein
31. Burkey D, Hanusa TP (1995) Organometallics 14:11
32. Forissier K, Ricard L, Carmichael D, Mathey F (1999) (unpublished)
33. Lemoine P, Gross M, Braunstein P, Mathey F, Deschamps B, Nelson JH (1984) Organometallics 3:1303
34. Lemoine P, Gross M, Braunstein P, Mathey F, Deschamps B (1986) J Organomet Chem 295:189
35. Román E, Leiva AM, Casasempere MA, Charrier C, Mathey F, Garland MT, Le Marouille J-Y (1986) J Organomet Chem 309:323
36. Roberts RMG, Silver J, Wells AS (1986) Inorg Chim Acta 126:61
37. Bartsch R, Hitchcock PB, Nixon JF (1988) J Organomet Chem 356:C1
38. Arnold PA, Cloke FGN, Nixon JF (1998) Chem Commun 797. This complex forms an asymmetric dimer in the solid state. Nixon JF personal communication
39. Cloke FGN, Hanks JR, Hitchcock PB, Nixon JF (1999) Chem Commun 1731
40. Cloke FGN, Green JC, Hanks JR, Nixon JF, Suter JL (2000) J Chem Soc Dalton Trans 3534
41. Cloke FGN, Flower KR, Hitchcock PB, Nixon JF (1995) Chem Commun 1659
42. Clark T, Elvers A, Heinemann FW, Hennemann M, Zeller M, Zenneck U (2000) Angew Chem Int Ed Engl 39:2807
43. Elvers A, Heinemann FW, Kummer S, Wrackmeyer B, Zeller M, Zenneck U (1999) Phosphorus Sulfur Silicon Relat Elem 144(6):725
44. Quin LD (1996) In: Katrizky AR, Rees CW, Scriven EFW (eds) Compr Heterocycl Chem II 2:757
45. Feher R, Köhler FH, Nief F, Ricard L, Rossmayer S (1997) Organometallics 16:4606
46. Hitchcock PB, Lawless GA, Marziano I (1997) J Organomet Chem 527:305
47. Kostic NM, Fenske RF (1983) Organometallics 2:1008
48. Sava X (2000) PhD thesis, Ecole Polytechnique, France
49. Ashe AJ III, Al Ahmad S, Pilotek S, Puranik DB, Elschenbroich C, Behrendt A (1995) Organometallics 14:2689
50. Waluk J, Klein H-P, Ashe AJ III, Michl J (1989) Organometallics 8:2804
51. Prins R (1970) Mol Phys 19:603
52. Atwood DA, Cowley AH, Dennis SM (1993) Inorg Chem 32:1527
53. Roberts RMG, Silver J, Wells AS (1986) Inorg Chim Acta 119:165
54. Birchall I, Drummond T (1971) Inorg Chem 10:399
55. Forissier K, Ricard L, Carmichael D, Mathey F (2000) Organometallics 19:954
56. Gloaguen B, Astruc D (1990) J Am Chem Soc 112:4607
57. Kölle U, Klaeui WL (1991) Z Naturforsch Teil B 46B:75
58. For example, Robbins JC, Edelstein N, Spencer B, Smart JC (1982) J Am Chem Soc 104:1882
59. Blümel J, Hebendanz N, Hudeczek P, Köhler FH, Strauss W (1992) J Am Chem Soc 114:4223
60. Collins JE, Castellani MP, Rheingold AL, Miller EJ, Geiger WE, Rieger AL, Rieger PH (1995) Organometallics 14:1232
61. Herberich G, Ganter B (2001) Inorg Chem Commun 4:100
62. Wendicke S, Forissier K, Carmichael D, Mathey F (2000) (unpublished)
63. Arliguie T, Ephritikhine M, Lance M, Nierlich M (1996) J Organometallic Chem 524:239
64. Cloke FGN, Flower KR, Jones C, Matos RM, Nixon JF (1995) J Organomet Chem 487:C21
65. Bartsch R, Hitchcock PB, Nixon JF (1989) J Organomet Chem 373:C17
66. Mathey F (1986) J Organomet Chem 154:C13
67. Garrett CE, Fu GC (1997) J Org Chem 62:4534
68. Sava X, Ricard L, Mathey F, Le Floch P (2000) Organometallics 19:4899

69. Ahlers W, Mackewitz T, Roeper M, Mathey F, Ganter C, Breit B (BASF) Ger Offen DE 19 921 730 (2000) Chem Abstr 133:349,964b
70. Ganter C, Brassat L, Glinsböckel C, Ganter B (1997) Organometallics 16:2862
71. Ganter C, Brassat L, Ganter B (1997) Tetrahedron: Asymmetry 8:2607
72. Ganter C, Brassat L, Ganter B (1997) Chem Ber/Recueil 130:1771
73. Ganter C, Glinsböckel C, Ganter B (1998) Eur J Inorg Chem 1163
74. Qiao S, Fu GC (1998) J Org Chem 63:4168
75. Tanaka K, Qiao S, Tobisu M, Lo MM-C, Fu GC (2000) J Am Chem Soc 122:9870
76. Tani K (1985) Pure Appl Chem 57:1845
77. Ganter C, Kaulen C, Englert U (1999) Organometallics 18:5444
78. Shintani R, Lo MM-C, Fu GC (2000) Org Lett 2:3695
79. Poizat O, Sourisseau C (1981) J Organomet Chem 213:461
80. Janiak C, Versteeg U, Lange KCH, Weimann R, Hahn E (1995) J Organomet Chem 501:219
81. Janiak C, Lange KCH, Versteeg E, Lentz D, Budzelaar PHM (1996) Chem Ber 129:1517
82. de Boer EJM, Gilmore IJ, Korndorffer FM, Horton AD, Van der Linden A, Royan BW, Ruisch BJ, Schoon L, Shaw RW (1998) J Mol Catal A 128:155
83. Brown SJ, Gao X, Harrison DG, Koch L, Spence REH, Yap GPA (1998) Organometallics 17:5445
84. Sone M, Yoshida O, Sato M (2000) (Tosoh) JP 2000 273 114 Chem Abstr 133:252,873h

Benzyne-Zirconocene Reagents as Tools in Phosphorus Chemistry

Jean-Pierre Majoral[1], Alain Igau[1], Victor Cadierno[1], Maria Zablocka[2]

[1] Laboratoire de Chimie de Coordination CNRS, 205 route de Narbonne, 31077 Toulouse Cedex 04, France. *E-mail: majoral@lcc-toulouse.fr*

[2] Centre of Molecular and Macromolecular Studies, Polish Academy of Sciences, Sienkiewicza 112, 90–363, Lodz, Poland

The use of η^2-benzyne and η^2-phosphabenzyne zirconocene in phosphorus chemistry is reviewed. The regiospecific reactions of these complexes with small unsaturated organic molecules incorporating phosphorus or not led to a variety of cyclic neutral or zwitterionic complexes showing a versatile behavior. New methodologies of synthesis of phosphorus heterocycles and of phosphorus ligands are described, as well as strategies of C-H and M-H (M=N, O, P, S) bond activations.

Keywords. η^2-Benzyne-zirconocene, η^2-Phosphabenzyne-zirconocene, α-Zirconated phosphines, Phosphorus heterocycles, Zwitterionic [phosphonium anionic zirconocene (IV)] complexes

Topics in Current Chemistry, Vol. 220

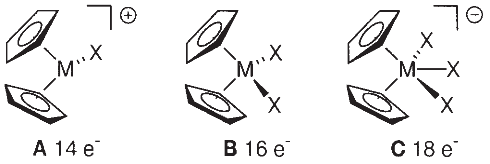

Fig. 1. Group 4 d^0-metallocene complexes Cp_2MX_n (**A** n=1, **B** n=2, **C** n=3)

1
Introduction

d^0-Bis(cyclopentadienyl)zirconocene complexes Cp_2ZrX_n (**A**, n = 1, **B**, n = 2, **C**, n = 3) with metal-ligand M-X bonds exhibit metal centers with 14, 16, and 18 electrons and valence coordination number from 3 to 5 (Fig. 1). During the last 20 years, bent cationic bis(cyclopentadienyl) complexes **A** have received considerable attention as those compounds have been identified as the active catalytic species in the homogeneous metallocene Ziegler-Natta process for the polymerization of olefins [1, 2]. The chemistry of **B** complexes has been extensively explored and has allowed the development of a rich chemistry based on interactions with organic reagents. The success of organo zirconium reagents **B** in synthesis can be explained in terms of chemo-, regio-, diastereo-, and enantioselectivity: these compounds are generally able to discriminate between similar functionalities that differ only slightly in their steric and/or electronic environment [3–5]. Anionic metallocene complexes **C** are postulated as intermediates in a number of stoichiometric and catalytic reactions and a very few of these metal **C** species have been spectroscopically and structurally characterized [6].

In the past decade, reports on the interactions between main group elements, including phosphorus derivatives, and zirconium species such as $[Cp_2ZrHCl]_n$ [7], Cp_2ZrMe_2 [8], $[Cp_2Zr]$ [9, 10], or others [11, 12] have appeared in the literature. The present review is focused on the use of η^2-benzyne-zirconocene and the parent η^2-phosphabenzyne-zirconocene in phosphorus chemistry. The versatile behavior of these complexes towards unsaturated phosphorus reagents and the versatile behavior of the resulting products will be more precisely reported.

2
η^2-Benzyne-Zirconocene in Phosphorus Chemistry

Photolysis or thermolysis of diarylzirconocenes or arylalkylzirconocenes lead to reactive aryne-zirconocene complexes which can be trapped with several types of electron-donating ligands including dienes, phosphines, and carbon monoxide [13–15]. After being postulated by Vol'pin et al. [14] and Erker [13], benzyne-zirconocene **1** (Eq. 1) was fully characterized by Buchwald et al. [16] by X-ray crystallographic studies of its trimethylphosphine complex adduct:

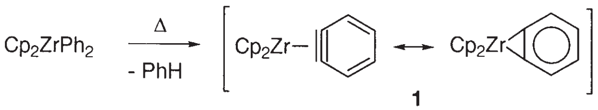

1

(1)

Equation (1). Generation of η^2-benzyne zirconocene

2.1
Reactions with Phospha-Imines

Thermolysis of $Cp_2ZrMePh$ or $(t\text{-}BuCp)_2ZrPh_2$ generates benzyne-zirconocene intermediates which in the presence of phospha-imines **2** afford azaphosphazirconaindenes **3** in a regiospecific way (Eq. 2) [17]:

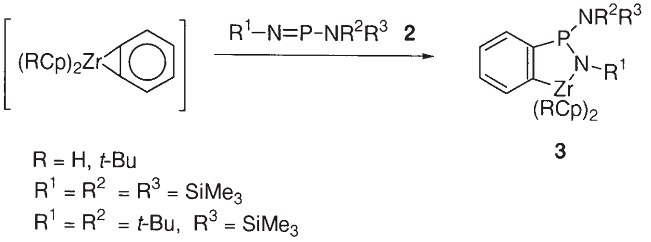

3

(2)

Equation (2). Insertion of phospha-imines into a Zr-C bond of η^2-benzyne zirconocene

2.2
Insertion of 2,3-Dihydrophosphole

There is an extensive literature on the topic of cyclic phosphines such as phospholanes, phospholenes, or phospholes [18]. In contrast only a limited number of fused bicyclic and tricyclic phosphines have been prepared and fused tricyclic systems incorporating two phosphorus atoms or phosphorus and other heavier main group elements remained unknown till the last five years.

A clean insertion reaction of the 2,3-dihydrophosphole **4** into the zirconium-carbon bond of the transient benzyne-zirconocene **1** occurs when **4** is heated with Cp_2ZrPh_2 at 80 °C for 6 h, leading to the tricyclic compound **5** (Scheme 1). The regioselective formation of **5** can be regarded as the result of a strong interaction between the phosphorus lone pair and zirconium. It can be noted that under the same experimental conditions, the corresponding oxide **4′** or the 3,4-dihydrophosphole **4″** do not react with **1**.

An exchange reaction involving **5** and various dichlorophosphines readily occurs at room temperature affording the tricyclic 1,1-diphosphines **6** [19] isolated as their disulfides adducts **7**. A *trans* arrangement of the lone pair of the two phosphorus atoms was shown for **6** (R = *t*-Bu) on the basis of the single crystal X-ray analysis of the corresponding disulfide. An analogous exchange reaction performed with $PhSbCl_2$ or Me_2SnCl_2 gives stiba- or tin-phosphorus-containing tricyclic systems **8** or **9** in high yield.

Remarkably the regioselectivity of the reaction of 2,3-dihydrophosphole **4** with a more hindered benzyne-zirconocene precursor as $(\eta^5\text{-}t\text{-}BuC_5H_4)_2ZrPh_2$ was found to be the same: the zirconaindene-phospholane **10** was formed quantitatively and no trace of **11** was detected (Scheme 2).

All the exchange reactions proceed with ring retention. This is not the case when the reactions are performed with monochlorophosphines instead of dichlorophosphines. A concomitant ring opening reaction with the exchange

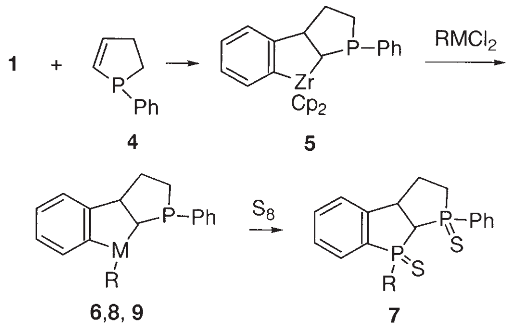

6, **7** M = P, R = Me, Ph, *t*-Bu, N-*i*-Pr_2
8 M = Sb, R = Ph
9 M = Sn, R = Me

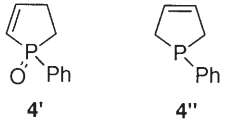

Scheme 1. Regioselective preparation of tricyclic 1,1-diphosphines from 2,3-dihydrophosphole **4** and η^2-benzyne zirconocene

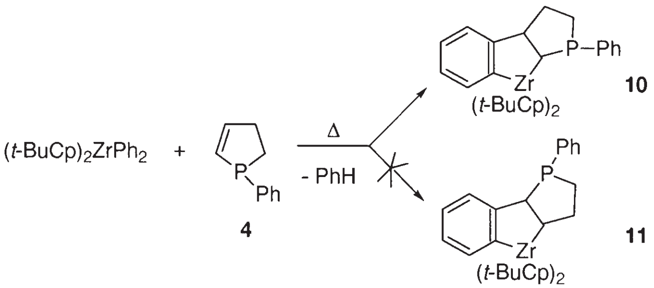

Scheme 2. Regioselective formation of the zirconaindene-phospholane **10**

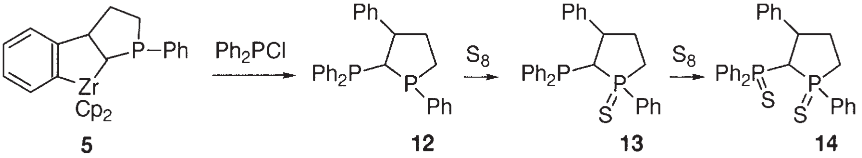

Scheme 3. Synthesis of 1,1-diphosphines and their sulfur adducts from the zirconaindane-phospholane **5**

reaction takes place when the tricyclic system **5** is reacted with Ph_2PCl. The 1,1-diphosphine **12** is obtained as two isomers in a 4:1 ratio. Monosulfurization occurs regioselectively on the intracyclic phosphorus atom. Further addition of sulfur leads to the formation of the corresponding disulfide **14** (Scheme 3) [19].

2.3
Insertion of Alkynes

2.3.1
Synthesis of 2-Phosphinophospholes

An efficient stereoselective synthesis of substituted zirconaindene compounds and their use as starting reagents for the formation of 2-phosphinophospholes was recently proposed [20]. It consists of the treatment of Cp_2ZrPh_2 with the alkynylphosphine **15a** in benzene at 80 °C for 6 h. The 2-phosphino-zirconaindene **16a** thus obtained is further reacted with phenyldichlorophosphine to give the 2-phosphinophosphole **17a** (Scheme 4). Such a stereoselective preparation of 2-phosphinophosphole was also observed with a non-terminal acetylenic phosphine such as **15b** and a more hindered diphenylzirconocene such as $(\eta^5\text{-}t\text{-}BuC_5H_4)_2ZrPh_2$. A similar exchange reaction from **16a** and dichlorostilbene led to the formation of the corresponding 2-phosphinostibole **18**.

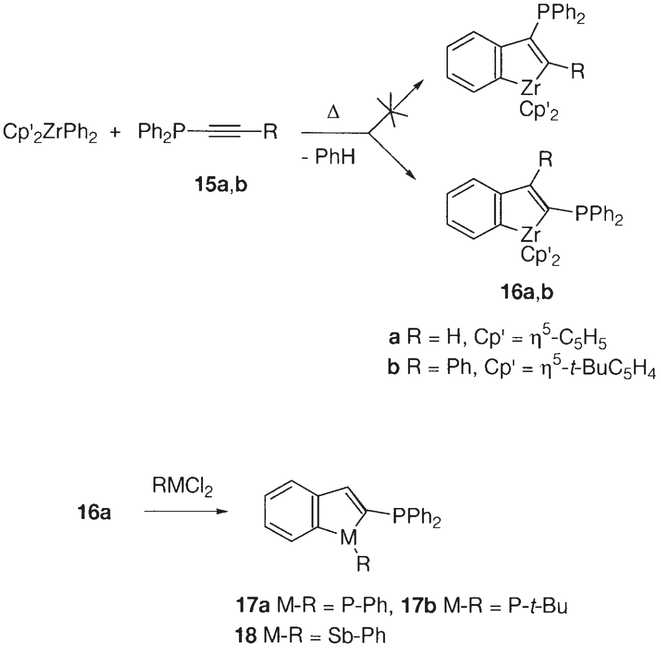

a R = H, Cp' = η^5-C_5H_5
b R = Ph, Cp' = η^5-t-BuC_5H_4

17a M-R = P-Ph, **17b** M-R = P-*t*-Bu
18 M-R = Sb-Ph

Scheme 4. Synthesis of 2-phosphino phospholes **17a,b** or stibole **18**

Addition of S_8 to **16b** gave the sulfide **19** (Eq. 3). X-ray structure analysis of **19** revealed an interaction between zirconium and sulfur: the P-S bond length was found to be slightly longer (2.005(1) Å) than those generally observed for thiophosphoryl groups (1.93–1.95 Å). Indeed the P-S bond length lies in between those of a single and a double bond, suggesting a zwitterionic character for **19** which can be formally considered as a zirconocene-ate zwitterionic complex:

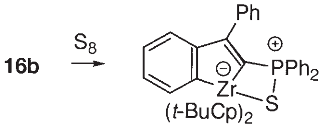

19

(3)

Equation (3). Addition of S_8 on the 2-phosphino-zirconaindene **16b**

2.3.2
[3+2] Cycloadditions Involving 2-Phosphino-Zirconaindenes

As already mentioned in the introduction, anionic early transition metallocene complexes of the type $[Cp_2Zr(R_1)(R_2)(R_3)]$ with R_1, R_2, R_3 = alkyl, alkenyl, or alkynyl, are unstable. Most of them exhibit electrostatic anion-cation pairing resulting in dimer, trimer, oligomer, or polymeric structures [21–25]. In marked contrast, stable 18 electron-zirconate complexes were prepared via a formal [3+2] cycloaddition reaction between 2-phosphino-zirconaindene **16a** and alkyne derivatives (Scheme 5) [26, 27].

X-ray diffraction data obtained for some of those ate complexes are consistent with a zwitterionic form incorporating a four coordinate cyclic phosphonium center and a pentavalent 18-electron zirconium metal center. It is reasonable to postulate that the first step of the reaction is the nucleophilic attack of the phosphino group in **16a** on an acetylenic carbon atom with formation of the corresponding transient zwitterion. In the second step, an intramolecular cyclization of the carbanionic center on the zirconium metal fragment occurs to form stable zirconate products **20a–f**. It was shown that the nature of the het-

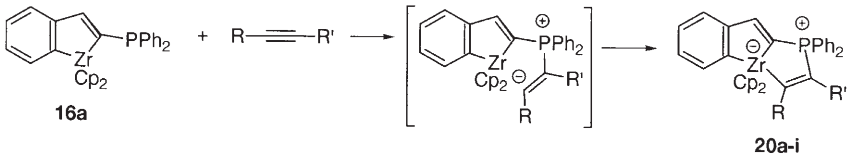

a R = R' = CO_2Me
b R = CO_2Me, R' = H
c R = C(O)Me, R' = H
d R = H, R' = OEt
e R = PPh_2, R' = H
f R = $P(S)Ph_2$, R' = H
g R = H, R' = CH_2OMe
h R = H, R' = CH_2OCH_2CCH
i R = H, R' = CH_2NMe_2

Scheme 5. [3+2] cycloadditions involving α-zirconated phosphines and alkynes eroelement directly bonded to the triple bond of the terminal acetylenic system directs the nucleophilic attack of the phosphine [27]. In all cases, only one regioisomer is observed. Surprisingly, the nucleophilic attack of the phosphine in **16a** occurs on propargyl derivatives to give the corresponding zwitterionic zirconate complexes **20g–i**.

Similar reactions were conducted with **16a** and various aldehydes [28]. It can be emphasized that the [3+2] cycloaddition reactions take place selectively on the carbonyl group allowing therefore the preparation of diversely functionalized zwitterionic zirconocene complexes such as compounds **21a–e** possessing either a free phosphino group (**21b**) or free alkenyl group (**21c–e**) (Eq. 4):

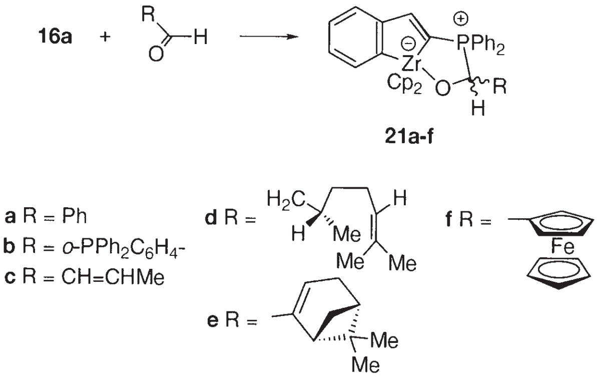

(4)

Equation (4). [3+2] cycloaddition involving the 2-phosphino-zirconaindene **16a** and aldehydes

The ability of **16a** to react with polyaldehydes was also investigated: the same strategy was used to graft on the surface of dendrimers of generation 4 (**22-G$_4$**) and of generation 8 (**22-G$_8$**) respectively 48 and 768 anionic zirconocene moieties (Scheme 6).

Moreover, a controlled number of anionic zirconocene units can be selectively introduced into the internal layers of a polydendritic macromolecule. The reaction of the multidendritic system **24-G$_3$G$_2$**, constituted by a central dendrimer of generation 3 and by six internal dendrimers of generation 2 possessing 24 internal aldehyde groups, with **16a** (excess) clearly leads to the polyzwitterionic zirconocene polydendritic structure **25-G$_3$G$_2$** in which all the early transition metal anions are located within the cascade structure (Scheme 6).

Other zwitterionic 18-electron d^0-anionic metallocene complexes **26–29** with one Zr-heteroelement σ-bond can be prepared following the same strategy. This implies the treatment of **16a** with an equimolecular amount of heterocumulenes (CO_2, CS_2, Cy-N=C=N-Cy, R-N=C=S, R-N=C=O) (Scheme 7) [29]. It is also reasonable to propose here that the formation of all these new systems is due first to a nucleophilic attack of the free phosphine of **16a** at the electrophilic center of the organic substrate. In the second step, cyclization reaction on the coordinatively unsaturated metal center occurs to form the stable pentavalent anionic zirconocene products. With isocyanates and isothiocyanates, the anionic charge

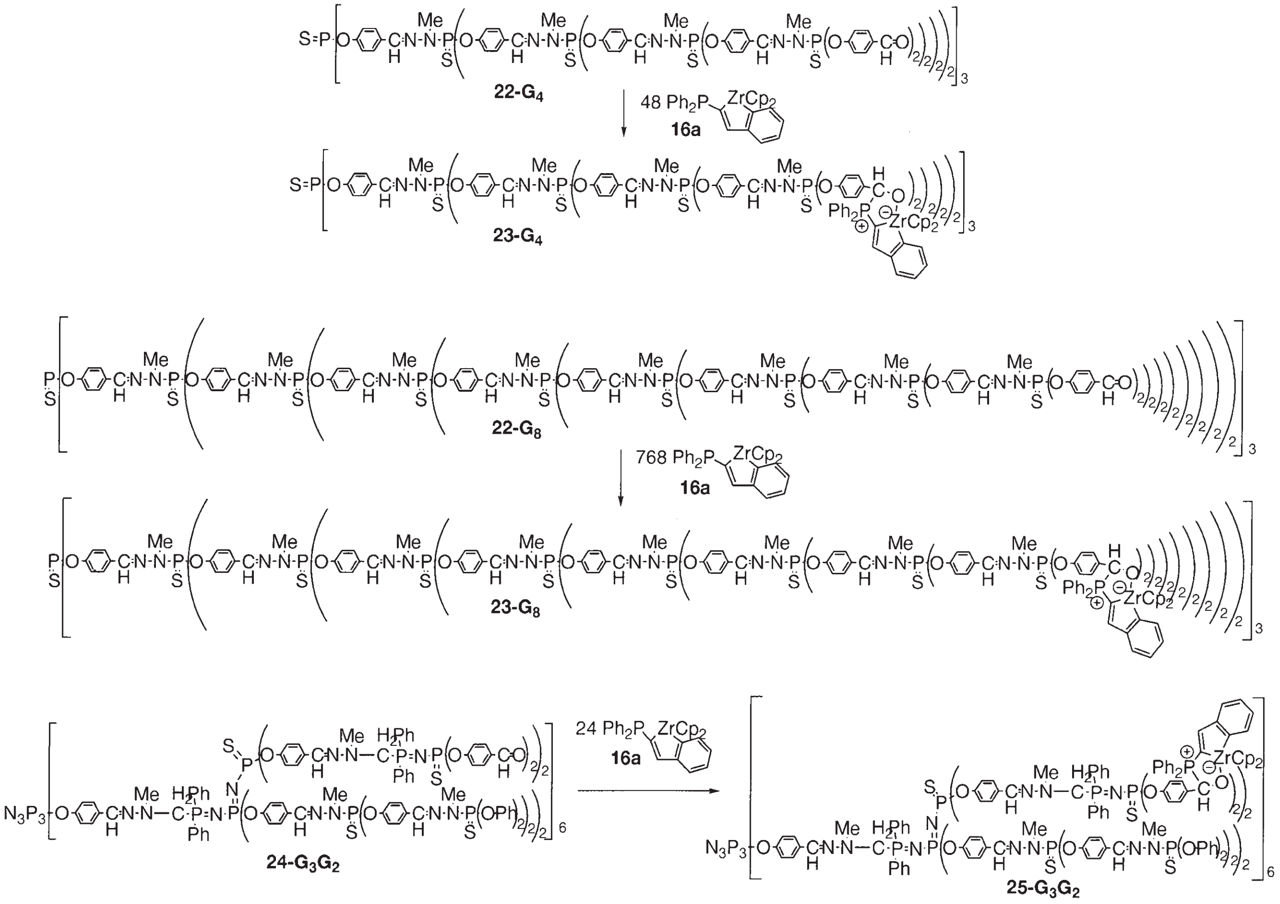

Scheme 6. Multiple [3+2] cycloadditions involving the α-zirconated phosphine **16a** and dendrimers with terminal or internal aldehyde groups

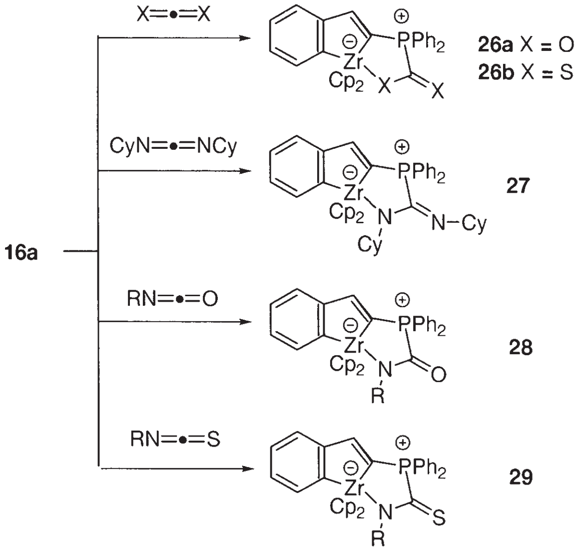

Scheme 7. [3+2] cycloadditions involving the α-zirconated phosphine **16a** and heterocumulenes

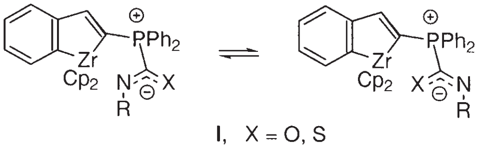

Fig. 2. Delocalization of the anionic charge in transient zwitterionic species **I**

is delocalized over the carbonyl skeleton in **I**, but the preferred coordination site in these systems is the nitrogen atom (Fig. 2). The η^1-bonding mode of the carbamoyl group in complexes **28** and **29** is very strong since no competition between nitrogen and oxygen or between nitrogen and sulfur was observed neither in the solid state, nor in solution.

This methodology of chemo- and regioselective cycloaddition for the synthesis of stable anionic zirconocene complexes can be extended to other phosphorus metallocenes. As an example, addition of phenylisothiocyanate to **5** led to the expected complex **30**. However, the same reaction performed with **5** and carbon disulfide afforded unique "dimeric" species **31** arising from successive (or concomitant) cycloaddition reactions on the two carbon sulfur double bonds of CS_2 (Scheme 8).

2.3.3
[3+1] Cycloadditions Involving 2-Phosphino-Zirconaindenes

The Staudinger reaction of azides with tertiary phosphines is one of the two major routes in the preparation of iminophosphoranes [30]. This reaction proceeds

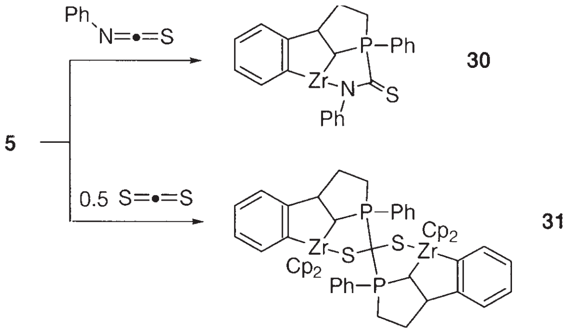

Scheme 8. [3+2] cycloadditions involving the tricyclic phosphine **5** and heterocumulenes

by nucleophilic attack of the phosphine on the terminal α-nitrogen atom of the azide to afford a linear phosphazide, rarely stable [31], which then dissociates to the iminophosphorane with elimination of nitrogen. Iminophosphoranes form complexes with a variety of metals by N-imino complexation (covalent or dative bond) [30].

In marked contrast, only a few phosphazide complexes have been prepared [32–34]. The unique seven-coordinate complex [WBr$_2$(CO)$_3$(Ar-N=N-=PPh$_3$)] **32** was characterized by X-ray diffraction studies: the phosphazide ligand is bounded to the tungsten metal fragment in a bidentate fashion through the α- and γ-nitrogen atoms [33]. More recently, the cyclic (Z)-phosphazide **33** was found to act as a monodentate two-electron donor through the less sterically hindered β-nitrogen atom [34] (Fig. 3).

A formal [3 + 1] cycloaddition is observed when 4-fluoro-3-nitrophenyl azide is reacted with **16a** with the formation of the phosphazide complex **34** [31]. Intramolecular donor-acceptor interactions only occur with the α-nitrogen atom which suggests that this nitrogen atom is a better donor than Nγ and that the polarization of the phosphazide moiety is more correctly represented as -P$^+$-N$^-$-N=N-R rather than -P$^+$-N=N-N$^-$-R, at least for the structure reported here. Complex **34** is stable at room temperature and slowly decomposed with loss of dinitrogen in refluxing toluene to give a new complex **35** in which the Nγ is linked both to zirconium and phosphorus. Analogous complexes **36** and **37** are directly isolated through the addition of $N_3P(O)(OPh)_2$ and N_3SiMe_3 on **16a**; transient formation of the phosphazide compound was not detected in these

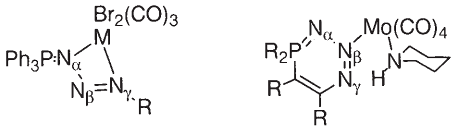

32 M = W or Mo

33

Fig. 3. Phosphazide complexes involving α and γ nitrogen complexation (**32**) or β nitrogen complexation (**33**)

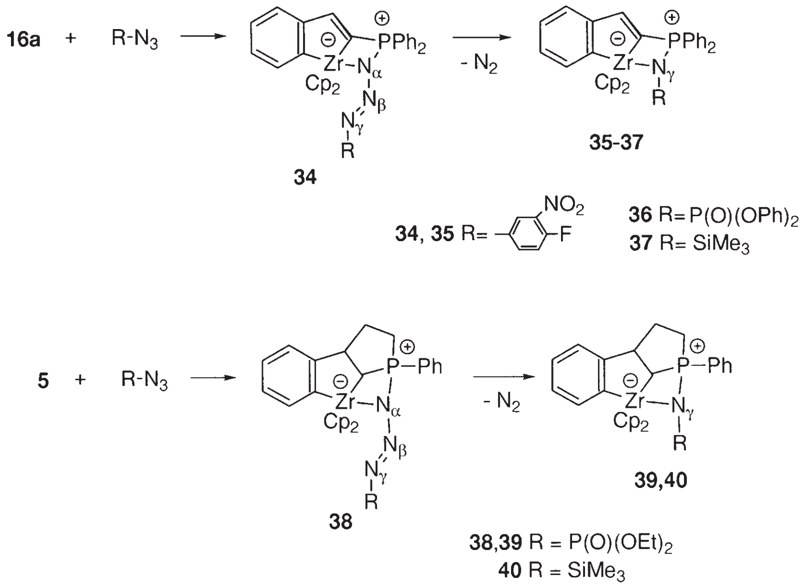

Scheme 9. [3+1] cycloadditions involving mono- and tricyclic-α-zirconated phosphines **16a** and **5** with azides

cases (Scheme 9). Such a formal [3+1] cycloaddition can be extended to the tricyclic system **5** to give the zwitterionic complexes **39** and **40** after addition of RN_3 ($R=P(O)OEt)_2$, $SiMe_3$).

Interestingly, no difference in the reactivity between the azido and the aldehyde groups of 4-azido tetrafluorobenzaldehyde is detected when this bifunctional reagent is reacted with **16a**: the expected [1+3] and [2+3] cycloadditions occurred concomitantly, even when stoichiometric conditions are used (Scheme 10). When the resulting complex **41** is heated in refluxing toluene, dinitrogen is liberated and adduct **42** is formed. A similar reactivity was observed when **16a** is treated with 4-azidophenylisocyanate with formation of complexes **43** and **44**. Reactions performed with **5** instead of **16a** (and with 4-azidotetrafluorobenzaldehyde or with 4-azidophenylisothiocyanate) allowed one to isolate the stable bis(zwitterionic) complexes **45** and **46**. Contrary to what was observed with the other phosphazide complexes, **45** and **46** do not lose dinitrogen cleanly when refluxed in toluene (Scheme 11).

2.3.4
Reactions of 2-Phosphino-Zirconaindenes with Isocyanides

Intramolecular coupling reactions of group 4 imino-acyl complexes yielding the corresponding free imines are rather rare and mainly involve titanium complexes [35–38]. The mechanism of these reactions still remains unclear although a concerted reductive elimination step, that initially leads to an η^1-imine intermediate complex of the type **II**, has already been postulated [35] (Fig. 4).

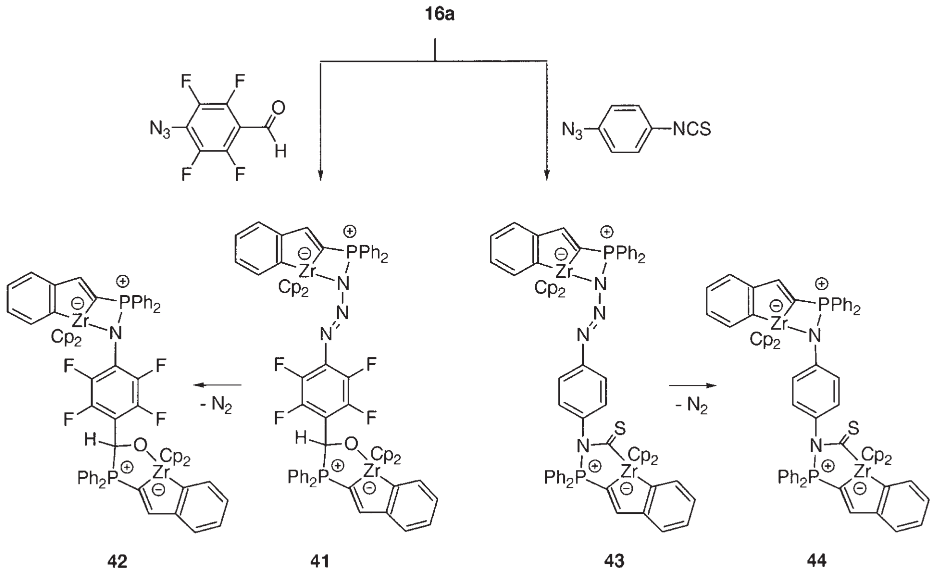

Scheme 10. [3+1] and [3+2] cycloadditions involving the α-zirconated phosphine **16a** and a 4-azidotetrafluorobenzaldehyde or 4-azidophenylisocyanate

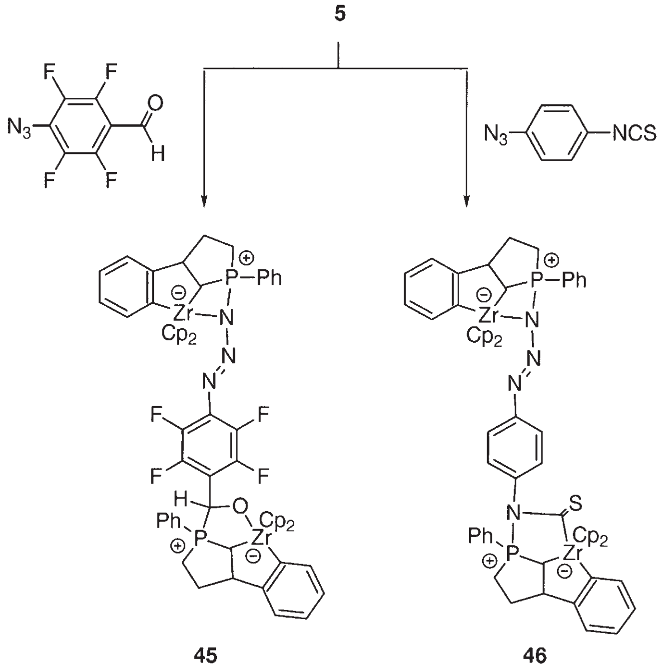

Scheme 11. [3+1] and [3+2] cycloadditions involving the tricyclic-α-zirconated phosphine **5** and 4-azidotetrafluorobenzaldehyde or 4-azidophenylisocyanate

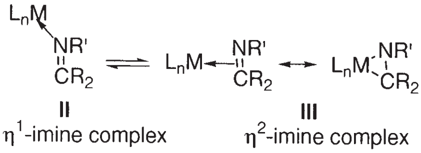

Fig. 4. η^1- and η^2-imine complexes

However, none of the previous reports described isolation and characterization of η^1-imine zirconocene complexes. Addition of isocyanides on organozirconocenes is known to give the corresponding iminoacyl complexes after insertion into a zirconium-carbon bond [5, 39–41]. These compounds have been conveniently converted for example to aldehyde [5, 39] or nitriles [42].

A powerful one pot synthesis of new bi- or tricyclic-β-phosphino-imines from **16a** and **5** and isocyanides was recently reported [43]. The process involves three successive and controlled steps: (i) a regioselective Zr-C isocyanide insertion reaction giving **47** followed by (ii) a carbon-carbon coupling reaction to form a neutral η^1-imine zirconocene complex **48** and (iii) subsequent reductive elimination of zirconocene fragment Cp_2Zr to give the corresponding β-phosphino-imines **49** (or **52** in the case of **5** as starting material). The phosphino group located in the close environment of the metal plays a key role in the course of the metal center displacement step. Therefore, this reductive elimination process extends the scope of the zirconocene-induced coupling reactions. Interestingly, addition of two equivalents of HCl on the η^1-imine complex **48** gave an access to β-aminophosphines **51** (Scheme 12).

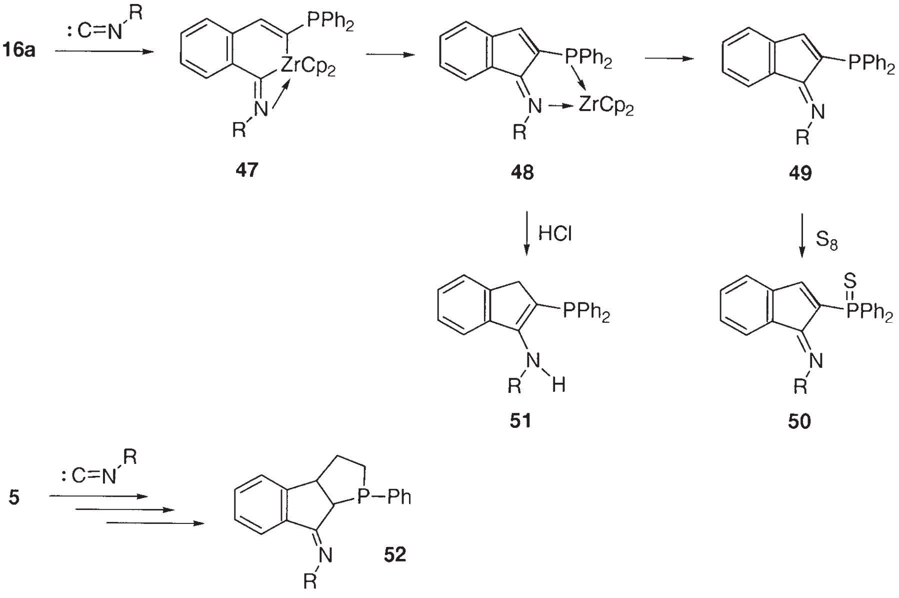

Scheme 12. Synthesis of bi- or tri-cyclic iminophosphines **49**, **52**, and the β-aminophosphine **51**

2.4
Insertion of Nitriles

Thermolysis of diphenylzirconocene in the presence of a wide variety of nitriles has previously been shown to generate azazirconacyclopentenes as dimers in the solid state in good to excellent yields [44]. A similar reaction undertaken with bis amino-cyanophosphines gives rise to new azazirconacyclopentenes **53** [45]. Treatment of these complexes with $R'PCl_2$ ($R' = Ph$, *t*-Bu) at room temperature led to elimination of Cp_2ZrCl_2 to form the unprecedented 1,2-azaphosphindoles **54** (Scheme 13). Exchange reaction involving **53a** and $PhSbCl_2$ led to the formation of the corresponding 1,2-azastilbindole **55**. Such a methodology can be applied to the preparation of derivatives incorporating more than one 1,2-azaphosphindole unit. As an example bis(1,2-azaphosphindole) **56** can be isolated as two diastereoisomers from the reaction of the diphosphine $Cl_2P(CH_2)_2PCl_2$ with complex **53a**.

2.4.1
C-H Bond Activation

The activation of C-H bonds is currently one of the most fascinating challenges encountered for the construction of organic molecules. Two recent reviews pointed out how important this process is from an economical point of view [46, 47]. In particular C-H activation initiated by transition metal complexes has

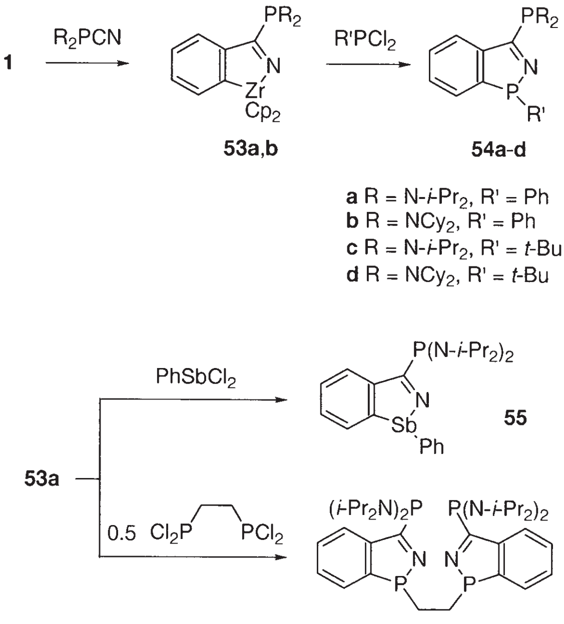

53a,b **54a-d**

a R = N-*i*-Pr$_2$, R' = Ph
b R = NCy$_2$, R' = Ph
c R = N-*i*-Pr$_2$, R' = *t*-Bu
d R = NCy$_2$, R' = *t*-Bu

55

56

Scheme 13. Synthesis of 1,2-azaphosphindoles and 1,2-azastilbindole been the topic of a number of reports: a lot of electronically unsaturated metal complexes were found to activate C-H bonds. Different strategies were proposed. Among them, one can cite 1,2-additions at M=X units (X=O, NR, CRR′), oxidative addition of a late transition metal, σ-bond metathesis, homolytic cleavage by UV-excited mercury atoms, activation at porphyrin Rh^{II} complexes, and heterolytic activation by late transition metals in polar media. C-H activation at d^0 metal centers was found to be effective due to the fact that these complexes remove hydrocarbons reversibly; in this case concerted processes are generally assumed to take place.

1-Aza-zirconacyclopentene complexes **53** contain a strongly electrophilic metal center mostly because of the inductive electron-withdrawing properties of the σ-bonded intracyclic nitrogen atom, and a rather nucleophilic imido group that does not share its lone pair electron density with the adjacent metal center because of the strain in metallacycle. **53a** has been found to activate C-H bonds of terminal acetylenic systems like methylpropiolate, diphenylphosphinoacetylene, and phenylacetylene to give complexes **57**–**59** [48] (Scheme 14). This carbon hydrogen bond activation is not limited to sp carbon hydrogen bond, since activation of an sp^3 C-H bond also easily occurs when **53a** is reacted with malonitrile or with diethylmalonate. Remarkably sp^3 C-H bond activation of vinyl acetate was also shown.

Furthermore, a novel electrophilic sp^2 C-H bond activation and its application for the preparation of α-diazomethylzirconium complexes were also recently reported. Treatment of complexes **53** with ethyldiazoacetate or with trimethylsilyldiazo methane affords the C-α-metallated diazo alkane complexes **63**–**66** (Scheme 15). When **53a,b** were allowed to react with the "non terminal" diazo derivative **67**, the pyrazoles **70** and **71** were obtained in good yield. Formation of the pyrazoles could be rationalized by O-H bond activation of the enol tautomer of **67**, leading to the zirconocene diazo intermediates **68** and **69** which

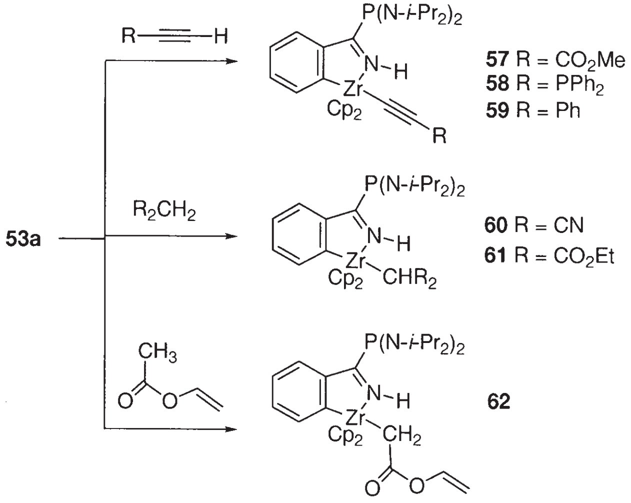

Scheme 14. Examples of C-H bond activation using 1-aza-zirconacyclopentene complex **53a**

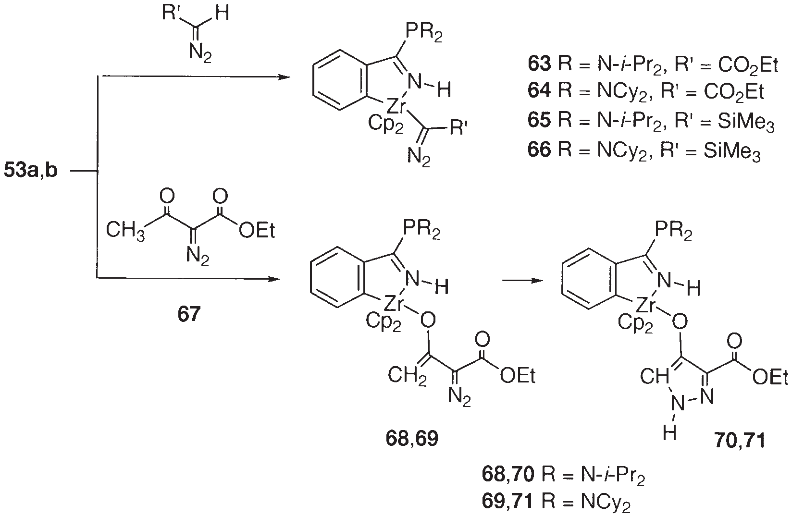

Scheme 15. Synthesis of α-diazo zirconium complexes

in turn rearrange by an intramolecular [3+2] cycloaddition to give the isolated products **70** and **71** [49].

The C-α-metallated diazo alkane complex **63** when reacted with phenylisocyanate is transformed into the 1,2,3-triazolato zirconocene enolate complex **74**. An identical reaction conducted with naphthyl isocyanate gave the triazole **75**. It is reasonable to propose for the formation of **74** and **75**, as a first step of the reaction, a [3+2] dipolar cycloaddition of the diazo function with the isocyanate group, with transient formation of **72** and **73** (Scheme 16). Then, due to the high

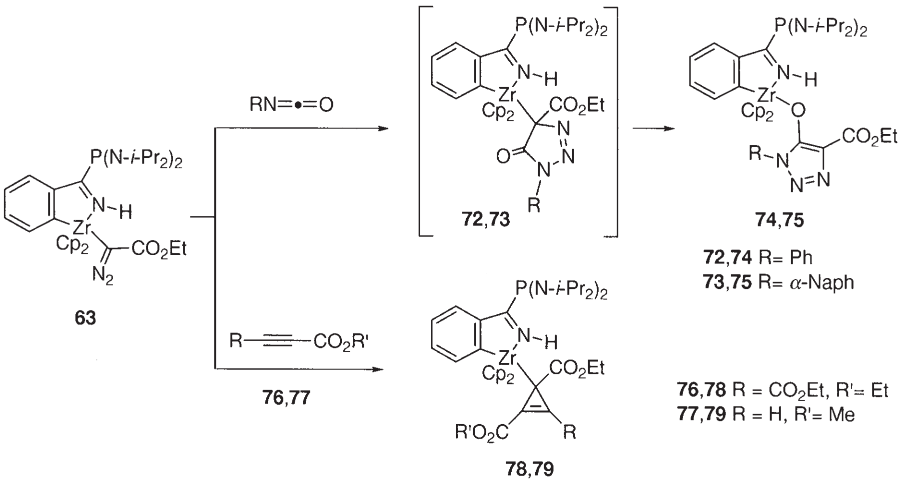

Scheme 16. Cycloaddition reactions of the α-diazomethyl zirconium complex **63**

oxophilicity of the zirconium atom and the resulting aromaticity of the five-membered ring in the final product, an intramolecular rearrangement occurs to give the metalonate triazole complexes **74** and **75** [49].

It is well known that transition metal complexes catalyze the decomposition of diazoacetates in the presence of acetylenes. Thus addition of **63** to the acetylenic species **76** and **77** resulted in loss of nitrogen and formation of the stable C-metallated cyclopropene compounds **78** and **79**. For the first time loss of nitrogen in the formation of cyclopropene rings is initiated by the presence of the zirconium metal fragment.

A clean cleavage of the exocyclic zirconium-carbon bond in **63** and **65** takes place when they are reacted with chlorophosphines as electrophiles. As an example, addition of $(^{i}Pr_2N)_2PCl$ to **63** or **65** resulted in transfer of the diazo $C(N_2)R'$ moiety to the phosphorus atom to give the α-diazophosphines **80** or **81**, respectively (Eq. 5) [49]:

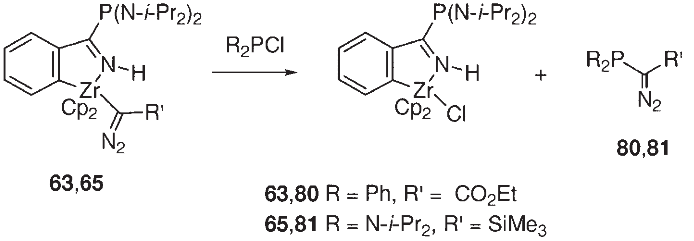

(5)

Equation (5). Formation of α-diazophosphines from azazirconaindenes **63**, **65**

2.4.2
X-H Bond Activation (X=N, O, P, S)

Reactions involving the addition of **53** to alcohols, enolisable ketones, amines, phenols, phosphonates, thiols, or an SH-terminated dendrimer of generation 2, lead via X-H bond activation (X=N, O, P, S) to new complexes **82**–**86** (Scheme 17).

Such a remarkable behavior is the result of the conjunction of two phenomena:

1. The presence of a phosphorus lone pair in **53a** which, through delocalization along the P-C-N unit, renders the cyclic imino nitrogen atom more basic. Analogous reactions can be performed with the complexes **87** which differ from **53a** by the replacement of the phosphorus group by an amino group. Neither C-H nor X-H bond activation reactions were observed when the donor group (phosphine or amine) was replaced by an alkyl group as in **88** (Fig. 5).
2. The presence of a 16 electron zirconium-nitrogen covalent bond in **53a** (or **87**) which allows the formation of an 18-electron zirconium-nitrogen dative bond incorporated in a stable heterosubstituted-cyclopentene bicyclic structure. Indeed, one can describe the later compounds as betaines with the imino nitrogen bearing the positive charge and zirconium bearing the negative charge.

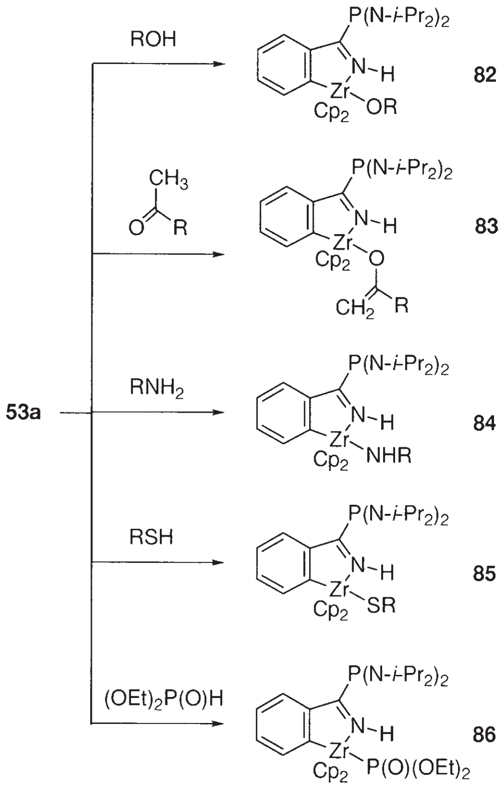

Scheme 17. Examples of X-H (X=O, N, S, P) bond activation using 1-aza-zirconacyclopentene complex **53a**

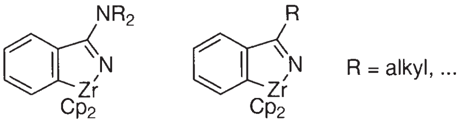

87 **88**

Fig. 5. 5. 1-Azazirconacyclopentene complexes **87**, **88**

Generally, the resulting Zr-X bonds (X=C, N, O, P, S) in complexes **57–66**, **70**, **71**, **74**, **75**, **78**, **79**, **82–86** can be easily cleaved by electrophiles offering access to various organic molecules (Eq. 6):

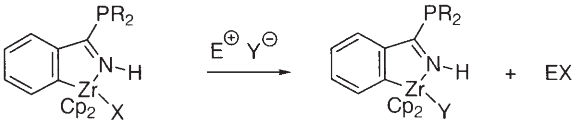

(6)

Equation (6). Cleavage of Zr-X bonds with electrophiles

2.5
Insertion of *tert*-Butylphosphaalkyne

1,1-Bis-(η^5-cyclopentadienyl)-1,3-zircona-3-phosphaindene **90** is obtained in good yield and high regioselectivity by reacting **1** with *tert*-butylphosphaalkyne **89** [50] (Eq. 7):

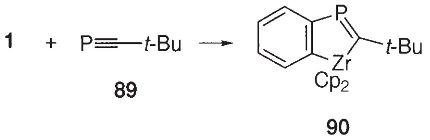

(7)

Equation (7). Insertion of *tert*-butylphosphaalkyne **89** on η^2-benzene zirconocene

2.6
Insertion of Bis(alkynyl)phosphines

The addition of the bis(alkynyl)phosphines *t*-Bu-P(C≡C-Ph)$_2$ **91** to one equivalent of the transient benzyne-zirconocene **1** resulted in the unexpected formation of the zirconacycle **93**, via the transient generation of complex **92** arising from insertion of one of the alkynyl group of **91** into a Zr-C bond of **1** [51] (Scheme 18). Treatment of **93** with HCl conveniently provided the phosphete **94**, a polyunsaturated cyclic phosphine, by cleavage of the two Zr-C bonds. The exchange reaction of **93** with PhSbCl$_2$ led to the corresponding tricyclic system **95**. Preliminary experiments show that such insertions can be envisaged with a variety of bis(alkynyl) reagents providing new ways for the formation of tricyclic systems incorporating one or two main group elements [52].

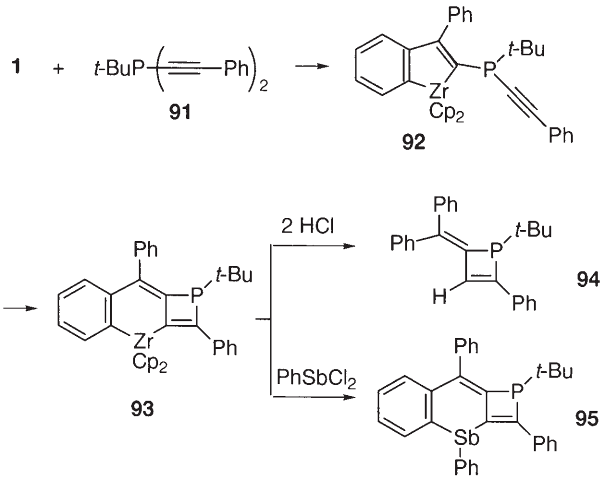

Scheme 18. Insertion of bis(alkynyl)phosphines on the Zr-C of benzyne zirconocene

3
η^2-Phosphabenzyne Zirconocene

3.1
Synthesis

It was only in 1994 that synthesis of heteroaryne derivatives was proposed. Following the methodology which was developed for the preparation of benzynes [16], Mathey et al. reported that the thermally promoted β-elimination of methane or benzene from (2-phosphinimyl) (phenyl or methyl) zirconocene complexes **98** led under mild conditions to η^2-phosphabenzyne-zirconocene complexes which can be isolated either as a PMe_3 adduct **99** or as dimers **100** when the elimination is carried out in the absence of phosphine [53, 54]. Preparation of complex **98** involved two steps: (i) insertion of zirconocene $[Cp_2Zr]$ into the C-X (X=Cl, Br) of 2-halogenophosphines **96** to give the (2-phosphinimyl)-halogenozirconocene **97** and (ii) addition of methyl or phenyllithium which takes place selectively on the Zr–Br bond without interfering with the P=C double bond to give **98** (Scheme 19).

The adduct **99** was only characterized in solution whereas an X-ray crystal structure of the dimer **100c** was recorded. The length of the carbon-carbon pseudo triple bond and the geometry of the corresponding ZrCC unit is similar to that of the η^2-benzyne zirconocene itself. The presence of phosphorus in the six-membered ring does not disturb the coordination sphere of zirconium. Interestingly the dimeric structure **100c** is not destroyed even under forcing conditions and the corresponding PMe_3-complex monomer is never observed.

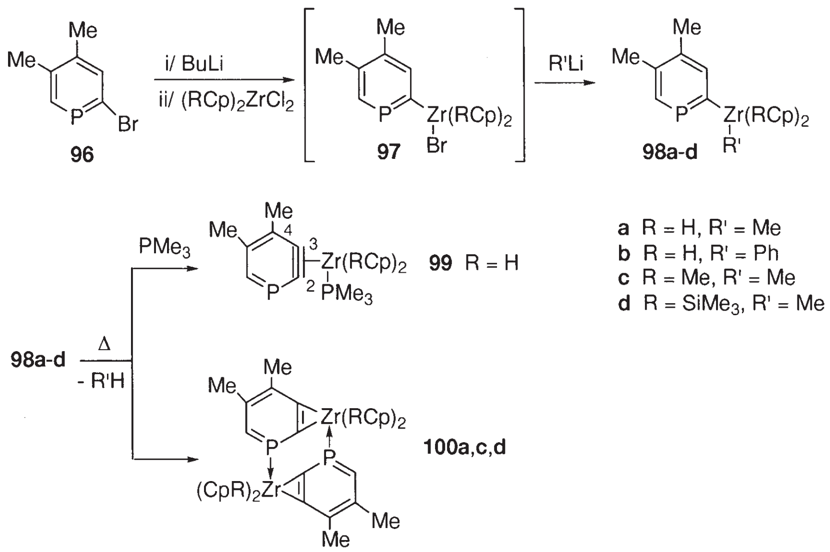

Scheme 19. Synthesis of η^2-phosphabenzyne-zirconocene monomers and dimers

3.2
Reactivity

Both monomer **98c** or dimer **100c** react with acetonitrile to give regioselectively an insertion product **101** into the Zr-C bond (Eq. 8):

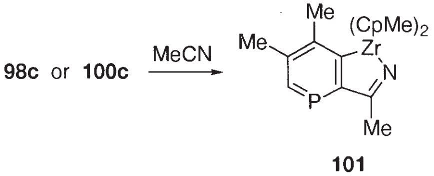

101

(8)

Equation (8). Insertion of acetonitrile on η^2-phosphabenzyne-zirconocene

A selective cleavage of the C_2-Zr bond was described when **100c** is submitted to react with triphenylphosphine sulfide as sulfur donor. The transient formation of a poorly soluble intermediate complex was observed with release of free triphenylphosphine. Upon hydrolysis with HCl, the thiol **102** is formed (Eq. 9):

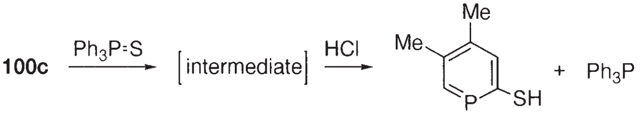

102

(9)

Equation (9). Synthesis of 2-thio-η^2-phosphabenzyne zirconocene **102**

The η^2-phosphabenzyne zirconocene **99** (or the complex **98a**) reacts with alkynes: insertion into the C_2-Zr bond was always observed with formation of the expected five-membered zirconacycles **103–106** (Scheme 20).

As in the case of the reactions conducted with η^2-benzyne zirconocene complex, the trimethylsilyl group of the starting alkyne $Me_3Si-C{\equiv}C-H$ is located on the α-carbon of the resulting five-membered ring. The same situation occurs for the phenyl group of the alkyne $Ph-C{\equiv}C-H$ while the reaction of $Ph_2P-C{\equiv}C-Ph$ with **99** affords two insertion complexes in a 95/5 ratio. Upon hydrolysis, functionalized phosphinines **107–110** are formed. The insertion of ketones or aldehydes takes place also selectively into the C_2-Zr bond of **99** or **98a** leading to

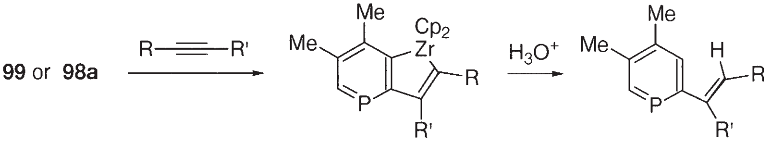

103-106 **107-110**

103,107 R = R' = Et
104,108 R = Ph, R' = H
105,109 R = PPh$_2$, R' = Ph
106,110 R = SiMe$_3$, R' = H

Scheme 20. Reaction of η^2-phosphabenzyne-zirconocenes **99** or **98a** with alkynes

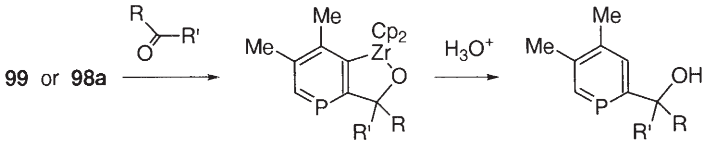

111-115 **116-120**

111,116 R = R' = Me
112,117 R = 4-MeC_6H_4, R' = Me
113,118 R = CpFe(C_5H_4), R' = Me
114,119 R = CpFe(C_5H_4), R' = H
115,120 R = 2-thienyl, R' = H

Scheme 21. Reaction of η^2-phosphabenzyne-zirconocenes **99** or **98a** with aldehydes

zirconacycles **111–115** which give phosphinines **116–120** after hydrolysis (Scheme 21).

Synthesis of homochiral phosphinines for enantioselective catalysis is a very attractive goal since the potential use of these phosphorus heterocycles as ligands in homogeneous catalysis was already mentioned [55]. The reaction of (+)-camphor with **98a** gave a single diastereoisomer in 55% yield after hydrolysis (Scheme 22): the phosphinine ring was selectively grafted onto the endo position of the norbonane skeleton giving enantiomerically pure functionalized phosphinine **122.** This can be explained by the fact that the other possible diastereoisomer of the metallacycle intermediate **121** is strongly disfavored because of the strong steric repulsion between the phosphorus lone pair and the dimethylated bridge [54].

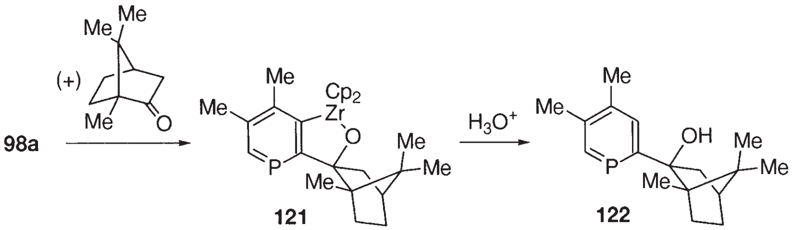

121 **122**

Scheme 22. Synthesis of an enantiomerically pure functionalized phosphinine

The 1-zircona-4-phosphaindene complex **103** was found to be a reagent of choice for the synthesis of functional 1,4-diphosphaindenes and then related anions. Exchange reactions between **103** and dichlorophenylphosphine or PBr_3 as transfer reagents afford 1-phenyl or 1-bromo-1,4 diphosphaindenes **123** and **124** respectively [56]. Addition of a stoichiometric amount of lithium leads to the anion **125** which can be used as a convenient source of functional derivatives **126–128** via reaction of electrophiles at the nucleophilic P atom of the phospholide unit (Scheme 23). Prolonged contact of anion **125** with excess of lithium or sodium cleanly affords the trianion **129** which gives back the anion **125** by oxidation with one equivalent of iodine.

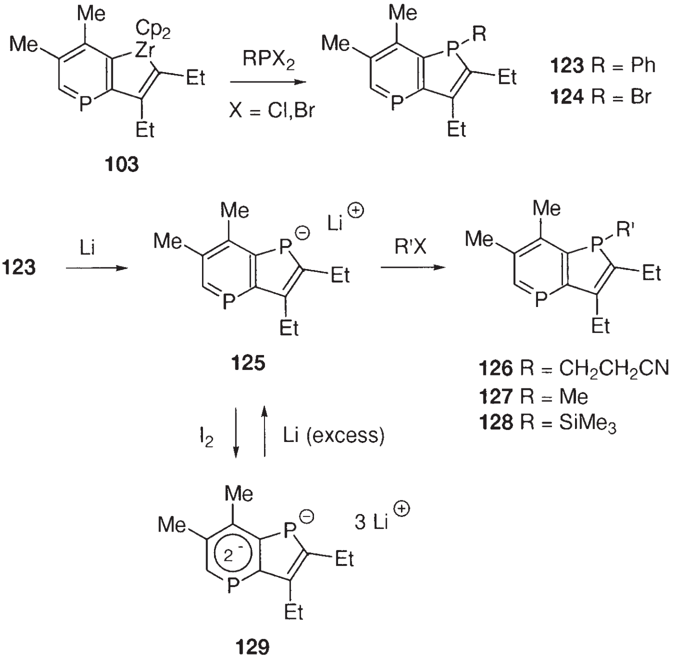

Scheme 23. Generation of mono- and tri-anions of the 1-zircona-4-phosphaindene complex 103

4
Conclusion

Throughout this review several points of primary importance can be pointed out. The first is the extraordinary regiospecificity of reactions involving η^2-benzyne-zirconocene or η^2-phosphabenzyne-zirconocene and unsaturated phosphorus or organic species. Indeed insertion of phosphino-alkyne, vinylphosphine, or 2,3-dihydrophosphole on η^2-benzyne-zirconocene exclusively gives the regioisomer in which phosphino substituent is located on the α-position of the five-membered zirconacycle as the result of a strong interaction between phosphorus lone pair and zirconium. Such a phenomenon was also observed when unsaturated phosphorus reagents were submitted to react with other zirconium species such as the Schwartz reagent $[Cp_2ZrHCl]_n$ [7]. Steric and electronic effects can be evoked to explain the regiochemical preference of the insertion reactions involving the parent phosphabenzyne-zirconocene: the presence of the methyl group at the C_4 position probably disfavors the insertion of alkynes into the C_3-Zr bond by hindering its approach to zirconium. However is was demonstrated [54, 57] that C_2 is more nucleophilic than C_3 in **100** and that the HOMO of phosphinines is mainly localized at P, C_2, and C_4. Besides, there is a much larger concentration of negative charge at C_2 than C_3. All these observations render rational the selective insertion into C_2-Zr bond.

Another main feature which has to be emphasized is the versatile behavior of the resulting phosphorus-zirconacycles which leads via exchange reactions, insertion reactions, [3+1], [3+2], or concomitant [3+1], [3+2] cycloaddition reactions to a large variety of new mono-, di-, tri-, tetra-, penta-, or polycyclic phosphorus derivatives.

Remarkably the use of benzyne-zirconocene allows the formation of unexpected new complexes as the first η^1-iminozirconocene **48**, the unprecedented phosphazide and iminophosphoranes complexes **34–46**, or the unique so far stable pentacoordinated organo zirconocene-ate complexes **20**, **21**, **22-G$_4$**, **22-G$_8$**, **24-G$_3$-G$_2$**, **25–31**.

Of special interest is the behavior of 1-aza-zirconacyclopentene complexes which allows electrophilic sp, sp^2, and sp^3 C-H bond activations as well as M-H bond activations (M=N, O, P, S) and the preparation of the first C-metallated diazoalkanes $L_nMC(N_2)R$ with an early transition metal.

Finally, the ability to prepare 1,4-diphosphaindenyl mono-and tri-anions and enantiomerically pure phosphorus ligands open new ways in organophosphorus chemistry and in asymmetric catalysis.

5
References

1. Jordan RF (1998) Metallocenes and single site olefin catalysts. J Mol Catal A: Chem 128:1
2. Piers WE (1998) Chem Eur J 4:13 and references cited therein
3. Negishi EI (1995) Recent advances in the chemistry of zirconocene and related compounds, Tetrahedron Symposia-in print n°57. Tetrahedron 51:4255
4. Erker G, Aulbach M, Mena M, Pfaff R, Sosna R (1989) Chem Scr 29:451
5. Buchwald SL, Nielsen RB (1998) Chem Rev 88:1047
6. Cadierno V, Zablocka M, Donnadieu B, Igau A, Majoral JP (1999) Organometallics 18:1882 and references cited therein
7. Majoral JP, Zablocka M, Igau A, Cenac N (1996) Chem Ber 129:879
8. Majoral JP, Igau A (1998) Coord Chem Rev 178/180:793
9. Majoral JP, Meunier P, Igau A, Pirio N, Zablocka M, Skowronska A, Bredeau S (1998) Coord Chem Rev 178/180:145
10. Avarvari N, Rosa P, Mathey F, Le Floch P (1998) J Organomet Chem 567:151
11. Hey-Hawkins E (1994) Chem Rev 94:1661
12. Stephan DW (2000) Angew Chem Int Ed 39:314
13. Erker G (1997) J Organomet Chem 134:189
14. Kolomnikov IS, Labeeva TS, Gorbachevskaya VV, Aleksandra GG, Struchkov YT, Vol'pin ME (1971) J Chem Soc Chem Commun 972
15. Rausch MD, Boon WH, Alt HG (1997) In: Slocum DW (ed) The place of transition metals in organic synthesis. Ann NY Acad Sci 295:103
16. Buchwald SL, Watson BT, Huffman JC (1986) J Am Chem Soc 108:7411
17. Dupuis L, Pirio N, Meunier P, Gautheron B, Mahieu A, Igau A, Majoral JP (1996) Bull Soc Chim Fr 133:611
18. See for example: Quin LD, Hughes AN (1990) In: Hartley FR (ed) The chemistry of organophosphorus compounds. Wiley, New York, vol I, chap 10
19. Zablocka M, Igau A, Donnadieu B, Majoral JP, Skowronska A, Meunier P (1997) Chem Commun 1239
20. Miquel Y, Igau A, Donnadieu B, Majoral JP, Dupuis L, Pirio N, Meunier P (1997) Chem Commun 279
21. Takagi K, Rousset CJ, Negishi EI (1991) J Am Chem Soc 113:1440

22. Ho SCH, Straus DA, Armantrout J, Schaefer WP, Grubbs RH (1984) J Am Chem Soc 106:2210
23. Luker T, Whitby RJ, Webster MJ (1995) J Organomet Chem 492:53
24. Etkin N, Hoskin AJ, Stephan DW (1997) J Am Chem Soc 119:11,420
25. Etkin N, Stephan DW (1998) Organometallics 17:763 and references cited therein
26. Miquel Y, Igau A, Donnadieu B, Majoral JP, Pirio N, Meunier P (1998) J Am Chem Soc 120:3504
27. Miquel Y, Cadierno V, Donnadieu B, Igau A, Majoral JP (2000) Organometallics 19:54
28. Cadierno V, Igau A, Donnadieu B, Caminade AM, Majoral JP (1999) Organometallics 18:1580
29. Cadierno V, Zablocka M, Donnadieu B, Igau A, Majoral JP (1999) Organometallics 18:1882
30. Johnson AW (ed) (1993) Ylides and imines of phosphorus. Wiley, New York
31. Cadierno V, Zablocka M, Donnadieu B, Igau A, Majoral JP, Skowronska A (2000) Chem Eur J 2:345 and references cited therein
32. Hilhouse GL, Haymore BL (1978) J Organomet Chem 162:C23
33. Hilhouse GL, Goeden GV, Haymore BL (1982) Inorg Chem 21:2064
34. Bieger K, Bouhadir G, Reau R, Dahan F, Bertrand G (1996) J Am Chem Soc 118:1038
35. Campora J, Buchwald SL (1995) Organometallics 14:2039
36. Scott CB, Grossman RB, Buchwald SL (1993) J Am Chem Soc 115:4912
37. Durfee LD, Hill JE, Fanwick PE, Rothwell IP (1990) Organometallics 9:75
38. Probert GD, Withby RJ, Coote SJ (1995) Tetrahedron Lett 36:4113 and references cited therein
39. Negishi EI, Swanson DR, Miller S (1998) Tetrahedron Lett 29:1631
40. Cuny GD Guttierez A, Buchwald SL (1991) Organometallics 10:537
41. Aoyagi K, Kasai K, Kondakov DY, Hara R, Susuki N, Takahashi T (1994) Inorg Chim Acta 220:319 and references cited therein
42. Buchwald SL, La Maire S (1987) Tetrahedron Lett 28:295
43. Cadierno V, Zablocka M, Donnadieu B, Igau A, Majoral JP, Skowronska A (1999) J Am Chem Soc 121:11,086
44. Buchwald SL, Sayers A, Watson BT, Dervan JC (1987) Tetrahedron Lett 28:3245
45. Cadierno V, Donnadieu B, Igau A, Majoral JP (2000) Eur J Inorg Chem 417
46. Dyker G (1999) Angew Chem Int Ed 38:1698
47. Kempe R (2000) Angew Chem Int Ed 39:468
48. Cadierno V, Zablocka M, Donnadieu B, Igau A, Majoral JP, Skowronska A (2001) Chem Eur J 1:221
49. Cadierno V, Zablocka M, Donnadieu B, Igau A, Majoral JP (2000) Angew Chem Int Ed 39:4254
50. Xia-Bo M, Regitz M (1995) Synthesis 667
51. Dupuis L, Pirio N, Meunier P, Igau A, Donnadieu B, Majoral JP (1997) Angew Chem Int Ed Engl 36:987
52. Pirio N, Meunier P, Dupuis L (unpublished results)
53. Le Floch P, Kolb A, Mathey F (1994) J Chem Soc Chem Commun 2065
54. Rosa P, Le Floch P, Ricard L, Mathey F (1997) J Am Chem Soc 119:9417
55. Breit B (1996) Chem Commun 2071
56. Rosa P, Ricard L, Mathey F, Le Floch P (1999) Chem Commun 537
57. Nyulaszi L, Keglevich G (1994) Heteroatom Chem 5:131

New Chiral Organophosphorus Catalysts in Asymmetric Synthesis

Jean Michel Brunel, Gérard Buono

ENSSPICAM, CNRS U.M.R. 6516, Faculté de St Jérôme, Av. Escadrille Normandie Niemen, 13397 Marseille, Cedex 20, France. *E-mail: buono@spi-chim.u-3mrs.fr*

Chiral organophosphorus compounds have been found to act as catalysts in numerous enantioselective reactions. This review highlights recent developments in this area and more precisely in the kinetic resolution of secondary alcohols, the enantioselective borane reduction of ketones, and in the asymmetric C-C bond formation with the introduction of asymmetric two-center catalysts.

Keywords. Chiral, Phosphorus, Asymmetric, Catalysis, Catalysts

Topics in Current Chemistry, Vol. 220

1
Introduction

Catalytic asymmetric processes based on organometallic chemistry have been intensively studied during the last 30 years [1–3]. In large part, catalytic asymmetric syntheses promoted by transition metal complexes involve the use of chiral phosphine ligands and particularly bidentate phosphine ligands. In this enantioselective catalysis, the key bonding interaction occurs at the transition metal center and the chiral phosphine ligand is responsible for the asymmetric induction during the reaction. Recent years have seen a steady growth in the use of chiral organophosphorus catalysts in asymmetric synthesis [4]. In this case, the organophosphorus catalyst activates by bonding either the reagent or/and the substrate. This review highlights some of the recent developments reported in the literature and will also serve to initiate potential researches in this area.

2
Use of Chiral Phosphines as Catalysts

2.1
Kinetic Resolution of Secondary Alcohols

In 1993, Vedejs et al. [5, 6] showed that tributylphosphine is a potent catalyst for the acylation of alcohols by acetic and benzoic anhydrides as efficient as 4-(dimethylamino)pyridine DMAP [7, 8]. However, the DMAP catalyst is more versatile since it presents catalytic activity in the reaction of alcohols with a larger variety of electrophiles. Due to these properties, Fu [9] realized the design and synthesis of a new family of chiral nucleophilic catalysts illustrated by the planar-chiral DMAP derivative **I** which is a very efficient catalyst in different enantioselective reactions such as addition of alcohols to ketenes [10], rearrangement of O-acylated azalactones [11], and kinetic resolution of secondary alcohols [12–14].

In the same way, Vedejs et al. [15] have explored the catalytic use of chiral phosphines in the enantioselective acylation of alcohols by the anhydrides. Moderate to good enantioselectivities were obtained using chiral phosphine **1a** as catalyst in the benzoylation of **2a**. In this case, the monobenzoate **3a** was obtained in 68% ee and 84% conversion.

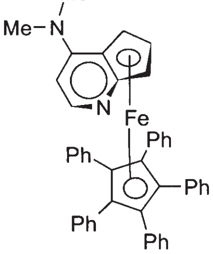

I

Scheme 1

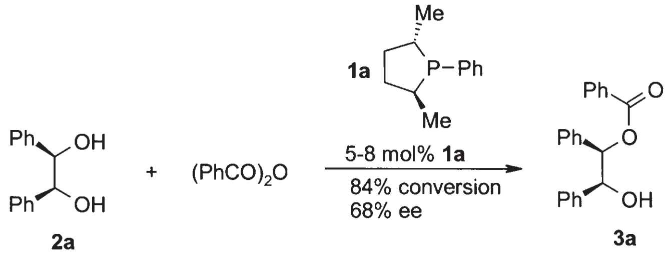

Scheme 2 2a 3a

This promising result have led Vedejs and Daugulis to design and synthesize efficient catalysts **1b**–**c** [16] belonging to the P-aryl-phospha-bicyclo [3.3.0] octane (PBO) family for the enantioselective catalyzed acylation of benzylic alcohols **2b**–**d** or unconstrained allylic alcohols **2e**–**l**.

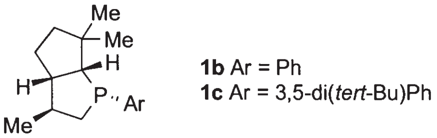

Scheme 3

The enantioselective key step for the reaction is the formation of a chiral acylphosphonium intermediate involving a nucleophilic addition of the phosphine to the carboxylic anhydride. This intermediate reacts preferentially with the alcohol (*R*)-**2** leading to the ester (*R*)-**3** and regenerating the catalyst.

The enantioselectivities are highly dependent on the alcohol structure, the nature of the catalyst, and the temperature. The following examples illustrate the efficiency of this new catalyst:

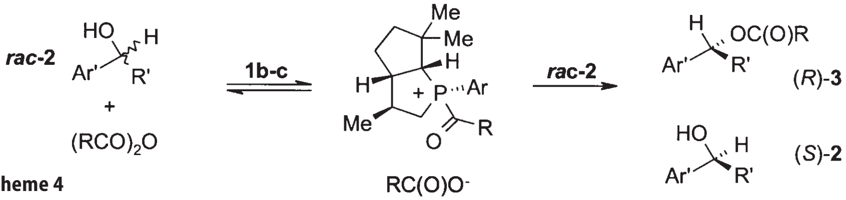

Scheme 4

- The *tert*-butylphenyl carbinol (*rac*)-**2b** (Ar′ = C_6H_5, R′ = *t*-C_4H_9) reacts with benzoic anhydride in toluene solution at –40 °C with 5 mol% of catalyst **1b** to afford after 45.8% conversion, the ester (*R*)-**3b** with 93.1% e.e and the unreacted alcohol (*S*)-**2b** with 78.7% e.e.
- The kinetic resolution of *o*-methylphenyl-1-ethanol (*rac*)-**2c** was realized by acylation with isobutyric anhydride in deoxygenated heptane, using 0.6 mol% catalyst **1c** with 99.7% e.e. After 14 h at –40 °C, the ester (*R*)-**3c** (48.5% conversion) was obtained with 95.7% ee (48% isolated), while 46% of (*S*)-**2c** was recovered (90.2% e.e.). The high enantioselectivity factor [17] s = 142 for this kinetic resolution shows the efficiency of the catalyst **1c**.

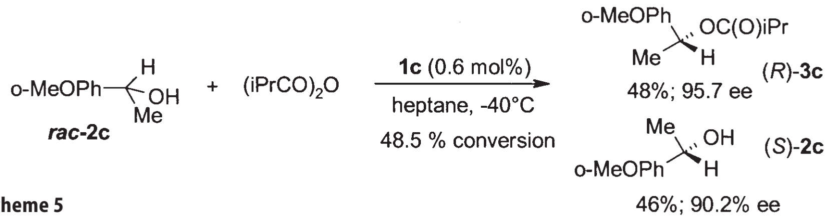

Scheme 5

Table 1. Kinetic resolution of allylic alcohols with isobutyric anhydride and **1c**[a]

Entry[a]	Alcohol	Conv. (%)	Ee % of (*S*)-**2**	Ee % of (*R*)-**3**	Enantio-selectivity factor s[c]
1		45.1	67.3	82.0	21
2	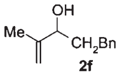	48.1	66.4	71.7	12
3	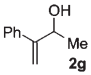	38.1	45.7	74.3	11
4	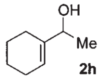	50.4	89.8	88.2	52[b]
5	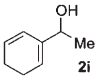	53.0	90.0	81.4	34
6	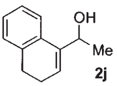	52.6	96.1	86.7	55
7	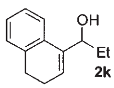	34.0	48.9	94.8	61
8	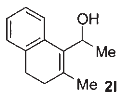	40.3	64.2	95.3	82[b]

---

[a] Reactions were performed at −40°C using 0.1 mol/l substrate, 2.5 equiv. of isobutyric anhydride, and 5 mol% of **2c** in toluene.

[b] Reaction in heptane solution.

[c] See [17].

- Alcohol **2d** (Ar′ = mesityl, R′ = Me) also proved to be an excellent substrate for kinetic resolution when **1c** was used in combination with acetic anhydride: s = 112 was measured at –40 °C in toluene. After 51.8% conversion **2d** (98.6% e.e.) and the ester (*R*)-**3d** (R = Me, 91.6% e.e.) were obtained.
- The PBO catalyst **1c** was recently applied to the kinetic resolution of allylic alcohols **2e–l** by acylation with isobutyric anhydride [18]. The enantioselectivity depends strongly on the structure of allylic alcohols and increases with the conformational flexibility of the substrate. The dienyl alcohols **2i–l** are good substrates for this kinetic resolution as shown by the high selectivity factors (30–80) obtained (Table 1).

2.2
Enantioselective C-C Bond Formation

Another example using chiral phosphines as catalysts has been described by Zhang et al. studying the enantioselective [3+2] cycloaddition of butadienoates with electron deficient olefins [19]. Thus, the use of catalytic amounts of catalysts **8–10** led to the formation of major adduct **6** in enantiomeric excesses varying from 12 to 93% ee. The best result was observed performing the reaction in toluene at 0 °C in presence of 10 mol% of catalyst **8** (entry 3, Table 2).

On the other hand, catalyst **8** has also been successfully applied in the alkylation of malonate-type nucleophiles **11** with activated allenic ester **4**. The adduct resulting from a γ-addition reaction was obtained in around 80% yield and 70% ee [20].

Asymmetric Baylis-Hillman reactions catalyzed by CAMP **9** [21] and BINAP **10** [22] have also been studied but in this case the products were isolated in low

Table 2. Enantioselective cycloaddition of butadienoates with olefins

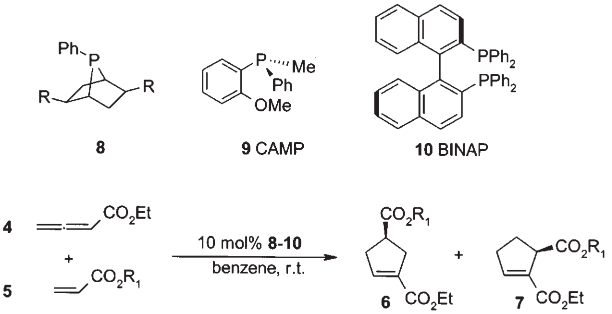

Entry	R_1	Solvent	Catalyst	T (°C)	Yield (%)	**6**:**7**	Ee (%) (**6**)
1	Me	Benzene	**8** (R = Me)	r.t.	87	96:4	79
2	*i*-Bu	Benzene	**8** (R = *i*-Pr)	r.t.	92	100:0	88
3	*i*-Bu	Toluene	**8** (R = *i*-Pr)	0	88	100:0	93
4	Et	Benzene	**9**	r.t.	33	73:27	12
5	Et	Benzene	**10**	r.t.	80	80:20	56

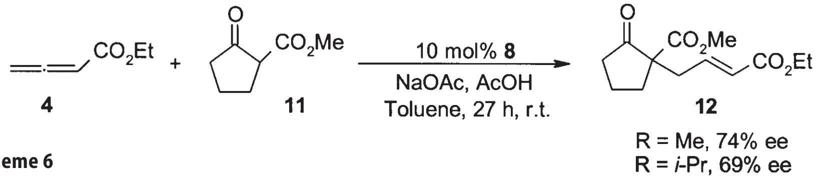

Scheme 6

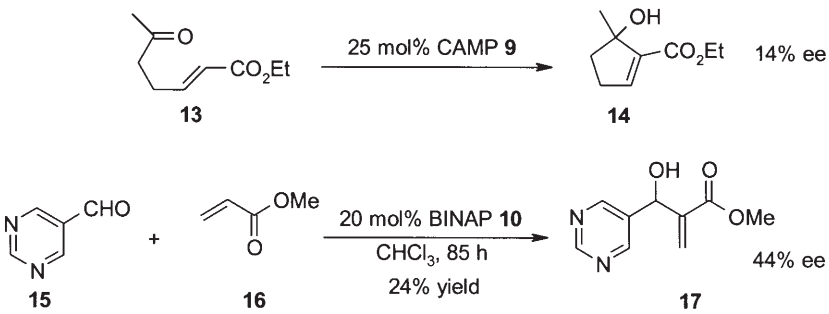

Scheme 7

chemical yields and poor enantioselectivities (respectively 14 and 44% ee for **14** and **17**).

3
Use of Chiral Phosphine-Borane Complexes in the Enantioselective Borane Reduction of Ketones

Parallel to the use of chiral phosphines as catalysts, other organophosphorus compounds have been found to be highly efficient promoters in numerous asymmetric reactions. For instance, in the early 1990s Buono et al. investigated the synthesis and reactivity of P-chirogenic oxazaphospholidine borane complexes [23, 24]. Such complexes are easy to prepare in a two-step sequence through an exchange reaction between a constrained aminoalcohol such as (*S*)-prolinol with a phosphorus(III) reagent such as bis(dimethylamino)phenylphosphine followed by complexation with borane [25]. The structure of these catalysts is analogous to those of the well established oxazaborolidine class which are highly efficient catalysts for the borane reduction of prochiral ketones [26, 27]. Thus, complex **18** turned out to be an effective catalyst for enantioselective reduction of acetophenone [23, 25].

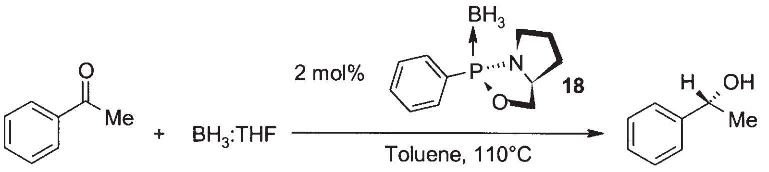

Scheme 8

Table 3. Enantioselective borane reduction of different ketones

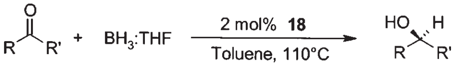

Entry	Ketone	Yield (%)	Ee (%)
1	Acetophenone	80	33
2	Propiophenone	63	38
3	Benzyl methyl ketone	81	55
4	*iso*-Propyl methyl ketone	75	92
5	*tert*-Butyl methyl ketone	67	36
6	2-Butanone	58	42
7	2-Hexanone	73	50
8	Ethylacetate	76	76
9	2-Acetyl furane	70	40

The best results in terms of enantioselectivity (33% using 2 mol% of **18**) were noticed in refluxing toluene whereas only 12% ee was obtained at 20 °C. Moreover, using a stoichiometric amount of **18** led to the formation of chiral (*R*)-phenethylalcohol in more than 95% ee. On the basis of these results, numerous ketones were reduced and also worked well with enantioselectivities up to 92% ee depending on the structure of the considered substrates (Table 3).

The mechanism of this reaction is still somewhat unclear but numerous results suggest that the hydride in the alcohol product comes from the borane attached to the phosphorus atom since its replacement by boron trideuterated led to the fully deuteration of the methine position of the alcohol (when one equivalent of catalyst, and of borane, was employed).

Moreover, it has been clearly demonstrated that catalyst **18** is converted at elevated temperature to the derivative **19** through ring opening of the heterocyclic ring upon exposure to borane. Derivative **19** appeared to be the effective catalyst in the enantioselective reduction of the ketone by the borane.

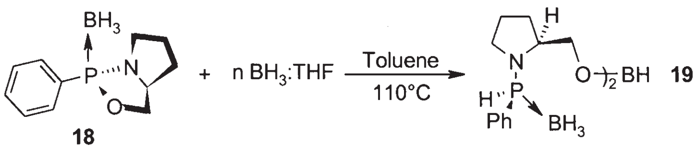

Scheme 9

This high activity of the catalyst **19** can be explained by its amphoteric properties since it is able to activate simultaneously both ketone and borane. This assumption led to a mechanistic proposal rationalizing the hydride transfer from the borane on the phosphorus atom to a ketone coordinated to the other boron atom acting as a Lewis acid.

Nevertheless, this mechanism cannot fully explain the enantioselectivity encountered. In the same area, Martens et al. have reported the synthesis of numerous oxazaphospholidine borane complexes and their use in the enantiose-

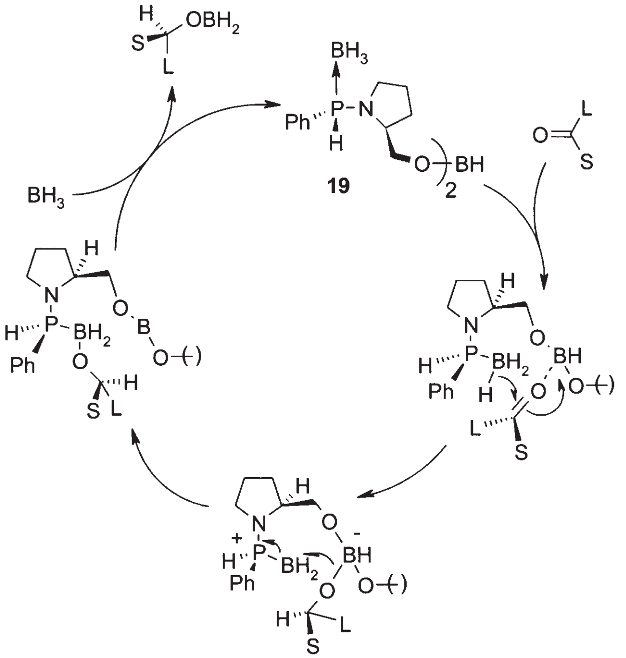

Scheme 10

lective borane reduction of ketones but only low ee varying from 0 to 12% have been observed. However, no detailed studies have been carried out to explain these results [28].

Based on these studies, Vasella et al. have described the synthesis of a glycosylphosphine-borane complex **20** and its use as catalyst (2 mol%) in asymmetric borane reduction of acetophenone at 110 °C with an enantioselectivity up to 24% ee [29].

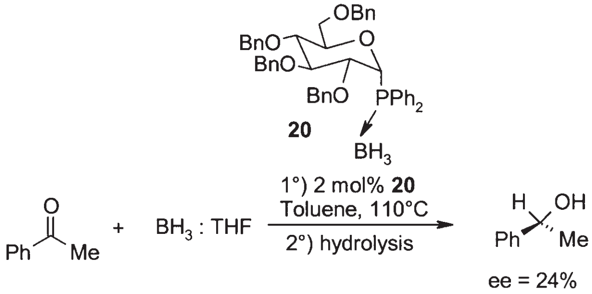

Scheme 11

On the other hand, Wills et al. reported in 1993 the synthesis of a new class of phosphine borane catalysts **21** which led to the formation of (*S*)-phenethylalcohol in 95% yield and 23% ee [30].

More recently, Muller et al. [31] and Chan et al. [32] have independently mentioned the highly enantioselective borane reduction of acetophenone in presence of a catalytic amount of organophosphorus borane complexes **22** and **23** is-

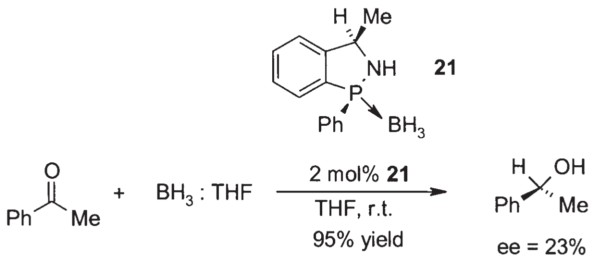

Scheme 12

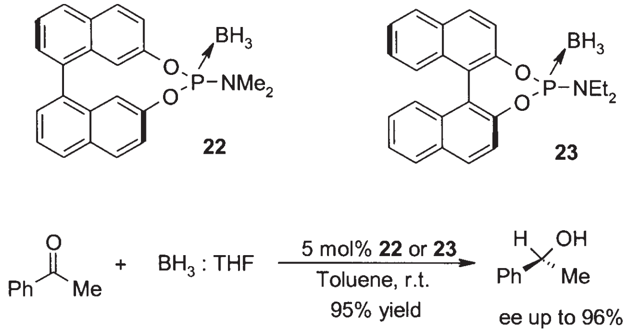

Scheme 13

sued from BINOL derivatives. In these cases, enantiomeric excesses up to 96% ee have been encountered but no hypothesis on the exact nature of the species involved have been proposed.

In 1996, the enantioselective borane reduction of imines catalyzed by an oxazaphospholidine-borane complex in refluxing toluene has been described. Thus, optically active amines have been obtained with enantioselectivities up to 63% [33].

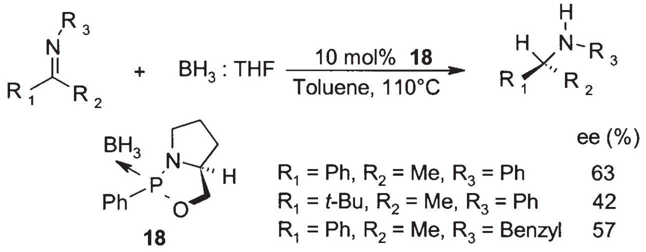

Scheme 14

4

Use of Chiral Phosphine-Oxide in the Catalytic Enantioselective Borane Reduction of Ketones

In 1996, our group initiated a program of research dealing with the asymmetric borane reduction of ketones using oxazaphospholidine oxide compounds as catalysts [34].

This research lays within the scope of the results obtained with the bifunctional catalyst **19** and the demonstration given by Wills et al. [35, 36] that the chiral phosphinamides R*NHP(O)Ph$_2$ were effective catalysts in the borane reduction of the ketones (see below). The use of such compounds was based on the known electron donor character of the oxygen atom of the highly polarized P=O bond better pictured as R_3P^+-O^- [37]. Such a property was demonstrated in numerous X-ray crystal structures of phosphoramides in complexes with salts such as lithium chloride in which the bonding between oxygen and metal cation is clearly apparent [38]. The interaction of the basic oxygen atom with borane would increase its reactivity with respect to the ketone. A secondary interaction may also takes place between the phosphorus atom (containing a partial positive charge) and the carbonyl group of the ketone, although this is likely to be considerably weaker than the primary interaction. Both interactions were illustrated by the model proposed by Wills in the reduction of acetophenone.

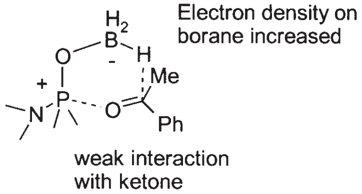

Scheme 15

On the basis of the achievements described above, the opening of the oxazaphospholidine ring would lead to the formation of a new bifunctional chiral catalyst possessing Lewis acid and Lewis base moieties [39]. This catalyst could activate both electrophiles and nucleophiles at defined positions.

On the basis of such hypothesis, the synthesis and use of new phosphine oxides from (*S*)-prolinol has been realized. Thus, enantioselective borane reduction of chloroacetophenone at 60 °C in THF in presence of 1 mol% of **24** led to the expected alcohols in up to 94% ee [34].

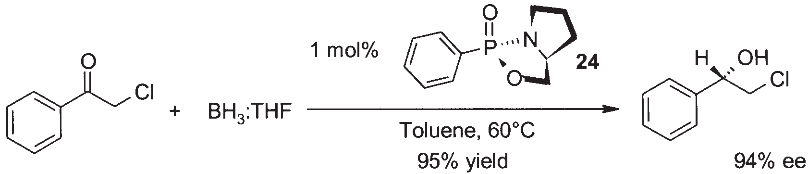

Scheme 16

As planned, the catalyst **24** underwent a cleavage of the endocyclic P-O bond early in the reduction reaction giving an active species **25** which was not recovered at the end of the reaction.

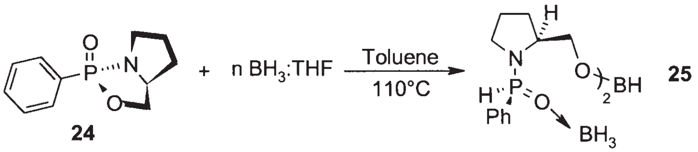

Scheme 17

As described in the catalytic enantioselective borane reduction of ketones using oxazaphospholidine-borane complexes, a mechanistic rationale has been proposed. Nevertheless, this mechanism cannot fully explain the enantioselectivity encountered.

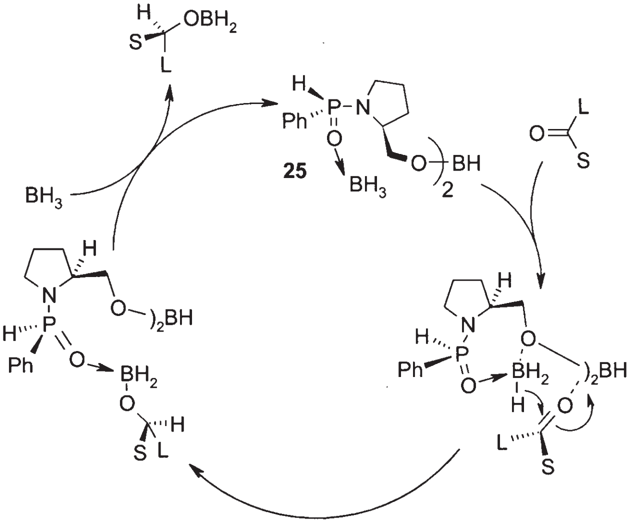

Scheme 18

Numerous ketones have been reduced under the best experimental conditions in 25 to 94% ee depending on the structure of the considered substrate.

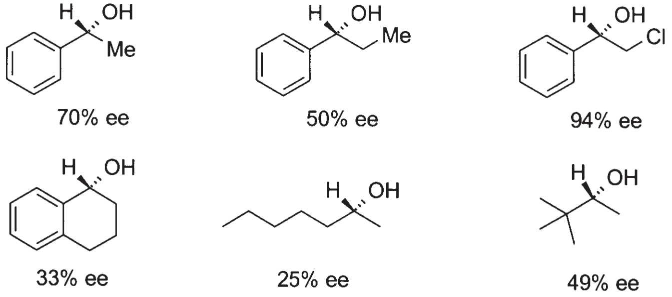

Scheme 19

A few months later, Peper and Martens reported similar results using a chiral phosphine oxide catalyst generated from (*S*)-diphenyl prolinol **26** and leading to similar or better results in terms of enantioselectivity [40]. Again, it is likely that this undergoes a reductive ring opening to a compound analogous to **25**.

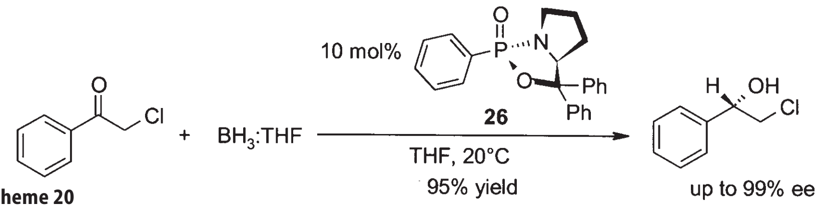

Scheme 20

A serial of related oxazaphospholidine oxides **27**–**31** were described, revealing that the presence of the second fused ring adjacent to the oxazaphospholidine was essential to obtain high catalytic activity.

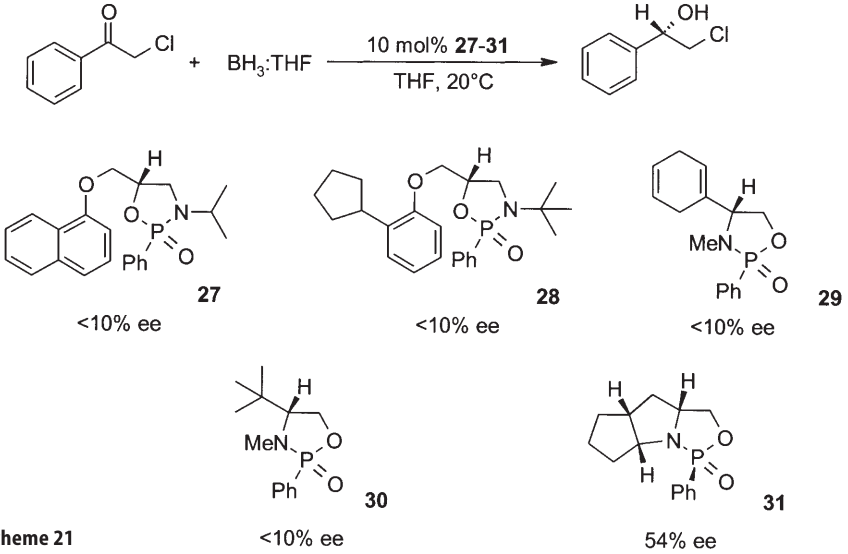

Scheme 21

Since these pioneering works, Wills et al. have widely developed the synthesis of different phosphine oxide compounds **32**–**44**, varying the structure of the chiral auxiliary bound to the phosphorus atom [41–44].

These different complexes have been used as catalysts in the enantioselective borane reduction of acetophenone (THF, r.t.) (Table 4) and the results obtained have permitted one to discover several key features about the catalyst essential for high activity.

Table 4. Enantioselective borane reduction of acetophenone in THF at r.t.

Entry	Catalyst	Yield (%)	Ee (%)
1	**32**	83	30
2	**33**	70	20
3	**34**	90	12
4	**35**	85	35
5	**36**	88	0
6	**37**	90	4
7	**38**	90	24
8	**39**	92	2
9	**40**	80	< 5
10	**41**	82	< 5
11	**42**	82	8
12	**43**	84	46
13	**44**	88	19

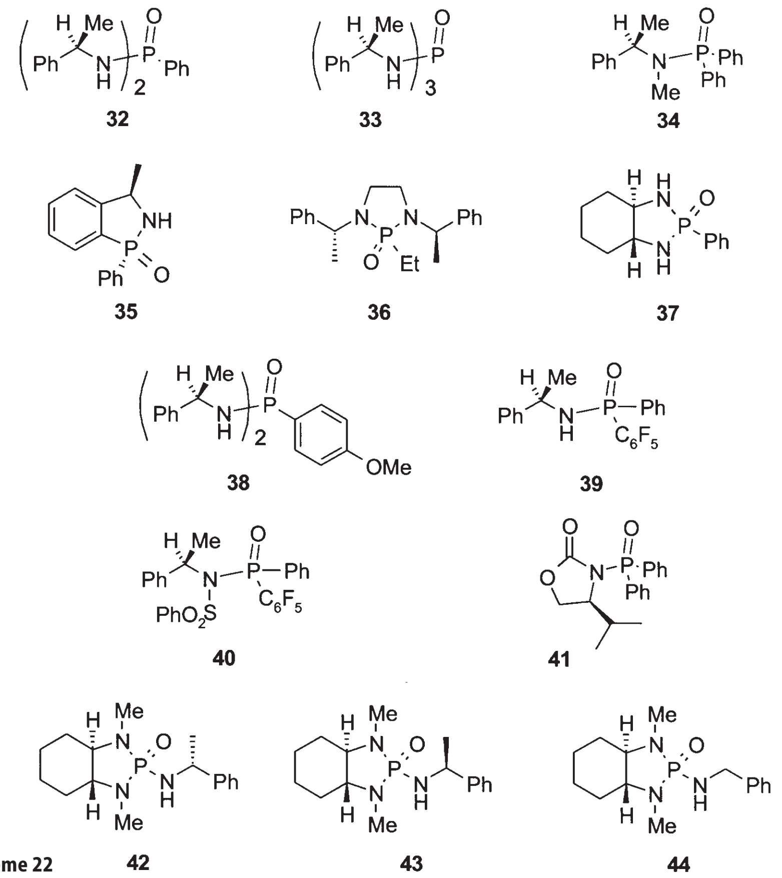

Scheme 22

Electron-rich catalysts such as **38** are rather better than electron-poor ones. In contrast, those containing electron withdrawing groups, i.e., **39**–**41**, are poor catalysts. A radical redesign of the catalyst structure led Wills and his coworkers to synthesize catalyst **45** derived from (*S*)-diphenyl prolinol [45]. In this case, upon reaction with borane, a borate ester would be formed and act as the Lewis acid site.

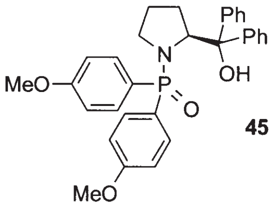

Scheme 23

This catalyst has been found to be highly efficient in terms of enantioselectivity performing the reactions in refluxing toluene. Enantioselectivities up to 90% were achieved in numerous cases.

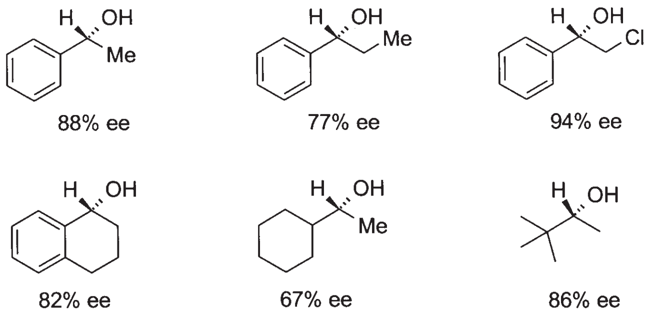

Scheme 24

A model for the control of asymmetric induction was proposed. It involves the formation of a complex in which the borane and ketone are held in place by the phosphinamide and borate ester, respectively.

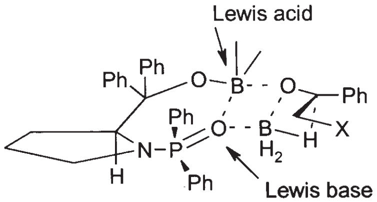

Scheme 25

As previously described, amphoteric catalysts featuring acidic-basic sites have appeared to be very effective. In this area, Buono's group has recently reported the synthesis of a novel class of chiral *o*-hydroxyaryl phosphine oxides possessing a basic (P=O) and acidic site (OH) [46]. The synthesis of diastereomerically pure *o*-hydroxyphenyl oxazaphospholidine oxide **46** was achieved from (*S*)-prolinol and applied as catalysts in the enantioselective borane reduction of numerous ketones [47] (Table 5).

Enantiomeric excesses varying from 10 to 68% ee have been encountered depending on the nature of the considered substrate.

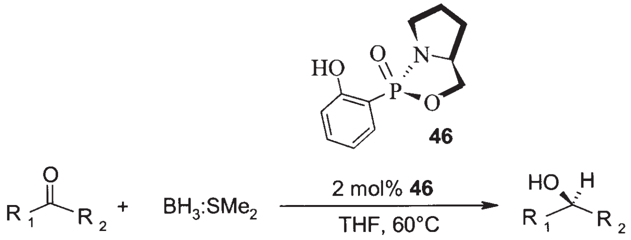

Scheme 26

Table 5. Enantioselective borane reduction of various ketones with 2 mol% of **46**

Entry	Ketone	Yield (%)	Ee (%)
1	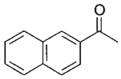	82	10 (*R*)
2	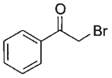	81	11 (*S*)
3	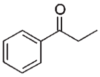	92	19 (*R*)
4	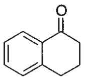	75	18 (*R*)
5	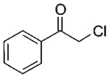	86	68 (*S*)
6	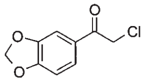	67	44 (*S*)

5
Use of Chiral Phosphine-Oxide Complexes in the Catalytic Enantioselective C-C Bond Formation

5.1
Catalytic Enantioselective Addition of Diethylzinc to Aldehydes

As for the reduction of the ketones, the amphoteric catalysts featuring acidic-basic sites have been found to be very effective for the enantioselective catalysis of C-C bond formation. Thus, Soai et al. were the first to report the enantioselective addition of dialkylzincs to aldehydes using enantiomerically pure phosphinamides and analogues as chiral catalysts in the presence of titanium tetraisopropoxide. Numerous chiral organophosphorus compounds have been prepared and applied in a test reaction between benzaldehyde and diethylzinc [48, 49]. An important difference in terms of enantioselectivity was observed between the behavior of P=S (**47**–**48**) and P=O (**49**) groups. Thus, the enan-

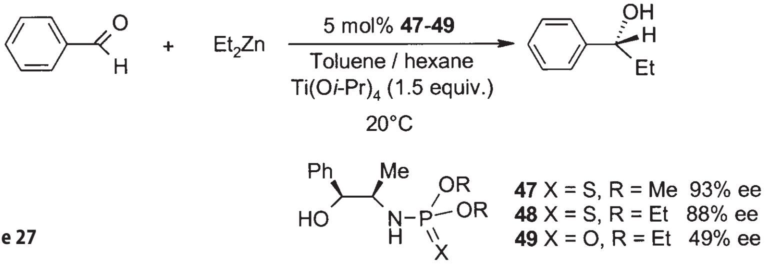

Scheme 27

tiomeric excesses of 1-phenylpropan-1-ol were higher using sulfur-containing chiral catalyst than using the corresponding oxygen analogue.

A mechanism has been postulated suggesting that the hard Lewis acid atom (titanium) bound to the oxygen of the catalyst may control the steric position of the aldehyde whereas the basic site (oxygen or sulfur atom) activates the diethylzinc.

Kellog et al. have also reported that catalysts **50** and **51** led to similar results in terms of chemical yields but improve the enantiomeric excesses up to >98% ee by replacement of the hydroxyl moiety by a thiol group [50, 51].

Scheme 28 **50** >98% ee **51** >93% ee

On the other hand, chiral *o*-hydroxyarylphosphine oxides such as **52** have been widely applied as catalysts in the asymmetric addition of diethylzinc to a series of aromatic aldehydes [52–54].

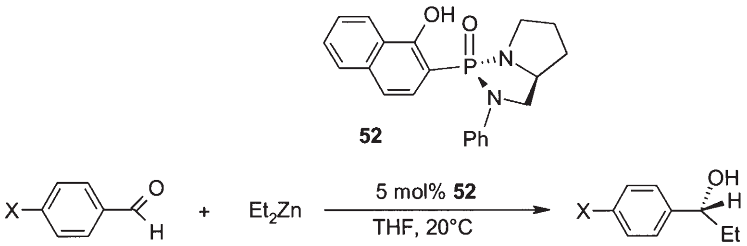

X = H 73% ee
X = NMe_2 71% ee
X =Cl 86% ee
X = CN 99% ee

Scheme 29

It appears that better enantioselectivities were obtained performing the reaction on aromatic aldehydes bearing electron-withdrawing groups on the para-position. Although the nature of the active species involved in this reaction are unclear, a plausible mechanism has been envisioned involving a six-center transition state.

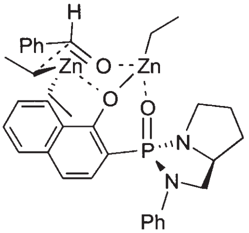

Scheme 30

In this area, the addition of dialkylzinc reagents to aldehydes facilitated by aminoalcohols as bidentate ligands is generally accepted to generate dimeric species. Thus, in order to substantiate this assumption, the use of non-linear effects to identify a higher order molecularity of the catalyst has been realized. The results obtained in presence of 5 mol% of **52** clearly demonstrate a positive non-linear effect and support the hypothesis of involvement of structures with more than one *o*-hydroxyaryldiazaphosphonamide molecule. Thus, assuming the mechanism proposed by Noyori and Kitamura [55], we can suppose that this positive non-linear effect was a result of autoassociation of the chiral reagent formed by the reaction between **52** and the organozinc compound.

Thus, when a mixture of (–)- and (+)-**52** was used, two types of dimeric species were formed: homochiral **53**-(*S*) and **53**-(*R*) and heterochiral *meso* (5*S*,*S*p,5′*R*,*R*p′) dimer. The enantiomeric monomers are the active catalysts in this reaction and each one produces predominantly one enantiomer of phenyl propanol. In this alkylation with diethylzinc, it is logical to conclude that if dimers are formed the heterochiral that retains the minor enantiomer of the catalyst should be less implicated in the reaction, leaving the homochiral-enriched dimer free to operate as the active agent or its precursor.

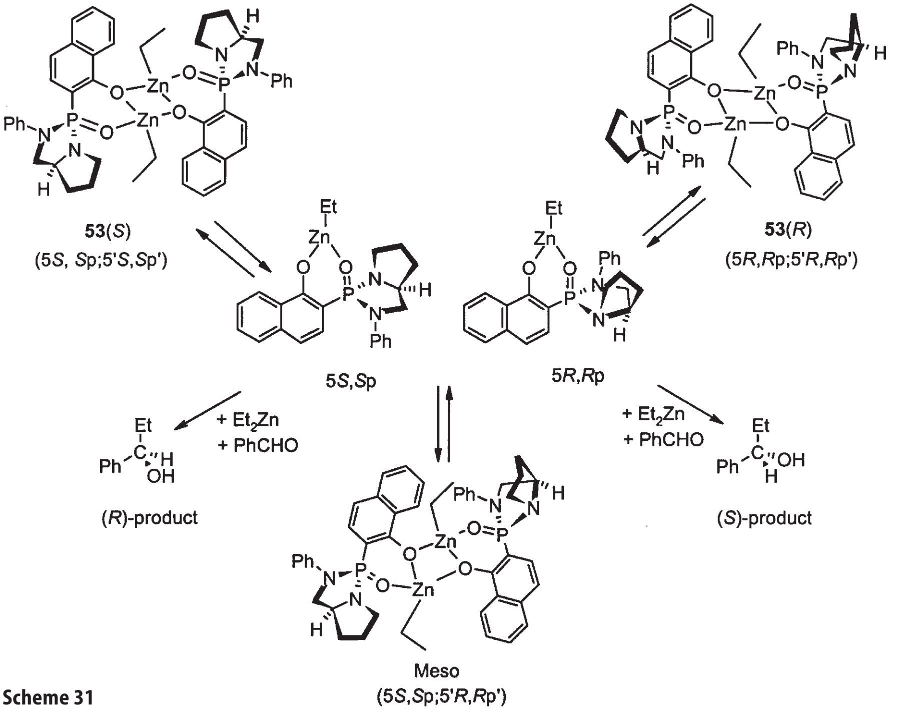

Scheme 31

5.2
Catalytic Enantioselective Trimethylsilylcyanation of Aldehydes and Aldimines

Due to their metal complexation properties, Buono et al. have envisioned the use of titanium alkoxide-chiral *o*-hydroxyarylphosphine oxides complexes in a catalytic enantioselective trimethylsilylcyanation reaction of various aromatic aldehydes [56] (Table 6).

A significant variation of the enantiomeric excess was observed depending on the nature of the aldehydes, the best results being obtained with benzaldehyde, 1-naphthylaldehyde and *p*-methoxybenzaldehyde leading respectively to 90, 94 and 98% ee.

Table 6. Enantioselective titanium catalyzed trimethylsilylcyanation of various aldehydes using **54** as chiral ligand

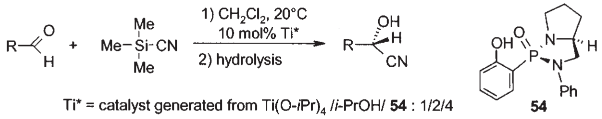

Ti* = catalyst generated from $Ti(O\text{-}iPr)_4$ /*i*-PrOH/ **54** : 1/2/4

54

Entry	Aldehyde	Yield (%)	Ee (%)
1	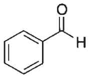	95	94 (*S*)
2	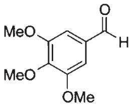	85	33 (*S*)
3	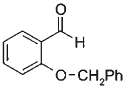	75	42 (*S*)
4	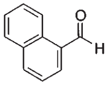	92	90 (*S*)
5	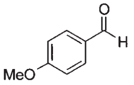	86	98 (*S*)
6	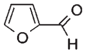	79	3 (*S*)

In the same area, Shibasaki et al. described a new Lewis acid-Lewis base bifunctional catalyst **55** highly efficient in the cyanosilylation of aldehydes [57, 58] (Table 7).

The origin of the highly enantioselective catalysis by **55** is the simultaneous activation of aldehydes and TMSCN by the Lewis acid (Al) and the Lewis base (the oxygen atom of the phosphine oxide), respectively. The enantioselectivity of the reaction may be explained by the working model depicted in Fig. 1, with the

Table 7. Enantioselective catalyzed trimethylsilylcyanation of various aldehydes using catalyst **55**

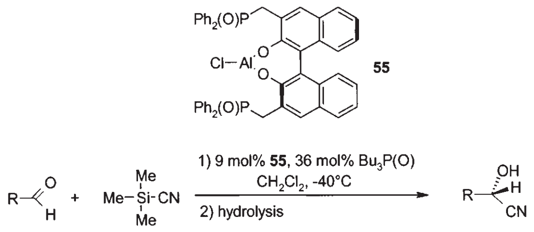

55

Entry	Aldehyde	Yield (%)	Ee (%)
1	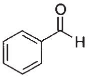	98	96 (*S*)
2	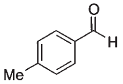	87	90 (*S*)
3	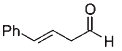	99	98 (*S*)
4	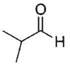	98	83 (*S*)
5	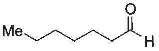	100	98 (*S*)
6	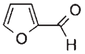	86	95 (*S*)
7	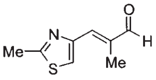	97	99 (*S*)

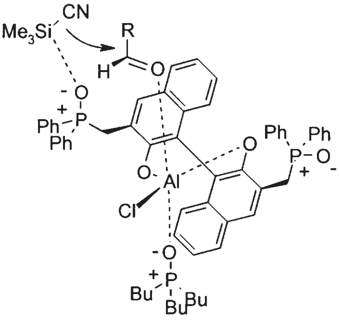

Fig. 1. Working model for the addition of TMSCN to aldehydes catalyzed by **55**

external phosphine oxide coordinating to the aluminum, thus giving a pentavalent aluminum. This geometry would allow the aldehyde to position itself at the apical site of the trigonal bipyramidal structure close to the internal phosphine oxide. Trimethylsilylcyanide, interacting with the internal phosphine oxide, could then transfer cyanide to the aldehyde, thus giving the observed *S*-product. This highly efficient cyanosilylation of aldehydes catalyzed by **55** is practical and was applied to the catalytic asymmetric total synthesis of Epothilone A starting from highly functionalized aldehyde (entry 7) [59, 60].

The bifunctional Lewis acid-Lewis base catalyst **55** has been applied with success to the asymmetric Strecker type reaction [61] (Table 8).

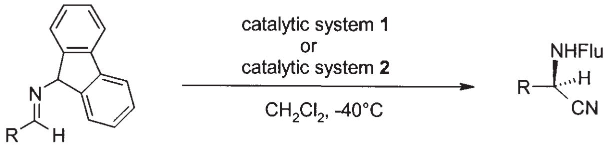

Catalytic system **1** : **55** (9 mol%), TMSCN (2 mol equiv.), PhOH (20 mol%, slow addition over 17 h)

Catalytic system **2** : **55** (9 mol%), TMSCN (20 mol%), HCN (1.2 mol equiv., slow addition over 24 h)

Scheme 32

Table 8. Catalyzed asymmetric Strecker reaction

Entry	R	System **1**		System **2**	
		Yield (%)	Ee (%)	Yield (%)	Ee (%)
1	Ph	92	95	92	92
2	3-Furyl	92	90	92	92
3	*trans*-PhCH=CH	80	96	78	78
4	$CH_3(CH_2)_5$	80	80	75	75
5	*i*-Pr	89	72	92	92
6	*tert*-Bu	97	78	98	98

Shibasaki et al. demonstrate that PhOH and/or HCN work as proton source to protonate the negative charge at the nitrogen atom without changing the catalytic species. TMSCN is more active than HCN in the presence of 20 mol% of PhOH which made it possible to use the catalytic system 2.

From analogy with the cyanosilylation of aldehydes a working model for the catalytic cycle has been proposed in which the Lewis acid (Al) and the Lewis base (phosphine oxide) activate the imine and TMSCN respectively.

More recently, Shibasaki et al. have extended this methodology to the enantioselective cyanosilylation of ketones by designing a novel bifunctional catalyst **56** containing titanium and phosphine oxide (Table 9). Thus, enantiomeric excesses up to 95% in numerous cases have been obtained [62].

On the other hand, Yang and Fang reported the use of a chiral bis-oxazaphospholidine oxide catalyst **57** in the trimethylsilylcyanation of aromatic aldehydes leading to enantiomeric excesses varying from 12 to 90% ee depending on the nature of the considered substrate [63].

Table 9. Enantioselective cyanosilylation of ketones using bifunctional catalyst **56**

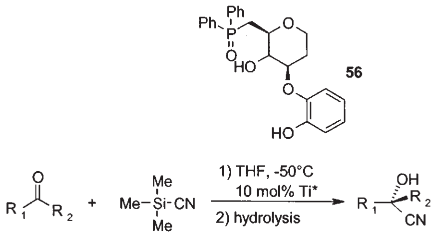

Ti* = catalyst generated from Ti(O-*i*Pr)$_4$ / **56** : 1/1

Entry	Ketone	Yield (%)	Ee (%)
1	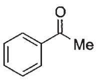	85	92 (*R*)
2	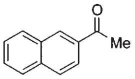	82	95 (*R*)
3	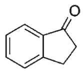	72	69 (*R*)
4	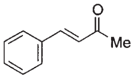	72	91 (*R*)
5	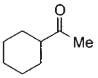	85	90 (*R*)
6	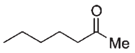	88	76 (*R*)

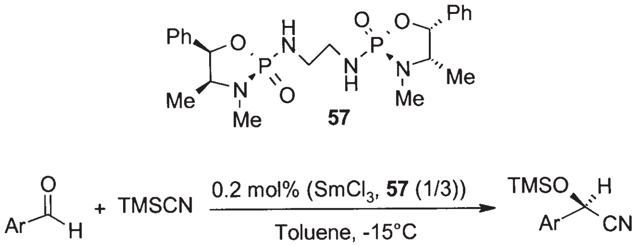

Scheme 33

ee varying from 12 to 90%

5.3
Catalytic Asymmetric Allylation of Aldehydes

In 1994, Denmark et al. found that chiral phosphoramides such as **58** may act as Lewis base in the enantioselective addition of trichloroallylsilane and aldehydes [64] (Table 10).

Table 10. Enantioselective addition of trichloroallylsilane on aldehydes catalyzed by phosphoramides **58**

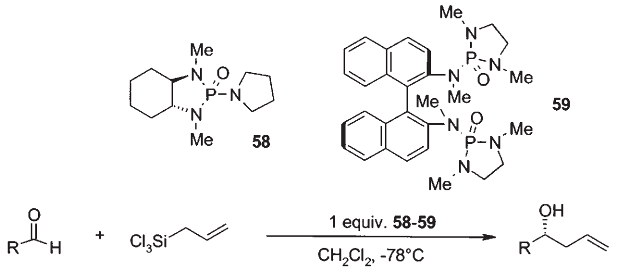

Entry	R	Catalyst	Yield (%)	Ee (%)
1	Ph	**58**	81	60
2	Ph	**59**	76	80
3	2-MeC_6H_4	**58**	81	65
4	4-$NO_2C_6H_4$	**58**	76	21
5	4-$MeOC_6H_4$	**58**	80	50
6	4-$NMe_2C_6H_4$	**58**	69	33
7	PhCH=CH	**58**	67	38

It is noteworthy that this reaction can also be performed in presence of a substoichiometric amount of catalysts **58** and **59** (25 mol%) affording the expected products in only slightly eroded yields and the same enantioselectivity. Moreover, this method gives *syn* and *anti* homoallylic alcohols diastereoselectively from (*Z*)- and (*E*)-crotyltrichlorosilane. The demonstration of a non-linear effect and higher order dependence on phosphoramide requires that the trichloroallylsilane undergoes ionization of a chloride to accommodate all of the components in a hexacoordinate array. The simultaneous operation of both mono- and diphosphoramide pathways provided a unique explanation for the less than spectacular enantioselectivities obtained. Generalized hypothetical transition structures for both pathways clearly show how the monophosphoramide pathway, if operative through a trigonal bipyramidal pentacoordinate siliconate (Fig. 2), would be less enantioselective than a diphosphoramide pathway involving an octahedral hexacoordinate siliconate due to the diminished influence of the singular chiral promoter in the former [65].

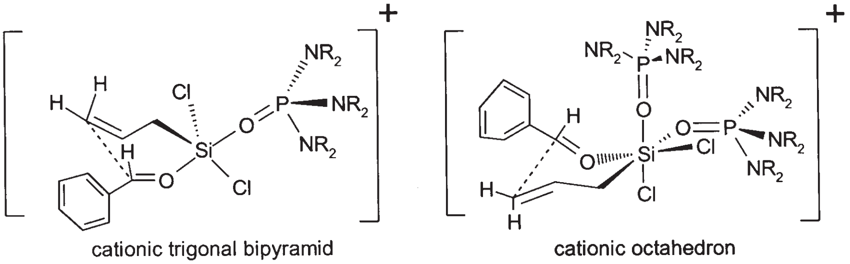

cationic trigonal bipyramid

cationic octahedron

Fig. 2. Hypothetical transition structures for the catalytic asymmetric allylation of aldehydes

Kobayashi et al. also demonstrated the efficiency of reagent **60** derived from (*S*)-proline generating asymmetric inductions of up to 88% ee for the catalytic allylation of benzaldehyde [66, 67].

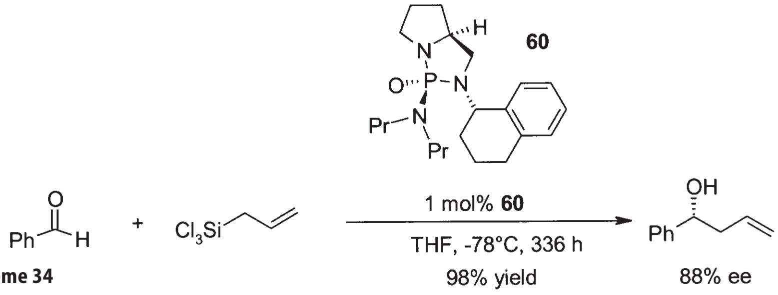

Scheme 34

5.4
Catalytic Asymmetric Ring Opening of *meso*-Epoxides with Silicon Tetrachloride

Denmark et al. have extended this study to the enantioselective ring opening of *meso*-epoxides with silicon tetrachloride catalyzed by chiral phosphoramide **71** (Table 11). In this case, enantiomerically enriched chlorohydrins have been synthesized in enantiomeric excesses varying from 7 to 87 depending on the structure of the considered substrate [68].

Table 11. Enantioselective ring opening of *meso*-epoxides by $SiCl_4$ catalyzed by phosphoramide **71**

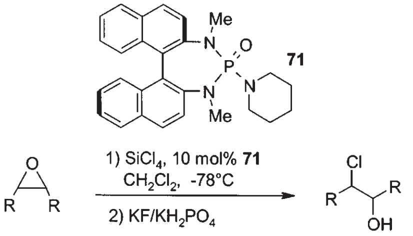

Entry	Substrate	Reaction Time (h)	Yield (%)	Ee (%)
1	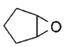	0.3	87	7
2	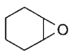	0.3	90	51
3	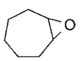	3.0	95	2
4	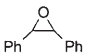	3.5	94	87
5		3.5	95	71

5.5
Catalytic Asymmetric Aldolisation

This concept of Lewis base catalysis has been widely developed by Denmark and coworkers in the asymmetric aldol additions of trichlorosilyl enolates on aldehydes. These reactions were shown to be highly susceptible to acceleration by catalytic quantities of chiral phosphoramides [69–77]. In particular, a phosphoramide derived from (*S*,*S*)-stilbenediamine was remarkably effective not only in accelerating the reaction but also in modulating the diastereoselectivity and in providing the aldol addition products in good to excellent enantioselectivity. For example, trichlorosilyl enolate **61** reacts with benzaldehyde in very high enantio- and diastereoselectivity with 10 mol% of phosphoramide **62** in favor of the *anti* diastereomer (*anti*/*syn*: 60/1). The catalyzed aldol reaction depends on the bulkiness and loading of the catalyst. On the other hand, the hindered phosphoramide (*S*,*S*)-**63** afforded the *syn* aldol product in excellent diastereoselectivity (*anti*/*syn*: 1/97) but with modest enantioselectivity.

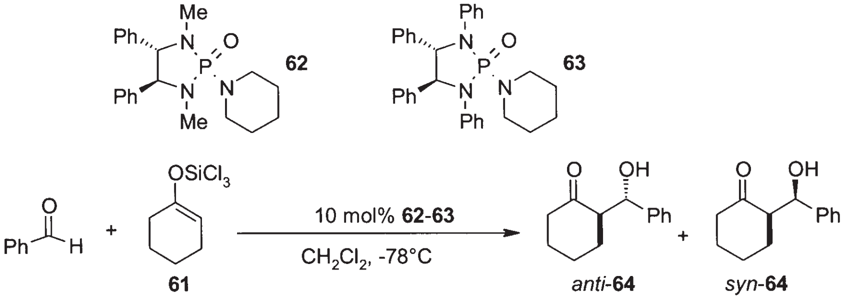

cat. **62** 95% yield *anti*/*syn*, 60/1 (*anti*, 92% ee)

Scheme 35 cat. **63** 94% yield *anti*/*syn*, 1/97 (*syn*, 51% ee)

Furthermore, the diasteroselectivity observed using catalyst (*S*,*S*)-**62** depends on the nature of the latent trichlorosilyl enolates. Thus, propiophenone-derived enolate **65** possessing the *Z*-configuration reacts with benzaldehyde in presence of 15 mol% of (*S*,*S*)-**62** to afford the *syn* adduct **66** with very high enantioselectivity.

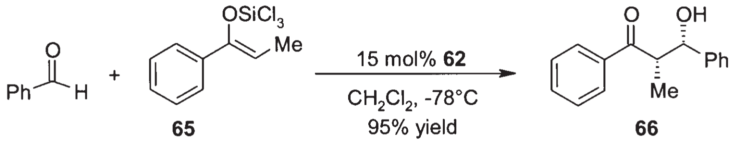

95% yield

Scheme 36 *anti*/*syn*, 1/18 (*syn*, 95% ee)

The formation of **64** using catalyst (*S*,*S*)-**62** exhibits a positive nonlinear effect, fitting well with Kagan's two ligand model [78] whereas the more hindered catalyst (*S*,*S*)-**63** led to a perfect linear asymmetric induction suggesting that the product arose from a transition structure involving only one chiral phosphoramide. The kinetic study of this aldol reaction is in accordance with these results; the reaction catalyzed by bulky chiral phosphoramide **63** exhibited first order dependence on the catalyst, while the aldol reaction catalyzed by **62** displayed second-order dependence on phosphoramide.

From experimental evidence, Denmark proposes two mechanistic pathways [79]: by coordination of the Lewis basic phosphoramide to silicon the trichlorosilyl enolate undergoes ionization of chloride to give rise a cationic tetracoordinate silicon moiety **67** in equilibrium with **68**, a trigonal bipyramidal silicon cation by coordination of a second molecule of the catalyst. This equilibrium is displaced in favor of **68** by using smaller phosphoramide such as **62** or at higher catalyst loading. Upon binding of the aldehyde the intermediates **67** and **68** undergo respectively aldolization through a boat and chair like transition structure (**69** and **70**) organized around a cationic pentacoordinate and hexacoordinate silicon atom.

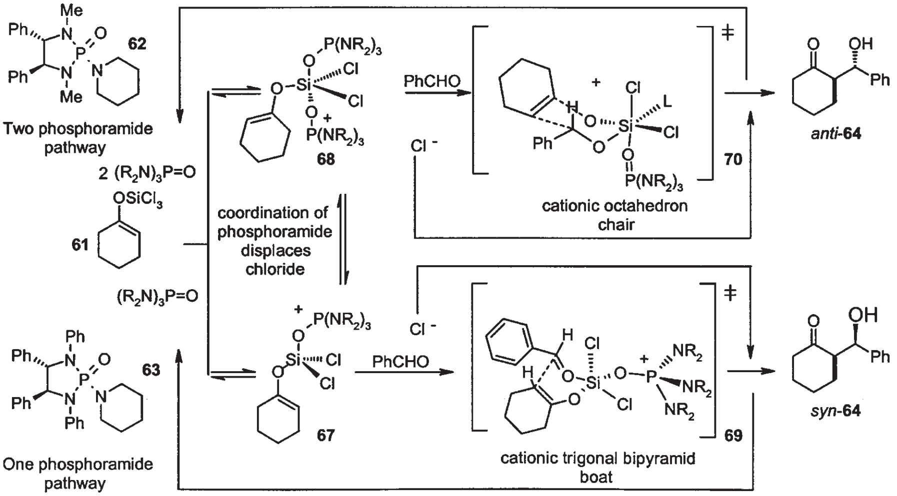

Scheme 37

The formation of *syn*-**64** and *anti*-**64** diastereomer aldol products emerges from the transition states **69** and **70**, respectively. Thus, the Zimmerman-Traxler model [80] involving a six-membered like assembly of the reactants provide a reasonable explanation of the (*Z*)-*syn*, (*E*)-*anti* correlation.

6
Conclusion

In this review, we have illustrated by different applications the importance of chiral organophosphorus compounds as catalysts opening up a new field in asymmetric catalysis. From the diversity of trivalent (pyramidal) $\lambda^3\sigma^3$ compounds and pentavalent (tetrahedral) $\lambda^5\sigma^4$, there are many possibilities for the design of asymmetric one- or two-center catalysts. It can be reasonably envisioned that new chiral phosphines, phosphine oxides, and phosphazenes, together with other related multifunctional organophosphorus compounds such as chiral hydroxyphosphines or phosphine oxides, will play an important role in the development of new multifunctional catalysts and their applications in catalytic asymmetric syntheses.

7
References

1. Noyori R (1994) Asymmmetric catalysis in organic synthesis. Wiley, New York
2. Ojima I (1993) Catalytic asymmetric synthesis. VCH, Berlin
3. Ojima I (2000) Catalytic asymmetric synthesis, 2nd edn. Wiley-VCH, New York
4. Buono G, Chiodi O, Wills M (1999) Synlett 377
5. Vedejs E, Diver ST (1993) J Am Chem Soc 115:3358
6. Vedejs E, Bennett NS, Conn LM, Diver ST, Gingras M, Lin S, Oliver PA, Peterson MJ (1993) J Org Chem 58:7286
7. Hassner A, Krepski LR, Alexanian V (1978) Tetrahedron 34:2069
8. Höfle G, Steglich W, Vorbrüggen H (1978) Angew Chem Int Ed Engl 17:569
9. Fu GC (2000) Acc Chem Res 33:412
10. Hodous BL, Ruble JC, Fu GC (1999) J Am Chem Soc 121:2637
11. Ruble JC, Fu GC (1998) J Am Chem Soc 120:11,532
12. Ruble JC, Latham HA, Fu GC (1997) J Am Chem Soc 119:1492
13. Ruble JC, Tweddell J, Fu GC (1998) J Org Chem 63:2794
14. Tao B, Ruble JC, Hoic DA, Fu GC (1999) J Am Chem Soc 121:5091
15. Vedejs E, Daugulis O, Diver ST (1996) J Org Chem 61:430
16. Vedejs E, Daugulis O (1999) J Am Chem Soc 121:5813
17. Kagan HB, Fiaud JC (1988) Top Stereochem 18:249
18. Vedejs E, Mackay JA (2001) Org Lett 3:535
19. Zhu G, Chen Z, Jiang Q, Xiao D, Cao P, Zhang X (1997) J Am Chem Soc 119:3836
20. Chen Z, Zhu G, Jiang Q, Xiao D, Cao P, Zhang X (1998) J Org Chem 63:5631
21. Roth F, Grgax P, Frater G (1992) Tetrahedron Lett 33:1045
22. Hayase T, Shibata T, Soai K, Wakatsuki Y (1998) Chem Commun 1271
23. Brunel JM, Pardigon O, Faure B, Buono G (1992) J Chem Soc, Chem Commun 287
24. Buono G, Brunel JM, Faure B, Pardigon O (1993) Phosphorus Sulfur Silicon 75:43
25. Brunel JM, Chiodi O, Faure B, Fotiadu F, Buono G (1997) J Organomet Chem 529:285
26. Deloux L, Srebnik M (1993) Chem Rev 93:763
27. Walbaum S, Martens J (1992) Tetrahedron: Asymmetry 3:1475
28. Peper V, Stingl K, Thumler H, Saak W, Haase D, Pohl S, Juge S, Martens J (1995) Liebigs Ann 2123
29. Lopusinski A, Bernet B, Linden A, Vasella A (1993) Helv Chim Acta 76:94
30. Burns B, Merifield E, Mahon MF, Molloy KC, Wills M (1993) J Chem Soc Perkin Trans I:2243
31. Muller P, Nury P, Bernardinelli G (2000) Helv Chim Acta 83:843
32. Ma MFP, Li K, Zhou Z, Tang C, Chan ASC (1999) Tetrahedron: Asymmetry 10:3259
33. Brunel JM, Buono G (1996) Synlett 177
34. Chiodi O, Fotiadu F, Sylvestre M, Buono G (1996) Tetrahedron Lett 37:39
35. Burns B, King NP, Studley JR, Tye H, Wills M (1994) Tetrahedron: Asymmetry 5:801
36. Burns B, Studley JR, Wills M (1993) Tetrahedron Lett 34:7105
37. Chesnut DB (1998) J Am Chem Soc 120:10,504
38. Denmark SE, Miller PC, Wilson SR (1991) J Am Chem Soc 113:1468
39. Shibasaki M (2000) Asymmetric two center catalysis, in Stimulating concepts in chemistry (Vögtle F, Stoddart F, Shibasaki M ed.) Wiley-VCH, Weinheim, p 105
40. Peper V, Martens J (1996) Tetrahedron Lett 37:8351
41. Burns B, Gamble MP, Simm ARC, Studley JR, Alcock NW, Wills M (1997) Tetrahedron: Asymmetry 8:73

42. Burns B, King NP, Tye H, Studley JR, Gamble MP, Wills M (1998) J Chem Soc, Perkin Trans I:1027
43. Gamble MP, Studley JR, Wills M (1996) Tetrahedron: Asymmetry 7:3071
44. Gamble MP, Studley JR, Wills M (1996) Tetrahedron Lett 37:2853
45. Gamble MP, Smith ARC, Wills M (1998) J Org Chem 63:6068
46. Legrand O, Brunel JM, Constantieux T, Buono G (1998) Chem Eur J 4:1061
47. Brunel JM, Legrand O, Buono G (2000) Eur. J Org Chem 3313
48. Soai K, Hirose T, Ohno Y (1993) Tetrahedron: Asymmetry 4:1473
49. Soai K, Ohno Y, Inoue Y, Hirose T (1995) Recl Trv Chim Pays Bas 114:145
50. Hulst R, Heres H, Fitzpatrick K, Peper NCW, Kellog RM (1996) Tetrahedron: Asymmetry 7:2755
51. Hulst R, Heres H, Peper NCW, Kellog RM (1996) Tetrahedron: Asymmetry 7:1373
52. Brunel JM, Constantieux T, Legrand O, Buono G (1998) Tetrahedron Lett 39:2961
53. Legrand O, Brunel JM, Buono G (1998) Tetrahedron Lett 39:9419
54. Legrand O, Brunel JM, Buono G (2000) Tetrahedron Lett 41:2105
55. Noyori R, Kitamura M (1991) Angew Chem Int Ed Engl 30:49
56. Brunel JM, Legrand O, Buono G (1999) Tetrahedron: Asymmetry 10:1979
57. Hamashima Y, Sawada D, Kanai M, Shibasaki M (1999) J Am Chem Soc 121:2641
58. Hamashima Y, Sawada D, Nogami H, Kanai M, Shibasaki M (2001) Tetrahedron 51:805
59. Sawada D, Kanai M, Shibasaki M (2000) J Am Chem Soc 122:10,521
60. Sawada D, Shibasaki M (2000) Angew Chem Int Ed 39:209
61. Takamura M, Hamashima Y, Usuda H, Kanai M, Shibasaki M (2000) Angew Chem Int Ed 39:1650
62. Hamashima Y, Kanai M, Shibasaki M (2000) J Am Chem Soc 122:7412
63. Yang WB, Fang JM (1998) J Org Chem 63:1356
64. Denmark SE, Ce DM, Pratt NE, Griedel BD (1994) J Org Chem 59:6161
65. Denmark SE, Su J (2000) J Am Chem Soc 122:12021
66. Iseki M, Kuroki Y, Takahashi M, Kobayashi Y (1996) Tetrahedron Lett 37:5149
67. Iseki M, Kuroki Y, Takahashi M, Kishimoto S, Kobayashi Y (1997) Tetrahedron 53:3513
68. Denmark SE, Barsanti PA, Wong KT, Stavenger RA (1998) J Org Chem 63:2428
69. Denmark SE, Winter SBD, Su X, Wong KT (1996) J Am Chem Soc 118:7404
70. Denmark SE, Wong KT, Stavenger RA (1997) J Am Chem Soc 119:2333
71. Denmark SE, Winter SBD (1997) Synlett 1087
72. Denmark SE, Stavenger RA, Wong KT (1998) J Org Chem 63:918
73. Denmark SE, Stavenger RA, Wong KT (1998) Tetrahedron 54:10,389
74. Denmark SE, Su X, Nishigaichi Y (1998) J Am Chem Soc 120:12,990
75. Denmark SE, Stavenger RA (1998) J Org Chem 63:9542
76. Denmark SE, Stavenger RA, Wong KT, Su X (1999) J Am Chem Soc 121:4982
77. Denmark SE, Stavenger RA (2000) J Am Chem Soc 122:8837
78. Kagan HB, Fenwick D (1999) Top Stereochem 22:257
79. Denmark SE, Pham SM (2000) Helv Chim Acta 83:1846
80. Zimmerman HE, Traxler MD (1957) J Am Chem Soc 79:1920

Metal-Mediated Degradation and Reaggregation of White Phosphorus

Markus Ehses[1], Antonio Romerosa[2], Maurizio Peruzzini[3]

[1] Auf der Klause 5, 55597 Wöllstein, Germany
[2] Área de Química Inorgánica, Facultad de Ciencias, Universidad de Almería, 04071, Almería, Spain
[3] ISSECC-CNR, V. Jacopo Nardi 39, 50132 Florence, Italy. *E-mail: peruz@fi.cnr.it*

Dedicated to Professor Otto J. Scherer on the occasion of his 68th birthday

A critical survey of the coordination chemistry of white phosphorus illustrating the metal-mediated degradation of the P_4 tetrahedron is presented. The underlying principles to account for the activation and stepwise fragmentation of this molecule in the presence of transition metal complexes are presented with emphasis given to mechanistic aspects. A collection of ^{31}P-NMR spectral data for the known polyphosphorus P_x compounds ($x \leq 4$) is also presented and briefly commented.

Keywords. White phosphorus, Transition metal complexes, ^{31}P NMR spectroscopy, Polyphosphorus ligands, Mechanistic studies

Topics in Current Chemistry, Vol. 220

List of Abbreviations

t-Bu	*tert*-Butyl
COD, cod	Cyclo-octa-1,5-diene
Cp	Cyclopentadienyl
Cp^{Et}	Ethyltetramethylcyclopentadienyl
Cp^{Me}	Methylcyclopentadienyl
Cp^{Pr}	Pentaisopropylcyclopentadienyl
Cp^{Si}	1,3-Bis(trimethylsilyl)cyclopentadienyl
Cp^{x}	Generic cyclopentadienyl ligand
Cp*	Pentamethylcyclopentadienyl
Cp′	*tert*-Butylcyclopentadienyl
Cp″	1,3-Bis(*tert*-butyl)cyclopentadienyl
Cp‴	1,2,4-Tris(*tert*-butyl)cyclopentadienyl
Cy	Cyclohexyl
DCM	Dichloromethane
dppe	1,2-Bis(diphenylphosphino)ethane
dppm	1,2-Bis(diphenylphosphino)methane
Et	Ethyl
i-Pr	Isopropyl
NMR	Nuclear magnetic resonance
NP_3	Tris(2-(diphenylphosphino)ethyl)amine
OTf	Triflate
Ph	Phenyl
PP_3	Tris(2-(diphenylphosphino)ethyl)phosphane
THF, thf	Tetrahydrofuran
triphos	1,1,1-Tris(diphenylphosphinomethyl)ethane
VE	Valence electron

1
Introduction

At the turn of the twentieth century, the coordination chemistry of white phosphorus, that may be broadly considered as the chemistry of transition metal complexes incorporating either the tetraphosphorus molecule or fragments thereof, is becoming a mature field at the borderline between coordination and inorganic chemistry. Since the discovery of the first tetraphosphorus complex, $[(PPh_3)_2ClRh(\eta^2\text{-}P_4)]$, in 1971 [1], the metal-mediated chemistry of this unique molecule has indeed flourished and a variety of complexes featuring naked P_1, P_2, P_3, and P_4 ligands in combination with all d-block transition metals, with the only exception of technetium and the group-3 triad, have been prepared. Remarkably, the assortment of coordination compounds arising from the metal-promoted P_4 activation is greatly enriched by the straightforwardness of diverse aggregation processes involving polyphosphorus units. Therefore, formation of P_5, P_6, and even larger P_x units, up to twelve phosphorus atoms, is a relatively common process. This peculiar feature, in line with the formal analogy between

$(CH)_x$ and P_x species, represents an important conceptual advancement towards the full development of a phosphorus-based *"inorganometallic chemistry"* [2].

Most of the early studies in the coordination chemistry of white phosphorus and polyphosphorus fragments were aimed at investigating this apparently neglected area of inorganic chemistry and beautiful examples of transition metal complexes incorporating phosphorus as well as other main group 15 elements (As, Sb, Bi) have been described [3–10]. Nowadays, when a manifold of coordination modes entailing P_x ligands have been accomplished, a different and more ambitious goal is attracting the attention of synthetic inorganic chemists, i.e., the use of transition-metal complexes as a platform to carry out the metal-mediated functionalization of white phosphorus, a process leading to new P-H and P-C bonds directly from elemental phosphorus and an organic substrate [4, 5].

In order to take further steps towards this intriguing and industrially relevant field, it is mandatory to have a rational view of the general principles governing the metal-mediated activation of white phosphorus. Although several reviews covering different aspects of transition-metal chemistry of naked phosphorus atoms and units have been published [4–12], no attempt has been made to provide a rationale picture of the metal-promoted stepwise degradation of white phosphorus that highlights the multiform pathways transforming an intact P_4 ligand into a variety of smaller and larger P_x units embedded into a variety of coordination architectures. This article, although updating precedent reviews on the coordination chemistry of white phosphorus, is not intended to provide a comprehensive coverage of the field. It attempts to provide a homogeneous picture of the present knowledge of the metal-assisted P_4 activation from the viewpoint of the stepwise demolition of the P_4 tetrahedron. Therefore, emphasis will be laid less on structural than on mechanistic aspects of the multiform compounds individuated along the degradation pathways of P_4.

2
White Phosphorus as a Ligand

2.1
The Coordination Chemistry of the Intact P_4 Molecule

Transition metal complexes featuring an intact, *tetrahedro*-tetraphosphorus ligand, i.e., η^1-P_4 metal complexes, are quite scarce despite the increasing interest in this chemistry and the growth of the general knowledge concerning the reactivity of white phosphorus with transition metal species [3–12]. Until a few years ago, the seminal complexes $[(NP_3)M(\eta^1\text{-}P_4)]$ (M=Ni, **1**; Pd, **2**), prepared in the late 1970s by Sacconi and coworkers by treating the strong Lewis acid complexes $[(NP_3)M]$ (M=Ni, **3** [13]; Pd, **4** [14]) with white phosphorus in THF/benzene solution (Eq. 1), remained the only well documented members of this class of compounds:

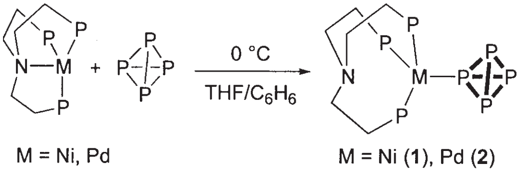

(1)

The nickel derivative, which is slightly air sensitive in the solid state, was authenticated by X-ray diffraction analysis. The crystallographic study confirmed the occurrence of an η^1-P_4 metal coordination with the nickel atom surrounded by the three donor atoms of the tripodal polyphosphane.

Apart from these sparse examples, no other transition metal complex featuring the intact P_4 molecule as a two-electron ligand was reported for the next 20 years. This fact is quite surprising in retrospect because these two decades witnessed an unexpected and rapid growth of the coordination chemistry of white phosphorus and related molecules [3–12]. Invariably, the many reactions of transition metal fragments with P_4 carried out during this period usually led to more or less drastic transformations of the tetrahedral-P_4 unit. Therefore, it was tempting to look at the η^1-P_4 complexes of Sacconi et al. as chemical curiosities whose stability was a consequence of the peculiar properties of the NP_3 ligand, particularly the shielding effects due to the six phenyl rings wrapping the Ni-P_4 assembly [15]. Accordingly, it was hypothesized that similar species without comparable steric stabilization would have only a fleeting existence along the reaction pathways starting with the activation and ending with the degradation of the P_4 tetrahedron. Nevertheless, the interest in understanding the first steps of the metal-to-P_4 interaction preceding the P-P bond activation encouraged several researchers to reorient their studies in order to explore the metal-mediated reactivity of white phosphorus under less harsh conditions than those usually used. Remarkable results in this area were obtained at the turn of the century by Scheer et al. [16] and, soon thereafter, by Peruzzini et al. [17] and Stoppioni et al. [18] who synthesized other *tetrahedro*-tetraphosphorus complexes using metal precursors invariably supported by sterically demanding phosphane coligands. In all of these cases, a coordinatively unsaturated metal fragment, namely $[M(CO)_3(PR_3)_2]$ (M=Mo, W; R=Cy; M=W; R=*i*-Pr) [19], $[(triphos)\ Re(CO)_2]^+$ [20] and $[(PP_3)M]^+$ (M=Co, Rh), [21, 22] generated in solution by either displacement of a weak agostic interaction in the educt [19, 20] or reductive elimination of weakly coordinated ligands [20–22], was straightforwardly reacted with white phosphorus to yield $[M(CO)_3(PR_3)_2(\eta^1\text{-}P_4)]$ [M=W, R=Cy (**5**), *i*-Pr (**6**); M=Mo, R=Cy (**7**)], $[(triphos)Re(CO)_2(\eta^1\text{-}P_4)]Y$ [Y=OTf, BPh_4 (**8**)] and $[(PP_3)M(\eta^1\text{-}P_4)]OTf$ (M=Co (**9**), Rh (**10**)] (Eqs. 2–4).

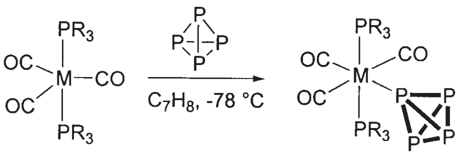

M = W; R = Cy (**5**), R = *i*-Pr (**6**)
M = Mo; R = Cy (**7**)

(2)

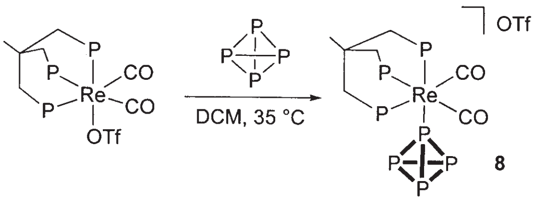

8

(3)

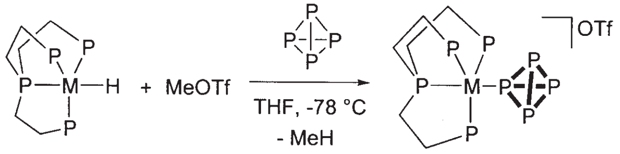

M = Co, **9**; Rh, **10**

(4)

Noticeably, all the new *tetrahedro*-tetraphosphorus complexes, apart from **8**, are unstable in solution at room temperature and decompose between −40 °C (**9**) and 0 °C (**5**). They were characterized by ^{31}P NMR spectroscopy in solution and, for complex **5** only, by X-ray crystallography (Fig. 1). In all cases the unquestionable presence of an η^1-P_4 ligand was ascertained.

The reaction of the hydrogenation catalyst [$(PPh_3)_3RuCl_2$] with white phosphorus in toluene was briefly investigated by Peruzzini et al. during a study aimed at exploring the possibility of hydrogenating P_4 homogeneously [23]. Notwithstanding that systems capable of accomplishing the hydrogenation of elemental phosphorus have not yet been individuated [4, 5], the reaction resulted in the formation of [$(PPh_3)_2RuCl(\mu\text{-}Cl)_3Ru(PPh_3)_2(\eta^1\text{-}P_4)$] (**11**) which has been the first dinuclear species containing a monohapto-P_4 ligand (Eq. 5). Unfortunately, the stability of **11** was insufficient to grow crystals suitable for an X-ray study as slow decomposition in solution to an intractable brown material took place even under an inert atmosphere.

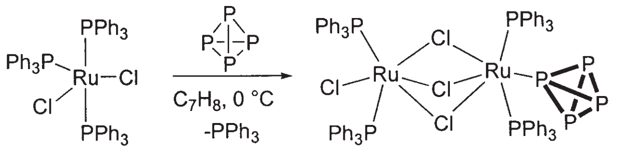

11

(5)

Solution characterization of the known η^1-P_4 metal complexes was mainly based on $^{31}P\{^1H\}$ NMR spectroscopy, which is a reliable tool to assign promptly the monohapto coordination mode of the P_4 molecule (see Sect. 3). Indeed, with the

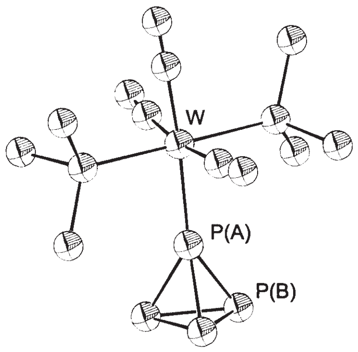

Fig. 1. Crystal structure of [$W(CO)_3(PCy_3)_2(\eta^1\text{-}P_4)$] (**5**). Only the P-bonded carbon atoms of the cyclohexyl substituents are shown for the sake of clarity. Adapted from [16]

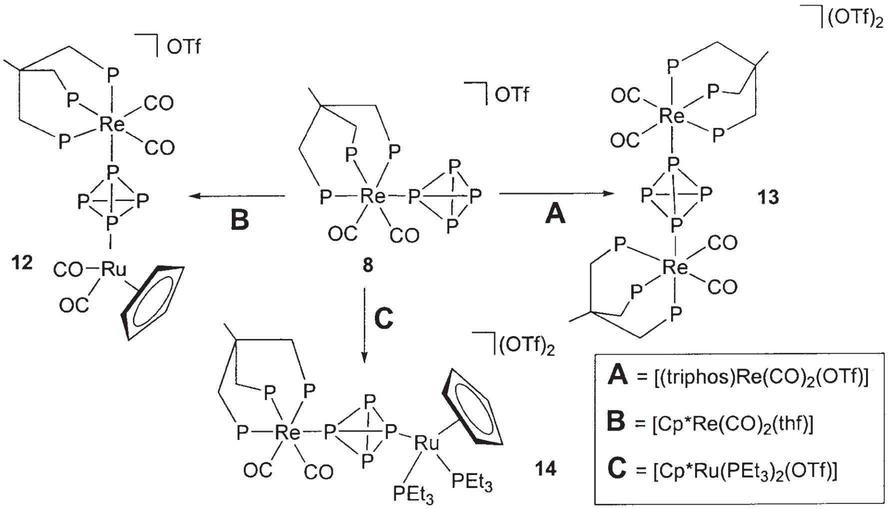

Scheme 1. Use of $[(\mathrm{triphos})\mathrm{Re(CO)_2}(\eta^1\text{-}P_4)]^+$ (**8**) as building block to synthesize dinuclear $\mu,\eta^{1:1}$-P_4 complexes

single exception of **1**, which was completely insoluble in common solvents [13], all the known *tetrahedro*-P_4 complexes, in the absence of additional coupling to NMR active nuclei (usually P-atoms of ancillary phosphanes or the metal itself), feature a well resolved AB_3 splitting pattern in the very high field region of the spectrum. The three uncoordinated phosphorus atoms (P_B) have exohedral *sp*^{3}-hybridized lone pairs and therefore may still act as a donor towards further transition-metal moieties. Nevertheless, the use of η^1-P_4 complexes as a building unit for multimetallic complexes has been scarcely considered, probably as a consequence of the thermal instability of most of these species, and further experimental investigations of the coordination chemistry in this area would be valuable. For **8**, the only thermally stable complex of this type yet reported, clear evidence of the bonding capabilities of the P_3 subunit has been provided. Thus, treatment of **8** with strongly acidic metal complexes such as $[(\mathrm{triphos})\mathrm{Re(CO)_2(OTf)}]^+$ [17], $[\mathrm{Cp^*Re(CO)_2(thf)}]$ [24], and $[\mathrm{Cp^*Ru(PEt_3)_2Cl}]$ [25] readily affords dinuclear complexes of formula $[(\mathrm{triphos})\mathrm{Re(CO)_2}(\mu,\eta^{1:1}\text{-}P_4)\mathrm{ML_n}]^{x+}$ (x=1, $\mathrm{ML_n}=\mathrm{Cp^*Re(CO)_2}$ (**12**); x=2, $\mathrm{ML_n}=(\mathrm{triphos})\mathrm{Re(CO)_2}$ (**13**), $\mathrm{Cp^*Ru(PEt_3)_2}$ (**14**)] (Scheme 1). A prima facie evidence for the formation of dimetallic species sandwiching an $\eta^{1:1}$-P_4 ligand between two metal fragments, is provided by the ^{31}P-NMR spectrum where the P_3 doublet in the high field region is replaced by the M_2 portion of the ABM_2 splitting pattern.

2.2
Metal-Mediated Rearrangement of P_4

In order to accomplish the synthesis of functionalized phosphorus compounds starting from white phosphorus, it is necessary that P_4 is activated in the presence of suitable reagents [26]. Following the activation step and the consequent P_4-degradation, free connectivities are generated, which may be saturated by a variety of organic fragments bearing heteroatoms such as N, P, O, S, C, or hydrogen atoms. Compounds in which the P_4 molecule, or fragments thereof, interacts with one or more transition metal centers may serve as suitable models for mimicking the sequential loss of the P_4 integrity and, therefore, the whole degradation process. The intensive experimental and theoretical studies aimed at identifying the resulting products have fed an ever growing, fascinating, and esthetical chemistry that has paved the way for bridging different disciplines such as inorganic, organic, and solid state chemistry. However, it is only in the last few years that systematic efforts have been undertaken to gain insights into the mechanisms of these reactions and some valuable clues in this area have been obtained.

2.2.1
P-P Bond Breaking of the P_4 Tetrahedron

Setting up the degradation of P_4 in the presence of both transition metal complexes and suitable substrates is crucial to accomplish the direct functionalization of white phosphorus [27, 28]. In many cases, the combination of P_4 with a transition metal system affords a variety of hardly predictable compounds containing unsubstituted phosphorus (P_x) ligands ($x \leq 12$) in which the original tetrahedral phosphorus structure is no longer evident [3, 4, 6–12]. The topologies exhibited by these ligands, conforming to acyclic, cyclic, and polycyclic units, suggest that in most instances the reactions proceed via a cascade of degradation and aggregation steps. Trapping the intermediates with suitable organic and inorganic molecules, and in situ studies by ^{31}P-NMR spectroscopy, represent the methods of choice to follow these intriguing processes.

Scheme 2 illustrates the formalism we have adopted to sort the P_x fragments according to the number of bonds cleaved in the P_4 molecule.

The scission of a single P-P bond in the P_4 molecule (**I**) leads to a butterfly arrangement of the P_4 polyhedron (**II**) (*bicyclo*-[1.1.0]tetraphosphabutane), which is usually incorporated in transition-metal complexes as a formal P_4^{2-} dianion. Cleavage of a second bond may afford tetraphosphorus ligands with either three- or four-membered rings depending on the position where the second P-P bond breakage occurs. Thus, if the additional cleavage takes place close to the first one, the three-membered cycle (**III**) is generated, whereas when the P-P scission takes place opposite to the first one, a *cyclo*-tetraphosphorus ligand is left (**IV**). From there on, three alternative ways of P-P breakage may generate tetraphosphorus ligands with "tripodal" (**V**), or linear chain arrangements (**VI**), or may result in two separated fragments, i.e., one *cyclo*-P_3 ring and a single P atom (**VII**). The cyclic three-membered ring (**VII**) and the tripodal P_4 ligand (**V**) may formally be transformed into the open P_3 structure (**VIII**), leaving again a single P atom apart. Two separate P_2 ligands (**IX**) are produced by cleavage of the central bond in the linear P_4 chain (**VI**), whereas disruption of one of the peripheral bonds leads again to topology **VIII**. Further degradation of **VIII** or **IX** eventually provides single phosphorus atoms and P_2 units.

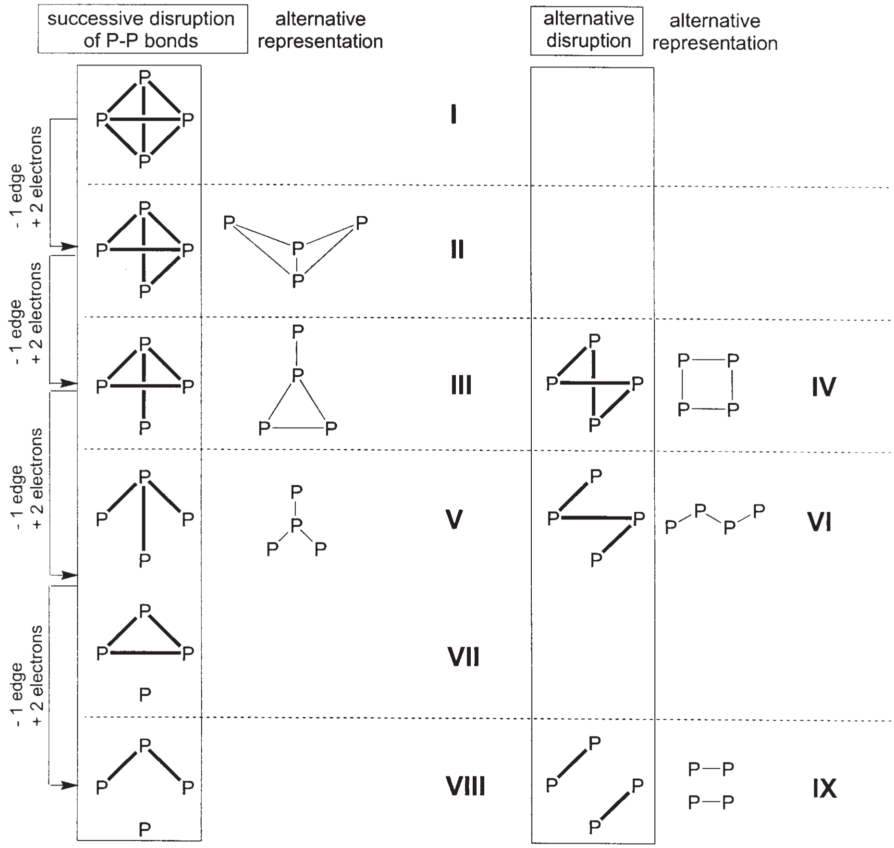

Scheme 2. Chart showing the formalism adopted to classify the P_x ligands as a function of the increasing number of P-P bond cleavages

The polyphosphorus units described above encompass the stepwise degradation of the P_4 molecule and may be described, from a formal electronic viewpoint, as polyphosphido or polyphosphorus ligands with multiple P-P bonds. In the latter case the formal charge of the P_x ligand is progressively reduced as the multiple P-P bond character increases.

2.2.2
Mechanistic Aspects of the Metal-Mediated Degradation of White Phosphorus

Complexes containing a weakly coordinated P_4 ligand epitomize the initial interaction of electronically and sterically unsaturated transition metal fragments with white phosphorus. However, as outlined above in Sect. 2.1, complexes bearing an intact P_4 ligand are quite rare in coordination chemistry owing to their sparing solubility and high reactivity. Therefore, it is not surprising that most of the reactivity patterns of P_4 with transition metal species result in a more or less pronounced degradation of the tetrahedral topology.

A perusal of the relevant literature suggests that there are two major pathways accounting for white phosphorus degradation that share the opening of one edge of the P_4-tetrahedron to yield a butterfly ligand as the initial step. Once the *bicyclo*-tetraphosphane unit has been generated, the first process goes on with a symmetrical cleavage forming a *cyclo*-P_4 ligand and eventually two diphosphorus units. In contrast, the alternative pathway leads to *cyclo*-P_3 and P_1 fragments via an unsymmetrical degradation.

The symmetric cleavage has been observed with both 16 and 17 VE fragments, producing mononuclear and bridging dinuclear P_4 butterfly complexes, $L_nM(\eta^2\text{-}P_4)$ and $L_nM(\mu,\eta^{1:1}\text{-}P_4)M'L'_m$, respectively. Remarkably, the first polyphosphorus complex ever described, $[(PPh_3)_2ClRh(\eta^2\text{-}P_4)]$ (**15**), fits in this class of compounds containing a distorted butterfly-like η^2-P_4 tetrahedron [1]. Thus, reaction of P_4 in dichloromethane with the Wilkinson complex (Eq. 6) or other square planar rhodium(I) and iridium(I), $[MX(PR_3)_3]$, complexes at −78 °C gave the slightly soluble and thermally unstable $[(PR_3)_2XM(\eta^2\text{-}P_4)]$ [M=Rh, X=Cl, R=Ph (**15**), *p*-tol (**16**), *m*-tol (**17**); X=Br, R=Ph (**18**); X=I, R=Ph (**19**). M=Ir, X=Cl, R=Ph (**20**)] [1,29]. The structure of **15** was determined by X-ray crystallography, which confirmed the presence of a dihapto coordinated, P-P elongated, P_4 ligand ($d_{P\text{-}P} = 2.4616$ Å). This arrangement was theoretically predicted by Albright et al. for the model complex $[(PH_3)_2ClRh(\eta^x\text{-}P_4)]$ (x=1, 2) for which the optimized side-on coordination was calculated to be 15 kcal mol^{-1} more stable than the optimized η^1-bonding isomer [30].

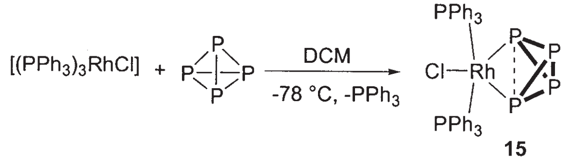

(6)

Complex **15** marks the borderline between a simple two-electron σ-type coordination of the P-P bond to a metal center and its oxidative addition to it. More distorted *bicyclo*-tetraphosphane-P_4 complexes have been installed on a variety of transition metals moieties containing as coligands either Cp^x [31–35] or monodentate [36] and polydentate phosphanes [18,28,37]. Double edge activation of the opposite bonds in the P_4 tetrahedron has been documented for the reaction of the 16 VE fragment $\{Cp^*Co(CO)\}$ obtained via *Co=Co* breakage from the dinuclear precursor $[\{Cp^*Co(CO)\}_2]$ [32]. Remarkably, the dicobalt species, which forms, $[\{Cp^*Co(CO)\}_2(\mu,\eta^{2:2}\text{-}P_4)]$ (**21**), together with $[\{Cp^*Co(CO)\}(\eta^2\text{-}P_4)]$ (**22**), may also be obtained by thermolysis of $[Cp^*Co(CO)_2]$ with **22** (Scheme 3) [32]. The high temperature cothermolysis or cophotolysis of $[\{Cp^*Co(CO)_n\}_m]$ (n+m=2) with P_4 goes a step forward in the direction of disrupting the tetraatomic topology [38–40]. Thus, diphosphorus and monophosphorus ligands have been isolated in bi-, tri-, and tetranuclear complexes of formula $[\{Cp^xCo\}_2(\mu,\eta^{2:2}\text{-}P_2)_2]$ (**23**) (Cp^x=Cp″, Cp‴, Cp^{Si}), $[\{Cp''Co\}_3(\mu_3\text{-}P)_2]$ (**24**), $[\{Cp^xCo\}_3(\mu\text{-}CO)(P_4)]$ (**25**) (Cp^x= Cp″, Cp^{Si}), and $[\{Cp^xCo\}_4(\mu_3\text{-}P)_4]$ (**26**) (Cp^x=

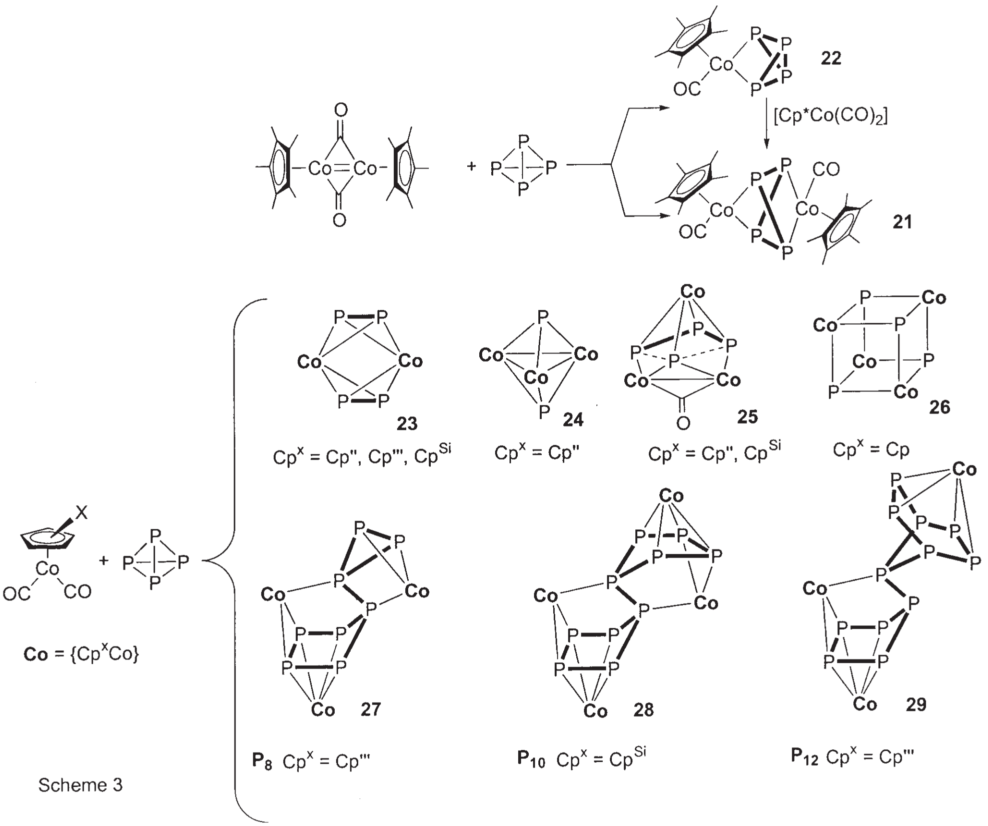

Scheme 3. Reaction of [{$Cp^xCo(CO)$}$_2$] and [$Cp^xCo(CO)_2$] (Cp^x=Cp*, Cp″, Cp‴, Cp^{Si}) with P_4

Cp, Cp″), which incorporate the totally decarbonylated 14 VE fragment {Cp^xCo}. As frequently observed in metal-mediated P_4 chemistry, the reaction is not unidirectional and a variety of polymetallic-polyphosphorus ligands such as P_8 (**27**), P_{10} (**28**), and P_{12} (**29**) (see Sect. 2.2.4.3) have been isolated after chromatographic workup (Scheme 3) [38, 39]. Replacing white phosphorus with yellow arsenic, As_4, has been successfully used to demonstrate the amazing richness and complexity of the products arising from interaction of a transition metal fragment with elemental pnicogen and has also served to clarify some reaction mechanisms involving P_4 [41].

Analogous reactivity is shown by the cognate Rh and Ir complexes, [{$Cp^xM(CO)_n$}$_m$] (m+n=2; M=Rh, Ir) during their cothermolysis with P_4 [31, 38, 42–45]. From a mechanistic viewpoint the stepwise loss of carbonyl ligands in the complexes [{$Cp^xM(CO)_m$}$_n$] (m+n=2; M=Co, Rh, Ir) is the key step as it provides increasing coordinative vacancies at the metal which are suitable to interact with the pnicogen molecule.

The reaction of white phosphorus with $[\{Cp^xM(CO)_n\}_m]$ complexes ($m+n=2$; M=Co, Rh, Ir), also highlights the possibility of achieving further, often unusual, polyphosphorus topologies and nicely addresses the non-innocent role played by the electronic and stereochemical requirements of the Cp-ring substituents. As an example, $[\{Cp^xCo\}_3(\mu\text{-}CO)(P_4)]$ (**25**) ($Cp^x=Cp''$, Cp^{Si}) is formed from the photochemical reaction of P_4 with $[Cp^xCo(CO)_2]$ (Scheme 3) [38]. Complex **25** contains a unique $\eta^{3:2}$-P_4Co_3 assembly where an asymmetric *cyclo*-P_4 ligand is capped by a $\{Cp^xCo\}$ moiety. It corresponds to an advanced stage in the unsymmetrical P_3/P_1 activation of P_4 and represents a minor product of the reaction that ultimately leads to $[\{Cp^xCo\}_2(\mu,\eta^{2:2}\text{-}P_2)_2]$ (**23**) ($Cp^x=Cp''$, Cp''', Cp^{Si}) [38, 46]. Remarkably, the formation of these tricobalt clusters does not occur when $[Cp^*Co(CO)_2]$, containing the sterically less demanding Cp* ligand, is employed under comparable reaction conditions [7, 32, 46].

Additional stabilization can be provided by further reaction with Lewis-acid fragments such as $\{M(CO)_5\}$ that may coordinate to the residual lone pairs of the P atoms (Scheme 4). Using this three-components protocol, Scheer and coworkers were able to develop a rich chemistry through one-pot-reactions by which they could trap a variety of intermediates caught during their transformation pathways [33–35, 47].

The photochemical or thermal activation of dinuclear iron cyclopentadienyl carbonyl complexes, $[\{Cp^xFe(CO)_2\}_2]$, containing sterically demanding coligands was used to elucidate the degradation of P_4 in the presence of fragments with uneven electron count (Scheme 5) [48]. During the photolysis of $[\{Cp''Fe(CO)_2\}_2]$, after cleavage of the first P-P bond by two 17 VE iron fragments, the reaction proceeds through internal rearrangements which affords in cascade the complexes $[\{Cp''Fe(CO)_2\}_2(\mu,\eta^{1:1}\text{-}P_4)]$ (**30**) and $[\{Cp''Fe(CO)_2\}\{Cp''Fe(CO)\}(\mu,\eta^{1:2}\text{-}P_4)]$ (**31**) by leaving the butterfly geometry of the P_4 ligand substantially unchanged. Subsequent photochemical elimination of CO from the partially decarbonylated iron moiety produces a 13 VE fragment that readily inserts into the bridgehead P-P bond of the butterfly ligand, yielding the "quasi-sandwiched" complex $[\{Cp''Fe\}\{Cp''Fe(CO)_2\}(\mu,\eta^{4:1}\text{-}P_4)]$ (**32**) containing a flat cyclic P_4 ligand. The second iron fragment may then decarbonylate and, after inserting into the third P-P bond, expands the tetraphosphorus assembly to an almost planar five-membered ring incorporated into the sandwich complex $[\{Cp''Fe\}\{\eta^5\text{-}P_4Fe(CO)Cp''\}]$ (**33**). Eventually, loss of the last CO ligand causes an internal rearrangement of the FeP_4 cycle and forms $[\{Cp''Fe\}_2(\mu,\eta^{4:4}\text{-}P_4)]$ (**34**) in which an open P_4-chain bridges two equivalent $\{Cp''Fe\}$ moieties.

The existence of a doubly metallated P_4 butterfly ligand in $[\{Cp^xFe(CO)_2\}_2(\mu,\eta^{1:1}\text{-}P_4)]$, which was postulated for some years on the basis of spectroscopic data [48–50], was recently ascertained by X-ray methods in $[\{Cp'''Fe(CO)_2\}_2(\mu,\eta^{1:1}\text{-}P_4)]$ (**35**) [51].

The transformation of P_4 in the coordination sphere of 15 VE fragments has been studied by allowing group-6 carbonyls, $[M(CO)_6]$ (M=Cr, Mo, W), and nickel cyclopentadienyl carbonyl complexes to react using Scheer's one-pot/three-components practice under thermal or photochemical conditions. Remarkably, the combination of P_4, $[Cr(CO)_6]$, and the nickel dimer $[\{Cp^*Ni(CO)\}_2]$ under UV irradiation yields complexes incorporating P_1, P_2, and P_3 lig-

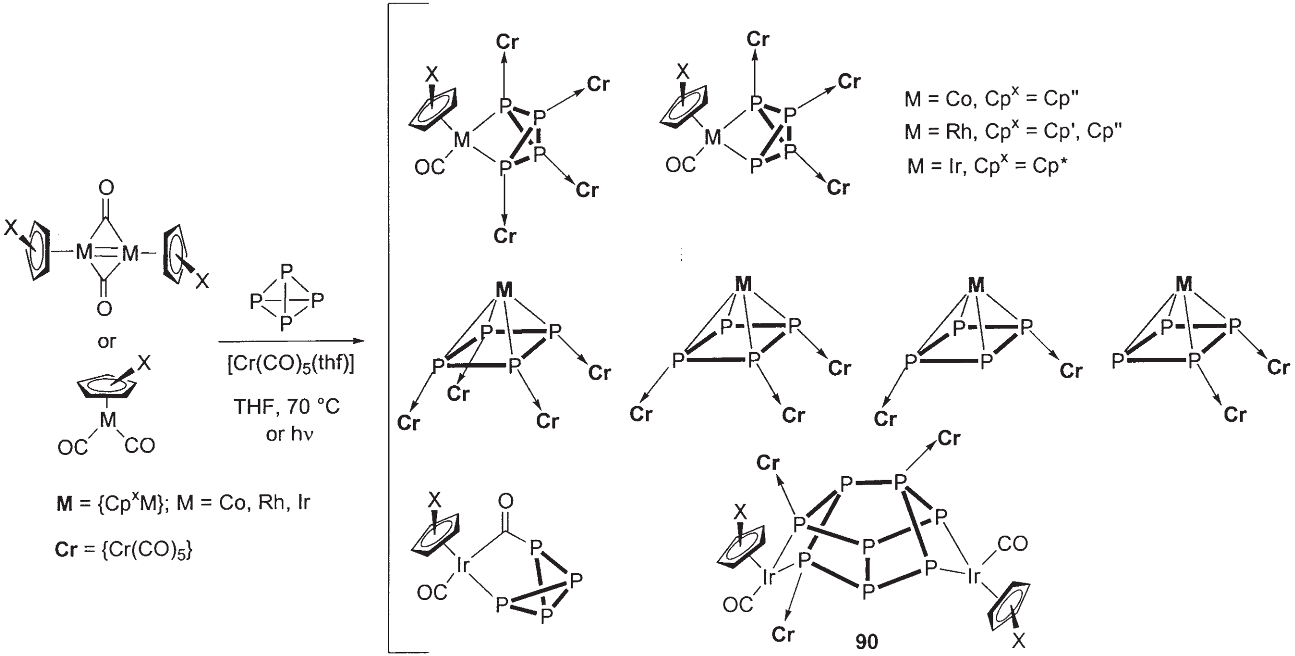

Scheme 4. Reaction of $[\{Cp^xM(CO)_n\}_m]$ (n + m = 2; M=Co, Rh, Ir) with P_4 in the presence of $[Cr(CO)_5(thf)]$

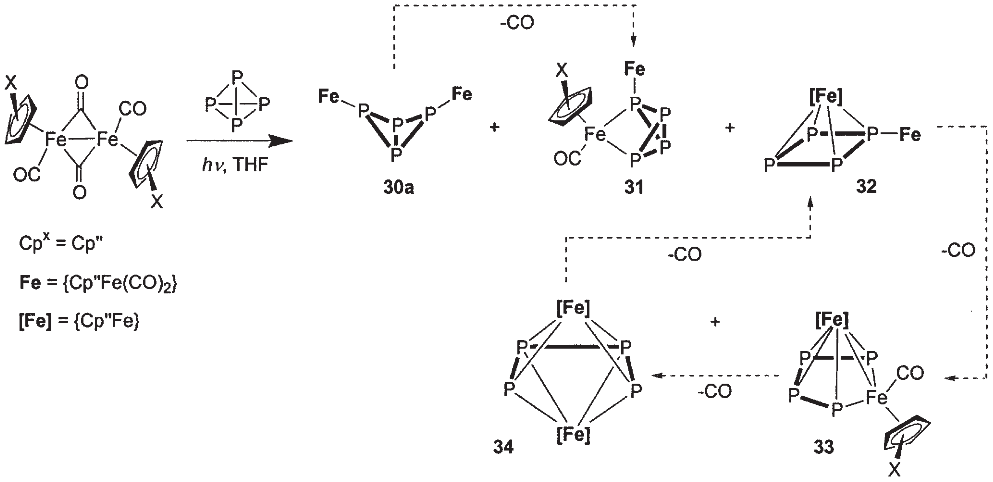

Scheme 5. Photolytic reaction of $[\{Cp''Fe(CO)_2\}_2]$ with P_4

ands together with $[\{Cp^*Ni\}(\eta^{3:1}\text{-}P_4)\{Cp^*Ni(CO)\}\{Cr(CO)_5\}_3]$ (**36**) in which a unique bent *cyclo*-P_4 ligand behaves as a ten electron donor (Scheme 6) [52]. The asymmetric bonding to both 15 and 17 VE metal fragments suggests the preliminary separation into P_3/P_1 units. Photolysis of **36** furnishes the impressive $P_4Ni_2Cr_2$ prismane complex $[\{Cp^*Ni\}_2(\eta^{3:3:1:1}\text{-}P_4)\{Cr(CO)_5\}_2]$ (**37**) featuring an open P_4-chain. From this reaction, the *cyclo*-P_3 complex $[\{Cp^*Ni\}(\eta^{3:1:1:1}\text{-}P_3)\{Cr(CO)_5\}_3]$ (**38**) and the dinickeladiphosphatetrahedrane $[\{Cp^*Ni\}_2(\mu,\eta^{1:1:1:1}\text{-}P_2)\{Cr(CO)_5\}_2]$ (**39**) are also isolated as minor products. Complex **39** is intriguing as it probably forms via dimerization of the undetected intermediate $[Cp^*Ni{\equiv}P \rightarrow Cr(CO)_5]$. Starting from the bent-P_4 complex **36**, the thermal reaction yields **37** as well as, at higher temperature, the novel P_4/P_1Ni_3 cubane $[\{Cp^*Ni\}_3(P_5)\{Cr(CO)_5\}]$ (**40**) with separated μ_3-P and tripodally arranged P_4 ligands. The formation of such a large variety of products (P_1, P_2, P_3, P_4-prismane, P_4/P_1-cubane) also takes place from the direct reaction between P_4 and several $[\{Cp^xNi(CO)\}_2]$ complexes under appropriate thermal or photolytic conditions (Scheme 6) [53, 54]. However, the intermediate species **36**, which is mechanistically central in this chemistry, has been accessible only through the three component reaction thank to the presence of the sterically encumbering $\{Cr(CO)_5\}$ auxiliary [52].

Thermolysis in THF of a mixture of the 17 VE molybdenum dimer $[\{Cp'Mo(CO)_3\}_2]$ (*Mo-Mo*), white phosphorus and excess of $[Cr(CO)_5(thf)]$ gives $[\{Cr(CO)_4\} < (\mu,\eta^{4:1:1:1:1:1}\text{-}P_4)\{Cr(CO)_5\}_4>]$ (**41**) (Scheme 7) [47]. Complex **41** does not contain molybdenum and exhibits a bent and asymmetrically coordinated *cyclo*-P_4 ligand, which is also accessible from direct cophotolysis of white phosphorus and $[M(CO)_6]$ (M=Cr, W) [55, 56]. However, when the same reaction is carried out under ultraviolet irradiation, the molybdenum precursor actively participates in the reaction yielding a mixture of the P_2Mo_2 tetrahedrane $[\{Cp'Mo(CO)_2\}_2<\{\mu,\eta^{2:2:1:1}\text{-}P_2\}\{Cr(CO_5)_2\}>]$ (**42**) and the unusual complex

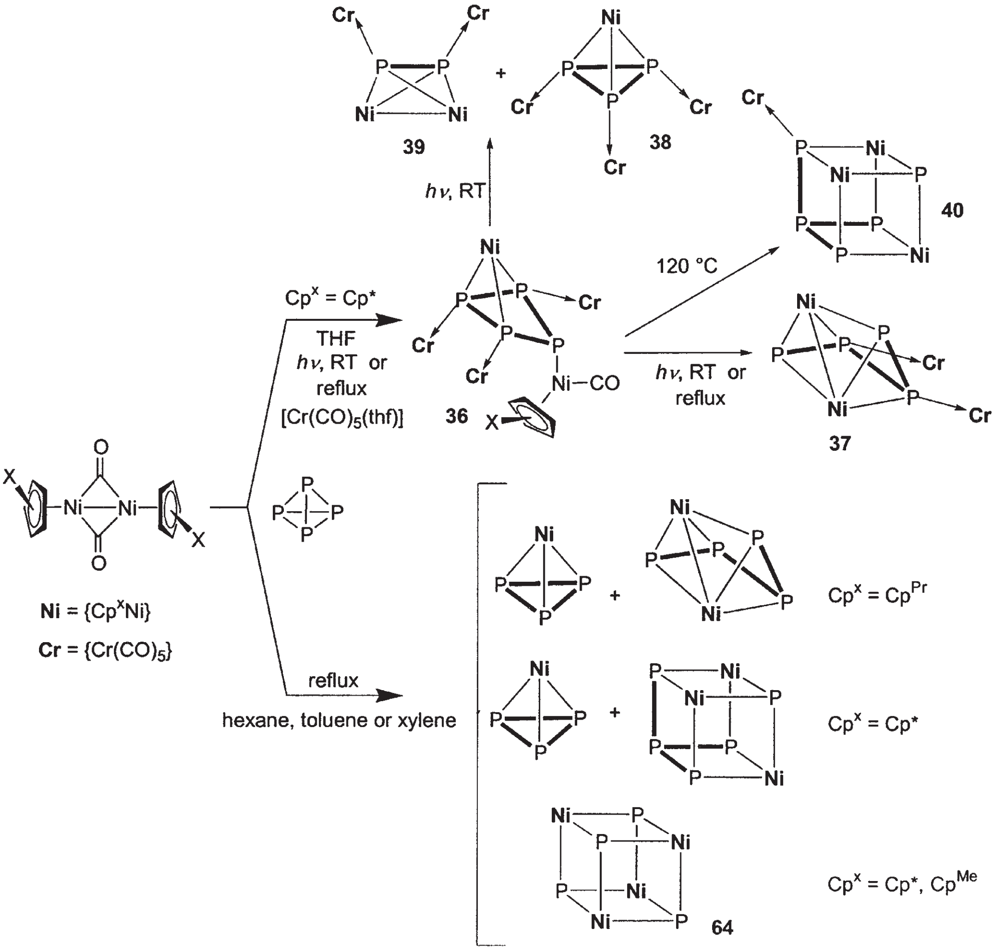

Scheme 6. Reaction of [{$Cp^xNi(\mu\text{-}CO)\}_2$] and P_4 with or without [$Cr(CO)_5(thf)$]

[{$Cp'Mo(CO)_2$}<{$\eta^{3:1:1:1:1}\text{-}P_4H$}{$Cr(CO_5)_2$}$_4$>] (**43**) where the P-H bond likely originates from adventitious water. In contrast, by replacing molybdenum with the lighter homologue [{$CpCr(CO)_3\}_2$] (*Cr-Cr*) in the two-component reaction, tetrahedral clusters, [{$CpCr(CO)_2\}_2(\mu,\eta^{2:2}\text{-}P_2)$] (**44**) and [$CpCr(CO)_2(\eta^3\text{-}P_3)$] (**45**), were obtained after CO loss together with the unprecedented P_{10} complex [{$CpCr(CO)_2\}_5(P_{10})$] (**46**) (see below) [57]. A radical mechanism involving attack of [$CpCr(CO)_x]^{\bullet}$ ($x = 2, 3$) to P_4, consequential homolysis of P-P bonds and formation of the key intermediate radical, [$CpCr(CO)_2(P)]^{\bullet}$, has been proposed (Scheme 7) [58].

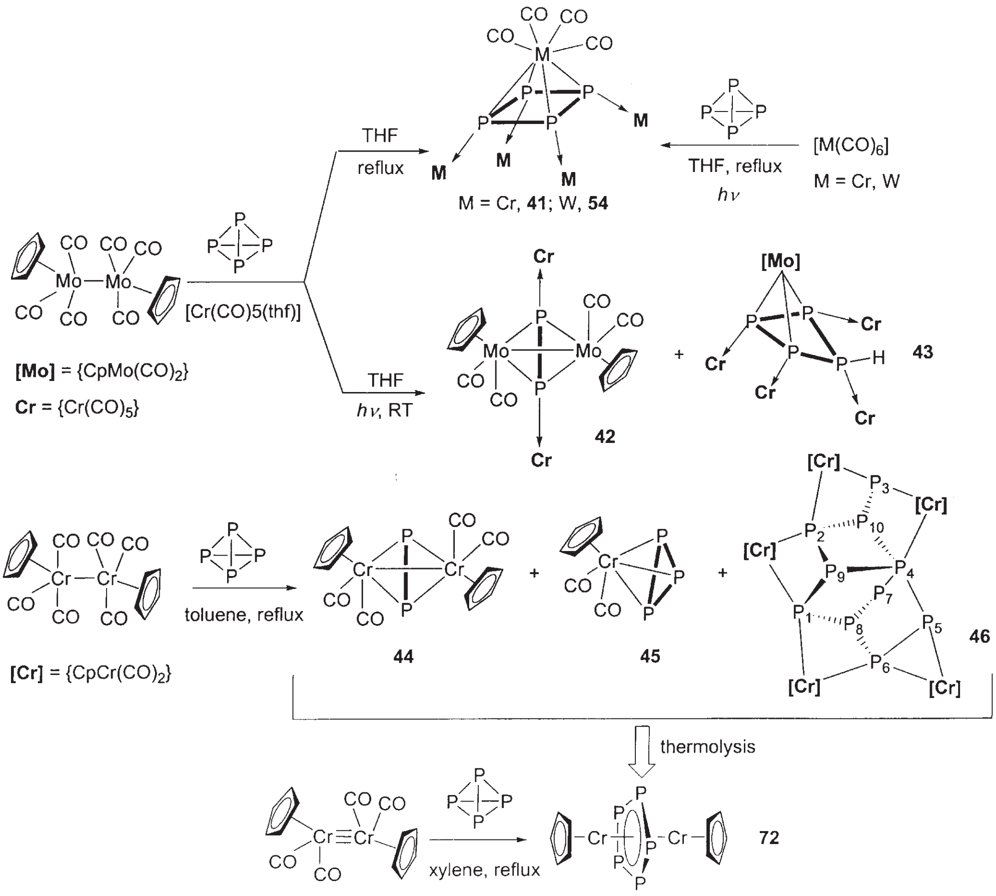

Scheme 7. Thermal and photolytic reaction of [{CpM(CO)$_x$}$_2$] (x = 2,3; M=Cr, Mo) and P_4 with or without [Cr(CO)$_5$(thf)]

2.2.3
P_4 Fragmentation to P_x Species (x < 4)

2.2.3.1
Symmetrical Degradation of P_4 to P_2 Ligands

Diphosphorus ligands stemming from P_4 activation are usually quenched in multinuclear complexes, where they generally adopt the side-on coordination mode. As mentioned in the mechanistic section, multinuclear diphosphorus complexes coordinated to 15 VE metal fragments may form via dimerization of reactive P_1 intermediates and are incorporated into dimetalla-diphosphorus tetrahedranes. However, when P_2-complexes are derived from the direct reaction of even-electron metal precursors and P_4, it is likely that they form from the direct degradation of tetraphosphorus since the intermediacy of terminal P_1 species is highly improbable. Thus, dimetallic bis-diphosphorus pseudo-triple decker derivatives are formed with group-9 metal fragments while group-7 fragments (16 VE) usually adopt the M_2P_2 butterfly arrangement. Accordingly, when the 16 VE fragment $\{Cp^*Re(CO)_2\}$, generated from $[\{Cp^*Re(CO)_2\}_2]$ (*Re=Re*), is treated with white phosphorus, di- and tetrametallic complexes containing two mesomeric diphosphorus ligands, $[\{Cp^*Re(CO)_2\}_2(\mu,\eta^{2:2}\text{-}P_2)]$ (**47**) and $[\{Cp^*Re(CO)_2\}_4(\mu,\eta^{1:1:1:1}\text{-}P_2)]$ (**48**), are formed depending on the reaction conditions (Scheme 8) [59, 60]. Interestingly, with the isoelectronic fragment $[(triphos)Re(CO)_2]^+$ the stable complexes, $[\{(triphos)Re(CO)_2\}(\eta^1\text{-}P_4)]^+$ (**8**), and $[\{(triphos)Re(CO)_2\}_2(\mu,\eta^{1:1}\text{-}P_4)]^{2+}$ (**13**), containing an end-on coordinated P_4 ligand are formed (see above) [17]. Once more, these results emphasize the importance of steric effects in controlling the reactivity of a metal fragment towards P_4 and underline the fundamental role played by ancillary ligands in driving the activation/degradation pathways of the P_4 tetrahedron.

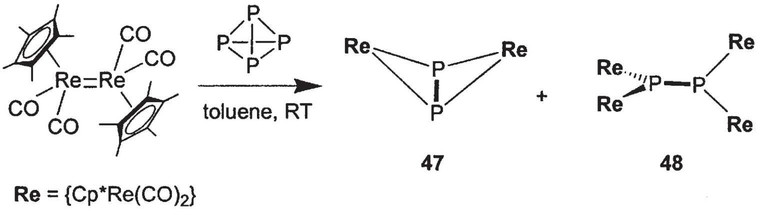

Scheme 8. Reaction of $[\{Cp^*Re(CO)_2\}_2]$ with P_4

2.2.3.2
Unsymmetrical Degradation of P_4 to P_3 and P_1 Ligands

Only few complexes resulting from the unsymmetrical cleavage of the P_4 cage to a P_3 moiety and an isolated P atom have been individuated. Noticeably, in all these cases, the fate of the four P atoms belonging to the reacting P_4 molecule has successfully been followed in the resulting reaction mixture.

An intensively investigated system providing clear-cut evidence for the occurrence of an unsymmetric cleavage of a P_4 ligand to P_3 and P_1 units has recently been reported for the reaction of white phosphorus with the rhodium and iridium trihydrides $[(triphos)MH_3]$ (M=Rh, Ir) (Scheme 9) [37]. The reaction results in the formation of complexes $[(triphos)M(\eta^{2:1}\text{-}P_4H)]^+$ [M=Rh (**49**), Ir (**50**)], where the partially hydrogenated ligand P_4H includes an appendant P atom singly bonded to a P_3 cycle. Further hydrogenation of the partially substituted P atom and extrusion of PH_3 traps the remaining triphosphorus unit (corresponding to one face of the original P_4 tetrahedron) in the thermodynamically stable *cyclo*-P_3 species $[(triphos)M(\eta^3\text{-}P_3)]$ [M=Rh (**51**), Ir (**52**)] [15]. A related process may be envisaged in the reaction of $[(triphos)Rh(R)(C_2H_4)]$ (R=H, Me, Et, Ph) with white phosphorus [28]. In the case at hand, a two-step mechanism involving first the activation of white phosphorus by the 16 VE metal moiety $[(triphos)Rh(R)]^+$, and then the metal-to-phosphorus migration of the organic

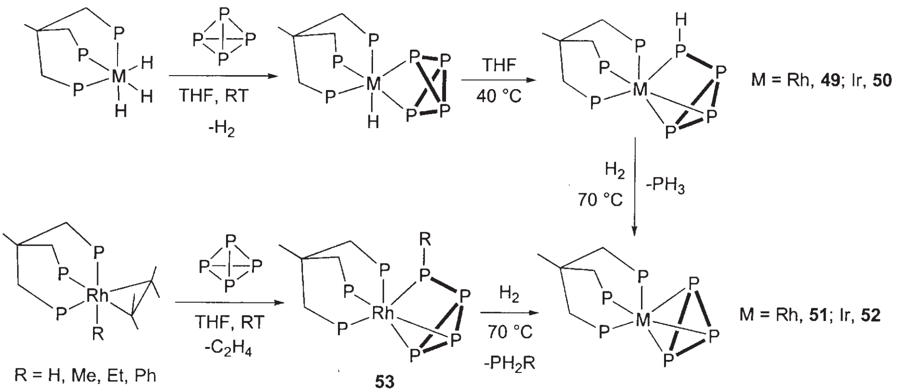

Scheme 9. Reaction of white phosphorus with [(triphos)MH_3] (M=Rh, Ir) and [(triphos) Rh(R)(C_2H_4)] (R=H, Me, Et, Ph)

residue, yields [(triphos)Rh($\eta^{2:1}$-P_4R)] (**53**) where a P_4R ligand is coordinated through three not adjacent P atoms.

Extrusion of a P_3 ligand either from the P_4 cage and other P_x-sources [61–64] commonly takes place in the metal assisted degradation of white phosphorus and related molecules in the presence of triphos metal complexes [5, 7–12, 61–64]. The reaction generally results in the stabilization of *cyclo*-P_3 complexes of formula [(triphos)M(η^3-P_3)]$^{n+}$ (n=0, M=Co, Rh, Ir; n=1, M=Ni, Pd, Pt) and [(triphos)M(μ,$\eta^{3:3}$-P_3)M′(triphos)]$^{n+}$ (n=0–2, M, M′=Fe, Ru, Os, Co, Rh, Ir, Ni, Pd, Pt) exhibiting a more or less distorted octahedral coordination around the metal [15, 65, 66]. However, mechanistic studies on the formation of such species are almost missing, being limited to few unpublished observations [67]. As a summary, THF mixtures of triphos and [(cod)Rh(μ-Cl)]$_2$ in the presence of non-coordinating anions react with one equivalent of white phosphorus within minutes at room temperature to form the *cyclo*-P_3 complex [(triphos) Rh(η^3-P_3)]. A redox process takes place in the reaction between [(triphos)Co (NCMe)$_3$]$^{2+}$ and P_4 in THF/EtOH and likely proceeds via formation of the paramagnetic triple-decker complex [{(triphos)Co}$_2$(μ,η^3-P_3)]$^{2+}$ before yielding [(triphos)Co(η^3-P_3)] [67]. From a mechanistic viewpoint, a chlorophosphinidene fragment "PCl" is formally extruded in the case of rhodium, whereas in the reaction with cobalt a monoelectronic reduction should occur formally extruding a "P^{2+}" unit. In both reactions, however, the outcome of the extruded P atom remains unknown although in the cobalt reaction mixture, the ester (EtO)$_2$EtPO, likely generated from the mechanistically non-innocent ethanol solvent, has been identified by combined HPLC and mass spectrometry [67–69].

2.2.3.3
Polyphosphorus Ligands from Progressive P-P Breakage

Entrenched in the formal P-P activation scheme and the mechanistic rules outlined in the previous sections, we intend to provide in this section a critical ac-

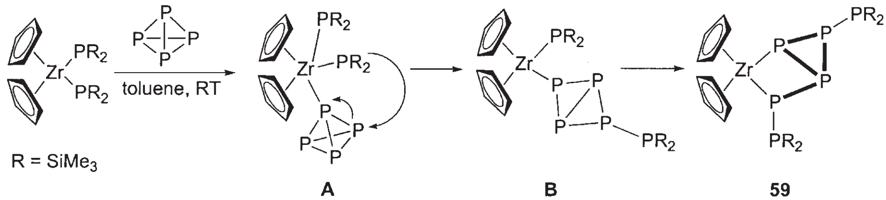

Scheme 10. Proposed mechanism accounting for the reaction of $[Cp_2Zr\{P(SiMe_3)_2\}_2]$ with white phosphorus

count of the final, thermodynamically stable, products deriving from the direct reaction of P_4 with transition metal complexes. Thus, in the following part we will order the activation/degradation products, for which insufficient mechanistic details are given, according to the numbers of P-P bonds cleaved. Sorting the P_x-containing complexes by this modus operandi may be helpful to rationalize the basic patterns exhibited by the reaction of transition metal complexes with elemental phosphorus and may contribute to better approach the directed syntheses of P_x complexes. Moreover, working out the polyphosphorus ligands within this general frame could eventually set the basis for the development of a rational approach to specific reactions aimed at functionalizing white phosphorus in the coordination sphere of a transition metal complex [68, 69].

As the cleavage of the first P-P bond to yield P_4-butterfly complexes has extensively been discussed in the previous sessions, we will now skip to illustrate those polyphosphorus ligands formed via rupture of a second bond in the tetraphosphorus tetrahedron.

2.2.3.3.1
Cleavage of Two P-P Bonds

The simultaneous cleavage of two P-P bonds in the P_4 tetrahedron occurs during the photochemical reaction between group-6 metallocarbonyls and P_4 and affords the *cyclo*-P_4 complexes $[\{M(CO)_4\} < (cyclo\text{-}P_4)\{M(CO)_5\}_4 >]$ [M=Cr (**41**), W (**54**)] (Scheme 7) [55, 56]. In such derivatives, the planar P_4 ring acts as 12 electron donor via face-capping and lone-pair coordination. Formation of *cyclo*-P_4 complexes also takes place from the photochemical reaction of $[Cp^xM(CO)_4]$ (M=V, Cp^x=Cp* [70]; M=Nb, Cp^x=Cp* [71]; M=Ta, Cp^x=Cp″ [72]) with P_4. These reactions usually result in complicated product mixtures from which the P_4 complexes $[Cp^*V(CO)_2(cyclo\text{-}P_4)]$ (**55**), $[\{Cp^*V(CO)_2\}(\mu,\eta^{1:4}\text{-}P_4)\{Cp^*V(CO)_3\}]$ (**56**) [70], $[Cp^*Nb(CO)_2(\eta^4\text{-}P_4)]$ (**57**) [71], and $[\{Cp''Ta\}_3(\mu_3\text{-}P_4)(\mu_3\text{-}P_2)]$ (**58**) [72] were isolated after chromatographic workup. In the niobium derivative a slightly bent tetraphosphorus cyclic ligand was determined by X-ray crystallography. The small distortions of the P-P network suggest the presence of an allylic P_3 chain/P_1 pre-separation.

The alternative cleavage of two P-P bonds (sketch **III** in Scheme 2) has so far been described only for polyphosphorus complexes stabilized by further bonds with organic residues. To the best of our knowledge, these conditions are matched only in two cases, i.e., the reaction of P_4 with either $[Cp_2Zr(PR_2)_2]$ (R=$SiMe_3$) [73] or with the rhodium and iridium complexes [(triphos)M(R)(C_2H_4)] (M=Rh; R=H, Me, Et, Ph; M=Ir, H) detailed above [28, 37]. In the reaction with the zirconocene derivative, a mechanism has been proposed (Scheme 10) which entails a concerted pre-coordination of one P atom to the electrophilic zirconium center (**A**) accompanied by the nucleophilic attack of one phosphido ligand to the activated η^1-coordinated P_4 ligand (**B**). P-P bond scission, phosphido-migration, and intramolecular rearrangement yields the P_6-complex $[Cp_2Zr\{\eta^{1:1}\text{-}P_4(PR_2)_2\}]$ (**59**) where the organic residues are attached to two peripheral phosphorus atoms [73].

2.2.3.3.2
Cleavage of Three P-P Bonds

Cleavage of three P-P bonds in the molecule of white phosphorus occurs during the thermal reaction of Co(II) salts with P_4 in the presence of dppm (Eq. 7) [74]. The reaction affords $[Co\{Ph_2PCH_2P(Ph)_2PPPP(Ph_2)PCH_2PPh_2\}]^+$ (**60**), which features a unique P_8-ligand with a *zig-zag* P_6-chain formed by the four atom of P_4 and two PPh_2 ends from two distinct dppm ligands which have undergone the nucleophilic attack of the activated tetraphosphorus ligand:

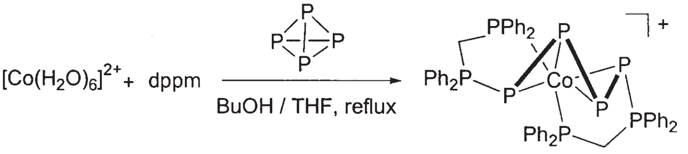

60

(7)

Open chain naked polyphosphorus ligands in a cisoid conformation are found only in multinuclear complexes. A beautiful example of this P_4-topology was reported by Scherer et al. in 1988 [31] in a study aimed at investigating the reaction of $[Cp^{Et}Rh(CO)_2]$ with P_4 in refluxing xylol (Eq. 8). After workup, crystals of $[\{Cp^{Et}Rh\}(\mu,\eta^{4:2}\text{-}P_4)\{Cp^{Et}Rh(CO)\}]$ (**61**) were separated. Compound **61** is not the thermodynamic sink of the reaction and decarbonylates after prolonged heating to transform into the bis(diphosphorus) complex $[\{Cp^{Et}Rh\}_2(\mu,\eta^2\text{-}P_2)_2]$ (**62**). The same topology is also found in group-8 complexes $[\{Cp^xM(CO)_2\}_2(P_4)]$ (M=Fe, Cp^x=Cp″ [48], Cp‴, Cp^{Pr} [51]; M=Ru, Cp^x=Cp″ [75]):

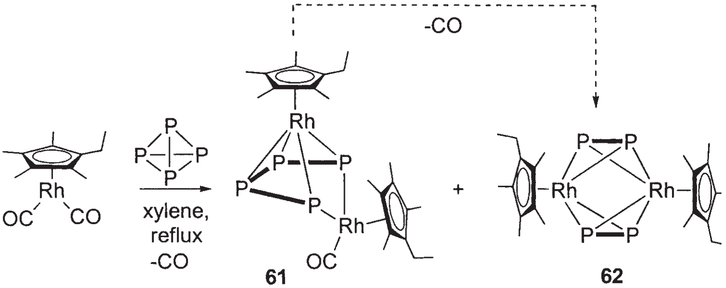

61 **62**

(8)

The tripodal topology (**V** in Scheme 2) has already been introduced (see Sect. 2.2.3.3.1) when we briefly mentioned the tantalum cluster $[\mathrm{Cp}''_3\mathrm{Ta}_3(\mu_3\text{-}\mathrm{P}_4)(\mu\text{-}\mathrm{P}_2)]$ (**58**) [72, 76, 77] and the trinickelatetraphosphacubane $[\{\mathrm{Cp}^*\mathrm{Ni}\}_3(\mathrm{P}_5)\{\mathrm{Cr(CO)}_5\}]$ (**40**) (see Scheme 6) [78] which are genuine examples of complexes containing this uncommon opened P_4 ligand.

2.2.3.3.3
Cleavage of Four P-P Bonds

An intriguing example of P_4 activation, en route to the separation into two diphosphorus units, has been recognized in the complex $[\mathrm{Fe}_6(\mathrm{CO})_{20}(\mu_3,\eta^{1:1:1}\text{-}\mathrm{P}_4)]$ (**63**), which is straightforwardly generated from the thermal reaction of white phosphorus and $[\mathrm{Fe}_2(\mathrm{CO})_9]$ in boiling benzene (Eq. 9) [79]:

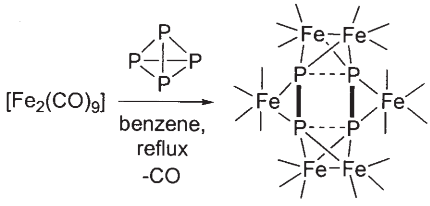

63

(9)

Two completely separated P_2 ligands originating from P_4 activation are present in the previously mentioned complexes $[\{\mathrm{Cp^xM}\}_2(\mu,\eta^{1:1}\mathrm{P}_2)_2]$ (M=Co, Rh, Ir). Orthogonally arranged P_2 ligands similar to a diphosphido dumbbell were found in the dodecahedral cluster $[\{\mathrm{Cp'Fe}\}_4(\mu,\eta^{1:2:2:1}\text{-}\mathrm{P}_2)]$ which is generated via high temperature cothermolysis of $[\{\mathrm{Cp'Fe(CO)}_2\}_2]$ with P_4 [80].

2.2.3.3.4
Cleavage of Six P-P Bonds

Transition metal complexes incorporating single P atoms originating from the cleavage of all the six P-P bonds contained in the P_4 tetrahedron were found in the tetraphosphatetrametalla cubanes $[\{\mathrm{Cp^xNi}(\mu_3\text{-P})\}_4]$ (**64**) (Scheme 6) [56] and $[\{\mathrm{CpCo}(\mu_3\text{-P})\}_4]$ (**26**) (Scheme 3) [38–40, 81, 82]. In keeping with the spatial disposition of the pnicogen atoms, the structures of both **26** and **64** can also be described as a P_4 tetrahedron with each face capped by a transition metal moiety. Complex **26**, which was reported by Dahl and coworkers in 1973, is historically relevant being the first example ever reported of a metal complex incorporating naked P atoms (Fig. 2). No hint about the mechanistic course leading to the formation of these M_4P_4 clusters has been yet reported. The intriguing possibility that the cubane may be assembled via a concerted tetramerization of terminal $[\mathrm{Cp^xM}{\equiv}\mathrm{P}]$ phosphido moieties cannot be excluded.

Splitting up of P_4 into four separate P ligands integrated in four molecules of $[\mathrm{P}{\equiv}\mathrm{Mo(NRR')}_3]$ (**65**) ($\mathrm{R}=3,5\text{-}\mathrm{C}_6\mathrm{H}_3\mathrm{Me}_2$, $\mathrm{R'}=\mathrm{C(CD_3)_2CH_3}$), takes place, under surprisingly gentle conditions, from the direct interaction of the trigonal planar paramagnetic complex $[\mathrm{Mo(NRR')}_3]$ with white phosphorus in diethyl ether [83, 84]. The reaction runs via not yet identified intermediates.

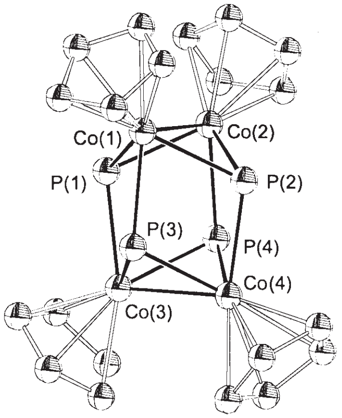

Fig. 2. Structure of the tetracobaltatetraphospha cubane [{CpCo(μ_3-P)}$_4$] (**26**). Adapted from [81]

Extrusion of single P atoms and their stabilization in transition metal complexes is a common feature in the reactivity of P_4 with metal complexes. Terminal phosphido species, M≡P, either as putative or intercepted intermediates, play a key role in the reaction of P_4 with 15 VE fragments. Thus, starting from either [$W_2(OR)_6L_2$] ($W \equiv W$) (R=*i*-Pr) [6, 85, 86] or the isolobal [$Co_2(CO)_8$] [87–89], the formation of M_xP_{4-x} tetrahedranes (x=3) incorporating P_1, P_2, and P_3 ligands has been observed. Mechanistic insights have been obtained for the reaction involving the tungsten reagent [6,86], and it has been proposed that the generation of the terminal phosphido species [$(OR)_3W{\equiv}P$] is mandatory to account for the formation of P_1 and P_2 complexes.

2.2.4
Aggregation to P_x Species (x > 4) Following P_4 Activation

The formation of polyphosphorus P_x ligands with more than the four atoms dowry provided by the P_4 reagent is a relatively common process during the interaction of P_4 with transition metal systems. This behavior can be explained by assuming that the initial P_x (x < 4) units resulting from the disruption of the P_4 tetrahedron can aggregate to assemble larger polyphosphorus ligands. Mechanistic investigations in this field are very sparse although some of these complexes have had paramount importance for the development of the isolobal-based chemistry between P atoms and CH units [2].

2.2.4.1
Pentaphosphacyclopentadienyl, P_5, Complexes

The direct reaction of white phosphorus with dinuclear metallocenes is the most useful entry to compose the planar *cyclo*-P_5 ligand isolobal with the Cp anion [5] although Baudler et al. demonstrated that ionic metathesis may be used to prepare similar derivatives [90]. The pentaphosphacyclopentadienyl ligand

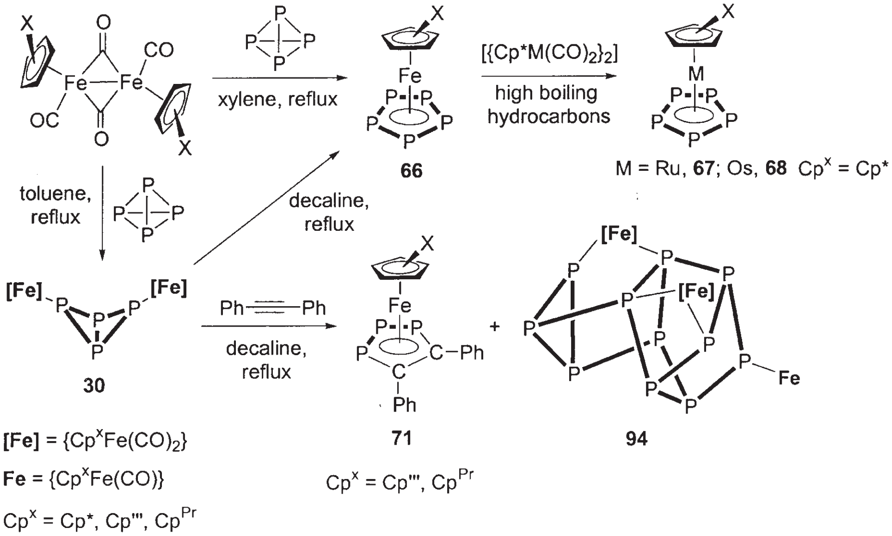

Scheme 11. Synthesis of η^5-P_5 iron complexes and related chemistry

may either be incorporated in group-8 cyclopentadienyl metal-complexes $[Cp^xM(\eta^5\text{-}P_5)]$ [M=Fe (**66**) [91,92], Ru (**67**) [93], Os (**68**) [93] (Scheme 11) or act as internal slice in triple decker compounds containing iron, $[\{CpFe\}(\mu,\eta^{5:5}\text{-}P_5)\{Cp^*Fe\}]PF_6$ [94a], or group-6 metals, $[\{Cp'''M\}_2(\mu,\eta^{5:5}\text{-}P_5)]$ [M=Cr (**69**), Mo (**70**)] [94b]. Careful investigation of the high temperature generation of $[Cp'''Fe(\eta^5\text{-}P_5)]$ from $[\{Cp'''Fe(CO)_2\}_2]$ and P_4, reveals that **66** forms via the P_4 butterfly complex $[\{Cp'''(OC)_2Fe\}_2(\mu,\eta^{1:1}\text{-}P_4)]$ (**30**) [51]. A tentative mechanistic hypothesis entails that a P_3 fragment is first extracted from the bicyclo-P_4 ligand and then coupled with a P_2 fragment. In keeping with this mechanistic picture, prolonged thermolysis of **30** with diphenylacetylene affords the intriguing 1,2,3-triphospholylyl species $[\{Cp'''Fe\}(\eta^5\text{-}P_3C_2Ph_2)]$ (**71**) where a P_3 unit originating from the tetraphosphorus ligand is coupled with the alkyne (Scheme 11) [95]. Thermolysis in the absence of any external ligand leads to the known pentaphosphacyclopentadienyl species $[\{Cp'''Fe\}(\eta^5\text{-}P_5)]$ in which the P_3 unit has been incorporated in a *cyclo*-P_5 ring [95]. The mechanistic evidence arising from this detailed investigation represents a milestone to understand the formation of P_5 sandwich complexes and stresses the isolobal relationship between $P{\equiv}P$ and $HC{\equiv}CH$.

Cothermolysis of dinuclear chromium complexes $[\{Cp^xCr(CO)_n\}_2]$ [n=2, (*Cr*≡*Cr*); 3, (*Cr-Cr*)] with white phosphorus has been used by Goh and coworkers to generate a family of derivatives incorporating P_2, P_3 and P_5 ligands (Scheme 7) [58, 96]. Remarkably, the paramagnetic dichromium triple decker derivative $[\{Cp^*Cr\}_2(\mu,\eta^5\text{-}P_5)]$ (**72**) has been the first *cyclo*-P_5 complex characterized by X-ray crystallography [94b].

The unexpected formation of the unique tetrachromium derivative $[<\{CpCr(CO)\}_2(\mu\text{-}PH)>\{(CpCr)_2(\eta^{5:5:1:1}\text{-}P_5)\}]$ (**73**), which is the first η^5-P_5 triple

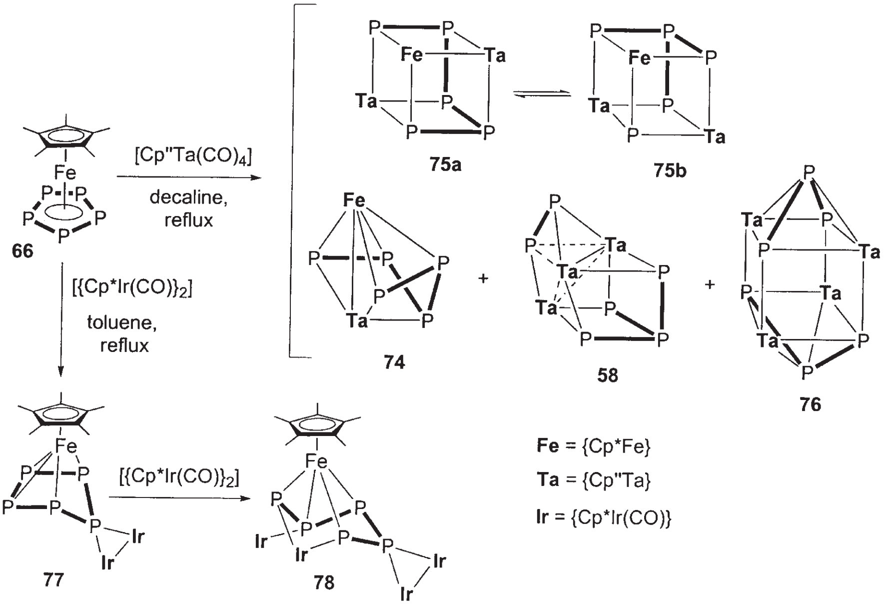

Scheme 12. Reaction of [Cp*Fe(η^5-P_5)] with [Cp″Ta(CO)$_4$] and [{Cp*Ir(CO)}$_2$]

decker complex coordinated to exocyclic transition-metal moieties, has recently been reported by Scheer et al. from the reaction of [{Cp(CO)$_2$Cr}$_2$(μ,$\eta^{2:2}$-P_2)] with LiHBEt$_3$ [97].

Rearrangements of preformed polyphosphorus units play a major role during the reaction of organometallic species with P_x complexes and often makes unpredictable the outcome of the reaction. However, in some cases, especially starting with *cyclo*-P_5 complexes, the primary products could be isolated and characterized. Thus, cothermolysis of [Cp*Fe(η^5-P_5)] with [Cp″Ta(CO)$_4$] in boiling decaline (Scheme 12) yields the previously mentioned tritantalum cluster **58** and the mixed complex [{Cp*Fe}(μ,$\eta^{4:3}$-P_5){TaCp″}] (**74**), where the Ta fragment inserts into the *cyclo*-P_5 ligand forming a folded P_5 chain [72, 75]. Insertion of a second tantalum into the adjacent P-P bond gives the trimetallic species [{Cp*Fe}(μ,$\eta^{2:2:3}$-P_5){TaCp″}$_2$] (*Fe-Ta*) (**75a**) which equilibrates with [{Cp*Fe}(μ,$\eta^{2:3:3}$-P_5){TaCp″}$_2$] (**75b**) [75]. In the latter complex, separated P_1 units and tripodal P_4 ligands may be distinguished, while in the former derivative an edge-opened folded P_5-chain is stabilized. The P_5 topology is lost in the bis-triphosphorus tetratantalum species [{Cp″Ta}$_4$(P_3)$_2$] (**76**) which forms together with **58** and the Fe/Ta mixed species.

In contrast, the reaction of [Cp*Fe(η^5-P_5)] with [{Cp*Ir(CO)}$_2$] transforms the planar P_5 ligand into a folded *cyclo*-P_5 envelope (**77**), which, after addition of a second iridium complex, is definitely cleaved to a P_5 chain (**78**) (Scheme 12) [98].

Cothermolysis of **66** with [Cp^{x}Co(CO)$_2$] yields complexes with P_4 and P_1 ligands incorporated in a distorted cubane or in trigonal bipyramidal polyhedron

[82]. Similarly, during the cothermolysis of **66** with [$\{Cp^xFe(CO)_2\}_2$] [80] or [$\{Cp^*Co(CO)\}_2$] [82, 99, 100], diphosphorus ligands may be installed into a dodecahedron, while P_1 ligands may be incorporated in a distorted trigonal pyramid. The formation of these heterometal complexes through a synthetic procedure, which leaves out the use of white phosphorus, nicely illustrates the potentiality of P_5 complexes to serve as sources of phosphorus units.

As a closing note on *cyclo*-P_5 chemistry, it is worth mentioning that transfer of the intact *cyclo*-P_5 ring from the [$Cp^xM(\eta^5\text{-}P_5)$] to the heavier congeners [Cp^xM] (M=Ru, Os) is a suitable method to prepare different phosphametallocenes [93]. The possibility to exchange intramolecularly polyphosphorus units between different transition metal systems has only occasionally been reported. Well documented examples are the transfer of a P_2 ligand from [$\{Co(CO)_3\}_2(\mu,\eta^{2:2}\text{-}P_2)$] to [$\{(i\text{-}PrO)_3W\}\{(i\text{-}PrO)_2(py)W\}$] yielding [$\{(i\text{-}PrO)_3W\}\{(i\text{-}PrO)_2(py)W\}(\mu,\eta^{2:2}\text{-}P_2)$] [85a], and the relocation of the entire E_2X cyclic-unit in the reaction of [$(triphos)Co(\eta^3\text{-}E_2X)$]$^+$ with [$\{(cod)Rh(\mu\text{-}Cl)\}_2$] and triphos to afford the dirhodium complexes [$\{(triphos)Rh\}_2(\mu,\eta^{3:3}\text{-}E_2X)$]$^+$ (E=P, As; X=S, Se) [101].

2.2.4.2
Hexaphosphabenzene, P_6, Complexes

The amazing complex [$\{Cp^*Mo\}_2(\mu,\eta^{6:6}\text{-}P_6)$] (**79**), containing a triple decker dimolybdenum complex sandwiching a hexaphosphabenzene *cyclo*-P_6 ring, was first described by Scherer and coworkers in 1985 during a study aimed at ex-

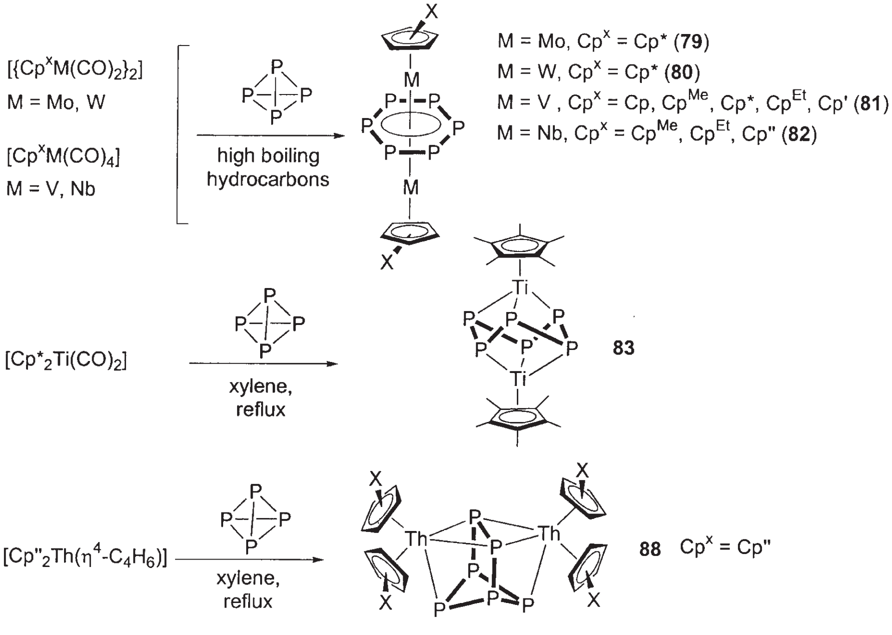

Scheme 13. Synthesis of the hexaphosphabenzene complexes [$\{Cp^xM\}_2(\mu\text{-}P_6)$]

ploring the coordination abilities of molybdenum carbonyls stabilized by cyclopentadienyl ligands towards white phosphorus (Scheme 13) [102]. The outstanding importance of this complex lies in the stabilization of the six-membered *cyclo*-P_6 as a bridging hexahapto ligand, a molecule which represents the all-phosphorus counterpart of benzene.

At present, the intriguing *cyclo*-P_6 ligand has been stabilized in a variety of triple decker complexes of general formula $[\{Cp^xM\}_2(\mu\text{-}P_6)]$ (M=Mo (**79**) [102], W (**80**) [103], V (**81**) [70, 103], Nb (**82**) [71, 104], and Ti (**83**) [105]) via cothermolysis of an appropriate half-sandwich precursor with white phosphorus in high boiling aromatic hydrocarbons. Depending on the transition metal and the overall electron count of the triple decker complex, severe distortions from the idealized D_{6h} symmetry can occur. As a matter of fact, deformations towards bisallylic or puckered *cyclo*-P_6 geometries have been crystallographically confirmed for niobium $[\{Cp^xNb\}_2(\mu,\eta^{6:6}\text{-}P_6)]$ (**82**) and titanium $[\{Cp^*Ti\}_2(\mu,\eta^{3:3}\text{-}P_6)]$ (**83**) complexes, respectively.

From a mechanistic viewpoint, the formation of the *cyclo*-P_6 ligand from P_4 has not yet been completely clarified. Nevertheless, suggestive hypotheses based on the dimerization of P_3 units or the trimerization of P_2 units have been proposed [70, 102, 106]. The latter mechanism is particularly intriguing as it parallels the well-known metal-mediated cyclotrimerization of acetylenes in the coordination sphere of cobaltocenes [107].

Supporting evidence for the formation of the hexaphosphorus ligand via cyclotrimerization of P_2 fragments, is provided by the formation of the *cyclo*-P_6 ligand in the seminal Scherer's complex $[\{Cp^*Mo\}_2(\mu,\eta^{6:6}\text{-}P_6)]$ by cothermolysis of $[\{Cp^*(CO)Mo\}_2(\mu,\eta^2\text{-}P_2)_2]$ (**84**) with white phosphorus [108]. In agreement with this alternative mechanistic picture, it has recently been observed that the heterometallic sandwich complex $[\{Cp^*Fe\}\{Cp^*Mo\}(\mu,\eta^{4:2}\text{-}P_4)(\mu,\eta^{2:2}\text{-}P_2)]$ (**85**), generated via cothermolysis of $[\{Cp^*(CO)Mo\}\{Cp^xFe\}(\mu,\eta^{2:2}\text{-}P_2)_2]$ (**86**) and P_4 [109], may transform into **79** and $[\{Cp^xFe\}(\eta^5\text{-}P_5)]$ under suitable thermal conditions [110].

The isolation of stable valence isomers is a not yet completely accomplished goal in the chemistry of transition-metal complexes incorporating polycyclic P_6 ligands. Nevertheless, bimetallic derivatives exhibiting an isolated valence isomer of *cyclo*-P_6 have also been synthesized and characterized by spectroscopic and crystallographic methods. A beautiful X-ray authenticated example is provided by the actinide complex $[\{Cp''Th\}_2(\mathit{bicyclo}\text{-}\mu,\eta^{3:3}\text{-}P_6)]$ (**88**) where the P_6 unit endorses to a formally edge-opened all-phosphorus ligand resembling benzvalene [111]. Figure 3 compares the X-ray structure of the remarkable complexes $[\{Cp^*W\}_2(\mu,\eta^6\text{-}P_6)]$ (**80**), $[\{Cp^*Ti\}_2(\mu,\eta^{3:3}P_6)]$ (**83**), and $[\{Cp''Th\}_2(\mathit{bicyclo}\text{-}\mu,\eta^{3:3}\text{-}P_6)]$ (**88**) which exhibit different forms of *cyclo*-P_6 ligand (planar, puckered and bicyclic ring, respectively).

2.2.4.3
High Nuclearity Polyphosphorus P_x Complexes ($x > 6$)

Polyphosphorus P_x ligands with nuclearity higher than 6 are usually obtained as byproducts from thermal reactions involving white phosphorus. Therefore,

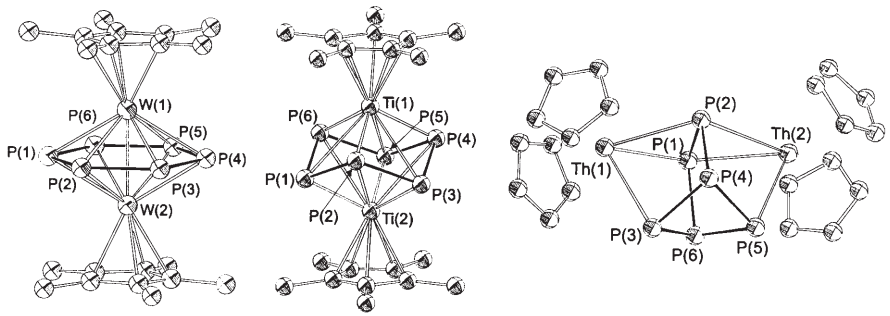

Fig. 3. Structure of the hexaphosphabenzene complexes $[\{Cp^*W\}_2(\mu,\eta^{6:6}\text{-}P_6)]$ (**80**), $[\{Cp^*Ti\}_2(\mu,\eta^{3:3}\text{-}P_6)]$ (**83**), and $[\{Cp''Th\}_2(bicyclo\text{-}\mu,\eta^{3:3}\text{-}P_6)]$ (**88**). Adapted from [104, 106, 112] respectively

their synthesis, which is accompanied by the formation of several, often more abundant, low-nuclearity species, appears typically to be driven by serendipity. Remarkably, the possible architectures accessible with high-nuclearity polyphosphorus ligands are still far from being entirely exploited. A number of possible P_x topologies (x > 6) have not yet been synthesized directly from white phosphorus. For example, complexes containing P_7 ligands in either norbornadiene (**A**) or nortricyclane (**B**) skeletons (Scheme 14), have never been prepared from white phosphorus. The known way to prepare P_7-complexes starts from the Zintl anion P_7^{3-} [112]. Noticeably, when Li_3P_7 is reacted with $[NiCl_2(PBu_3)_2]$, head-to-head dimerization of the P_7^{3-} ligand occurs to afford the richest P_x ligand so far known, i.e., $[\{Ni(PBu_3)_2\}_4(P_{14})]$ (**89**), where two P_7 ligands are held together by an elongated P-P bond [113].

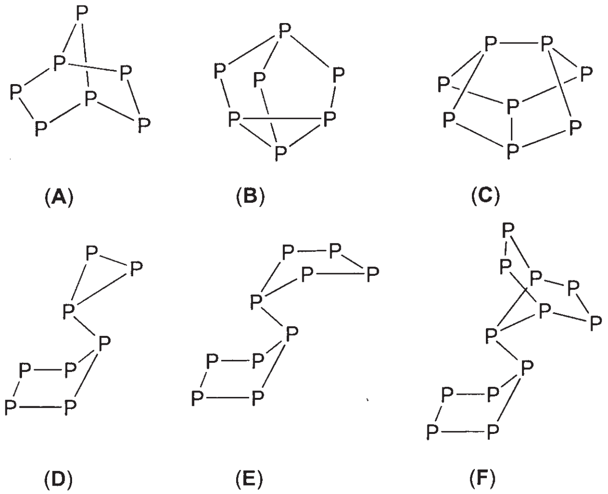

Scheme 14. Sketches of some polyphosphorus P_x ligands with x > 6

According to theoretical calculations [114], the most stable modification of a neutral P_8 ligands is expected to be the cuneane structure (**C**), which is found in the phosphorus allotrope known as Hittorff's phosphorus [115, 116]. Surprisingly, a ligand conforming to this structural motif has been stabilized in the mixed iron/iridium complex $[\{Cp^*Ir(CO)\}_2(\mu,\eta^{2:2:1:1:1}\text{-}P_8)\{Cr(CO)_5\}_3]$ (**90**), prepared either by photolysis or thermolysis of $[Cp^*Ir(CO)_2]$ with P_4 in the presence of excess $[Cr(CO)_5(thf)]$ (Scheme 4) [35]. The same unit has also been recognized in the iron derivatives $[\{Cp^{Me}Fe(CO)\}_2(\mu,\eta^{2:2:1:1}\text{-}P_8)\{Cp^{Me}Fe(CO)_2\}_2]$ (**91**) and $[\{Cp^{Me}Fe(CO)\}_2(\mu,\eta^{2:2:1:1:1:1}\text{-}P_8)\{Cp^{Me}Fe(CO)_2\}\{Fe(CO)_4\}\{Cp^{Me}Fe_2(CO)_5\}]$ (**92**) prepared by photolysis of $[\{Cp^{Me}Fe(CO)\}_2]_2$ and P_4 [115].

Starting from the *bicyclo*-(P_5-P_3) polyhedron (**D**) the "homologation" of polycyclic polyphosphorus ligands with stepwise increments corresponding to P_2 units has been accomplished. Complexes of general formula $[\{Cp'''Co\}_x(P_{12-n})]$ [x=3; n=0 (**29**), 4 (**28**), x=4, n=2 (**27**)] have been isolated and, for the P_8 and P_{10} complexes, characterized by X-ray methods [38, 39]. The related P_{10}-rhodium derivative $[\{Cp''Rh\}_4(P_{10})]$ (**93**) is also known [42]. Remarkably, all these complexes, whose astounding structures are summarized in Scheme 3 share the same basic motif (**D–F**) consisting of a bent P_5 envelope connected through an isolated P-P bond to a second uneven-numbered P_x fragment (x=3, 5, 7).

A quite unusual geometry is encountered in Goh's P_{10} complex $[\{CpCr(CO)_2\}_5(P_{10})]$ (**46**) generated by cothermolysis of $[\{CpCr(CO)_3\}_2]$ (*Cr-Cr*) with P_4 (Scheme 7) [117]. The genesis of **46** is unclear as it is the formation of the P_{11} ligand in $[\{Cp^{Pr}Fe(CO)_2\}(\mu,\eta^{1:2:2}\text{-}P_{11})\{Cp^{Pr}Fe(CO)\}_2]$ (**94**) from the reaction of $[\{Cp^{Pr}Fe(CO)_2\}_2(\mu,\eta^{1:1}\text{-}P_4)]$ (**30**) with tolane (Scheme 11) [95]. The latter compound is particularly remarkable being the first polyphosphorus complex with an uneven number of P atoms (apart from P_3 and P_5) directly accessible from white phosphorus [5].

3
^{31}P-NMR Spectral Data for Transition Metal Complexes Containing P_x Ligands from P_4 Degradation

The huge variation of ^{31}P-NMR chemical shifts and the big magnitude of $^1J(P,P)$ coupling constants exhibited by transition metal complexes incorporating P_x ligands represent a formidable tool to get accurate and easily accessible information about the solution structure of the compounds obtained from the reaction of P_4 and transition metal complexes. The NMR information is also useful to clarify the product of the synthetic procedures and the reactivity patterns as well. However, notwithstanding the paramount importance played by ^{31}P-NMR spectroscopy in the coordination chemistry of white phosphorus and of the compounds described in this report, no in-depth study aimed at critically analyzing the vast collection of ^{31}P-NMR data available for these compounds has been published till now. In view of the limited space available, it is not our intention to provide a comprehensive survey of the reported NMR data; rather, we intend to outline the general trends of the ^{31}P-NMR chemical shifts for the several degradation products formed from P_4-metal activation. A comprehensive statistical study addressing the relationships between the chemical shifts and coupling constants vs the structural and bonding properties of transition metal complexes containing naked phosphorus ligands is currently under development and will be presented in due course. Thus, only some general trends will be presented in this chapter with the purpose of providing the reader with useful information about the ^{31}P-NMR properties of naked P_x ligands. As a helpful assist to the reader, we have collected in Fig. 4, in a simple pictorial way, the range of chemical shifts exhibited by polyphosphorus complexes as a function of the P_x ligand ($x \le 4$).

The ^{31}P-NMR signal of white phosphorus appears as a singlet near -526.9 ppm at room temperature in CD_2Cl_2. Upon coordination, the four phosphorus atoms of the P_4 tetrahedron invariably move downfield with respect to the resonance of the free molecule. The extent of such a shift strongly depends on the nature of the metal, its oxidation state, and the electronic properties of the ancillary ligands. Although the paucity of the collected data should be critically considered; nevertheless some meaningful conclusions can be drawn. Thus, it appears that the metallated P_A atom experiences the larger downfield shift with respect to free P_4 with Δ-values ranging from about 100 ppm for the tungsten(0) derivatives $[W(CO)_3(PR_3)_2(\eta^1\text{-}P_4)]$ (**5**, **6**) [16], to more than 200 ppm for the ruthenium(II) complex $[(PPh_3)_2RuCl(\mu\text{-}Cl)_3Ru(PPh_3)_2(\eta^1\text{-}P_4)]$ (**11**) [23]. In contrast, the three magnetically equivalent P_B atoms show a less pronounced shift with a narrow distribution of values $[\delta(P_B)_{ave} = -478]$. The temperature invariance of the AB_3 spin system points to the absence of any dynamic process exchanging P_A and P_B atoms. In addition, the lack of coalescence for the high field P_B-doublet in the ^{31}P-NMR spectrum of $[(triphos)Re(CO)_2(\eta^1\text{-}P_4)]^+$ (**8**) down to -105 °C is in line with a P_4-ligand freely rotating about the P_A-metal axis [17].

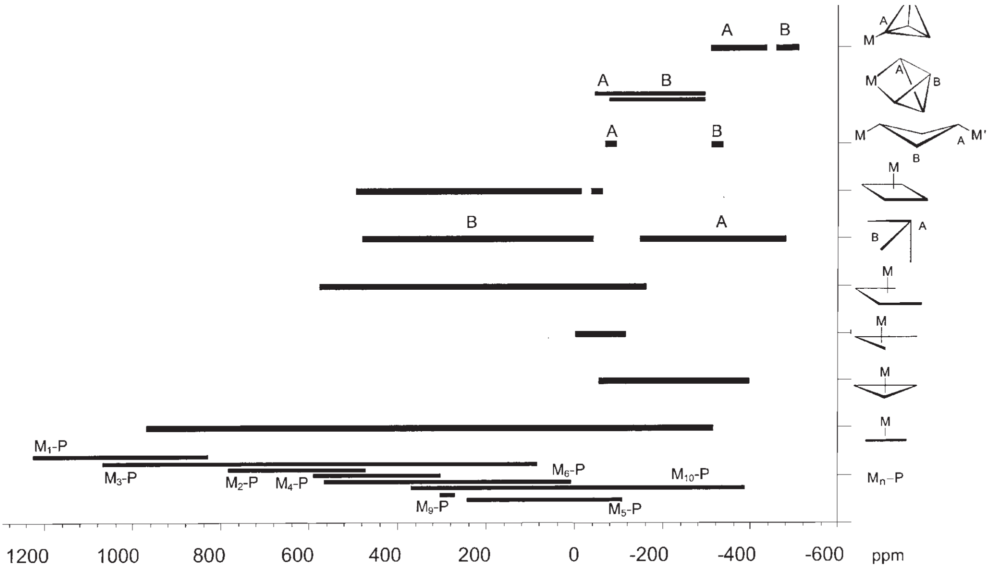

Fig. 4. Range of ^{31}P-NMR spectral data for polyphosphorus P_x compounds ($x \le 4$) [85% H_3PO_4 reference with downfield values taken as positive ($\delta = 0$)]

Once the P_4-tetrahedron undergoes a metal-promoted activation with a more or less drastic disruption of the original geometry, the NMR resonances due to the naked P atoms generally move low-field to a largely variable extent depending on both the achieved P_x topology and the nature of the coordinated metal ligand fragment. Inspection of Fig. 4 allows one to draw some useful conclusions, which are illustrated below, paralleling the stepwise demolition of the η^1-*tetrahedro* tetraphosphorus ligand. As a general rule, the metallated P atoms are more deshielded than the P-atoms not coordinated to the metal in line with the Lewis-acid properties ascribable to metal centers.

In keeping with these general trends, the ^{31}P-NMR spectra of η^2-P_4 complexes usually exhibit A_2B_2 splitting patterns downfield shifted in comparison to the signals of both free P_4 and η^1-P_4 complexes. Generally, the metal coordinated phosphorus atoms (P_A) are less electron-rich and resonate to lower fields than P_B. The interesting complex $[\{Cp''Co\}(\mu\text{-}CO)(P_4)]$ (**25**) (see Scheme 3) [58], which is the only known example of P_4-complex containing an almost separated P_3/P_1 array of phosphorus atoms, shows an averaged signal at –50.2 ppm for the four P atoms. Remarkably, the dynamic behavior of **25** represents a pervasive feature in transition metal-P_x chemistry, which often makes extremely complicated the assignment of solution structure for these complexes by ^{31}P-NMR spectroscopy.

The few data available for compounds featuring the P_4-butterfly geometry (A_2B_2 spin system) fall in a very narrow range of δ values, and, in keeping with the general rule outlined above, in all the known examples the metallated P atom (P_A) is significantly more deshielded than P_B $[\Delta(P_B\text{–}P_A)_{ave} \approx 140$ ppm$]$. An even larger deshielding is shown by the P atoms incorporated in planar *cyclo*-P_4 ligands which span a wide range of positive chemical shifts ($487 \leq \delta \leq -3$). Further degradation of the P_4 ligand to the tripodal disposition yields a very peculiar ^{31}P-NMR spectrum (AB_3 system if one assumes the magnetic equivalence of the three peripheral P atoms) with the three metal-coordinated P atoms resonating within a broad range of values almost overlapped with those determined for the complexes containing a *cyclo*-P_4 ligand. In contrast, the non-coordinated phosphorus atom (P_A) roughly resonates in the interval between –161 and –466 ppm pointing to a modest electronic perturbation. The alternative disposition of four P atoms coordinated to the metal in an acyclic chain fashion displays a wide range of chemical shifts between 567 and 147 ppm, similar to that observed for cyclic P_4 ligands. At first glance it appears that the chemical shift of such acyclic PPPP chains strongly depends on the adopted way of wrapping around the metal center.

Removing the P_4 topology first leaves P_3 ligands, which may coordinate to transition metal fragments by adopting one of two possible dispositions, i.e., open chain and *cyclo*-P_3 structures. The triangular arrangement causes ^{31}P-signals to fall in a relatively narrow range from ca. –69 to –381 ppm, which largely depends on the overall charge of the complex, as well as the metal and the coligands nature [12, 65]. In general, mononuclear *cyclo*-P_3 complexes display high field signals with respect to triple-decker complexes where the P_3 unit bridges two metals forming homo- or heterodinuclear systems. However, there is a large overlap between the range of chemical shifts covered by mono- and dinuclear species, which broadly range from -133 to -300 ppm. Coordination of further exocyclic metal fragments (up to three as in $[(\text{triphos})\text{Co}(\eta^{3:1:1:1}\text{-P}_3)\{\text{CpMn}(\text{CO})_2\}_3]$ [118]), usually σ-bonded to the P atoms of the *cyclo*-P_3 moiety, does not extensively affect the chemical shift of the *cyclo*-P_3 ring. Triangular opened disposition of the P_3 ligand gives a smaller array of chemical shifts ($-18.8 \le \delta \le -103.6$), which are normally downfield shifted in comparison with *cyclo*-P_3 complexes.

A completely different behavior is found for the well assorted set of species featuring P_2 ligands in which ^{31}P-NMR resonances fall in a range spanning more than 1300 ppm: from 959 ppm for $[\{\text{Cp*Zr}\}_2(\mu,\eta^{2:2}\text{-P}_2)]$ [119] to ca. -300 ppm for $[\{\text{CpW}(\text{CO})_2\}_2(\mu,\eta^{1:1}\text{-P}_2)]$ [120]; however, the data located at positive fields are fewer than those falling at high field. The impressive variation of chemical shifts displayed by compounds containing diphosphorus ligands is certainly due to the many coordination modes and dispositions exhibited by this simple ligand which entails examples covering the large range of chemical shifts indicated in Fig. 4. It may be rationalized in terms of multiform participation of the excited states of the P_2 ligand which possess a high degree of radical character [121].

The final step in the degradation pathways of the P_4 molecule provides single phosphorus atoms coordinated to one (terminal phosphido, $M{\equiv}P$, species) or more transition metals (bridging phosphido, μ_n-P, species). Related resonances cover a wide range of chemical shifts from -369 to 1216 ppm. A simple inspection of Fig. 4 reveals that it is possible to associate a roughly distinct chemical shift region to each class of known phosphido ligands with more or less significant overlapping in some cases. In principle, there is not a direct connection between the displayed range of chemical shifts for a certain type of phosphido ligand (μ_x-P) with the coordination number exhibited by the phosphorus atoms. However, some care should be applied in extrapolating predictable information from these data because the known categories of phosphido ligands span from monometallic species (μ_1-P) to high nuclearity clusters, encapsulating a phosphido atom embedded in the core of a decametallic polyhedron [122]. It is also worth mentioning that some of the possible μ_x-phosphido categories are scarcely represented [123] or are even not yet known, as for μ_7-P and μ_8-P species.

Acknowledgement. We thank the EC for financial support through the INCO Copernicus project ERB ic15ct960746. Thanks are also expressed to INTAS (grant 00-0018).

4
References and Notes

1. Ginsberg AP, Lindsell WE (1971) J Am Chem Soc 93:2082
2. Dillon KB, Mathey F, Nixon JF (1998) Phosphorus: the carbon copy. Wiley, Chichester (UK); Fehlner TP (1992) Inorganometallic chemistry. In: Fehlner TP (ed) Modern inorganic chemistry. Plenum Press, New York, NY
3. Whitmire KH (1998) Adv Organomet Chem 42:2
4. Peruzzini M, de los Rios I, Romerosa A, Vizza F (2001) E J Inorg Chem 593
5. Scherer OJ (1999) Acc Chem Res 32:751
6. Scheer M (1997) Coord Chem Rev 163:271
7. Scheer M, Herrmann E (1990) Z Chem 29:41

8. Scherer OJ (1990) Angew Chem 102:1137; (1990) Angew Chem Int Ed Engl 29:1104
9. Scherer OJ (1990) In: Regitz M, Scherer OJ (eds) Multiple bonds and low coordination in phosphorus chemistry. Thieme, Stuttgart
10. Scherer OJ (1985) Angew Chem 97:905; (1985) Angew Chem Int Ed Engl 24:924
11. Scherer OJ (1987) Comments Inorg Chem 6:1
12. Di Vaira M, Stoppioni P, Peruzzini M (1987) Polyhedron 6:351
13. Dapporto P, Midollini S, Sacconi L (1979) Angew Chem 91:510; (1979) Angew Chem Int Ed Engl 18:469
14. Dapporto P, Sacconi L, Stoppioni P, Zanobini F (1981) Inorg Chem 20:3834
15. Di Vaira M, Sacconi L (1982) Angew Chem 94:338; (1982) Angew Chem Int Ed Engl 21:330
16. Gröer T, Baum G, Scheer M (1998) Organometallics 17:5916
17. Peruzzini M, Marvelli M, Romerosa A, Rossi R, Vizza F, Zanobini F (1999) Eur J Inorg Chem 931
18. Di Vaira M, Ehses M, Peruzzini M, Stoppioni P (2000) Eur J Inorg Chim 2193
19. Wasserman J, Kubas GJ, Ryan RR (1986) J Am Chem Soc 108:2294
20. Bergamini P, Fabrizi DeBiani F, Marvelli L, Mascellani N, Peruzzini M, Rossi R, Zanello P (1999) New J Chem 207
21. Bianchini C, Mealli C, Peruzzini M, Zanobini F (1992) J Am Chem Soc 114:5905
22. Bianchini C, Masi D, Meli A, Peruzzini M, Zanobini F (1988) J Am Chem Soc 110:6411
23. Peruzzini M, Mañas S, Romerosa A, Vacca A (2000) Mendeleev Commun 134
24. Schmidt G, Peruzzini M (1999) (unpublished results)
25. de los Rios I, Peruzzini M, Romerosa A (2000) (unpublished results)
26. The direct synthesis of organophosphorus compounds from white phosphorus has some precedents See, for example: Rauhut MM, Semsel AM (1963) J Org Chem 28:471; Rauhut MM, Semsel AM (1963) J Org Chem 28:473; Rauhut MM, Bernheimer R, Semsel AM (1963) J Org Chem 28:478; Rauhut MM (1964) In: Grayson M, Griffith EJ (eds) Topics in phosphorus chemistry. Interscience, New York, NY (USA); Maier L (1966) Helv Chim Acta 49:2458; Staendeke H (1972) Chem Zeit 96:494; Brown C, Hudson RF, Wartew GA (1978) Phosphorus and Sulfur 5:67; Brandsma L, van Doorn JA, de Lang R-J, Gusarova NK, Trofimov BA (1995) Mendeleev Commun 14
27. Tamulis A, Abdreimova RR, Tamuliene J, Peruzzini M, Balevicius ML (2000) Inorg Chim Acta 307:71
28. Barbaro P, Peruzzini M, Ramirez JA, Vizza F (1999) Organometallics 18:4237
29. Ginsberg AP, Lindsell WE, McCullough KJ, Sprinkle CR, Welch AJ (1986) J Am Chem Soc 108:403
30. Kang S-W, Albright TA, Silvestre J (1984) Croat Chem Acta 57:1355
31. [Cp″M(η^2-P_4)] (M=Zr, Hf): Scherer OJ, Swarowsky M, Wolmershäuser G (1988) Angew Chem 100:738; (1988) Angew Chem Int Ed Engl 27:694
32. [Cp*Co(CO)(η^2-P_4)]: Scherer OJ, Swarowsky M, Swarowsky H, Wolmershäuser G (1989) Organometallics 8:841
33. (a) [{Cp″Co(CO)}($\eta^{2:1:1:1:1:1}$-P_4){$Cr(CO)_5$}$_4$]: Scheer M, Becker U, Huffman JC, Chisholm MH (1993) J Organomet Chem 461:C1; (b) Scheer M, Becker U (1997) J Organomet Chem 545/546:451
34. [{Cp^{x}Rh(CO)}($\eta^{2:1:1:1:1:1}$-P_4){$Cr(CO)_5$}$_4$] (Cp^x=Cp′, Cp″): Scheer M, Troitzsch C, Hilfert L, Dargatz M, Kleinpeter E, Jones PG, Sieler J (1995) Chem Ber 128:251
35. [{Cp*Ir(CO)}($\eta^{2:1:1:1:1:1}$-P_4){$Cr(CO)_5$}$_4$]: Scheer M, Becker U, Matern E (1996) Chem Ber 129:721
36. [$(PPh_3)_2$Pt($\eta^{2:1:1}$-P_4){$Cr(CO)_5$}$_2$]: Scheer M, Dargatz M, Rufińska A (1992) J Organomet Chem 440:327
37. [(triphos)IrH(η^2-P_4)]: Peruzzini M, Ramirez JA, Vizza F (1998) Angew Chem 110:2376; (1998) Angew Chem, Int Ed Engl 37:2255
38. Scherer OJ, Völmecke T, Wolmershäuser G (1999) Eur J Inorg Chem 945
39. Scherer OJ, Berg G, Wolmershäuser G (1996) Chem Ber 129:53
40. Weigel S, Wolmershäuser G, Scherer OJ (1998) Z Anorg Allg Chem 624:559
41. Scherer OJ, Pfeiffer K, Wolmershäuser G (1992) Chem Ber 125:2367

42. Scherer OJ, Höbel B, Wolmershäuser G (1992) Angew Chem 104:1042; (1992) Angew Chem, Int Ed Engl 31:1027
43. Detzel M (1995) PhD Thesis, University of Kaiserslautern
44. Scheer M, Troitzsch C, Jones PG (1992) Angew Chem 104:1395; (1992) Angew Chem Int Ed Engl, 31:1377
45. Scheer M, Becker U (1994) Phosphorus, Sulfur and Silicon Rel Elem 93/94:257
46. Scheer M, Becker U, Chisholm MH, Huffman JC, Lemoigne F, Eisenstein O (1995) Inorg Chem 34:3117
47. Scheer M, Becker U, Magull J (1998) Polyhedron 17:1983 and references cited therein
48. Scherer OJ, Schwarz G, Wolmershäuser G (1996) Z Anorg Allg Chem 622:951
49. Jutzi P, Opiela S (1991) J Organomet Chem 124:725
50. Weber L, Sonnenberg U (1991) Chem Ber 725:124
51. Scherer OJ, Hilt T, Wolmershäuser G (1998) Organometallics 17:4110
52. Scheer M, Becker U (1996) Chem Ber 129:1307
53. Scherer OJ, Braun J, Wolmershäuser G (1990) Chem Ber 123:471
54. Scherer OJ, Braun J, Walther P, Wolmershäuser G (1992) Chem Ber 125:2661
55. Scheer M, Herrmann E, Sieler J, Oehme M (1991) Angew Chem 103:1023; (1991) Angew Chem Int Ed Engl 30:969
56. Barr ME, Smith SK, Spencer B, Dahl FL (1991) Organometallics 10:3983
57. Goh LY, Chu CK, Wong RCS, Hambley TW (1989) J Chem Soc Dalton Trans 1951
58. Goh LY (1999) Coord Chem Rev 185/186:257 and references cited therein
59. Scherer OJ, Ehses M, Wolmershäuser G (1997)) J Organomet Chem 531:217
60. Scherer OJ, Ehses M, Wolmershäuser G (1998) Angew Chem 110:530; (1998) Angew Chem Int Ed Engl 37:507
61. Extrusion of *cyclo*-P_3 to form $[(\text{triphos})M(\eta^3\text{-}P_3)]^{n+}$ takes place from a variety of phosphorus containing compounds other than P_4. This list include: P_{red}, P_4S_3, P_4S_5, P_4S_7, P_4Se_3, P_2Te_3, *cyclo*-P_5Me_5: Peruzzini M, Stoppioni P (unpublished results)
62. Wachter J (1998) Angew Chem 110:782; (1998) Angew Chem Int Ed Engl 37:751
63. Di Vaira M, Stoppioni P (1992) Coord Chem Rev 120:259
64. Di Vaira M, Stoppioni P, Peruzzini M (1990) Comm Inorg Chem 11:1
65. Di Vaira M, Sacconi L, Stoppioni P (1983) J Organomet Chem 250:183
66. Mealli C, Costanzo F, Ienco A, Peruzzini M, Perez-Carreño E (1998) Inorg Chim Acta 275/276:366
67. Ehses M, Stoppioni P (unpublished results)
68. Catalytic synthesis of organophosphates from alcohol and white phosphorus has been accomplished – see: Dorfman YA, Aleshkova MM, Polimbetova GS, Levina LV, Petrova TV, Abdreimova RR, Doroshkevich DM (1993) Russ Chem Rev 62:877
69. Bianchini C, Peruzzini M, Abdreimova RR, Akbayeva DN, Polimbetova GS (2000) Italian Patent FI2000 A000021
70. Herberhold M, Frohmader G, Milius W (1996) J Organomet Chem 522:185
71. Scherer OJ, Vondung J, Wolmershäuser G (1989) Angew Chem 101:1395; (1989) Angew Chem Int Ed Engl 28:1355
72. Scherer OJ, Winter R, Wolmershäuser G (1993) Z Anorg Allg Chem 619:827
73. Hey E, Lappert MF, Atwood JL, Bott SG (1987) J Chem Soc Chem Comm 597
74. Cecconi F, Ghilardi CA, Midollini S, Orlandini A (1986) Inorg Chem 25:1766
75. Scherer OJ, Mohr T, Wolmershäuser G (1997) J Organomet Chem 529:379
76. Scherer OJ, Winter R, Wolmershäuser G (1993) J Chem Soc Chem Commun 313
77. Scherer OJ, Dave T, Braun J, Wolmershäuser G (1988) J Organomet Chem 350:C20
78. Scheer M, Dargatz M, Schenzel K (1992) J Organomet Chem 435:123
79. Scherer OJ, Kemény G, Wolmershäuser G (1995) Chem Ber 128:1145
80. Koch B, Scherer OJ, Wolmershäuser G (2000) Z Anorg Allg Chem 626:1797
81. Simon GL, Dahl LF (1973) J Am Chem Soc 95:2175
82. The more regular cubane $[\{Cp''Co(\mu_3\text{-}P)\}_4]$ has been prepared, without using P_4, from $[Cp^*Fe(\eta^5\text{-}P_5)]$ and $[\{Cp''Co(CO)\}_2]$: Scherer OJ, Weigel S, Wolmershäuser G (1998) Chem Eur J 4:1910

83. Cummins CC (1998) J Chem Soc Chem Comm 1777
84. Laplaza CE, Davis WM, Cummins CC (1995) Angew Chem 107:2181; (1995) Angew Chem Int Ed Engl 34:2042
85. (a) Chisholm MH, Folting K, Huffman JC, Koh JJ (1985) Polyhedron 4:893; (b) Chisholm MH, Huffman JC, Pasterczyk JW (1987) Inorg Chim Acta 133:17; (c) Chisholm MH, Folting K, Pasterczyk JW (1988) Inorg Chem 27:3057; (d) Chisholm MH, Folting K, Scheer M (1998) Polyhedron 17:2931
86. Scheer M (1995) Angew Chem 107:2151; (1995) Angew Chem Int Ed Engl 34:1997
87. Kruck T, Sylvester G, Kunau JP (1973) Z Naturforsch B28:38
88. Vizi-Orosz A, Pályi G, Markó L (1973) J Organomet Chem 60:C25
89. Campana CF, Vizi-Orosz A, Palyi G, Markó L, Dahl LF (1979) Inorg Chem 18:3054
90. Baudler M, Akpapoglou S, Ouzonis D, Wasgestian F, Meinigke B, Budzikiewicz H, Münster H (1988) Angew Chem 100:288; (1988) Angew Chem Int Ed Engl 27:280
91. Scherer OJ, Brück T (1987) Angew Chem 99:59; (1987) Angew Chem Int Ed Engl 26:59
92. Scherer OJ, Brück T, Wolmershäuser G (1988) Chem Ber 121:935
93. Rink B, Scherer OJ, Wolmershäuser G (1995) Chem Ber 128:71
94. (a) Scherer OJ, Brück T, Wolmershäuser G (1989) Chem Ber 122:2049; (b) Scherer OJ, Schwalb J, Wolmershäuser G, Kaim W, Gross R (1986) Angew Chem 98:349; (1986) Angew Chem Int Ed Engl 25:358
95. Scherer OJ, Hilt T, Wolmershäuser G (2000) Angew Chem 112:1484; (2000) Angew Chem Int Ed Engl 39:1426
96. Goh LY, Wong RCS, Chu CK, Hambley WH (1990) J Chem Soc Dalton Trans 977
97. Sekar P, Scheer M, Voigt A, Kirmse R (1999) Organometallics 18:2833
98. Detzel M, Mohr T, Scherer OJ, Wolmershäuser G (1994) Angew Chem 106:1142; (1994) Angew Chem Int Ed Engl 33:1110
99. Detzel M, Friedrich G, Scherer OJ, Wolmershäuser G (1995) Angew Chem 107:1454; (1995) Angew Chem Int Ed Engl 34:1321
100. Friedrich G, Scherer OJ, Wolmershäuser G (1996) Z Anorg Allg Chem 622:1478; Hänisch C, Fenske D, Weigend F, Ahlrichs R (1997) Chem Eur J 3:1494
101. Di Vaira M, Mani F, Moneti S, Peruzzini M, Sacconi L, Stoppioni P (1985) Inorg Chem 24:2230
102. Scherer OJ, Sitzmann H, Wolmershäuser G (1985) Angew Chem 97:358; (1985) Angew Chem Int Ed Engl 24:351
103. Scherer OJ, Schwalb J, Swarowsky H, Wolmershäuser G, Kaim W, Gross R (1988) Chem Ber 121:443
104. Reddy AC, Jemmis ED, Scherer OJ, Winter R, Heckmann G, Wolmershäuser G (1992) Organometallics 11:3894
105. Scherer OJ, Swarowsky H, Wolmershäuser G, Kaim W, Kohlmann S (1987) Angew Chem 99:1178; (1987) Angew Chem Int Ed Engl 26:1153
106. Halivi EA, Bock H, Roth B (1984) Inorg Chem 23:4376
107. Schore NE (1988) Chem Rev 88:1081
108. See for example: Scherer OJ, Bach I, Schwalb J, Sitzmann H, Wolmershäuser G, Kaim W, Gross R (1987) Phosphorus and Sulfur 30:269
109. Hofmann C, Scherer OJ, Wolmershäuser G (1998) J Organomet Chem 559:219
110. Hofmann C (1997) PhD Thesis, University of Kaiserslautern
111. Scherer OJ, Werner B, Heckmann G, Wolmershäuser G (1991) Angew Chem 103:562; (1991) Angew Chem Int Ed Engl 30:553
112. Charles S, Danis JA, Fettinger JC, Eichhorn BW (1997) Inorg Chem 36:3772; Bolle U, Tremel W (1994) J Chem Soc Chem Comm 217
113. Ahlrichs R, Fenske D, Fromm K, Krautscheid H, Treutler O (1996) Chem Eur J 2:238
114. Böcker S, Häser M (1995) Z Anorg Allg Chem 621:258
115. Barr ME, Adams BR, Weller RR, Dahl LF (1991) J Am Chem Soc 112:3052
116. Corbridge DEC (1995) Phosphorus – an outline of its chemistry and technology, 5th edn. Elsevier SA, Lausanne (Switzerland)
117. Goh LY, Wong RCS, Sinn E (1990) J Chem Soc Chem Comm 1484
118. Mealli C, Midollini S, Moneti S, Sacconi L (1980) Cryst Struct Commun 9:1017

119. Fermin MC, Ho J, Stephan DW (1994) J Am Chem Soc 116:6033
120. Davies JE, Klunduk MC, Mays MJ, Raithby PR, Shields GP, Tompkin PK (1997) J Chem Soc Dalton Trans 715
121. Chesnut DB, Byrd EFC (1996) Heteroatom Chem 7:307; Kutzelnigg W, Fleischer U, Schindler M (1990) NMR Bas Princ Progr 23:165; Challoner R, McDowell CA, Yoshifuji M, Toyota K, Tossel JA (1993) J Magn Res A 104:258; Lazzeretti P, Tossell JA (1987) J Phys Chem 91:800
122. Examples of μ_{10}-P complexes include: Vidal JL, Walker WE, Schoening CR (1981) Inorg Chem 20:238; Heaton BT, Strona L, Della Pergola R, Vidal JL, Schoening RC (1983) J Chem Soc Dalton Trans 1941
123. For example, $[Rh_9(\mu_9\text{-}P)(CO)_{21}]^{2-}$ is the only known example containing a μ_9-P phosphido ligand: Vidal JL, Walker WE, Pruett RL (1980) Inorg Chem 102:2449

New Inorganic Polymers Containing Phosphorus

Andrew R. McWilliams, Hendrik Dorn, Ian Manners

Department of Chemistry, University of Toronto, Toronto, Ontario, Canada, M5S 3H6
E-mail: imanners@chem.utoronto.ca

The relatively unexplored area of main group polymer chemistry continues to offer fertile ground for scientific study. In this chapter recent developments in the area of linear inorganic polymers based on phosphorus are reviewed. The 1990s saw the development of a number hybrid polymer systems where elements such as carbon and sulfur were incorporated into polymer backbones along with phosphorus and nitrogen. Many of these novel materials were synthesized via the ring-opening polymerization of cyclic heterophosphazenes. Polythionylphosphazenes, hybrids of "classical" polyphosphazenes and polyoxothiazenes, are discussed in particular detail. In addition, polyphosphinoboranes, with a main chain comprising alternating phosphorus and boron atoms, have been recently prepared via the transition metal catalyzed dehydrocoupling of phosphine-borane adducts. These novel materials are also described.

Keywords. Phosphorus, Polymers, Heterophosphazenes, Thionylphosphazenes, Phosphinoboranes

Topics in Current Chemistry, Vol. 220

1
Introduction

The preparation of new classes of inorganic polymers provides a substantial synthetic challenge but is motivated by the possibility of accessing new materials with interesting and useful properties [1]. Advances in the last two decades or so of the twentieth century have led to the preparation of a variety of new polymers which contain main group elements, transition metals, and even lanthanides [1]. It is plausible that some of these new materials will possess properties which are difficult or impossible to achieve with existing organic materials and may in the future fulfill the requirements of specialized markets. Phosphorus is one of the most abundant elements on Earth and the development of the polymer chemistry of this fascinating non-metal is clearly of both fundamental and applied interest. In this chapter we survey recent progress made in the development of linear inorganic polymers where phosphorus is contained in the polymer main chain.

The most widely studied class of phosphorus-containing inorganic polymers are the polyphosphazenes, **1**, which have a backbone composed of alternating phosphorus and nitrogen atoms [2, 3]. The side groups, R, can be alkoxy, aryloxy, amino, alkyl, aryl, inorganic, or organometallic groups. This large range of accessible structural variations is accompanied by a wide range of polymer properties that are highly dependent upon the nature of the side groups.

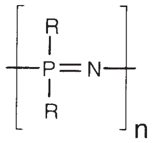

$[-PR_2{=}N-]_n$

1

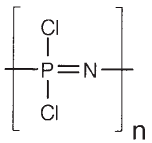

$[-PCl_2{=}N-]_n$

2

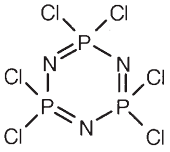

3

The first polyphosphazene, polydichlorophosphazene (**2**), was prepared in crosslinked form by Stokes at the end of the nineteenth century by the thermal ring-opening polymerization ROP of the cyclic trimer $[Cl_2PN]_3$ (**3**) [4]. This material, referred to as "inorganic rubber," remained a chemical curiosity due its intractability and hydrolytic instability until the mid-1960s when it was shown by Allcock and Kugel that if the (ROP) of pure **3** is carried out carefully, uncrosslinked polydichlorophosphazene (**2**), which is soluble in organic solvents, is formed [5]. Subsequent reaction of this highly reactive polymeric species with nucleophiles has been shown to yield a wide range of hydrolytically stable polyorganophosphazenes by the pioneering work of Allcock and coworkers [4, 6–8]. Since that time, the development of condensation routes to polydialkylphosphazenes and polydichlorophosphazene have also been reported [9, 10]. This chapter focuses on new polymer systems and on the recent interest in the synthesis of hybrid systems which incorporate phosphorus and nitrogen together with other elements in the polymer main chain.

2
Synthesis and Properties of Polycarbophosphazenes

In the past decade reports of a series of polyheterophosphazenes have appeared in the literature. Among these are the polycarbophosphazenes, which possess a backbone of phosphorus, nitrogen, and carbon atoms and can be regarded as derivatives of "classical polyphosphazenes" **1** in which every third phosphorus atom is replaced by carbon. The first examples of these materials were discovered in 1989 by Allcock, Nuyken et al. [11]. Thermal ROP of a cyclic carbophosphazene was used to prepare the chlorinated polymeric species **4** which undergoes halogen replacement reactions with nucleophiles such as aryloxides to yield hydrolytically stable poly(aryloxycarbophosphazenes) **5** (M_w = ca. 10^5) which are isolated as white, solid materials. The polymer backbone in these materials was found to be less flexible than in classical polyphosphazenes [11–14]. For example, the halogenated polymer **4** possesses a glass-rubber transition (T_g), which reflects the onset of large-scale conformational motions of the polymer chain, of −21 °C compared to a value of −66 °C for polydichlorophosphazene **2**:

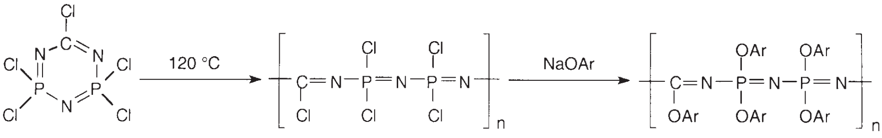

4 **5** (1)

The reaction of **4** with alkylamines has also been studied [14]. The resulting poly(alkylaminocarbophosphazenes) are sensitive to hydrolysis. However, arylamino derivatives are moisture stable and, in addition, a novel, regioselectively substituted polymer **6** was successfully prepared via the sequential reaction with $NHPh_2$ and trifluoroethoxide anions:

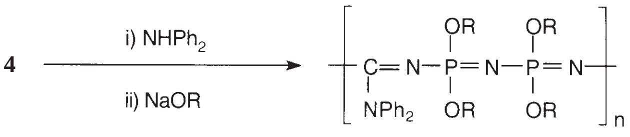

(2)

$OR = OCH_2CF_3$

6

3
Polymers Containing Phosphorus and Transition Elements

Examples of polymers which contain both transition metals and phosphorus atoms in the main chain remain relatively rare. In 1989, Roesky and Lücke briefly reported the synthesis of the first polymetallaphosphazenes where every third phosphorus atom from a classical phosphazene is replaced by a metal atom (M=Mo, W) [15]. Polymetallaphosphazenes (**7**) were isolated through the ROP of cyclic metallaphosphazenes in refluxing xylenes. However, detailed characterization of these materials has yet to be reported:

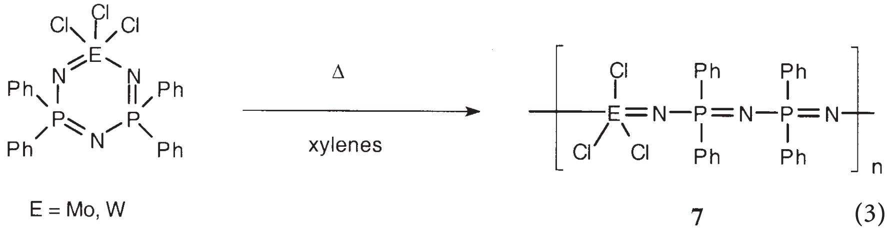

7 (3)

Examples of "organometallic" polymers containing both phosphorus atoms and transition metals in the backbone include polyferrocenylphosphines **8** (and the corresponding phosphine sulfides **9**), which are accessible via the thermal ROP of phosphorus-bridged [1] ferrocenophanes [16, 17]. Polymers of this type have been previously prepared by condensation routes and the catalytic potential of some of their transition metal derivatives has already been noted [18]. Living anionic ROP of phosphorus-bridged [1]ferrocenophanes has recently been demonstrated and provides a route to block copolymers such as **10** (PI = polyisoprene) [19]:

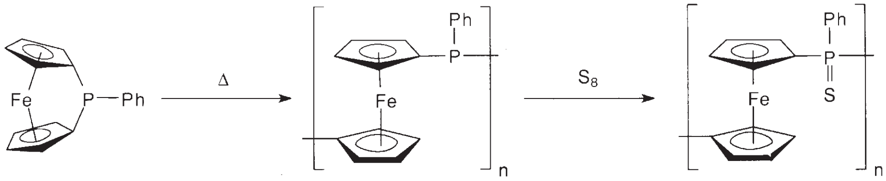

8 **9** (4)

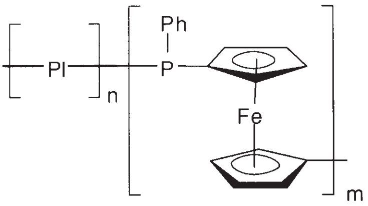

10

4
Sulfur-Nitrogen-Phosphorus Rings and Polymers

4.1
Polythiophosphazenes

Sulfur-nitrogen-phosphorus polymers possess backbones which can be regarded as compositional hybrids of those present in sulfur-nitrogen polymers, such as the solid state polymer poly(sulfur nitride) $[SN]_x$ or polyoxothiazenes

$[RS(O)=N]_n$ and classical polyphosphazenes, $[R_2P=N]_n$ **1** [20,21]. The first well-characterized examples of these materials, polythiophosphazenes, were also reported by Allcock et al. [22]. These polymers were prepared via the thermal ROP of a cyclothiophosphazene. This yielded the hydrolytically sensitive polythiophosphazene **12** with a backbone of three-coordinate sulfur(IV), nitrogen, and phosphorus atoms. Although reaction of **12** with nucleophiles such as aryloxides yielded materials **13** with improved hydrolytic stability, degradation in the presence of moisture was still rapid except where very bulky substituents such as *o*-phenylphenoxy were present:

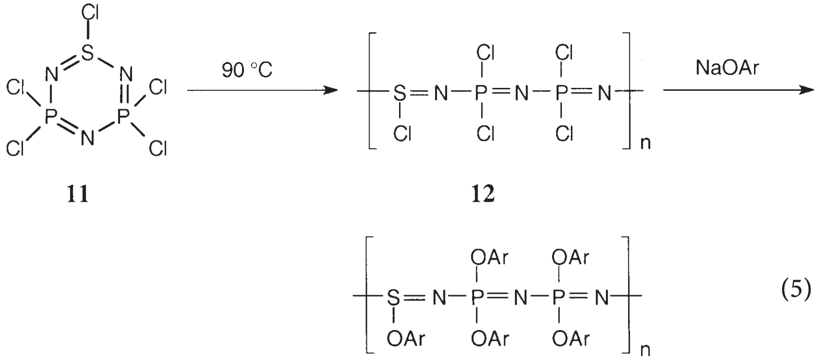

11 **12**

13

(5)

Although the backbone of polythiophosphazenes appears to be quite fragile, a particularly interesting feature of the substitution reactions of **12** is that the S-Cl bond is much more reactive than the P-Cl bonds. Regioselective substitution at the sulfur center is possible to yield macromolecules **15** with different aryloxy substituents at sulfur and phosphorus. [22,23]:

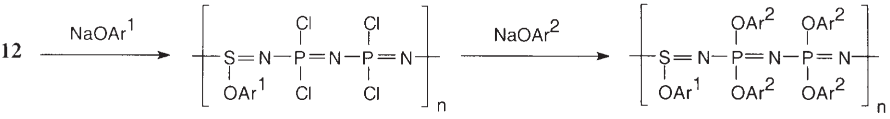

14 15 (6)

4.2
Polythionylphosphazenes

4.2.1
Cyclic Thionylphosphazene Monomers

One of the most well studied heterophosphazenes is the cyclic thionylphosphazene **18** which was first prepared in 1972 by two different low yield routes. Van de Grampel et al. reported the synthesis of small quantities of this species via the vacuum thermolysis of $Cl_3P=N\text{-}PCl_2=N\text{-}SO_2Cl$ [24]. An alternate, low yield route was provided by Klingebiel and Glemser using a [3+3] cyclocondensation route between $[Cl_3P{=}N{=}PCl_3]PCl_6$ and sulfamide $SO_2(NH_2)_2$ [25]. The best synthetic route to **18** is that described by Suzuki et al. in 1983 [26] which involves the reaction of sulfamide with PCl_5 followed by a [5+1]cyclocondensation reaction between the bis(phosphazo)sulfone **16** with hexamethyldisilazane. The chlorination of the cyclic species **17** is accomplished by reaction with PCl_5 in a mixture of $EtOH/CHCl_3$ affording **18** in yields of 40–75%. Two comprehensive reviews on the chemistry of **18** with particular emphasis on halogen side group replacement reactions have been published by van de Grampel in 1981 and 1992 [27,28]:

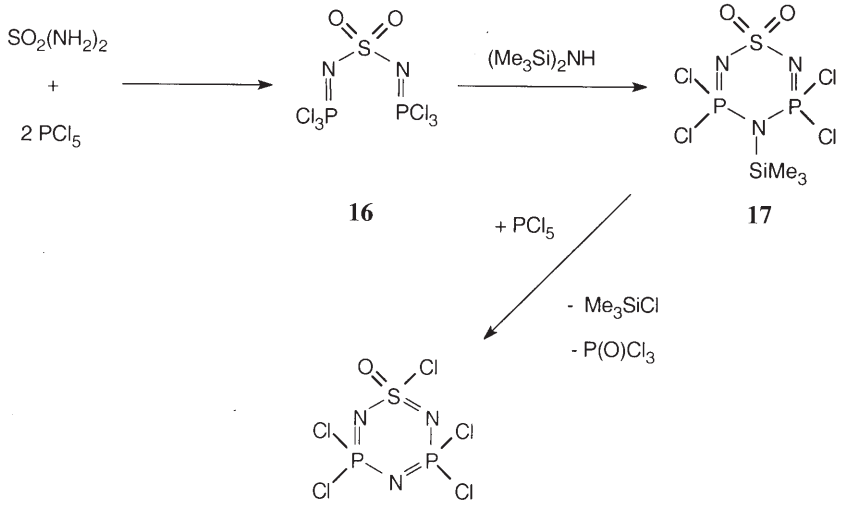

16 **17** **18**

(7)

4.2.2
Thermal ROP of Cyclic Thionylphosphazenes

In 1991, Liang and Manners reported that when the cyclic thionylphosphazene **18** is heated in the melt at 165 °C, thermal ROP takes place to yield the polythionylphosphazene **19** with chlorine substituents at both sulfur and phosphorus [23]:

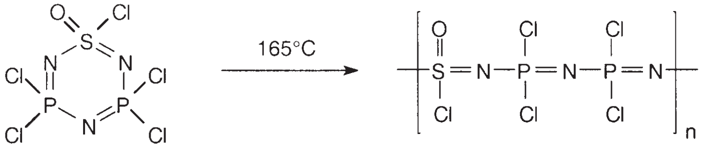

18 **19**

(8)

The fluorinated derivative **20** which can be prepared by reaction of the perchlorinated thionylphosphazene with AgF_2 [29], $HgF_2/AlCl_3$ [30], or alternatively with $AgBF_4$ [31], also undergoes thermal ROP when heated in the melt at 180 °C yielding **21** [32]:

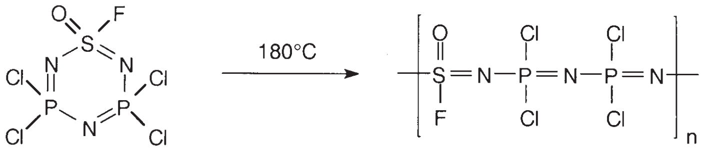

20 **21** (9)

As a consequence of the hydrolytically sensitive main group element-halogen bonds the gummy polymers **19** and **21** are sensitive to moisture and must be handled under an inert atmosphere. Therefore, molecular weight measurements on these perhalogenated polythionylphosphazenes have not yet been reported. Nevertheless, insight into the conformational flexibility of the main chain present in these new polymer structures was obtained from an analysis of their thermal transition behavior by Differential Scanning Calorimetry (DSC). T_gs were detected at −46 °C for **19** and −56 °C for **21**. These values are intermediate between those of related polyphosphazenes $[N{=}PCl_2]_n$ (T_g= −63 °C) [2] and polyoxothiazenes such as $[NS(O)Me]_n$ (T_g=55–65 °C)[33] reflecting the hybrid nature of the polymer structure. This increase in T_g suggests that there is a decrease in conformational flexibility of the perhalogenated polymers when S(O)Cl or S(O)F groups replace a PCl_2 unit in the backbone. This is probably a consequence of (i) the smaller size of sulfur relative to phosphorus and (ii) increased intermolecular interactions when a highly polar S=O moiety is present. The lower T_g (−56 °C) of polymer **21** which has fluorine at sulfur, compared with that of **19** (−46 °C) which has a chlorine substituent, can be attributed to the smaller size and lower polarizability of a fluorine side group compared with a chlorine. This trend is also observed with polyphosphazenes and organic polymers. For example, the T_g of $[N{=}PF_2]_n$ (−96 °C) is significantly lower than that of $[N{=}PCl_2]_n$ (−66 °C) and the T_g of poly(vinylidenefluoride) $[CH_2CF_2]_n$ (−39 °C) is lower than that of poly(vinylidenechloride) $[CH_2CCl_2]_n$ (−19 °C).

Ab initio molecular orbital calculations on short-chain model compounds of polythionylphosphazenes **19** and **21** have also been carried out to study the conformations and bonding present, and to provide insight into the factors that influence chain flexibility [34]. Geometry optimizations show that the model compounds adopt a non-planar *trans-cis* structure which has been attributed to the presence of two different substituents on sulfur. The calculations suggest that the isotactic polymer (i.e., one in which the sulfur(VI) stereocenters have the same configuration) would form a 12/5 helix in an extended conformation and that highly polar S-N and P-N bonds are present where sulfur and phosphorus are electron-deficient and nitrogen is electron-rich. The torsional flexibility was also studied, and revealed that the torsional barriers for rotation of the S-N-P and P-N-P bond angles decrease when changing from chlorine on sulfur in **19** to fluorine on sulfur in **21**. This calculated increase in flexibility in **21** is consistent with the observed lowering of the T_g when fluorine replaces chlorine as a substituent on sulfur.

4.2.3
Isolation of Macrocycles from Thermal ROP Mixtures

The dominant compounds present in the crude reaction mixture after heating **18** for 4 h at 165 °C are unreacted cyclic thionylphosphazene **18** and polymer **19** (ca. 80%). In addition to these species several other minor products can be detected by ^{31}P NMR [35]. Furthermore, Fast Atom Bombardment mass spectrometry indicated that 12-, 18-, 24-, 30-, and 36-membered rings, $[(NSOCl)(NPCl_2)_2]_n$ (n=2–6), are also formed. From this mixture the *cis* and *trans* isomers of the 12-membered ring **22a** and **22b** have been successfully isolated and characterized by X-ray diffraction (see Fig. 1a). The two rings were found to be significantly non-planar and the P-N-P bond angles are highly expanded [134(1)-163(1)°] relative to **18** [122°], whereas the S-N-P angles are only slightly expanded. Interestingly, the angles at sulfur are much smaller in **22a** and **22b** than in **18**, whereas the angles at phosphorus are similar. The bond lengths in the heterocycles are typical for P-N and S-N double bonds.

Fractional recrystallization also yielded the remarkable 24-membered macrocycle **23** which was characterized via crystallographic analysis (see

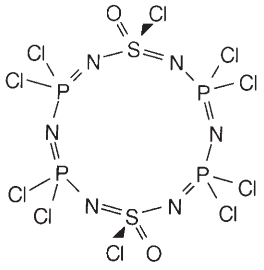

22a

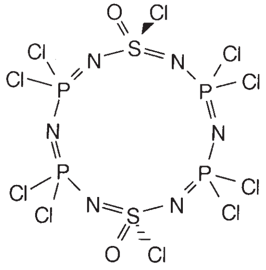

22b

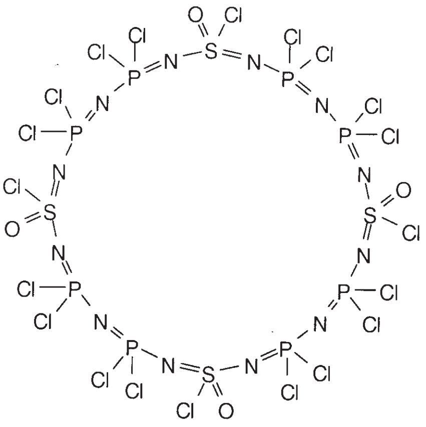

23

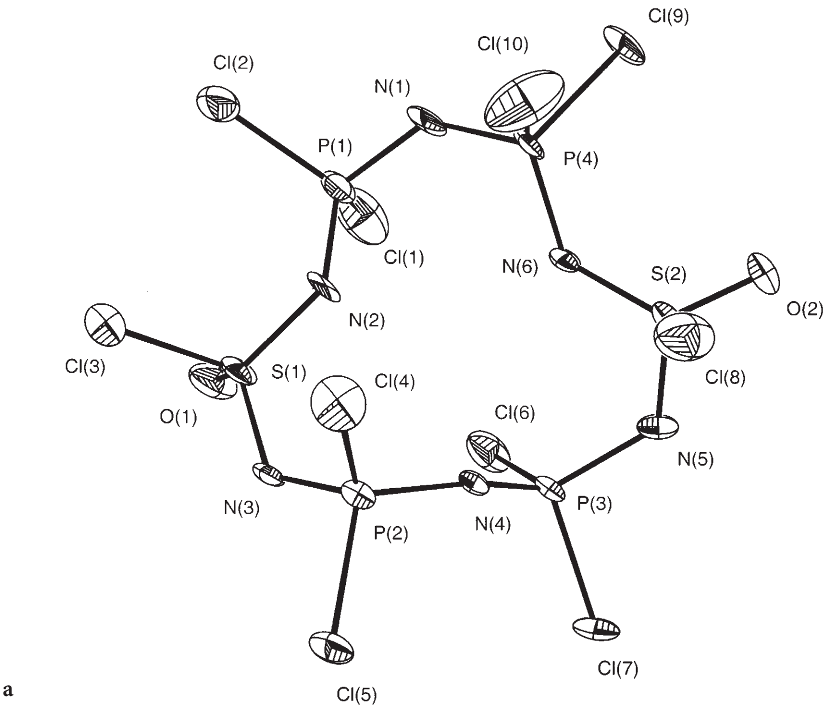

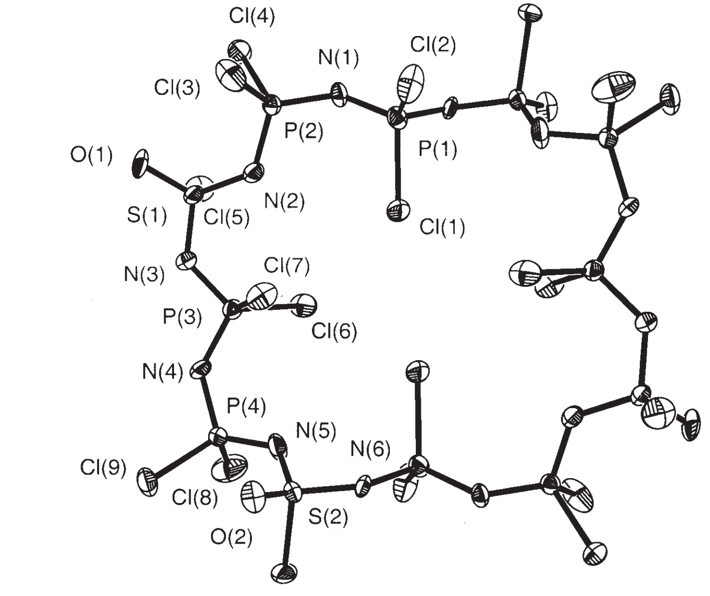

Fig. 1. Molecular structures of: **a** a 12-membered thionylphosphazene ring (**22a**); **b** a 24-membered thionylphosphazene ring (**23**). Reproduced from [35] with permission

Fig. 1b). Compound **23** is among the largest inorganic heterocycles to be characterized structurally to date [36]. The structural features of **23** are similar to those of **22a** and **22b**; however, in this case the crystal contained only the *cis/trans/cis/trans* isomer in which the PCl_2 fragments alternate between being exo- and endocyclic. Studies of this type may provide insight into the mechanism(s) of polymerization/oligomerization and may also provide access to novel complexes with metal ions.

4.2.4
Synthesis and Properties of Hydrolytically-Stable Polythionylphosphazenes

In order to prepare hydrolytically stable polythionylphosphazenes the perchlorinated polymers were reacted with nucleophiles to substitute the hydrolytically sensitive main group-element halogen bonds [2]. This type of post-polymerization structural modification is well-established in polyphosphazene chemistry [2, 8]. Thus, aryloxide nucleophiles or primary amines were used to substitute the polymers leading to poly(aryloxythionylphosphazenes) **24** and poly(aminothionylphosphazenes) **25** respectively [35, 37]:

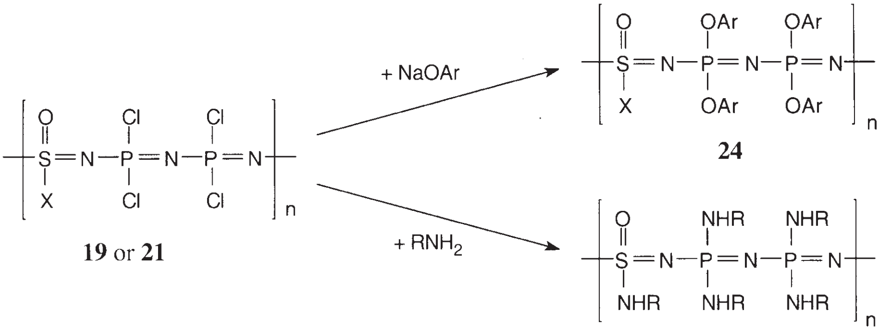

19 or **21**

24

25 (10)

In the case of the reaction with aryloxides, only substitution of the P-Cl bonds can be achieved even after prolonged reaction times. Interestingly, the sulfur-chlorine (in **19**) or sulfur-fluorine (in **21**) bonds remain intact. This regioselective substitution pattern is exactly the opposite to that observed with polythiophosphazenes **12** which contain sulfur(IV) centers where perhalogenated derivatives substitute with aryloxides preferentially at sulfur [38]. In contrast to aryloxides, amines readily substitute at both the phosphorus and sulfur sites at ambient temperature. The resulting moisture stable polythionylphosphazenes range from colorless elastomeric materials (see Fig. 2) to glassy polymers which are isolated as white powders (see Table 1).

The poly(aryloxythionylphosphazenes) **24** and poly(aminothionylphosphazenes) **25** show no noticeable change after storage in air for several years. However, in solution, polymer **24** rapidly decomposes in the presence of strong bases such as NaOH or excess sodium aryloxide at elevated temperatures. These reactions are presumably initiated by nucleophilic attack at the sulfur(VI) center.

Fig. 2. A typical polythionylphosphazene elastomer (**27c**)

The molecular weights of the polymers **24** and **25** have been estimated by Gel Permeation Chromatography (GPC) relative to polystyrene standards (Table 1). In addition, an absolute value of the weight average molecular weight (M_w) for polymer **24b** was determined by low-angle laser light scattering (LALLS) studies in THF solution and gave a value of $M_w = 64{,}000$ compared to the value determined by GPC (140,000). This result showed that GPC, a relative technique, overestimates the molecular weight of aryloxy-substituted polythionylphosphazenes by a factor of 2. In contrast, LALLS for **25d** gave $M_w = 105{,}000$ which is substantially greater than that determined by GPC ($M_w = 49{,}000$). Thus, poly(aryloxythionylphosphazenes) appear to be poorly solvated in THF and thus the effective hydrodynamic size of the polymer coils is compact with respect to polystyrene, whereas for poly(aminothionylphosphazenes) the exact opposite is true. Thus, polymer molecular weights of **24** are overestimated and underestimated for **25**, since GPC separation of polymers is based on effective hydrodynamic size.

The thermal transition behavior of the aryloxy polymers was studied by DSC and, as expected, bulkier aryloxy side-groups, such as *p*-phenylphenoxide, led to an increase in T_g over less bulky side-groups such as phenoxide. For poly[(amino)thionylphosphazenes], the T_g values can be easily modified by varying the type and length of side-chain used. The use of bulky amines, such as aniline to substitute the polymer leads to a relatively high T_g of 82 °C for **25f**. The T_g values show a general decrease as the length of the alkyl chain is extended from methyl (**25a**) ($T_g = 22\,°C$) to hexyl (**25e**) ($T_g = -18\,°C$). This effect arises from the free volume increase as the longer alkyl side groups push the polymer chains further apart. Interestingly, in contrast to the situation for perhalogenated

Table 1. Characterization data for selected polythionylphosphazenes[a]

	R	R′	Molecular weight (M_w)	PDI[b]	T_g (°C)	Type of material
19	Cl	Cl	–	–	–46	Gum
21	F	Cl	–	–	–56	Gum
24a	Cl	OPh	58,000	1.4	10	Gum
24b	Cl	OC_6H_4Ph-*p*	140,000	2.7	55	Glass
24c	F	OPh	38,000	1.5	–15	Gum
24d	F	OC_6H_4Ph-*p*	90,000	1.6	48	Glass
25a	NHMe	NHMe	5000[c]	1.5	22	Glass
25b	NHEt	NHEt	37,000	2.3	4	Gum
25c	NHPr	NHPr	49,000	1.9	6	Gum
25d	NHBu	NHBu	49,000	2.0	–16	Gum
25e	NHHex	NHHex	71,000	1.9	–18	Gum
25f	NHPh	NHPh	130,000	1.8	82	Glass
27a	NHBu	OCH_2CF_3 (51%) NHBu (49%)	140,000	1.7	–14	Gum
27b	NHBu	OCH_2CF_3 (76%) NHBu (24%)	33,000	1.7	–20	Gum
27c	NHBu	OCH_2CF_3 (95%) NHBu (5%)	39,000	1.4	–30	Gum
28a	NC_5H_{10}	NC_5H_{10}	42,000	3.1	27	Glass
28b	NC_4H_8	NC_4H_8	57,000	2.6	24	Glass
29a	NHBu	NHBu (18%) NEt_2 (82%)	52,400	1.9	1	Gum
29b	NHBu	NHBu (29%) NEt_2 (71%)	53,500	1.8	–9	Gum
29c	NHBu	NHBu (47%) NEt_2 (53%)	63,700	1.8	–13	Gum
29d	NHBu	NHBu (26%) NC_5H_{10} (74%)	35,700	4.9	20	Glass
29e	NHBu	NHBu (56%) NC_5H_{10} (44%)	113,700	2.3	6	Gum
29f	NHBu	NHBu (36%) NC_4H_8 (64%)	33,500	10.9	14	Gum
31	NHBu	NHBu	150,000	1.9	–70 (PTHF) –16 (PTP)	Gum

---

[a] R indicates the substituents on the sulfur atom (S-R), R′ indicates the substituents on the phosphorus atoms (P-R′).

[b] Polydispersity index (PDI) is the measure of the breadth of the molecular weight distribution of a polymer sample and is defined as the weight average molecular weight (M_w) divided the number average molecular weight (M_n).

[c] The molecular weight of this water soluble polymer is probably a dramatic underestimate because of its anticipated small hydrodynamic size in THF solution.

polythionylphosphazenes, the aryloxy and amino-substituted materials generally possess lower T_gs than the analogous classical polyphosphazenes. For example, the butylamino polymer **25d** has a significantly lower T_g (–17°C) than $[N{=}P(NHBu)_2]_n$ ($T_g = 8$°C) [39] This is a consequence of the presence of the small S=O group which leads to only five substituents of significant size per six skeletal atom repeat unit in polythionylphosphazenes compared to six substituents for polyphosphazenes. Providing that the substituents are not small this effect overrides the lower flexibility introduced by the replacement of a phosphorus atom by a sulfur(VI) moiety discussed above. Another interesting difference from polyphosphazenes is that all of the polythionylphosphazenes prepared so far are amorphous and, to date, none show melting transitions by DSC. Their amorphous nature has been confirmed by wide-angle X-ray scattering studies which give featureless diffractograms.

Attempts to substitute completely the halogen substituents of polymers **19** and **21** with alkoxide nucleophiles have led only to degradation of the polymer backbone. The unexpected regioselectivity of substitution of the polythionylphosphazenes with aryloxide nucleophiles and the rapid degradation of the polymer backbone with alkoxide nucleophiles prompted us to model this behavior by studying the reactions of the cyclic thionylphosphazenes **18** and **20** towards representative aryloxide and alkoxide reagents [40]. The substitution reactions with NaOPh were found to conform to the following general order of reactivity: $PCl_2 > PCl(OPh) > S(O)X$ (X=Cl or F). As in the case of the polymer, the substitution of the S-Cl bonds did not take place under normal reaction conditions, but it was found that, upon the addition of an excess of NaOPh and reaction for several days at 25°C or reflux for 4 h, the fully substituted cyclic

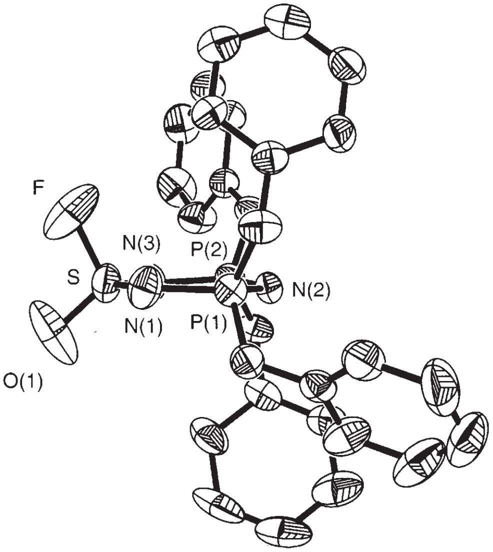

Fig. 3. The molecular structure of a regioselectively phenoxide substituted thionylphosphazene, $NSOF[NP(OPh)_2]_2$. Reproduced from [40] with permission

thionylphosphazene could be formed. In the case of the fluorinated cyclic thionylphosphazene, even after prolonged reflux in excess NaOPh, no substitution of the S-Cl bond was detected and only the regioselectively tetrasubstituted thionylphosphazene could be isolated (see Fig. 3).

Two alkoxide nucleophiles trifluoroethoxide and butoxide were chosen to model the substitution pattern of **18** and **20**. The reaction of cyclic thionylphosphazene with NaOBu was found to follow the same order of reactivity as NaOPh; however, unlike NaOPh the substitution of the S-Cl bond was facile at room temperature and the substitution of the S-F bond required an excess of nucleophile. Interestingly, although the reaction of the cyclic thionylphosphazenes with the $NaOCH_2CF_3$ was found to follow the same general order of reactivity as NaOPh or NaOBu ($PCl_2 > PCl(OPh) > S(O)X$), a significant enhancement in reaction rate was detected with each equivalent of trifluoroethoxide added.

Although the reason for the backbone degradation in the reaction of **19** and **21** with alkoxides is still not clear, these results have encouraged the recent synthesis of amorphous poly[alkoxy(amino)thionylphosphazenes] with high loadings of trifluoroethoxide [41]. Polymers **27a–c** were synthesized through the reaction of **19** with $Na(OCH_2CF_3)$ in various ratios, followed by the reaction with $BuNH_2$. The substitution was found to proceed regioselectively with reaction of alkoxide only at P, and subsequent substitution of the remaining P-Cl and S-Cl bonds with butylamine.

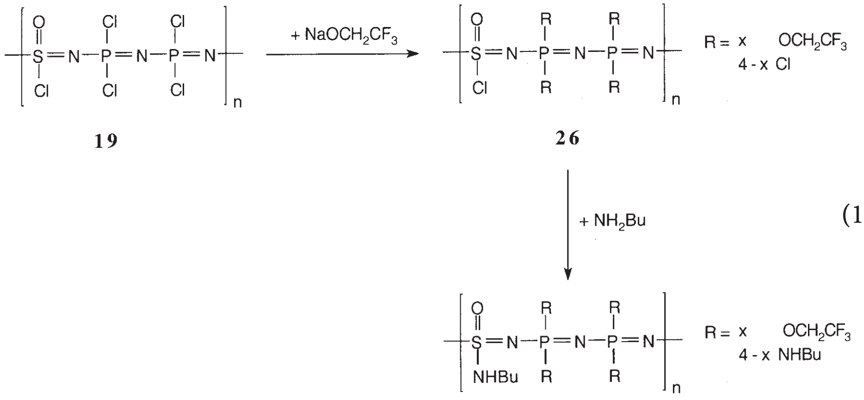

19 **26** **27**

(11)

These polymers have the lowest T_gs determined to date from hydrolytically stable polythionylphosphazenes. Upon an increase in the loading of trifluorethoxide from **27a–c**, the T_g decreased from −14 °C to −30 °C. This decrease in T_g is expected as lower glass transition temperatures are observed for polyphosphazenes with trifluoroethoxy side groups {$[P(OCH_2CF_3)_2N]_n$, $T_g = -66\,°C$} than with butylamino side groups {$[P(NHBu)_2N]_n$, $T_g = 8\,°C$}.

In order to expand further the polythionylphosphazene system, the polymers **28a, b** and **29a–f** were prepared with secondary amines [42]. While complete substitution of chlorine atoms was observed for cyclic secondary amines, treatment of **19** with the sterically more demanding $HNEt_2$ resulted in only a partial substitution. The hydrolytically stable poly(aminothionylphosphazenes) (**29a–f**) were prepared through reaction of partially substituted polythionylphosphazenes with *n*-butylamine. Complete substitution of chlorine by cyclic secondary amines led to materials with ambient T_gs (**28a,** $T_g = 27\,°C$) when compared to analogs derived from primary amines. As expected, an increase in the amount of *n*-butylamino substituents in the mixed systems resulted in a decrease in the T_g of the final material (**29e,** $T_g = 6\,°C$):

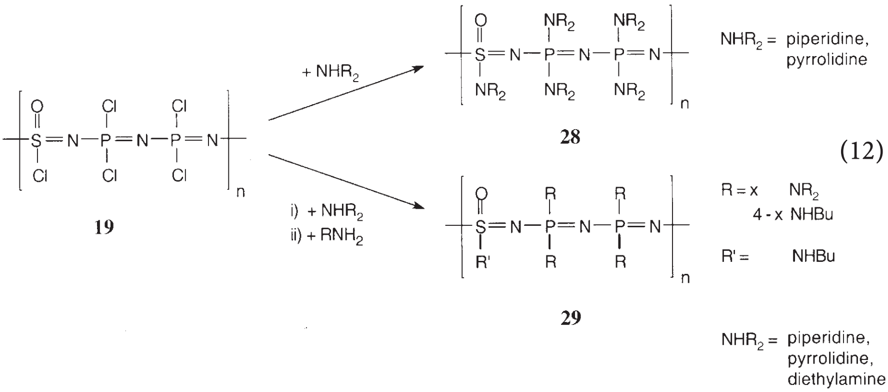

(12)

4.2.5
Applications of Polythionylphosphazenes as Matrices for Oxygen Sensors

Polythionylphosphazenes represent an interesting class of new polymers and the possible applications of these materials are under exploration. One area where significant potential has already been established involves their use as phosphorescent oxygen sensor matrices [43]. Phosphorescent sensors based on composites comprising transition metal-based dyes (e.g., $[Ru(phenPh_2)_3]^{2+}$) with oxygen quenchable excited states dispersed in polymer matrices of high gas permeability (e.g., crosslinked polysiloxanes) have attracted attention as oxygen sensors for biomedical applications [44]. In addition, much interest exists in the use of such sensors for barometric applications such as the determination of the air pressure distribution over aircraft models in a wind tunnel. Information of this type plays a vital role in aircraft design and testing. However, current techniques involve the use of solid state pressure taps which are monitored individually. This technology is very expensive, gives pressure information only at points where the taps are located, and is limited to stationary objects. The use of pressure sensing composites has the potential to overcome all of these problems. For example, simply spray-coating a film of the composite on a surface of interest allows the pressure distribution over the whole surface to be readily monitored via illumination of the excitation wavelength of the dye and data acquisition in the region of phosphorescent emission, the intensity of which depends on the air (i.e., oxygen) pressure at that point.

Manners, Winnik and coworkers have shown that poly(aminothionylphosphazenes), **25**, offer some significant advantages over existing materials for pressure-sensing composite technology (see Fig. 4) and it has even been found that

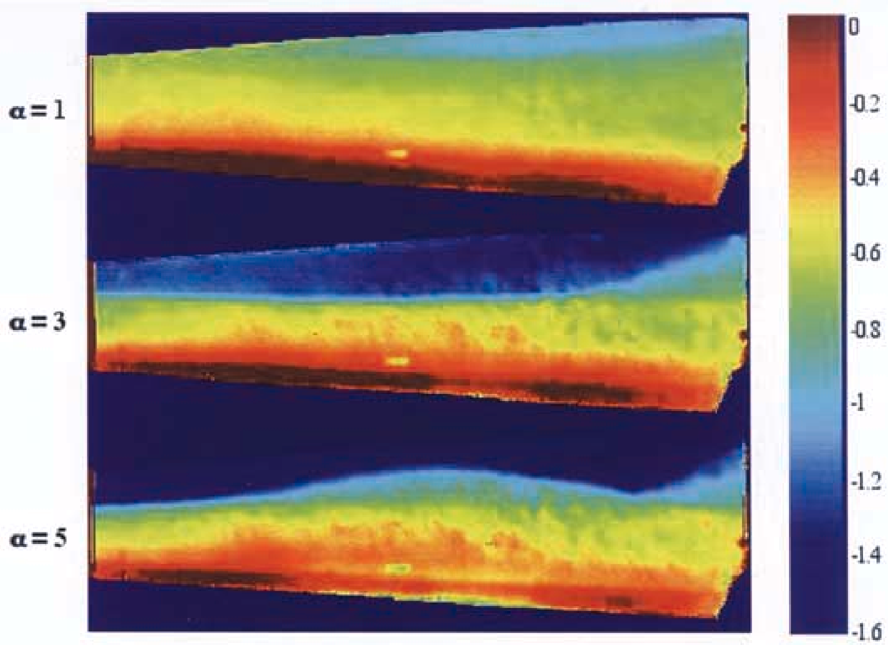

Fig. 4. Phosphorescent image of a section of a model aircraft wing showing the surface pressure distribution as a function of tilt angle (α) during a wind tunnel experiment. (The colors, whilst artificial, reflect the pressure at different points on the surface. In this case, the polymer matrix was composed of poly(aminothionylphosphazene)-*b*-poly[THF] (**31**) and the dye was $[Ru(phenPh_2)_3]Cl_2$. The images were obtained from a series of tests run at the National Research Council Wind Tunnel in Ottawa)

rotating objects such as propellers can be imaged. The key advantages of poly(aminothionylphosphazenes) for this type of application involves the high solubility and high diffusion coefficient for oxygen in these materials [45], the good compatibility with the dye due to the polar polymer structure, and the ability to access reasonable quality films without the need for crosslinking. In addition, the relatively low T_gs for **25** are important as large scale conformational motions are usually vital for effective gas diffusion in a material. T_g values of less than –10 °C, which represents a typical low temperature limit in a wind tunnel, are therefore critical.

Unfortunately, films formed by **25 d** are still quite tacky which make them unsuitable for these applications. Visualization of air flow over objects such as aircraft requires materials which provide a smooth, abrasive resistant surface. With this in mind, the cationic chain end of **19** (see Scheme 1) was reacted with tetrahydrofuran resulting in polythionylphosphazene-*b*-polytetrahydrofuran block copolymer (**30** and **31**) [46]:

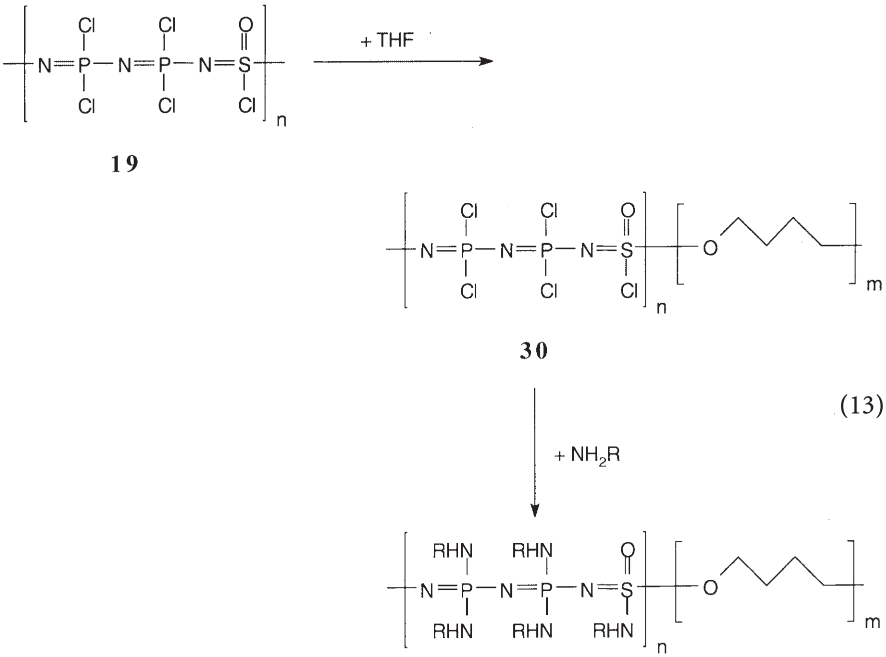

19

30

(13)

31

Black copolymer **31** forms free standing films which are non-tacky and have good mechanical properties while maintaining oxygen permeability which is fairly close to that of **25 d**.

4.2.6
Ambient Temperature Synthesis of Polythionylphosphazenes

It has been speculated that the thermal ROP of both **18** and **20** proceeds via the heterolytic dissociation of the sulfur-halogen bond as the initiation step, forming the highly reactive thionylphosphazene cation (**32**) (see Scheme 1) [20]. Propagation occurs via attack of **32** by another molecule of **18** (or **20**) to give a cationic cyclolinear species, which can subsequently be attacked resulting in continued chain propagation. Cationic mechanisms are common for the polymerization of cyclic organic molecules and a similar mechanism involving the ionization of a phosphorus-halogen bond has also been proposed for the thermal ROP of the cyclic phosphazene **3** [2]. Attempts to isolate **32** through the reaction of **18** with stoichiometric quantities of a variety of halide acceptors led instead to the synthesis of new S-substituted cyclic thionylphosphazenes [31].

In addition, these studies led to discovery of an ambient temperature route to **19** through reaction of **18** with substoichiometric amounts of Lewis acid catalysts (such as $GaCl_3$). As with the thermal ROP, reaction of **18** with 10 mol%

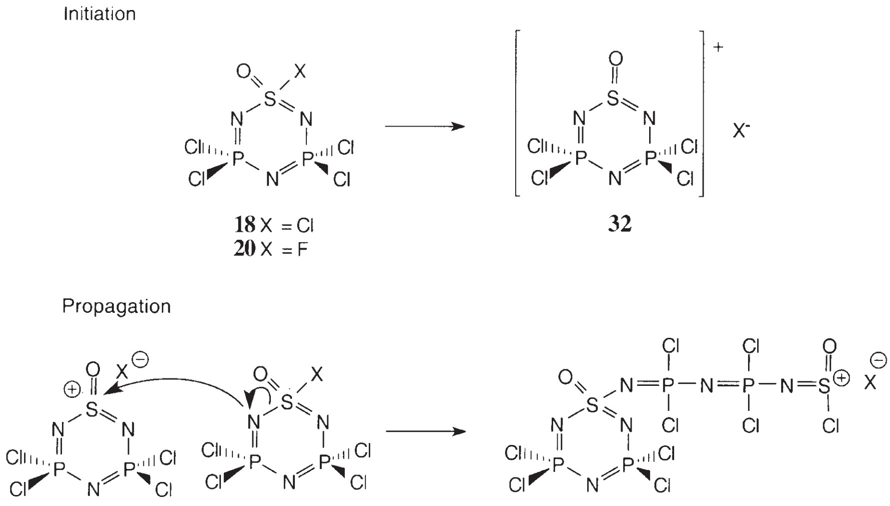

Scheme 1. Proposed mechanism for the thermal ring-opening polymerization (ROP) of cyclic thionylphosphazenes (**18** and **20**)

$GaCl_3$ produces 12-, 18-, 24-, and higher order macrocycles, in addition to high molecular weight polythionylphosphazene, **19**. Interestingly, the extent of reaction and distribution of products was shown to be highly dependent on the concentration of **18** in solution (see Table 2).

Highly concentrated solutions of **18** and 10 mol% $GaCl_3$ afforded only **19** and higher order macrocycles, whereas more dilute samples yielded **19** together with smaller macrocyclic products with lower conversions. Subsequent reaction of **19** with *n*-butylamine yielded **25d** with molecular weights in the range M_w 52,000–150,000; PDI = 1.26–2.52. Remarkably, dilute solutions of **18** (ca. 250 mg in 20 ml CH_2Cl_2) were found to be unreactive towards $GaCl_3$ (see Table 2). This points to the existence of a critical concentration (~0.15 mol/l) below which polymerization will not take place at ambient temperature. Although such observations are well-established for organic monomers (such as α-methylstyrene and THF) [47], very few examples have been established for inorganic systems [48].

4.3
Condensation Routes to Sulfur-Nitrogen-Phosphorus Polymers

Also noteworthy is the interesting condensation route reported by Turner et al. which leads to polymers with backbones of alternating S(O)=N and P=N units [49]. Although, polythionylphosphazenes could not be isolated through heating mixtures of *N*-silylphosphoranimines (**33**) and *N*-silylsulfonimides (**34**) at 140 °C, a regioselective coupling of the two compounds occurred by heating equimolar amounts of **33** and **34** between 80 °C and 140 °C. The resulting

Table 2. Conversion of **18** to polymer **19** using 10% $GaCl_3$ as an initiator in different volumes of CH_2Cl_2 upon equilibration[a]

Volume CH_2Cl_2 used (ml)	**18** (%)	**22** (%)	**19** (%)[b]	Yield **25d** (%)[c]	M_w **25d**	PDI **25d**
0.25	0	0	100	68[d]	84,750[d]	1.86[d]
0.50	4	12	84	83	91,500	2.18
1	15	20	65	62	89,000	1.72
2	33	32	35	34	60,500	1.78
3	52	23	25	25	59,000	1.32
4	61	23	16	5	58,000	1.26
5	77	23	0	0	–	–
10	88	12	0	0	–	–
20	100	0	0	0	–	–

[a] 0.76 mmol of **18** were used. The composition of the reaction mixture was determined using ^{31}P NMR integration. (**18** δ =27.1 ppm, **22** δ = −7.7, −7.9 ppm, **19** δ = −9.7 ppm).

[b] Estimate also includes higher membered rings (>12-membered).

[c] Isolated yield based on 252 mg of **18**.

[d] Average of 4 experiments. Yield of **25d.** 51–89%; M_n. 52,000–150,000; PDI 1.63–2.52.

thionylphosphazene monomers (**35**) were reacted with trifluoroethanol to give the alternate monomer **36**. Heating **35** and **36** (R=Me, OR=OCH_2CF_3) at 140°C and 100°C, respectively, resulted in low molecular weight polythionylphosphazenes, **37**. Polymer **37** represents the first polythionylphosphazenes with alkyl side groups:

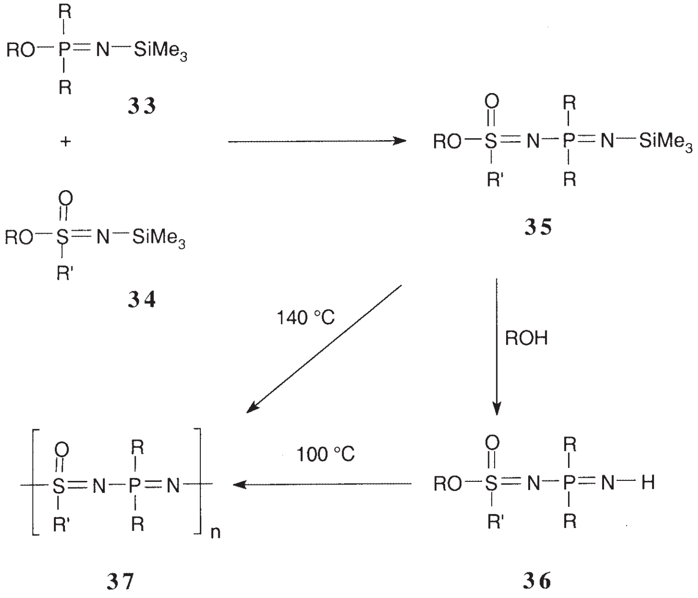

(14)

In addition, the first polythiazylphosphazenes (**38**), which contain two coordinate sulfur(III) atoms, were prepared from the reaction of $Cl_2PN_2(SiMe_3)_3$ with sulfur halides [50]. The materials, which also possess alternating S-N and P-N units in the polymer backbone, represent true hybrids of poly(sulfur nitrides) and polyphosphazenes and further developments in this area should prove to be particularly interesting:

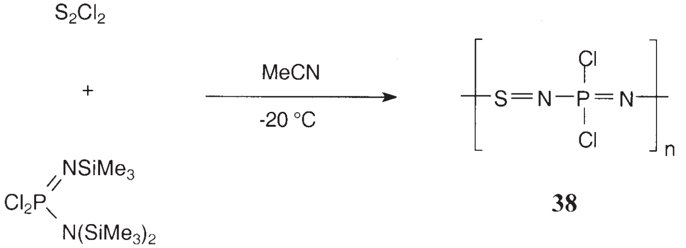

38

(15)

5
Synthesis of Polyphosphinoboranes

5.1
Early Pyrolytic Routes to Phosphinoboranes

Cyclic phosphinoboranes of the general formula $[R_2P\text{-}BH_2]_x$ (R=alkyl or aryl, x=3 or 4) are well known as a result of the pioneering work of Burg and Wagner in the 1950s. For instance, the pyrolysis of $Me_2PH \cdot BH_3$ at 150 °C for 40 h is reported to give a mixture of 90% $[Me_2P\text{-}BH_2]_3$ and 9% $[Me_2P\text{-}BH_2]_4$ [51]. Most interestingly, these cyclic structures show high thermal stability, and resistance to oxidation and hydrolysis.

The attempted synthesis of polymeric materials based on skeletons of alternating, four-coordinate phosphorus and boron atoms, polyphosphinoboranes, also received significant attention at that time, as such materials seemed likely candidates for accessing valuable, high performance properties such as high temperature stability and flame retardancy. However, the open literature on phosphinoborane polymer chemistry is very limited and most of this work is documented in patents and technical reports [52, 53]. The main synthetic methodology studied involved thermally-induced dehydrocoupling of phosphine-borane adducts $R_2PH \cdot BH_3$ at ca. 200 °C and above which was often performed in the presence of additives such as amines, which were claimed to prevent cyclization. For example, thermolysis of $Me_2P\text{-}PMe_2 \cdot BH_3$ or $RMePH \cdot BH_3$ (R=Me or Et) at 175–200 °C in the presence of amines was reported to give polymers $[RMeP\text{-}BH_2]_n$ with molecular weights of 1800–6000 [54, 55]. A patent claims a maximum molecular weight of 13,632 when the thermolysis of $Me_2PH \cdot BH_3$ is carried out at 200 °C for 17 h with a difunctional base but no further product characterization was reported in this particular case [56]. In addition, partially characterized, insoluble materials with three-coordinate phosphorus and boron atoms have been described [57]. However, none of the products were convincingly structurally characterized by present day standards and, where reported, the yields and molecular weights were generally very low. Since that time the area of phosphorus-boron polymer chemistry has generally been neglected.

5.2
Metal-Catalyzed Dehydrocoupling Routes to Phosphinoboranes

In 1999, a novel transition metal-catalyzed dehydrocoupling route to linear and cyclic oligomeric and also high molecular weight polyphosphinoboranes was developed [58, 59]. The dehydrocoupling of the phosphine-borane adduct $Ph_2PH \cdot BH_3$ in the presence of $[\{Rh(\mu\text{-}Cl)(1{,}5\text{-}cod)\}_2]$ or $[Rh(1{,}5\text{-}cod)_2][OTf]$ (0.5–1 mol% Rh) gives the linear compound $Ph_2PH\text{-}BH_2\text{-}PPh_2\text{-}BH_3$ (**39**) at 90 °C, and a mixture of the cyclic trimer $[Ph_2P\text{-}BH_2]_3$ (**40a**) and tetramer $[Ph_2P\text{-}BH_2]_4$ (**40b**) at 120 °C. In addition, the catalytic potential of other complexes (e.g., Ti, Ru, Rh, Ir, Pd, Pt) was investigated and was in many cases demonstrated:

$$\mathrm{Ph_2PH\text{-}BH_3} \xrightarrow[-\,\mathrm{H_2}]{\substack{[\mathrm{Rh}]\\ 90\ ^\circ\mathrm{C}}} \underset{\mathbf{39}}{\mathrm{Ph_2PH\text{-}BH_2\text{-}PPh_2\text{-}BH_3}} \tag{16}$$

$$\mathrm{Ph_2PH\text{-}BH_3} \xrightarrow[-\,\mathrm{H_2}]{\substack{[\mathrm{Rh}]\\ 120\ ^\circ\mathrm{C}}} \underset{\mathbf{40a}}{[\mathrm{Ph_2P\text{-}BH_2}]_3} + \underset{\mathbf{40b}}{[\mathrm{Ph_2P\text{-}BH_2}]_4} \tag{17}$$

In the absence of the rhodium catalyst, no conversion of $Ph_2PH \cdot BH_3$ was observed at this temperature. As previous work had shown, much higher temperatures (> 170 °C) are necessary before $Ph_2PH \cdot BH_3$ undergoes thermally-induced dehydrocoupling to give mainly $[Ph_2P\text{-}BH_2]_3$ (**40a**) [60]. Compounds **39**, **40a**, and **40b** were characterized by solution NMR spectroscopy (^1H, ^{11}B, ^{13}C, ^{31}P nuclei) and by single crystal X-ray crystallography (**39**, **40b**, see Figs. 5 and 6) [58, 59].

Early work on the pyrolysis of the primary phosphine-borane adduct $PhPH_2 \cdot BH_3$ by Korshak et al. in 1964 suggested that low molecular weight polymers of possible formula $[PhPH\text{-}BH_2]_n$ could exist. For instance, heating of $PhPH_2 \cdot BH_3$ at temperatures between 100 and 150 °C for a period of 13 h was reported to give a benzene-soluble polymer with an average composition unit $PhPH\text{-}BH_2$, as determined by elemental analysis, and a molecular weight (M_n) of 2150, which was measured ebullioscopically. Longer heating and elevated temperatures (up to 250 °C) led to the formation of insoluble material, without significant molecular weight increase of the benzene-soluble fraction (maximum $M_n = 2630$) [61].

When $PhPH_2 \cdot BH_3$ was refluxed in toluene overnight in the presence of approximately 0.5–1 mol% of $[Rh(1{,}5\text{-}cod)_2][OTf]$, dehydrogenative coupling was indeed observed. After precipitation into hexanes an off-white product was iso-

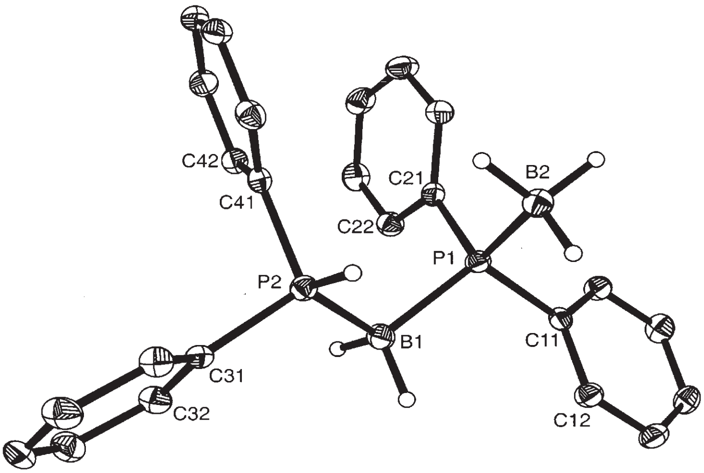

Fig. 5. The molecular structure of a linear phosphinoborane (**3a**). Reproduced from [59] with permission

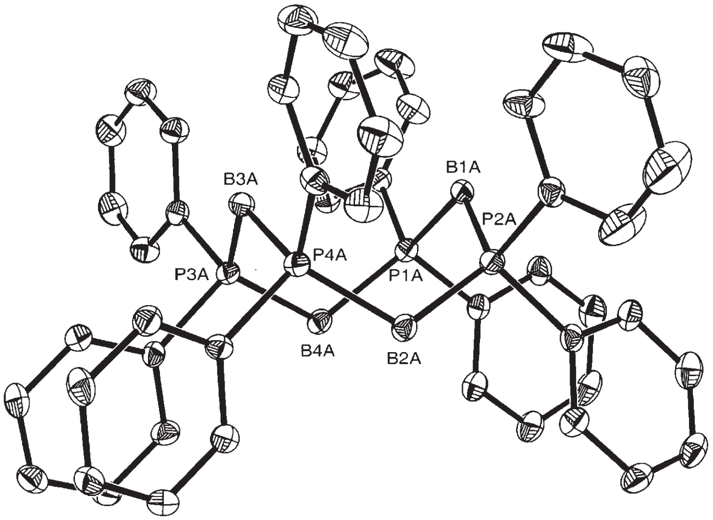

Fig. 6. The molecular structure of a cyclic phosphinoborane (**40**). Reproduced from [59] with permission

lated and subsequently identified as poly(phenylphosphinoborane) (**41**) [58, 59]:

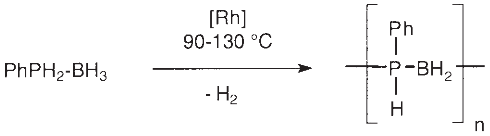

$$PhPH_2\text{-}BH_3 \xrightarrow[-\,H_2]{[Rh]\;90\text{-}130\ °C} \left[\underset{H}{\overset{Ph}{\overset{|}{\underset{|}{P}}}}\text{-}BH_2 \right]_n \qquad (18)$$

41

Polymer **41** was characterized by ^{1}H, ^{11}B, ^{13}C, ^{31}P NMR and IR spectroscopy, and elemental analysis. The molecular weight of **41** was determined by static light scattering (SLS) in THF. However, the absolute weight average molecular weight (M_w) of **41** prepared by this solution method was found to be relatively low ($M_w = 5600$), corresponding to a weight average degree of polymerization (DP_w) of only 46.

To obtain higher molecular weights by increasing the extent of reaction, $PhPH_2{\cdot}BH_3$ and a rhodium catalyst were heated in the absence of solvent at slightly more elevated temperatures. Neat $PhPH_2{\cdot}BH_3$ and a catalytic amount of $[\{Rh(\mu\text{-}Cl)(1,5\text{-}cod)\}_2]$ (ca. 0.6 mol% rhodium) were heated at 90 °C for 3 h and then at 130 °C for 3 h. The reaction mixture gradually became viscous at 90 °C and was completely solid after 3 h at 130 °C. Dissolution of the product in THF and subsequent precipitation into hexanes gave polymer **41** (ca. 75% yield) which was spectroscopically identical to that prepared in toluene. However, in this case the high molecular weight nature of **41** was confirmed by SLS, which afforded an absolute value of $M_w = 33{,}300$, corresponding to $DP_w = 273$. The SLS studies on solutions of polymers **41** in THF also revealed that the second virial coefficient A_2 equals zero. This indicates that THF is a poor solvent for $[PhPH\text{-}BH_2]_n$ at 22 °C and that the polymer is on the verge of precipitation (θ conditions). Attempts to analyze the molecular weight distribution of samples of **41** by GPC using styragel columns and THF as eluent were not successful. However, dynamic light scattering (DLS) experiments on solutions of **41** in THF were also performed. DLS is capable of obtaining the distribution of sizes in a polymer solution and provides a measurement of the hydrodynamic diameter (D_h) of the polymer. A sample of high molecular weight **41** (with $M_w = 33{,}300$) in THF showed a value of $D_h \approx 10$ nm. A small D_h value (ca. 1 nm) was measured for the sample of polymer **41** prepared by catalytic dehydrocoupling in solution which is consistent with the relatively low molecular weight subsequently determined by SLS ($M_w = 5600$).

Polyphenylphosphinoborane (**41**) is air- and moisture-stable in the solid state. It is soluble in THF and chlorinated hydrocarbons, moderately soluble in toluene and benzene, and is insoluble in aliphatic hydrocarbons such as hexanes or in hydrophilic solvents such as methanol or water. Prolonged storage of polymer **41** in THF solution in air results in slow decomposition, which is indicated by a number of additional resonances in the ^{31}P and ^{1}H NMR spectra and is probably peroxide-moderated. Additional experiments have shown that $[PhPH\text{-}BH_2]_n$ (**41**) is stable in solution toward triethylamine (no P-B bond cleavage was observed) and is inert to benzaldehyde (no hydrophosphination occurred).

In the absence of rhodium catalyst, thermally-induced dehydrocoupling of $PhPH_2 \cdot BH_3$ proceeds very slowly and forms only low molecular weight materials with complex NMR spectra. Hydrodynamic diameters obtained by DLS measurements in THF solution clearly revealed the low molecular weight nature of the material ($D_h \approx 1$ nm), which is consistent with the previous work by Korshak and co-workers where molecular weights M_n of ca. 2000 were reported. This suggests that the material probably consists of low molecular weight oligomers and perhaps cyclics or branched species.

Catalytic dehydrocoupling of the alkyl-substituted phosphine-borane adduct $i\mathrm{BuPH_2 \cdot BH_3}$ has also been investigated and was found to be much slower than that of $\mathrm{PhPH_2 \cdot BH_3}$. This produced polyisobutylphosphinoborane $[i\mathrm{BuPH\text{-}BH_2}]_n$ (**42**) under neat conditions at 120 °C (13 h) in the presence of $[\{\mathrm{Rh}(\mu\text{-}\mathrm{Cl})(1{,}5\text{-cod})\}_2]$ in 80% yield [59]. Polymer **42** was isolated as a tacky solid after precipitation into a mixture of 2-propanol/water from THF, and characterized by multinuclear NMR spectroscopy. Conclusive evidence for the polymeric character of **42** was obtained from DLS experiments in THF solution. However, the hydrodynamic diameter of polymer **42** ($D_h \approx 7$ nm) was slightly smaller than the one measured for high polymeric **41**. Making the approximation that polymers **41** and **42** exhibit similar hydrodynamic behavior in THF, the DLS data for **42** suggest a molecular weight of 10,000 to 20,000. Polyisobutylphosphinoborane (**42**) is stable to both oxygen and moisture and is soluble in THF, chlorinated solvents, toluene, and even hexanes, but is insoluble in water and methanol. Again, the dehydrocoupling of $i\mathrm{BuPH_2 \cdot BH_3}$ is very sluggish in the absence of rhodium catalyst.

Prolonged heating of polymers **41** and **42** at elevated temperatures in the presence of catalyst afforded insoluble products which were found to swell significantly upon addition of THF or $\mathrm{CH_2Cl_2}$. However, the $^{31}\mathrm{P}$ and $^{1}\mathrm{H}$ NMR spectra of these materials (immersed and swollen in $\mathrm{CDCl_3}$) were similar to those obtained for $\mathrm{CDCl_3}$-soluble polymers **41** and **42**. As branching positions could not be detected in the $^{31}\mathrm{P}$ and $^{11}\mathrm{B}$ NMR spectra, we assume that the polymers either become weakly crosslinked (through additional interchain P-B coupling) or increase in molecular weight above the solubility limit when heated for prolonged periods above 120–130 °C in the presence of catalyst.

Future work in this area will focus on detailed studies of the physical properties of polyphosphinoboranes, which can be regarded as analogs of poly(α-olefins) with a phosphorus-boron backbone. This should be very revealing from a fundamental perspective and useful properties such as flame retardancy and oxidative stability may emerge. Substantial differences in physical properties would be anticipated as the skeletal P-B bonds (typically >1.92 Å) should be much longer than C-C single bonds (1.54 Å). Opportunities also exist for the facile structural modification of polyphosphinoboranes such as **41** and **42** and analogs via exploitation of the P-H functionality using deprotonation/electrophilic addition reaction sequences. The dehydrocoupling mechanism is also of considerable interest; the catalytic chemistry may involve M-P and/or M-B bonds and studies in this area are in progress [62]. The extension of the synthetic methodology to other skeletons based on alternating atomic sequences of Group 13 and Group 15 elements may also be possible by analogous chemistry and such materials would be of potential interest as precursors to III/V semiconductor materials. We have shown that amine-borane adducts also undergo catalytic dehydrocoupling. For example, in the presence of $\mathrm{Rh^1}$ complexes (ca. 1–5 mol.%) $\mathrm{Me_2NH{\cdot}BH_3}$ yields the cyclic dimer $[\mathrm{Me_2N\text{-}BH_2}]_2$ at 25–45 °C [63] Such reactions may permit convenient routes to B-N polymers to be developed.

6
Summary

In this chapter key developments in the inorganic polymer chemistry of phosphorus are reviewed. A range of interesting new polymer systems have been prepared recently by using ROP routes or novel polycondensation methods. Further investigation of the generality of these types of synthetic approaches and the development of entirely new polymerization strategies and materials will be important. For example, dendritic systems, which are currently attracting much attention, have also been recently prepared with phosphorus as a key structural component [64]. A future challenge will also be to study and understand the properties of the new phosphorus-containing materials and to investigate possible applications.

7
References

1. Manners I (1996) Angew Chem Int Ed Engl 35:1602
2. Allcock HR (1972) Chem Rev 72:315
3. Allen CW (1994) Coord Chem Rev 130:137
4. Stokes NH (1895) Am Chem J 17:275; Stokes NH (1896) Am Chem J 18:629; Stokes NH (1897) Am Chem J 19:782; Stokes NH (1898) Am Chem J 20:740; see Mark JE, Allcock HR, West R (1992) Inorganic polymers. Prentice Hall, Englewood Cliffs, New Jersey
5. Allcock HR, Kugel RL (1965) J Am Chem Soc 87:4216
6. de Jaeger R, Gleria M (1998) Prog Polym Sci 23:179
7. Allcock HR (1994) Chem Mater 6:1476
8. Allcock HR (1994) Adv Mater 6:106
9. Allcock HR, Crane CA, Morrissey CT, Nelson JM, Reeves SD, Honeyman CH, Manners I (1996) Macromolecules 29:7740
10. Honeyman CH, Manners I, Morrissey C, Allcock HR (1995) J Am Chem Soc 117:7035
11. Manners I, Allcock HR, Renner G, Nuyken O (1989) J Am Chem Soc 111:5478
12. Allcock HR, Coley SM, Manners I, Nuyken O, Renner G (1991) Macromolecules 24:2024
13. Allcock HR, Coley SM, Manners I, Visscher KB, Parvez M, Nuyken O, Renner G (1993) Inorg Chem 32:5088
14. Allcock HR, Coley SM, Morrissey CT (1994) Macromolecules 27:2904
15. Roesky HW, Lücke M (1989) Angew Chem Int Ed Engl 28:493
16. Honeyman CH, Foucher DA, Dahmen FY, Rulkens R, Lough AJ (1995) Organometallics 14:5503
17. Peckham TJ, Massey JA, Honeyman CH, Manners I (1999) Macromolecules 32:2830
18. Withers HP, Seyferth D (1982) Organometallics 1:1275
19. Cao L, Manners I, Winnik MA (2001) Macromolecules 34:3353
20. Manners I (1994) Coord Chem Rev 137:109
21. Poly(sulfur nitride), $[SN]_x$, possesses remarkable properties such as electrical conductivity at room temperature and superconductivity below 0.3 K; see Labes MM, Love P, Nichols LF, (1979) Chem Rev 1; $[SN]_x$ is insoluble and has a polymeric structure in the solid state with interchain S···S interactions. As these interactions are crucial to the properties of the material, $[SN]_x$ is best regarded as a solid-state polymer rather than a polymeric material with discrete macromolecular chains of the type discussed in this section
22. Dodge JA, Manners I, Allcock HR, Renner G, Nuyken O (1990) J Am Chem Soc 112:1268
23. Liang M, Manners I (1991) J Am Chem Soc 113:4044
24. Baalmann HH, Velvis HP, van de Grampel JC (1972) Recl Trav Chim 91:935

25. Klingebiel U, Glemser O (1972) Z Naturforsch 27b:467
26. Suzuki D, Akagi H, Matsumura K (1983) Synth Commun 369
27. van de Grampel JC (1981) Rev Inorg Chem 3:1
28. van de Grampel JC (1992) Coord Chem Rev 112:247
29. Baalmann HH, van de Grampel JC (1973) Recl Trav Chim 92:1237
30. Gates DP (1997) The synthesis, structure, reactivity and polymerization behavior of boron- and sulfur-nitrogen-phosphorus heterocycles and highly strained chalcogen- and boron-bridged [1]. ferrocenophanes. PhD thesis, University of Toronto
31. McWilliams AR, Gates DP, Edwards M, Liable-Sands LM, Guzei I, Rheingold AL, Manners I (2000) J Am Chem Soc 122:8848
32. Liang M, Manners I (1991) Makromol Chem, Rapid Commun 12:613
33. Roy AK, Burns GT, Lie GC, Grigoras S (1993) J Am Chem Soc 115:2604
34. de Jaeger R, Lagowski JB, Manners I, Vansco GJ (1995) Macromolecules 28:539
35. Ni Y, Lough AJ, Rheingold AL, Manners I (1995) Angew Chem Int Ed Engl 34:998
36. To our knowledge, only two other examples of 24-membered inorganic heterocycles have been structurally characterized: (a) the 24-membered phosphazene $[N{=}PPh_2]_{12}$, see: Oakley RT, Rettig SJ, Paddock NL, Trotter J (1985) J Am Chem Soc 107:6923; (b) a 24-membered imidoantimony(III) metallacycle has also been reported, see: Beswick MA, Davies MK, Paver MA, Raithby PR, Steiner A, Wright DS (1996) Angew Chem Int Ed Engl 35:1508
37. Ni Y, Stammer A, Liang M, Massey J, Vancso GJ, Manners I (1992) Macromolecules 25:7119
38. Allcock HR, Dodge JA, Manners I (1993) Macromolecules 26:11
39. Allcock HR, Cook WJ, Mack DP (1972) Inorg Chem 11:2584
40. Gates DP, Park P, Liang M, Edwards M, Angelakos C, Liable-Sands LM, Rheingold AL, Manners I (1996) Inorg Chem 35:4301
41. Gates DP, McWilliams AR, Manners I (1998) Macromolecules 31:3494
42. Nobis MN, McWilliams AR, Nuyken O, Manners I (2000) Macromolecules 33:7707
43. Pang Z, Gu X, Yekta A, Masoumi Z, Coll JB, Winnik MA, Manners I (1996) Adv Mater 8:768
44. See: Weyenberg DR, Nelson LE (1965) J Org Chem 30:2618; Cundy CS, Eaborn C, Lappert MF (1972) J Organomet Chem 44:291
45. Masoumi Z, Stoeva V, Yekta A, Pang Z, Manners I, Winnik MA (1996) Chem Phys Lett 261:551
46. Ruffolo R, Evans CEB, Liu X, Pang Z, Park P, McWilliams AR, Gu X, Yekta A, Winnik MA, Manners I (2000) Anal Chem 72:1894
47. The polymerization of α-methylstyrene is only possible above concentrations of 2.2 mol/l at 25 °C; see Odian G (1991) Principles of polymerization, 3rd edn. Wiley-Interscience, New York, Chap 3
48. (a) The observation of a critical concentration below which polymerization is not observed is explained by a counterbalance of the ΔH_{ROP} and $T\Delta S_{ROP}$ contributions to ΔG_{ROP}. ΔS_{ROP} is generally negative. (b) For an example of a system that is a ring in solution and a polymer in the solid state see: Beckmann J, Jurkschat K, Schollmeyer D, Schürmann M (1997) J Organomet Chem 543:229
49. Chunechom V, Vidal TE, Adams H, Turner ML (1998) Angew Chem Int Ed 37:1928
50. Chivers T, Doxsee DD, Edwards M, Hilts RW (1992) In: Steudel R (ed) The chemistry of inorganic ring systems (Studies in Chemistry, vol 14). Elsevier, p 291
51. Burg AB, Wagner RI (1953) J Am Chem Soc 75:3872
52. Parshall GW (1967) In: Muetterties EL (ed) The chemistry of boron and its componds. Wiley, New York, p 617
53. Haiduc I, Sowerby DB (1987) The chemistry of inorganic homo – and heterocycles. Academic Press, Toronto, p 103
54. Wagner RI, Caseiro FF (1959) J Inorg Nucl Chem 11:259
55. Burg AB (1959) J Inorg Nucl Chem 11:258
56. Burg AB, Wagner RI (1963) US Patent 3,071,553
57. Coates GE, Livingstone JG (1961) J Chem Soc 5053
58. Dorn H, Singh RA, Massey JA, Lough AJ, Manners I (1999) Angew Chem Int Ed 38:3321

59. Dorn H, Singh RA, Massey JA, Nelson JM, Jaska CA, Lough AJ, Manners I (2000) J Am Chem Soc 122:6669
60. Gee W, Holden JB, Shaw RA, Smith BC (1965) J Chem Soc 3171
61. Korshak VV, Zamyatina VA, Solomatina AI (1964) Izv Akad Nauk SSSR Ser Khim 8:1541
62. Dorn H, Jaska CA, Singh RA, Lough AJ, Manners I (2000) Chem Commun 1041
63. Jaska CA, Temple K, Lough AJ, Manners I (2001) Chem Commun 962
64. Maraval V, Laurent R, Donnadieu B, Mauzac M, Caminade AM, Majoral JP (2000) J Am Chem Soc 122:2499

Recent Advances in Stereocontrolled Synthesis of P-Chiral Analogues of Biophosphates

Piotr Guga, Andrzej Okruszek, Wojciech J. Stec

Department of Bioorganic Chemistry, Centre of Molecular and Macromolecular Studies,
Polish Academy of Sciences, Sienkiewicza 112, 90–363 Łódź, Poland
E-mail: wjstec@bio.cbmm.lodz.pl

Oligonucleotides and their analogues have recently found broad application in biochemistry and molecular biology as new tools for studying interactions of nucleic acids with other biomolecules, and as potential candidates for therapeutics. In this chapter the synthetic methods leading to P-chiral oligonucleotide analogues are reviewed, including synthesis of isotopomeric phosphates and various nucleotide and oligonucleotide conjugates. In this respect special emphasis has been put on the application of oxathiaphospholane methodology, recently developed in the authors' laboratory, for the stereocontrolled synthesis of P-chiral biophosphate analogues.

Keywords. Oligonucleotides, P-chiral DNA analogues, Phosphorothioates, Isotopomeric phosphates, Bioconjugates

Topics in Current Chemistry, Vol. 220

List of Abbreviations

Ade	adenine
Bz	benzoyl
Cyt	cytosine
DBU	1,8-diazabicyclo[5.4.0]undec-1-ene
DMT	dimethoxytrityl
ESI	electrospray ionization
FAB	fast atom bombardment
Gua	guanine
HPLC	high performance liquid chromatography
MALDI TOF	matrix-assisted laser desorption ionization, time-of-flight
MMT	monomethoxytrityl
PAGE	polyacrylamide gel electrophoresis
Thy	thymine
Ura	uracil

1
Introduction

Nearly 25 years ago this Laboratory introduced asymmetric trifunctional phosphorylating reagents of general formula (ArO)(PhNH)P(X)Cl (**1**, X=O or S) [1, 2] allowing for the stereocontrolled synthesis of P-chiral analogues of mononucleotides and dinucleotides. Phosphorylation of the 3′-hydroxyl group of appropriately protected deoxyribonucleosides with **1** provided nucleoside-3′-*O*-(*O*-aryl-*N*-phenylphosphoramidate)s (**2a**) or corresponding phosphoramidothioates (**2b**), readily separable into diastereomeric forms [2, 3]. Subsequent stereoinvertive intramolecular substitution of aryloxy group with another hydroxyl function of the same nucleoside provided P-chiral nucleoside cyclic phosphoranilidates (**3**) [4, 5], while reaction with 5′-OH group of another nucleoside furnished the corresponding dinucleoside 3′,5′-phosphoranilidates (**4**) [5]. The subsequent PN→PX conversion (X=S or ^{18}O) [6] allowed for stereoretentive replacement of anilido function with sulfur or stable oxygen isotope giving rise to pure R_P and S_P diastereomers of nucleoside cyclic 3′,5′-phosphorothioates (**5a**), isotopomeric nucleoside cyclic 3′,5′-[^{18}O] phosphates (**5b**), or dinucleoside 3′,5′-phosphorothioates (**6**) [5].

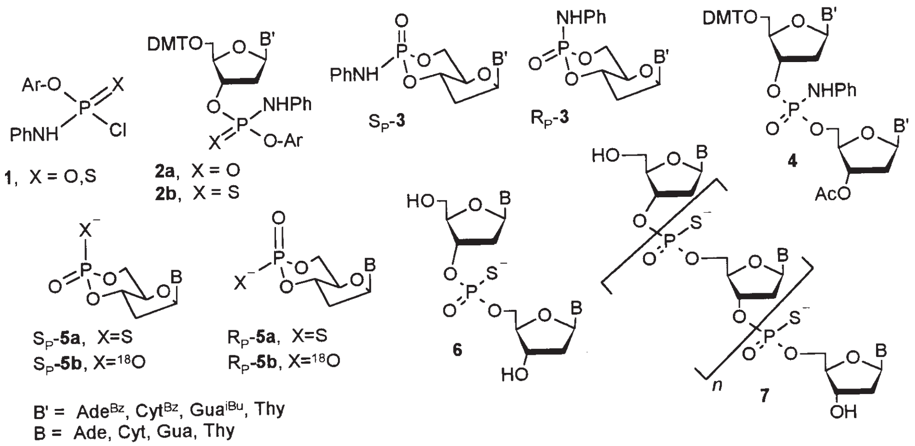

1, X = O,S

2a, X = O
2b, X = S

S_P-**3**

R_P-**3**

4

S_P-**5a**, X=S
S_P-**5b**, X=^{18}O

R_P-**5a**, X=S
R_P-**5b**, X=^{18}O

6

7

B' = Ade^{Bz}, Cyt^{Bz}, Gua^{iBu}, Thy
B = Ade, Cyt, Gua, Thy

The same methodology was applied for the synthesis of corresponding ribonucleoside derivatives [7]. Unfortunately, that approach did not allow for the chemical synthesis of P-chiral analogues of oligonucleotides, such as oligo(nucleoside 3′,5′-phosphorothioate)s (PS-Oligos, 7) [8], widely used as biochemical tools for investigation of numerous intracellular processes, or evaluation of antisense strategy for regulation of protein biosynthesis [9]. In the vast majority of so far published studies PS-Oligos have been used only as the random mixture of diastereomers, prepared according to phosphoramidite [10] or H-phosphonate [11] methods. Therefore, the curiosity in consequences of the sense of chirality at phosphorus atom for biological properties of PS-Oligos prompted us to search for a novel method allowing for stereocontrolled chemical synthesis of PS-Oligos [12].

2

Oxathiaphospholane Approach to the Stereocontrolled Synthesis of Biophosphates

2.1

The Principle of 1,3,2-Oxathiaphospholane Ring-Opening Condensation Strategy

The early attempts to use relatively easily available diastereomerically pure nucleoside 3′-*O*-(2-cyanoethyl-*N*,*N*-diisopropylphosphoramidite) monomers for the stereospecific synthesis of PS-Oligos failed because of inevitable racemization of P^{III} intermediate caused by an excess of 1*H*-tetrazole necessary for efficient elongation of oligonucleotide chain [13]. An idea to use for that purpose appropriately protected nucleosides functionalized at 3′-*O* position with 2-thio-1,3,2-oxathiaphospholane moiety arose from the studies on the reactions of disubstituted phosphorothioates with oxiranes [14, 15], and in particular from the observation that PS-PO exchange in *O*,*O*-diphenyl phosphorothioate (**8**) upon treatment with ethylene oxide in methanol solution resulted in formation of

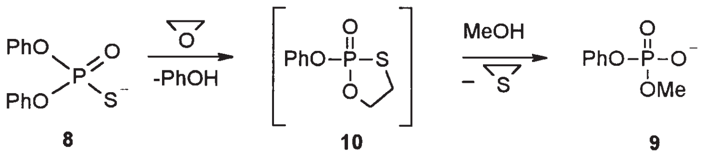

Scheme 1 **8** **10** **9**

O-phenyl-*O*-methyl phosphate (**9**) [16] (Scheme 1) while neither **8** nor *O*,*O*-diphenyl phosphate undergo methanolysis under applied conditions.

Further mechanistic studies provided evidence that the reaction proceeds with participation of 2-oxo-1,3,2-oxathiaphospholane intermediate **10** which reacts with a nucleophile present in the reaction mixture (methanol) with the cleavage of the endocyclic P-S bond and elimination of ethylene sulfide. Moreover, using diastereomerically pure R_P-thymidine-3′-*O*-(4-nitrophenyl phosphorothioate) we were able to prove that in the course of reaction with [^{18}O]oxirane and [^{17}O]water the opening of the oxathiaphospholane ring occurs with the stereoselectivity 98% [17]. Mechanistic considerations led to the conclusion that the replacement of the exocyclic oxygen atom with sulfur in **10** should provide a 2-alkoxy-2-thio-1,3,2-oxathiaphospholane that should react with alcohols to give a product with a phosphorothioate diester structure. To verify the applicability of this strategy for the synthesis of stereodefined PS-Oligos [12], phosphitylating reagent 2-*N*,*N*-diisopropylamino-1,3,2-oxathiaphospholane (**11**, R=H) was prepared by condensation of 2-mercaptoethanol with *N*,*N*-diisopropyl phosphoramidodichloridite. Reaction of appropriately protected nucleosides with **11** provides 2-alkoxy-1,3,2-oxathiaphospholanes (**12**) (Scheme 2) which are readily sulfurized with elemental sulfur to yield 2-alkoxy-2-thio-1,3,2-oxathiaphospholanes (**13**) [18].

Compounds **13** are fairly stable under neutral conditions and the nucleoside derivatives can be isolated by flash silica gel column chromatography. It was found that the 2-thio-1,3,2-oxathiaphospholanes **13**, similarly to their 2-oxo counterparts **10**, react with alcohols in the presence of base catalyst (preferably DBU) under rigorously anhydrous conditions with the cleavage of endocyclic

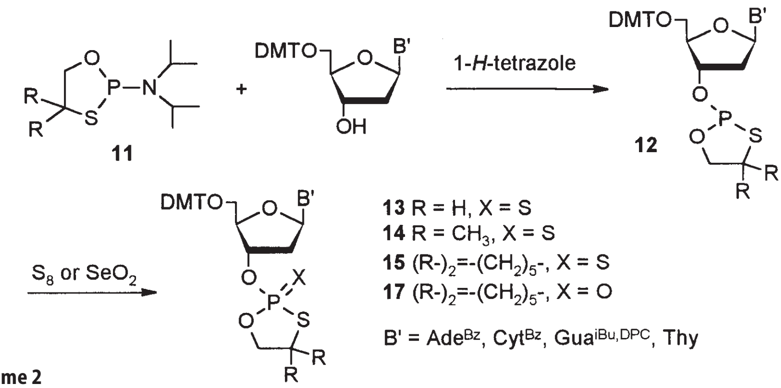

11 **12**

13 R = H, X = S
14 R = CH_3, X = S
15 $(R\text{-})_2$=$\text{-}(CH_2)_5\text{-}$, X = S
17 $(R\text{-})_2$=$\text{-}(CH_2)_5\text{-}$, X = O

B' = Ade^{Bz}, Cyt^{Bz}, Gua^{iBu,DPC}, Thy

Scheme 2

PS-bond, followed by spontaneous elimination of episulfide and formation of expected *O*,*O*-dialkyl phosphorothioates in high yield. It has also been demonstrated in model experiments that compounds **13** react with sodium methoxide with formation of sodium *O*-alkyl-*O*-methyl phosphorothioate. The ring opening condensation also occurred if potassium *tert*-butoxide was used as the base, while in the presence of tertiary amines other than DBU, such as triethylamine or diisopropyl ethyl amine (Hünig base), the condensation process occurred very slowly [19]. Importantly, the nucleoside monomers **13** could be chromatographically separated into *fast*- and *slow*-eluting P-diastereomers allowing for investigation of the stereochemical outcome of the methodology designed for the stereocontrolled formation of the internucleotide phosphorothioate linkage.

2.2
Stereocontrolled Synthesis of Oligo(nucleoside Phosphorothioate)s

For the purpose of solid-phase synthesis of PS-Oligos of predetermined P-chirality, three classes of 5′-*O*-DMT-deoxyribonucleoside 3′-*O*-(2-thio-1,3,2-oxathiaphospholane) monomers were developed (Scheme 2), bearing at position 4 of the oxathiaphospholane ring either hydrogen atoms (**13**) [18], methyl groups (**14**) [19], or pentamethylene ring in the spiro-arrangement (**15**) [20]. The corresponding 2,2-disubstituted-2-mercaptoalcohols necessary for the preparation of **14** and **15** were synthesized separately via published procedures [21]. The oxathiaphospholane monomers **13**–**15** were isolated in 80–90% yield as a mixture of diastereomers in ca. 55:45 ratio (^{31}P NMR). They were further separated into individual diastereomers by careful silica gel column chromatography. The separation was rather tedious and inefficient in the case of **13** and **14**. Fortunately, the monomers **15** could be much more easily obtained as diastereomerically pure species. It has been demonstrated that all separated diastereomers **13**–**15** react with appropriately 3′-*O*-protected or support-bound 5′-OH nucleosides (**16**) in a fully stereospecific manner (Scheme 3).

Fast- and *slow*-eluting monomers **13** give rise to **6** with internucleotide phosphorothioate linkages of S_P and R_P configuration, respectively. Interestingly, the presence of two methyl substituents in position 4 in **14**, as well as the presence of pentamethylene group in spiro-arrangement at the same position in **15**, changed the relative mobility of diastereomers, and *fast*-eluting monomers were precursors for internucleotide phosphorothioate linkages of R_P configuration. Accordingly, *slow*-eluting monomers of **14** and **15** yielded PS-Oligos with S_P configuration of phosphorothioate centers. For the purpose of solid phase synthesis of PS-Oligos it was necessary to use DBU-resistant supports with a sarcosinyl-succinoyl linker between 5′-*O*-DMT nucleosides (*N*-protected if necessary) and controlled pore glass [22].

Detailed studies on the stereocontrolled synthesis of oligo(nucleoside phosphorothioate)s by the oxathiaphospholane approach were performed with monomers **15** [20]. The optimization of the coupling step was performed [20, 23] involving the amount of the monomer (20 mg for 1 μmol synthesis), the concentration of DBU (1 mol/l) and the coupling time (450 s). To complete the pro-

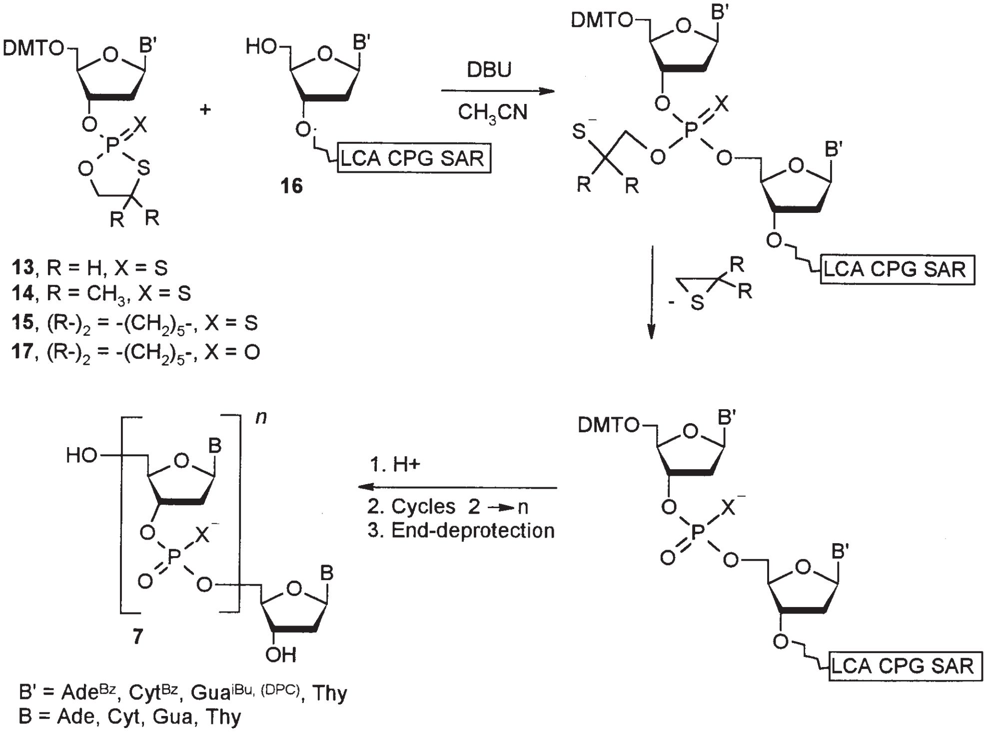

Scheme 3

cedure, standard detritylation and capping steps were added. The optimized synthetic protocol is given in Table 1.

The step-yield condensation in presented oxathiaphospholane methodology not exceeding 93 – 95 % does not allow for the synthesis of PS-oligos longer than 20-mers, albeit with a miserable yield stereodefined 28-mers of mixed-sequence were obtained as well. Using this procedure several stereodefined oligo(nucleoside phosphorothioate)s with the length up to 28 bases were synthesized for physicochemical studies and biological evaluation, although the final yields were lower than that resulting from the non-stereocontrolled phosphoramidite/sulfurization process [10]. The quality of HPLC-purified products obtained by both methods was comparable, as determined by PAGE, ion exchange HPLC, ESI or MALDI TOF mass spectrometry, and ^{31}P nuclear magnetic resonance. The resulting products were free of nucleobase- and sugar-phosphate backbone modifications. The stereoselectivity of ring opening condensation was not lower that 98 %, as proved by the synthesis of all 16 combinations of dinucleoside phosphorothioates, followed by reversed phase HPLC analysis. Importantly, the separated diastereomers of **15** were found to be more stable upon storage than the monomers **13** and **14**.

Table 1. Synthetic protocol for the 1-µmol scale automated solid-phase synthesis of PS-oligos using monomers **15**, or PO-oligos using **17**

Step	Reagent or solvent	Volume (ml)	Purpose	Time (s)
1	Dichloroacetic acid in CH_2Cl_2	2.3	Detritylation	50
	Acetonitrile	7.0	Wash	150
2	Activated **15**[a] or **17**[b] in CH_3CN	0.8	Coupling	470
	Methylene chloride	3.33	Wash	200
	Acetonitrile	7.0	Wash	150
3	DMAP/Ac_2O/lutidine in THF	0.33	Capping	20
	Acetonitrile	7.0	Wash	150

[a] A mixture of 270 µl of a solution of a monomer **15** in CH_3CN (75 mg/ml) and 530 µl of 1.5 mol/l DBU in CH_3CN.

[b] A mixture of 270 µl of a solution of a monomer **17** in CH_3CN (75 mg/ml) and 530 µl of 1.0 mol/l DBU in CH_3CN.

It must be pointed out that in a growing PS-oligonucleotide synthesized by oxathiaphospholane method, generated in each iterative step, internucleotide phosphorothioate bonds are of diester structure. Therefore, elongation of oligonucleotides possessing those phosphorothioate diester linkage(s) by the use of phosphoramidite/oxidation method was not possible, as already generated phosphorothioate linkages would be readily oxidized upon treatment with the oxidizing mixture I_2/H_2O/pyridine, typically used in aforementioned standard methods of synthesis of natural oligonucleotides [24]. Our attempts to find an efficient method for reversible protection of diester phosphorothioate bonds against oxidation were unsuccessful. To solve this problem we had to modify the oxathiaphospholane approach by preparing 5′-*O*-DMT-nucleoside 3′-*O*-(2-oxo-4,4-pentamethylene-1,3,2-oxathiaphospholane)s (**17**, Scheme 2). They were obtained by oxidation of P^{III} precursors **12** with selenium dioxide [20, 23]. The 2-oxo derivatives **17** were found to be much less stable compared to their 2-thio counterparts **15**, and had to be isolated with rigorous exclusion of moisture. All four deoxyribonucleoside monomers **17 a – d** (B′=Ade^{Bz}, Cyt^{Bz}, Gua^{iBu}, and Thy) were synthesized and used for the elongation of oligonucleotide chain with unmodified nucleotide units. Since in this case, contrary to phosphoramidite or H-phosphonate methods, the internucleotide phosphodiester linkages are formed directly, i. e., without oxidation step, the stereodefined phosphorothioate linkages already present in a growing oligomer are prevented from oxidation rendering possible the preparation of "chimeric" PS/PO oligonucleotides as well as unmodified oligonucleotides (PO-Oligos). Examples of stereodefined PS-Oligos and "chimeric" PS/PO-Oligos of predetermined structure and chirality are numerous and can be found in relevant papers [25 – 32].

2.3
The Mechanism and Stereochemistry of 1,3,2-Oxathiaphospholane Ring-Opening Process

Mechanistic considerations for the nucleophilic substitution at the phosphorus atom incorporated in 2-thio-1,3,2-oxathiaphospholane ring system involved two possible pathways. The first one assumed that a DBU activated alcohol molecule may approach the phosphorus atom according to an "in-line" type mechanism, via colinear attack from the side opposite to the endocyclic P-S bond, and that the resulting intermediate collapses with the ring opening and the cleavage of the P-S bond with net inversion of configuration at the phosphorus atom. Alternatively, the ring opening may result from an attack of the nucleophile from the side opposite to the most apicophilic endocyclic oxygen atom ("adjacent" type mechanism), resulting in a pentacoordinate intermediate with a trigonal bipyramid structure, which before collapse has to undergo intramolecular rearrangement (pseudorotation) placing the cleavable P-S bond in the apical position. The stereochemical outcome of the second pathway must be retention of configuration at phosphorus. In both cases the cleavage of the P-S bond is followed by fast and irreversible elimination of alkylene sulfide, leading to a final product. Our early model studies on the mechanism of nucleophilic substitution in elsewhere postulated intermediate thymidine-3′-*O*-(2-oxo-1,3,2-oxathiaphospholane) [17] supported the participation of the "adjacent" mechanism, but the presence of exocyclic sulfur instead of oxygen in position 2 of the oxathiaphospholane ring might affect the mechanism of ring opening process. This forced us to look for direct stereochemical evidence, rather than to apply conclusions resulting from the structural analogy between 2-thio- and 2-oxo-1,3,2-oxathiaphospholanes. As mentioned earlier, *fast*- and *slow*-eluting diastereomers of the nucleoside 3′-*O*-(2-thio-1,3,2-oxathiaphospholane) **13** were precursors of internucleotide bonds of S_P and R_P absolute configuration, respectively [18], but their configuration could not be correlated with any known P-chiral nucleotides. To solve that problem a set of model compounds was designed, namely 2-[(R_C)-1-(α-naphthyl)ethylamino]-2-thio-1,3,2-oxathiaphospholane (**18**) and *O*,*S*-dimethyl *N*-[(R_C)-1-(α-naphthyl)ethyl]phosphoramidothioate (**19**). Diastereoisomers of **18** and **19** were separated as pure specimens, and two of them, namely *slow*-eluting-**18** and *slow*-eluting-**19**, were obtained in the crystalline form. Their X-ray analysis revealed that both compounds have (R_P,R_C) configuration [33]. Since the *slow*-eluting-**18**, when subjected to DBU-catalyzed methanolysis, followed by alkylation of resulting phosphoroamidothioate with methyl iodide, yielded *fast*-eluting-**19** (Scheme 4), the conclusion has been drawn that the opening of the oxathiaphospholane ring in compound **18** occurs according to the "adjacent" type mechanism.

However, that model system did not provide final evidence as it suffered from the presence of amino substituent instead of alkoxy group attached to the phosphorus atom. Fortunately, the *fast*-eluting diastereomer of 5′-*O*-DMT-N^4-benzoyl deoxycytidine-3′-*O*-(2-thio-4,4-dimethyl-1,3,2-oxathiaphospholane) (**14**, B′=Cyt^{Bz}) after detritylation with *p*-toluenesulfonic acid, yielded N^4-benzoyl deoxycytidine-3′-*O*-(2-thio-4,4-dimethyl-1,3,2-oxathiaphospholane) (**20**) which

Scheme 4 *slow*-[R_PR_C]-**18** *fast*-[S_PR_C]-**19**

was successfully crystallized from a mixture of toluene, methylene chloride, and diethyl ether. An X-ray analysis of a single crystal of **20** allowed us to assign the absolute configuration as R_P [20]. Since the detritylation process does not change the configuration at phosphorus, the same configuration had to be assigned to its *fast*-5′-*O*-DMT derivative **14** (B′= Cyt^{Bz}), otherwise known to be the precursor of phosphorothioate dinucleotide d(C_{PS}C) of R_P-configuration. This correlation, based on unambiguous results of crystallographic analysis, supported the hypothesis that the coupling reaction proceeds via an "adjacent" mechanism with pseudorotation of the pentacoordinate phosphorus intermediate.

The results of ab initio calculations [34, 35] provided a theoretical basis for the explanation of experimental results, and indicated that an attack of nucleophile at phosphorus atom in **13** (and analogously in **14** and **15**) occurs from the side opposite to the endocyclic oxygen atom of 1,3,2-oxathiaphospholane moiety (Scheme 5).

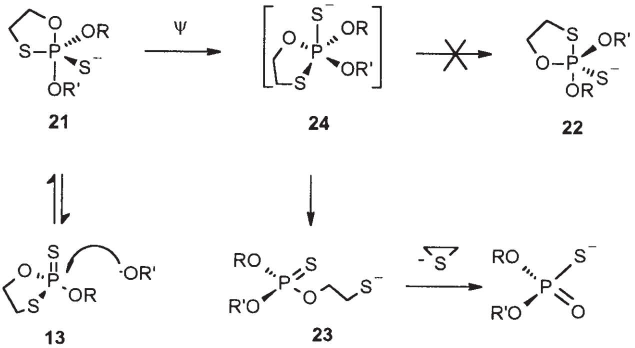

Scheme 5

The resulting pentacoordinate intermediate **21**, fulfilling Westheimer's rules of nucleophilic substitution at phosphorus [36] (apical entry – apical departure), should undergo pseudorotation. The calculations have shown that the pentacoordinate intermediate **22** with apical sulfur is energetically unfavorable, and the cleavage of the P-S bond leading to ring-opening product **23** most likely occurs via a tetragonal pyramid-like **24**, the hypothetical transition state between **21** and **23**, without involvement of **22**. Nonetheless, the elimination of ethylene sulfide from **23** provides product with phosphorothioate diester bond with overall retention of configuration at P-atom.

2.4
Stereocontrolled Synthesis of Isotopomeric Oligo(nucleoside $PS^{18}O$-Phosphorothioates and -$P^{18}O$-Phosphates)

Stereodefined PS-Oligos are often accepted as substrates by nucleolytic enzymes and can be used for stereochemical studies of their mode of action [37]. If the enzymatic hydrolysis is performed in the presence of isotopically labeled [^{18}O]water, an absolute configuration of the P-atom in the resulting nucleoside [^{18}O]phosphorothioate monoester can be determined, thus providing important information on the mechanism of the enzymatic reaction [38]. The same information can be gained when PS-Oligo possesses phosphorothioate linkage(s) labeled with heavy oxygen isotope ($PS^{18}O$-Oligo) and the unlabeled water is used for hydrolysis. Such modification of substrates is advantageous because the enzymes are usually available as solutions in unlabeled water, and also it is much easier and cheaper to prepare all buffers necessary for hydrolysis using $H_2{}^{16}O$, as compared to $H_2{}^{18}O$ (or even more expensive $H_2{}^{17}O$). Since recently developed techniques of configurational analysis of nucleoside [^{18}O]phosphorothioate monoester residues allow one to work with very small amounts of oligonucleotides [39], in many cases stereodefined $PS^{18}O$-Oligos may themselves be useful stereochemical tools in molecular biology. In our effort to obtain stereodefined $PS^{18}O$-Oligos and $P^{18}O$-Oligos by the oxathiaphospholane approach, at first we synthesized phosphitylating reagent 2-chloro-4,4-pentamethylene-

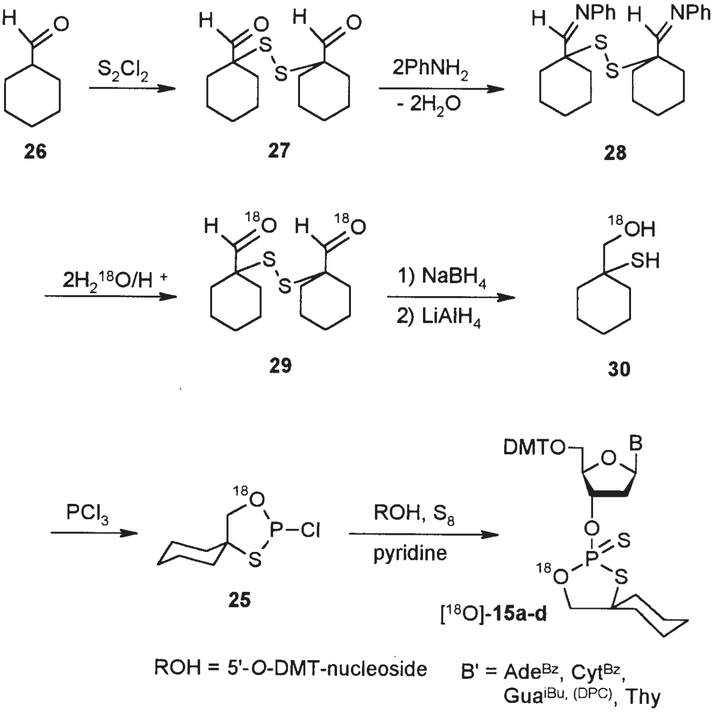

Scheme 6

1,3,2-[^{18}O]oxathiaphospholane (**25**) carrying an isotope label in endocyclic position (Scheme 6).

For that purpose, commercially available cyclohexanecarbaldehyde (**26**) was converted into 2,2′-dithiobis(cyclohexanecarbaldehyde) (**27**) [40] and subsequently transformed into 2,2′-dithiobis(cyclohexanecarbo-*N*-phenylimine) (**28**). Its HCl-promoted hydrolysis in the presence of [^{18}O]water yielded 2,2′-dithiobis([^{18}O]cyclohexanecarbaldehyde) (**29**) with almost unchanged isotopic enrichment. The two-step reduction of **29** gave 1-mercapto-1,1-pentamethyleneethan-2-[^{18}O]ol (**30**) which in reaction with PCl_3 provided **25**. Phosphitylation of 5′-*O*-DMT-nucleosides with **25**, followed by sulfurization, gave monomers [^{18}O]-**15a–d** (B′=Ade^{Bz}, Cyt^{Bz}, Gua^{iBu}, Thy), which subsequently were separated chromatographically into pure *fast*- and *slow*-eluting P-diastereomers of R_P and S_P absolute configuration, respectively. Configurational assignments based upon known stereochemistry of the condensation process (see above) allowed us to conclude that the *slow*- and *fast*-[^{18}O]-**15** provide [^{18}O]phosphorothioate internucleotide bonds of S_P and R_P absolute configuration, respectively. According to Cahn-Ingold-Prelog's rule, the isotopic replacement $^{16}O \rightarrow {}^{18}O$ in internucleotide phosphorothioates does not change either the sense of chirality or the absolute configuration of the phosphorus atom, as the atomic numbers of both oxygen isotopes are the same [38].

Monomers [^{18}O]-**15a–d** were successfully used for the synthesis of several stereodefined oligo(nucleoside [^{18}O]phosphorothioate)s. Their stereochemistry and isotopic enrichment were confirmed by a combined enzymatic-mass spectrometry method employing snake venom phosphodiesterase or calf spleen nuclease, and MALDI TOF mass spectrometry.

To obtain a set of monomers for direct synthesis of stereodefined P^{18}O-Oligos, diastereomerically pure monomers [^{18}O]-**15a–d** were stereospecifically (as judged by ^{31}P NMR spectroscopy) oxidized with selenium dioxide yielding 5′-*O*-DMT-nucleoside-3′-*O*-(2-oxo-4,4-pentamethylene-1,3,2-[^{18}O]oxathiaphospholane)s ([^{18}O]-**17a–d**). These monomers were characterized by FAB MS and ^{31}P NMR. Although we have already described the applicability of the unlabeled 2-oxo monomer **17d** (B′=Thy) for the synthesis of "chimeric" oligonucleotides [20, 23], the absolute configuration of the isotopomeric P^{18}O-Oligos had to be determined, because both stereochemistry of oxidation **15**→**17** as well as the stereochemical outcome of the DBU induced condensation utilizing monomers [^{18}O]-**17** were obscure. Our stereochemical analysis was based on stereoretentive oxidation of internucleotide [^{18}O]phosphorothioate bond in **31** into corresponding [^{18}O]phosphate in **32** by means of unlabeled 1,2-epoxybutane [15, 16] (Scheme 7).

The result of this correlation indicates that a sequence of reactions: *slow*-[^{18}O]-**15b** → [^{18}O]-**17b** → P^{18}O-dinucleotide **32** yields the [^{18}O]phosphate internucleotide bond of R_P absolute configuration. It seems reasonable to assume that the oxidation of [^{18}O]-**15** into [^{18}O]-**17**, as well as the condensation of [^{18}O]-**17** with 3′-*O*-acetylthymidine **16**, both occur with retention of configuration.

The two sets of ^{18}O-labeled monomers [^{18}O]-**15** and [^{18}O]-**17** described above and their unlabeled counterparts allowed for the synthesis of medium size oligonucleotides with any combination of internucleotide bonds with respect to

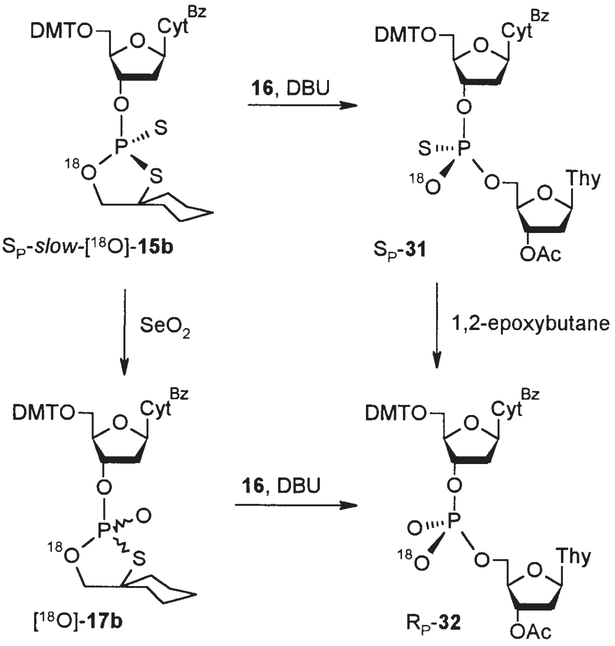

Scheme 7

their type (PS vs PO) or absolute configuration (R_P vs S_P), as well as to the position and the number of isotope labels along the chain. This flexibility was exemplified by the solid phase synthesis of partially stereodefined oligonucleotide $d(A_{PO}A_{Mix\text{-}PS}A_{Mix\text{-}PS}A_{Rp\text{-}PS}C_{Rp\text{-}PS18O}G_{Rp\text{-}PS}T_{Rp\text{-}PS}T_{Mix\text{-}PS}T_{PO}T)$ (**33**) with one isotope label (47 atom % of ^{18}O) in phosphorothioate linkage of R_P configuration between dC and dG residues. Construct **33** was hydrolyzed in unlabeled water by endonuclease from *Serratia marcescens*. This enzyme shows no sequence specificity with regard to natural oligonucleotides; however careful analysis of its activity towards substrates containing phosphorothioate linkages allowed us to select **33** as an appropriate target. Stereochemical analysis of $_{PS18O}G_{Rp\text{-}PS}T_{Rp\text{-}PS}T_{Mix\text{-}PS}T_{PO}T$ (**34**) possessing the chiral 5′-terminal [^{18}O]-phosphorothioate group, which was the predominant product of degradation of **33**, was based on the methodology developed by Mizuuchi et al. [39]. The procedure involved isolation of the oligomer **34** by HPLC, followed by its enzymatic ligation to a hairpin-like 44-base long template. Controlled degradation of the ligated material with S_P-specific nuclease P1 provided pentamer $_{PO}T_{PS18O}G_{Rp\text{-}PS}T_{Rp\text{-}PS}T_{Rp\text{-}PS}T$ (**35**) (Scheme 8).

The final MALDI TOF analysis of **35** showed the presence of two ions m/z 1626 and 1628 in the expected ratio, thus indicating the retention of isotopic enrichment. This observation provided evidence that the degradation of **33** by *Serratia marcescens* endonuclease proceeds with inversion of configuration at the phosphorus atom [41].

However, it is known that the presence of a sulfur atom influences the properties of internucleotide bonds, mostly due to different steric requirements of

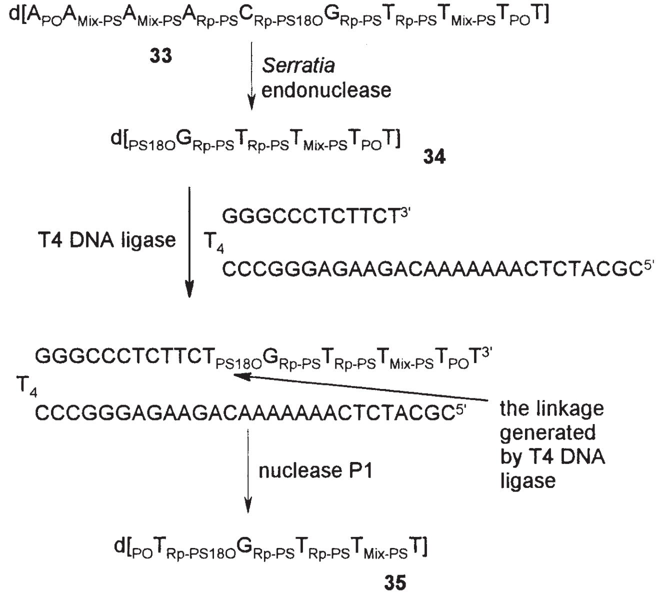

Scheme 8

sulfur atom, differences in P-S vs P-O bond length, altered affinity towards metal ions, modified hydration pattern, and changes in negative charge distribution within the ambident phosphorothioate anion [42]. Therefore, unquestionable results could be obtained by the use of P-chiral isotopomeric oligo(nucleoside [^{18}O]phosphate)s (P^{18}O-Oligos) which are stereochemical probes not distinguishable from natural oligomers by enzymes or other interacting biomolecules [43, 44]. Until recently, the synthesis of stereodefined P^{18}O-Oligos possessing isotopic labels at any preselected positions of the oligomer was not possible. The so-called "dimer approach" allowed one to label only a limited number of internucleotide bonds, no more than at every second position along the chain. Oligonucleotides containing a single P-chiral [^{18}O]phosphate internucleotide bond were for the first time used by Eckstein et al. [45] in pioneering studies on the mode of action of Eco RI endonuclease. Presented in this account is a methodology for synthesis of stereodefined P^{18}O-Oligos requiring development of new analytical tools allowing for measurement of the stereodependent isotope effect in their interactions with other molecules or metal ions with sufficient accuracy [46].

2.5

The Application of 1,3,2-Oxathiaphospholane Derivatives for 5′-End Modification of Oligonucleotides

It is well documented that covalent attachment of lipophilic biomolecules, e.g., lipids, cyclodextrins, steroids, or long-chain alcohols to oligonucleotides results in considerable improvement of cellular uptake, which is an important factor for biological activity [47]. Therefore, we applied the oxathiaphospholane approach

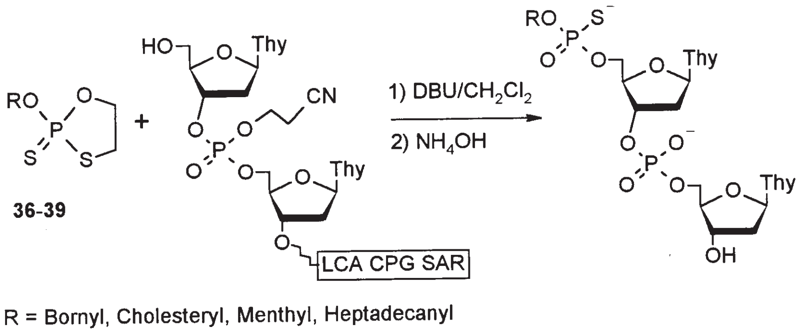

Scheme 9

to the synthesis of oligodeoxyribonucleotide conjugates bearing at the 5′-end lipophilic residues attached via a phosphorothioate linkage [48]. The 2-thio-1,3,2-oxathiaphospholane derivatives of optically active forms of borneol, cholesterol or menthol (**36**–**38**) as well as that of achiral heptadecanol (**39**) were prepared by standard procedure (as in Scheme 2) and reacted with 5′-OH group of either appropriately protected nucleosides or a thymidine dinucleotide (prepared by a standard phosphoramidite method) attached to the solid support (Scheme 9). In the model experiments, the most satisfactory yields of dithymidine conjugates were obtained with 30-fold molar excess of oxathiaphospholane (CH_2Cl_2 solution) and 400-fold molar excess of DBU with respect to support bound dinucleotide; reaction time 40 min. This protocol was further employed for lipophilic modification of the 5′-end of hexadecadeoxyribonucleotides (phosphodiesters or phosphorothioates) complementary to a fragment of human or rat mRNA of plasminogen activator inhibitor type 1 (PAI-1), which were used in antisense inhibition experiments [49, 50].

2.6

The Application of 1,3,2-Oxathiaphospholane Derivatives for the Synthesis of Stereodefined Oligo(ribonucleoside Phosphorothioate)s and their 2′,5′-Analogues

Stereodefined oligo(ribonucleoside phosphorothioate)s were available only by the enzymatic method [51–54] or by partially stereocontrolled H-phosphonate procedure [55, 56]. However, both procedures could provide only products with R_P configuration. Alternatively, compounds containing the single phosphorothioate modification were synthesized by nonstereospecific phosphoramidite or H-phosphonate methods and then separated into diastereomers by tedious HPLC procedure with various degree of success [57–59]. Such constructs became important tools for investigation of the mechanism of action of ribozymes.

In order to check the applicability of the oxathiaphospholane method for the stereocontrolled synthesis of oligo(ribonucleoside 3′,5′-phosphorothioate)s, appropriate oxathiaphospholane monomers possessing 2′-hydroxyl function protected with *tert*-butyldimethylsilyl group (**40a**–**d**) were synthesized and sepa-

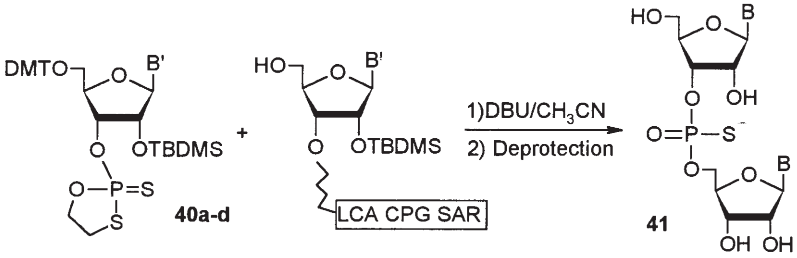

B' = Ade^{Bz}, Cyt^{Bz}, Gua^{iBu}, Ura
B = Ade, Cyt, Gua, Ura

Scheme 10

rated chromatographically into individual diastereomers [60]. Diastereomerically pure monomers **40** were reacted with support-bound ribonucleosides under DBU activation to yield dimers **41** (Scheme 10). It was found that the coupling proceeded with a stereoselectivity exceeding 98%. However, only for the case of the uridine monomer (**40d**) the yield of condensation was in the range acceptable for solid-support oligonucleotide synthesis (96–98%). For other monomers (**40a–c**) lower yields of condensation (66–83%) were observed. Since the coupling yields exceeding 90% are essential for successful iterative synthesis, further studies on the use of oxathiaphospholane methodology for preparation of stereodefined oligo(ribonucleoside phosphorothioate)s were abandoned.

Phosphorothioate analogues of 2′,5′-oligoadenylates have promising antiviral and anticancer properties and are able to elicit RNase L activation [61]. Short tri- and tetra-2′,5′-oligoadenylates were recently synthesized as a mixture of diastereomers and then separated into diastereomerically pure compounds [62]. For the purpose of their stereocontrolled synthesis, N^6-benzoyl-5′-*O*-DMT-3′-*O*-*tert*-butyldimethylsilyl adenosine-2′-*O*-(2-thio-1,3,2-oxathiaphospholane) was synthesized and chromatographically separated into P-diastereomers [63]. The separated monomers were used for synthesis of 2′,5′-tri- and tetra-adenosine analogues, which were cleaved from the support, deprotected, and identified by physicochemical and enzymatic methods. The step-yields 94–95% were achieved for attachment of consecutive adenosine 2′-*O*-phosphorothioate moieties.

2.7
The Synthesis of Stereodefined Oligonucleotide Phosphorothioates Possessing Modified Sugar Residues

2.7.1
Derivatives of xylo-Nucleosides

Oligonucleotides with incorporated *xylo*-nucleosides attract a lot of interest because they are more resistant towards nucleolytic enzymes compared to natural oligodeoxyribonucleotides [64, 65]. The corresponding oligodeoxy*xylo*-nucleotides with incorporated phosphorothioate linkages should be even more stable. Their biological activity could depend on their avidity to complementary DNA and RNA strands and might be influenced by the stereochemistry of internucleotide bonds. For the stereocontrolled synthesis of oligothymidylates containing *xylo*thymidine 3′-*O*-phosphorothioate moiety, 5′-*O*-DMT-*xylo*thymidine-3′-*O*-(2-thio-4,4-pentamethylene-1,3,2-oxathiaphospholane) (**42**) was prepared and chromatographically separated into P-diastereomers [66]. The separated isomers were reacted with 3′-*O*-acetylthymidine (**16**) to give R_P- and S_P-diastereomers of corresponding dinucleotides (**43**) (Scheme 11).

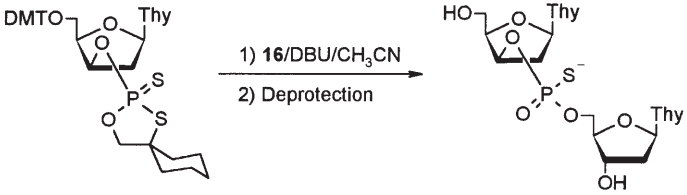

Scheme 11 *slow*-**42** (or *fast*-**42**) R_P-**43** (or S_P-**43**)

The *slow*- and *fast*-eluting isomers of **42** were also reacted with 5′-hydroxyl group at the end of support-bound hexathymidylate (synthesized by phosphoramidite methodology), followed by sequential addition of five 2-oxo-oxathiaphospholane monomers **17d**. On this way, "chimeric" dodecathymidylates of type 5′-T_5*xylo*$T_{PS}T_6$ were synthesized, containing either R_P- or S_P-*xylo*thymidine 3′-*O*-phosphorothioate moiety in the middle of the sequence [66]. An important conclusion from these studies, besides the assessment of hybridization properties and nucleolytic resistance of *xylo*nucleoside-containing oligomers, was the confirmation of stereospecificity of the ring opening condensation utilizing monomers **42**, which have significantly altered conformation of the sugar ring. In such a system the access to phosphorus atom is highly hindered due to the presence of DMT group, aglycone, and oxathiaphospholane ring at the same "side" of the sugar moiety.

2.7.2
Derivatives of Locked Nucleic Acids

Locked nucleic acids (LNA), defined as oligonucleotides containing one or more 2′-*O*-4′-*C*-methylene-β-D-ribofuranosyl nucleotide monomer(s), have been recently introduced as a new class of conformationally restricted oligonucleotide analogues [67]. LNA with incorporated internucleotide phosphorothioate linkages have also been reported [68]. By applying the oxathiaphospholane methodology, the first stereocontrolled synthesis of LNA dinucleoside phosphorothioates was performed [69]. Thus, the 5′-*O*-protected thymine LNA nucleoside was transformed into corresponding 3′-*O*-(2-thio-4,4-pentamethylene-1,3,2-oxathiaphospholane) (**44**), which was then separated into diastereomers by silica gel chromatography. The separated oxathiaphospholane monomers were reacted with 5′-OH nucleoside to give diastereomerically pure LNA dinucleoside phosphorothioates (**45**) (Scheme 12).

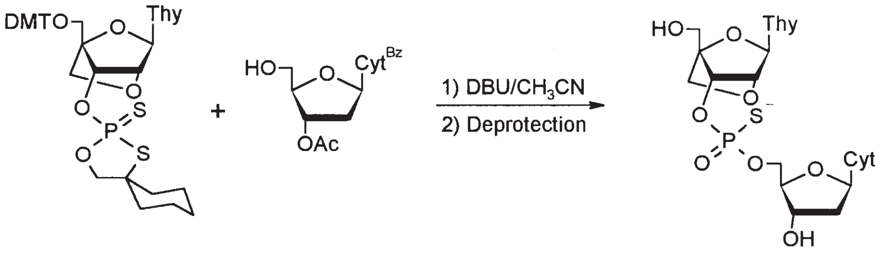

44 (*fast* or *slow*)

45a or **45b**

Scheme 12

Contrary to information that LNA oligonucleotides are resistant to digestion with nucleases [67], we have observed that diastereomer **45a** of LNA dinucleoside phosphorothioate (presumably R_P), obtained from *fast*-**44**, was readily digested by snake venom phosphodiesterase.

2.7.3
Dinucleoside N3′-O5′-Phosphoramidates and Phosphoramidothioates

The N3′-O5′ DNA analogues were found to have relatively low avidity for cellular proteins and high affinity to double-stranded DNA allowing the formation of stable triplex structures [70]. For these reasons, N3′-O5′ Oligos became widely tested for their use in antisense and antigene strategies [71,72], although their syntheses were reported as moderately efficient [73, 74]. In order to check the possibility of obtaining N3′-O5′-Oligos in a more convenient way, we phosphitylated base-protected 5′-*O*-DMT-3′-amino-2′,3′-dideoxyribonucleosides (**46**) with 2-chloro-4,4-pentamethylene-1,3,2-oxathiaphospholane (**47**) (Scheme 13).

The intermediate phosphoramidites were then in situ oxidized with *tert*-butyl hydroperoxide to form corresponding 5′-*O*-DMT-2′,3′-dideoxyribonucleoside-3′-*N*-(2-oxo-4,4-pentamethylene-1,3,2-oxathiaphospholane)s (**48**, B′= Ade^{Bz}, Cyt^{Bz}, Gua^{iBu}, Thy). They have been chromatographically isolated and characterized by

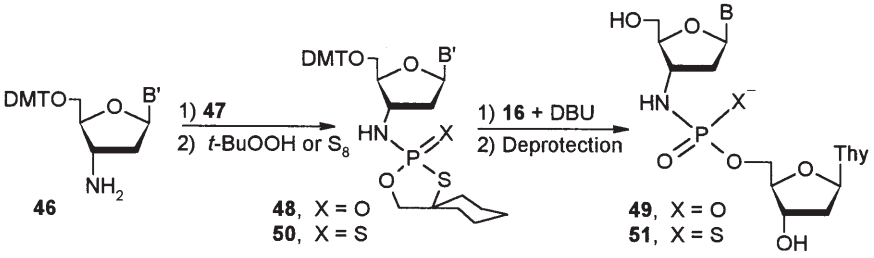

B′ = Ade^{Bz}, Cyt^{Bz}, Gua^{iBu}, Thy
B = Ade, Cyt, Gua, Thy

Scheme 13

^{31}P NMR and FAB MS. The condensation of **48** (B′= Thy) with **16** in the presence of DBU in acetonitrile solution led to dithymidine N3′-O5′-phosphoramidate (**49**) in 85% yield. Compounds **48** were also used in DBU-promoted condensation with thymidine 3′-*O*-immobilized on a solid support, which occurred in 89–93% yield furnishing **49**. To our disappointment, attempts at elongation of the oligonucleotide chain were not successful, as the yield of the second coupling step dropped to 50%. Further studies revealed that **49** was virtually insoluble in acetonitrile. This property of N3′-O5′ phosphoramidates seems to be responsible for the failure of effective elongation of the chain. Several different solvents (DMF, CH_2Cl_2, pyridine, pyridine-CH_3CN) were tested to improve the yield of condensation by increasing the solubility of $T_{NP}T$, but in no case was the coupling efficiency higher than that observed in acetonitrile as the reaction medium.

Replacement of **48** with 2-thio-analogues (**50**) for condensation with 3′-protected thymidine provided, after deprotection, diastereomeric mixture of N3′-O5′ phosphoramidothioates $T_{NPS}T$ (**51**). Also in this case the yield of the first coupling step was relatively high (90%), but under conditions of solid phase synthesis the yield of the second coupling dropped to 50%. It was assumed that S-alkylation of phosphorothioate linkages may improve solvation of the growing oligomer and increase the coupling yield. Unfortunately, attempts at alkylation of **51** with methyl iodide, 4-nitrobenzyl bromide, or 4-nitrobenzyl chloride-NaI-2,6-lutidine did not substantially increase the effectiveness of the process of chain extension. Using a pyridine solution of 4-nitrobenzyl bromide the coupling efficiency was increased up to 75%, but unfortunately we were unable to find experimental conditions to rise a coupling yield to at least 90%.Therefore, at the moment the oxathiaphospholane approach cannot be applied for satisfactory synthesis of N3′-O5′-Oligos longer than dinucleotides, like **49** and **51** [75].

2.8
Boranophosphates

Boranophosphates, containing negatively charged borane moiety (BH_3^-) in place of one of the non-bridging oxygen atoms, constitute a new class of backbone-modified oligonucleotides [76]. The boranophosphate group is isoelectronic to the natural phosphodiester group and isosteric to the methylphosphonate modification, and its introduction retains the ability of oligonucleotides to form reasonably stable complexes with the complementary DNA or RNA [77]. In order to check the applicability of oxathiaphospholane methodology to the stereocontrolled synthesis of oligo(nucleoside boranophosphate)s the borane complex of the 5′-*O*-*tert*-butyldimethylsilyl-thymidine-3′-*O*-1,3,2-oxathiaphospholane (**52**) was prepared from the corresponding P^{III} oxathiaphospholane **53** [78]. The complex **52** was reacted with 3-*N*-anisoyl-3′-*O*-acetylthymidine (**16a**) in THF solution in the presence of DBU to give, after deprotection, dithymidine boranophosphate (**54**) in 60% yield (Scheme 14).

Unfortunately, attempts to separate P-chiral diastereomers of complex **52** by column chromatography were unsuccessful due to its instability to moisture, so the stereochemical experiment could not be performed. That goal has been

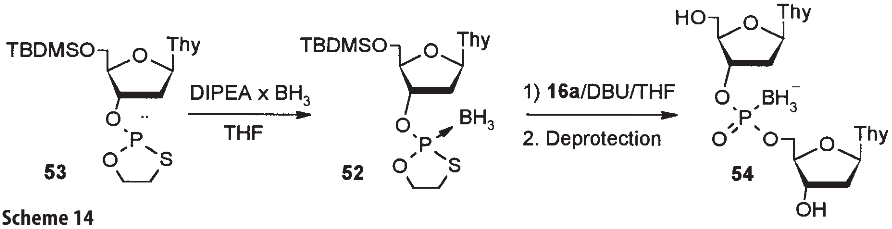

Scheme 14

achieved recently by Jin and Just [79], who obtained pure P-diastereomers of much more stable dithymidyl-2-cyanoethyl phosphite-borane complex and converted them into R_P- and S_P-isomers of **54**.

2.9

The Application of the Oxathiaphospholane Approach for the Synthesis of Conjugates of Nucleotides with Aminoacids

It has been reported recently that condensation of 3′-deoxy-3′-azidothymidine (AZT, **55**) with N-phosphorylated aromatic amino acids provides conjugates **56** of considerably higher activity against HIV-1 replication in PBM cells than that of parent AZT [80]. Compounds **56** are stable enough in human blood plasma, and are highly hydrophilic due to a negative charge present in phosphoramidate group. Among several amino acids tested, L-tryptophan gave the best results. In vitro studies showed that the L-tryptophan-AZT phosphoramidate **56** (R= 3-indolylmethyl) was eight times more active an HIV-1 RT inhibitor than AZT itself, without any symptoms of toxicity [81]. In this laboratory conjugates of aminoacid methyl esters with nucleotides have been obtained [82] using the oxathiaphospholane and/or dithiaphospholane methodology [83, 84]. The reaction of amino acid methyl esters (**57**) with 2-chloro-1,3,2-oxathiaphospholane (**58**) or 2-chloro-1,3,2-dithiaphospholane (**59**) in the presence of elemental sulfur gave nearly quantitative yields of *N*-(2-thio-1,3,2-oxathia(or dithia)phospholane) amino acids methyl esters **60** or **61** (Scheme 15), which were isolated from the reaction mixture by silica gel column chromatography, and characterized by ^{1}H NMR, ^{31}P NMR, and FAB MS.

Their reaction with azidothymidine in the presence of DBU furnished either phosphoramidothioate (**62**, X=O) or phosphoramidodithioate (**63**, X=S) derivatives of aminoacid carboxyesters. Due to asymmetry of the phosphorus atom, compounds **62** were formed as diastereomeric mixtures and were further separated into diastereomerically pure species by means of HPLC. Their antiviral activity is currently under investigation. Compounds **62** and **63** after their oxidation with potassium peroxymonosulfate ("Oxone", buffered solution) [85] provided phosphoramidate analogues **56.** It should be emphasized that the presented methodology allowed us to obtain not only the known compounds **56**, but also new classes of their monothio- and dithio-analogues, **62** and **63**, respectively. *N*-(2-Thio-1,3,2-oxathiaphospholane) derivative of L-tryptophane methyl ester **60** was chromatographically separated into P-diastereomers, and the crystal structure of *fast*-eluted isomer has been resolved indicating the ab-

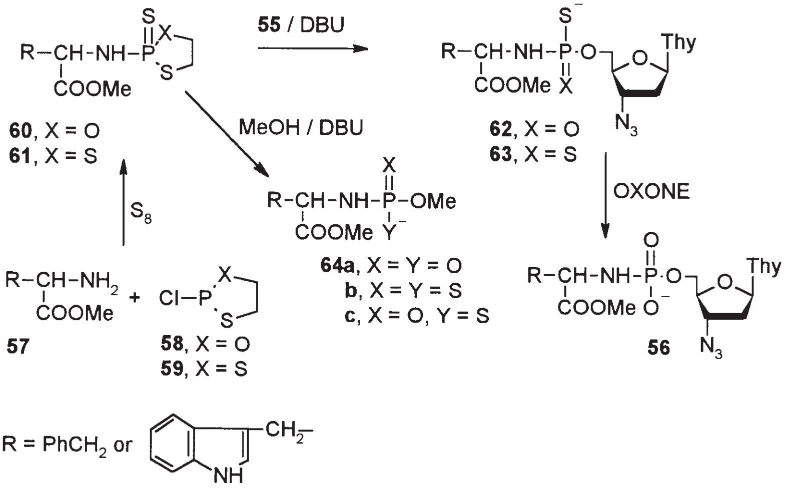

Scheme 15

solute configuration R at the phosphorus atom [86]. Since the stereochemistry of the oxathiaphospholane ring opening process with O-nucleophiles has been determined, the absolute configurations at P-atom in corresponding conjugates **62** are predictable.

Independent from studies oriented towards the search for better anti-AIDS drugs, compounds of general formula **60** and **61**, where R are natural aminoacid residues, were reacted with simple alcohols like methanol. In this way we prepared, with high purity and satisfactory yields, otherwise difficult to obtain phosphorothioate [87] and phosphorodithioate [88] amidoesters **64** considered as the analogues of transition state for the cleavage of peptide bond by proteases [89].

2.10
Oxathiaphospholane Ring Opening Condensation with Nucleophiles other than Alcohols

So far presented examples of the 1,3,2-oxathiaphospholane ring opening process have involved the attack of O-nucleophiles. Here we present evidence that other nucleophilic reagents such as amines, thiols, and fluoride anion react in the presence of DBU in a similar way. Primary and secondary amines, like *n*-butylamine, aniline, or morpholine, are themselves sufficiently nucleophilic to attack (albeit slowly), without assistance of other activators, phosphorus atom of 2-alkoxy-2-oxo(or thio)-1,3,2-oxathiaphospholanes yielding corresponding *O*-alkyl phosphoramidates or phosphoramidothioates, respectively [90]. Thus, for example, the reaction of $N^6,N^6,O^{2'},O^{3'}$-tetrabenzoyladenosine-5′-*O*-(2-oxo-1,3,2-oxathiaphospholane)s (**65**) with morpholine gives rise to adenosine-5′-*O*-phosphormorpholidates (**66**), important intermediates for the synthesis of nucleoside 5′-*O*-di- and triphosphates [91, 92] (Scheme 16).

In the presence of DBU, the ring opening condensation of **13** occurs even with weak nucleophiles such as imidazole [90]. It has also been demonstrated that

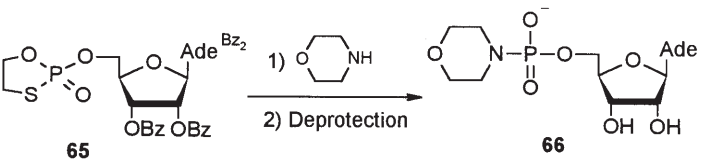

Scheme 16 **65**

3′-*O*-acetyl-thymidine-5′-*O*-(2-oxo- or 2-thio-1,3,2-oxathiaphospholanes) react smoothly with 5′-*O*-protected-3′-amino-3′-dideoxyribonucleosides (**46**) giving in high yield aforementioned dinucleoside N3′-O5′-phosphoramidates (**49**) [75] or -phosphoramidothioates (**51**).

S-Nucleophiles, like *n*-butyl mercaptan, react with nucleoside 2-thio-1,3,2-oxathiaphospholane monomers like **13**, yielding nucleoside *S*-*n*-butyl-phosphorodithioates (**67**) [93] (Scheme 17).

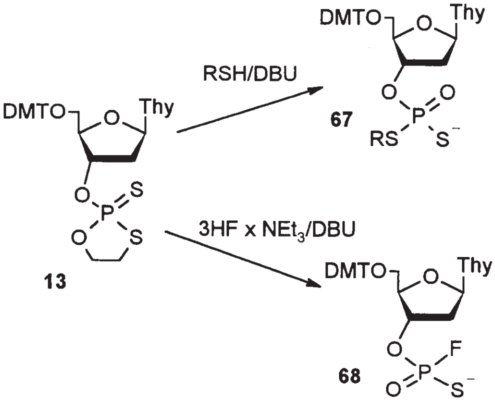

Scheme 17

Triethylamine tris(hydrofluoride) in the presence of DBU reacts quantitatively with **13**. Contrary to all examples so far presented of 1,3,2-oxathiaphospholane ring opening condensations, an attack of fluoride ion on phosphorus is not stereospecific; when performed with diastereomerically pure species, the mixture of diastereomeric compounds **68** is always produced [93, 94]. Oxathiaphospholane derivatives of 3′-amino-3′-deoxythymidine **48** and **50** under treatment with triethylamine tris(hydrofluoride) in the presence of DBU, followed by detritylation with acidic ion-exchange resin, provided 3′-deoxythymidine-3′-*N*-phosphoramidofluoridate (**69**) and 3′-deoxythymidine-3′-*N*-phosphoramidofluoridothioate (**70**) (Scheme 18), further purified by preparative TLC in ca. 80% yield [75].

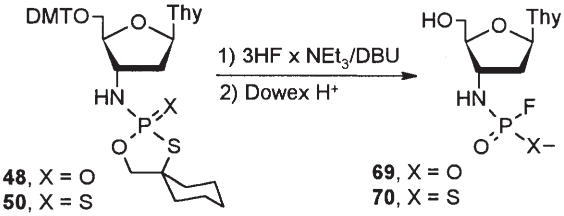

Scheme 18

Compound **70** (as a mixture of two diastereomers) in the presence of nuclease P1 (buffer pH 7.2, 24 h) underwent hydrolysis to the extent of 40%. In a control experiment without the enzyme, **70** was hydrolyzed to the extent of 36%. At pH 5.0, the P-F bond in **70** was hydrolytically stable independent of the presence of the enzyme. This observation provided evidence that the activity of nuclease P1 towards compounds like **70** is virtually negligible [75].

2.11
Oxathiaphospholane Approach to Phosphorothioylation of Polyols

Since the discovery by Zamecnik et al. in 1966 [95] that diadenosine polyphosphates ($A_{Pn}As$) are by-products of the lysyl-tRNA synthetase, dinucleoside polyphosphates have elicited wide interest [96]. However, their biological functions are not yet adequately understood. Symmetrical diadenosine tri- and tetraphosphates have been proposed to carry out various intracellular functions, including regulation of DNA replication and signaling stress responses. There is also considerable current interest in an extracellular role of $A_{P4}A$ and $A_{P3}A$ in blood platelet physiology [97, 98]. It was demonstrated only recently that the tumor suppressor Fhit protein [99] is an $A_{P3}A$ hydrolase [100], whose signaling appears to depend on $A_{Pn}A$ binding [101]. That result suggests that $A_{P3}A$ or similar dinucleoside polyphosphates may be essential factors in tumorigenesis [102]. A major problem in understanding the cellular function of $A_{Pn}As$ is their rapid degradation by both specific and non-specific hydrolases and phosphorylases. Much efforts have been put into chemical synthesis of their isopolar and isosteric analogues that would be stable to enzymatic cleavage or might serve as strong inhibitors of $A_{Pn}A$ hydrolases [103]. Searching for new inhibitors of Fhit protein we decided to replace the “middle” phosphate/pyrophosphate moiety in $A_{Pn}A$ with polyol derivatives [104]. Phosphorothioylation of hydroxyl functions of polyols of general formula **71** with N^6,N^6,$O^{2'}$,$O^{3'}$-tetrabenzoyladenosine-5′-*O*-(2-thio-1,3,2-oxathiaphospholane) (**72**) provided, after deprotection, corresponding phosphorothioate derivatives **73** in satisfactory yield (Scheme 19, path a). Alternatively, the same compounds **73** are readily available in reaction of corresponding poly-oxathiaphospholane derivatives (**74**) with N^6,N^6,$O^{2'}$,$O^{3'}$-tetrabenzoyladenosine (**75**, Scheme 19, path b).

The crude reaction mixtures were deprotected with aqueous ammonia and purified by preparative TLC and ion-exchange chromatography. So far, compounds of type **73** have been obtained as diastereomeric mixtures since the attempts at separation of diastereomers of **72** have failed. The ratio of substrates used in all condensation reactions depicted in Scheme 19 is important and determines the structure of final products, what can be well illustrated in the case of pentaerythritol (**76**).The reaction of **76** with less that four molar equivalents of **72** provided a mixture of mono-, di-, or tri- adenosine 5′-*O*-phosphorothioylated pentaerythritols, still containing free OH function(s) (**77**, Scheme 20).

Alternatively, tetra-oxathiaphosphorothioylated pentaerythritol (**78**) in reaction with less than four molar equivalents of **75**, followed by the treatment of the resulting mixture with 3-hydroxypropionitrile and subsequently with ammonia, provides pentaerythritols with each oxygen phosphorylated with adenosine 5′-

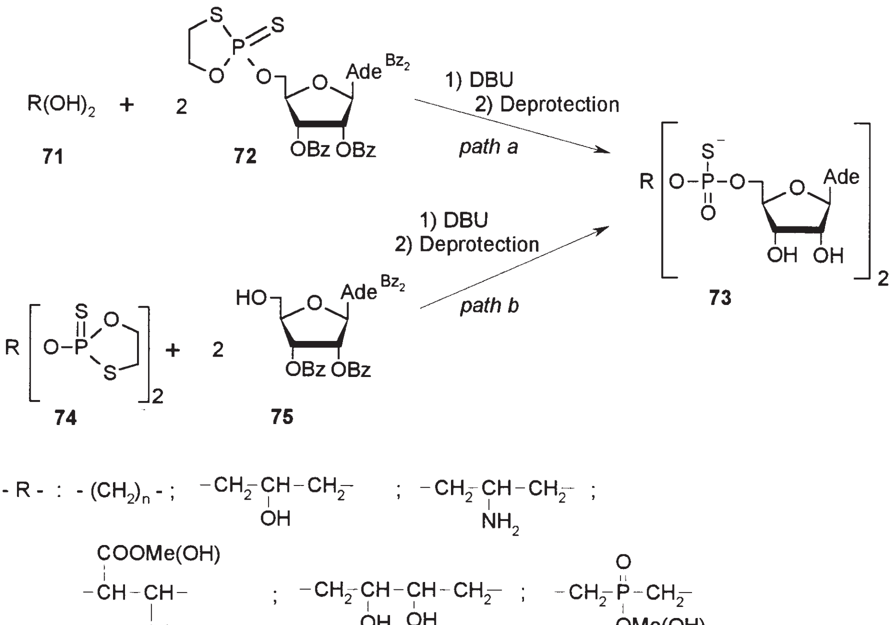

Scheme 19

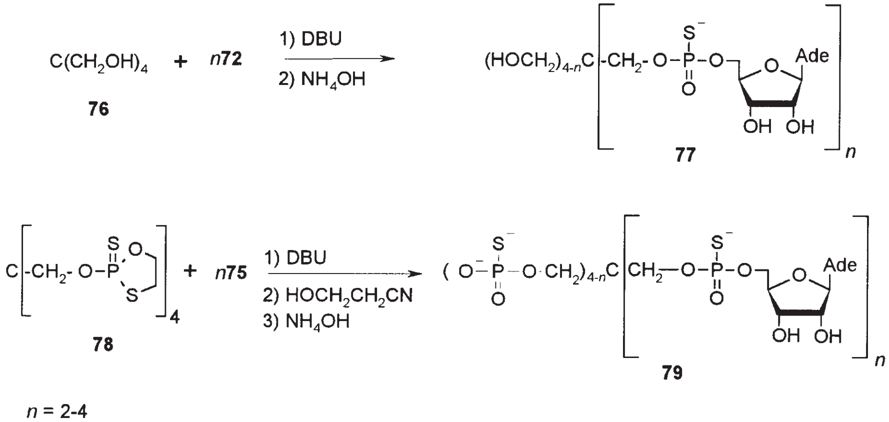

Scheme 20

O-phosphorothioyl or phosphorothioyl substituents (**79**). It has to be added that the reactions analogous to those presented in Schemes 19 and 20 were also performed with selected polyamine derivatives [88].

Among numerous compounds of general structure **73**, 1,3-bis(adenosine 5′-*O*-phosphorothioyl)glycerol (**80**) and tetrakis-(adenosine 5′-*O*-phosphorothioyl) pentaerythritol (**79**, n = 4), have been found to be the most potent inhibitors of Fhit hydrolase so far known. Interestingly, their phosphate congeners are ca. 100-fold weaker inhibitors of the same hydrolase [105]. Since both **79** and

80 were obtained and tested as a mixture of all possible diastereomers, success in obtaining diastereomerically pure R_P- and S_P-**72** will determine further progress in the studies on the mechanism of stereodependent inhibition of hydrolases. The above-mentioned $A_{Pn}A$ analogues were also tested as potential inhibitors of the platelet aggregation process. Strong inhibitory properties were found for newly synthesized compounds resulting from condensation of **72** with bis(hydroxymethylene)phosphinic acid *O*-methyl ester, followed by removal of all protecting groups. Platelet aggregation inhibitory properties comparable to clinically used Ticlopidine were also found for 1,4-bis(adenosine 5′-*O*-phosphorothioyl)erythritol (**77**, n = 2) [106].

2.12
Synthesis of Phosphorodithioate Analogues of Nucleotides and Oligonucleotides

P-Prochiral phosphorodithioate analogues of nucleotides and oligonucleotides were presented as potent inhibitors of viral reverse transcriptases and, therefore, are regarded as potential antiviral therapeutics [107]. Results of early studies on the electrophilic reactivity of organophosphorus compounds containing 1,3,2-dithiaphospholane moiety [83] prompted us to apply this reaction to the synthesis of nucleoside phosphorodithioates. Several 2-thio-1,3,2-dithiaphospholane-substituted nucleosides (**81**; X=S) were obtained and reacted with various oxygen nucleophiles in the presence of base catalysts. We have found that appropriately protected nucleoside 5′-*O*-(2-thio-1,3,2-dithiaphospholanes) (**81a**; X=S)) react with inorganic pyrophosphate in the presence of DBU to give nucleoside 5′-*O*-(1,1-dithiotriphosphates) (**82**, Scheme 21, path a) [108].

Similarly, appropriately protected deoxyribonucleoside 3′-*O*-(2-thio-1,3,2-dithiaphospholanes) (**81b**) were reacted with 5′-OH deoxyribonucleosides pro-

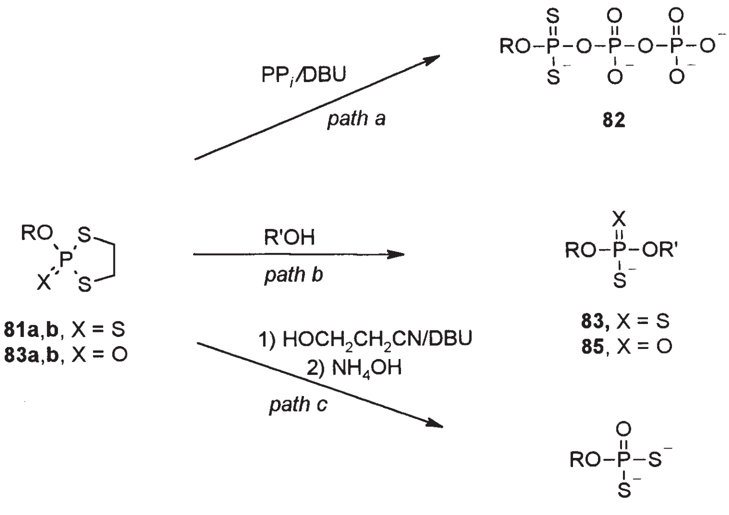

Scheme 21 **86a,b**

viding dinucleotides with phosphorodithioate internucleotide linkage (**83**, X=S) (Scheme 21, path b). Compounds **81b** were further developed as monomers for the efficient solid state synthesis of oligo(deoxyribonucleoside phosphorodithioate)s (**84**) [84].

Both **81a** and **81b** were also reacted with 3-hydroxypropionitrile in the presence of DBU to give, after ammonia treatment, the corresponding 5′-*O*- (**86a**) or 3′-*O*-phosphorodithioate mononucleotides (**86b**) (Scheme 21, path c) [109].

The 2-oxo analogues of dithiaphospholanes **81**, namely appropriately protected nucleoside 5′-*O*- (**83a**) or 3′-*O*-(2-oxo-1,3,2-dithiaphospholanes) (**83b**) have also been used as P-prochiral substrates for the potentially asymmetric synthesis of dinucleotides with P-chiral phosphorothioate internucleotide linkage (**85**, X=O) (Scheme 21, path b). For example, reaction of 5′-*O*-DMT-thymidine-3′-*O*-(2-oxo-1,3,2-dithiaphospholane) (**83b**) with N^2-isobutyryl-3′-*O*-acetyl deoxyguanosine in the presence of DBU provided corresponding dinucleoside 3′,5′-phosphorothioate of isomeric composition R_P/S_P=28/72 [110].

Among phosphorodithioate analogues of oligonucleotides useful as chemical tools for elucidation of the architecture of active site of metal-dependent endonucleases [111] P-chiral compounds of general formula **87** should be mentioned. First obtained by Cosstick and Vyle [112] by phosphoramidite approach, compounds **87** had to be separated into diastereomers by HPLC. We have recently found that 5′-*O*-MMT-3′-deoxy-3′-mercaptothymidine react with **58** in pyridine solution in the presence of elemental sulfur, providing in satisfactory yield 5′-*O*-MMT-3′-deoxy-3′-mercaptothymidine-3′-*S*-(2-thio-1,3,2-oxathiaphospholane) (**88**), then chromatographically separated into *fast*- and *slow*-migrating diastereomers. Their DBU-assisted condensation with **16** proceeds stereospecifically to give individual diastereomers of dithymidine S3′-O5′-phosphorodithioate (**87a, b**) in a fully stereocontrolled manner [110]. Although the absolute configuration at phosphorus in substrates and products of reaction presented in Scheme 22 has not been yet determined, our results proved that of two phosphorothiolate bonds present in **88** only endocyclic P-S bond is cleaved, as in the case of oxygen- or nitrogen-bound oxathiaphospholane derivatives. This observation confirms our claim that the 1,3,2-oxathiaphospholane ring opening condensation is driven by the ring-strain effect and fast irreversible elimination of episulfide.

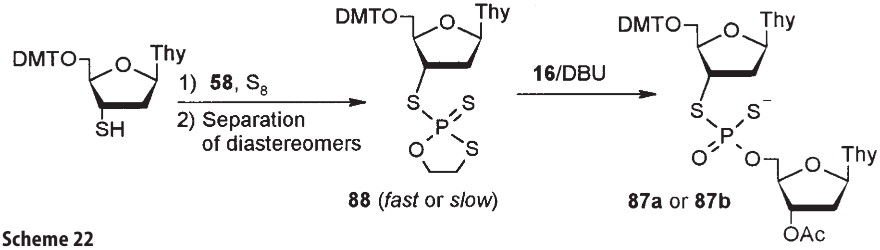

Scheme 22

3
Summary

Several new P-chiral compounds with phosphorus incorporated into the 1,3,2-oxathiaphospholane ring system were obtained and their structures have been assigned unambiguously by X-ray crystallography [113–117]. The chemistry of 1,3,2-oxathiaphospholanes, from the beginning full of ambiguities [118] and unprecedented reaction pathways [119–121], has been developed as a practical method of phosphorylation and phosphorothioylation of alcohols, thiols, and amines. The endocyclic P-O and P-S bonds of 1,3,2-oxathiaphospholanes differ substantially as far as the energy of dissociation is concerned, and ring strain effect is the major driving force of the ring opening process as the result of nucleophilic attack at phosphorus followed by fast and irreversible elimination of episulfide. These two factors are responsible for its chemoselectivity and stereospecificity, providing the basis for stereocontrolled transformations of diastereomerically pure oxathiaphospholane derivatives. The elucidation of the mechanism of ring opening condensation was possible due to crystallographic assignments of absolute configuration of oxathiaphospholane substrates and products resulting from them. Theoretical studies confirmed the correctness of earlier stereochemical correlations. Successful attempts at preparation of stereodefined P-chiral analogues of oligonucleotides, like PS-Oligos, were numerous and led to development of novel stereospecific syntheses of P-chiral *O*,*O*-dialkyl esters of phosphorothioic acid. Besides the methods presented in earlier reviews [12, 122], some recent results from other research establishments should be briefly mentioned. Just and co-workers made numerous attempts towards preparation of P-chiral cyclic phosphoramidites. Assuming their anancomeric stability and the preference of exocyclic substituent at P^{III}-atom (usually appropriately protected 3′-*O*-nucleosides) for occupying the axial position, cyclic phosphoramidites obtained from both enantiomers of corresponding aminoalcohols have to possess opposite absolute configuration at phosphorus. Therefore, the separation of diastereomeric precursors could be avoided, and the process of stereospecific ring-opening condensation followed by addition of elemental sulfur should furnish the desired diastereomers of protected dinucleoside phosphorothioates. 2-(3′-*O*-Thymidine)-1,3,2-oxazaphospholanes based upon 1,2-*O*,*O*-cyclopentylidene-5-deoxy-5-isopropylamine-*α*-D-*xylo*-furanose and its enantiomer were stereospecifically reacted with 3′-*O*-*tert*-butyldimethylsilylthymidine in the presence of 2-bromo-4,5-dicyanoimidazole yielding, after sulfurization and deprotection, nearly stereopure R_P- and S_P-diastereoisomers of dithymidine-3′,5′-phosphorothioate [123]. A conceptually similar approach to stereoselective synthesis of internucleotide phosphorothioate linkage has also been demonstrated by Agrawal and co-workers [124]. Nucleoside 3′-*O*-bicyclic azaphospholidines derived from R_P- and S_P-2-pyrrolidinemethanol have been used for highly stereoselective synthesis of R_P- and S_P-dinucleoside phosphorothioates, including 2′-methoxyribonucleoside analogues [125]. In parallel, Wang and Just [126] reported on the use of chiral indolyl-oxazaphosphorine derivatives which undergo DBU-assisted substitution at the P^{III} atom with another 5′-OH-nucleoside resulting in highly stereospecific cleavage of P-N bond, leading to the formation, after sulfurization and deprotection, of R_P- and S_P-dithymidine phosphorothioates.

Much more advanced and effective appeared to be the method reported recently by Beaucage et al. [127]. Starting from (±)-2-amino-1-phenylethanol (**88**) the authors performed chemoselective N-acylation with ethyl fluoroacetate (**89**) providing **90**, followed by its reaction with hexaethylphosphorous triamide (Scheme 23). Cyclic N-acylphosphoramidite **91** has been obtained as a mixture of diastereomeric rotamers. Condensation of N^4-benzoyl-5′-*O*-DMT-2′-deoxycytidine **92** with **91** in the presence of 1*H*-tetrazole gave, after silica gel chromatography, pure R_C,R_P-**93** and S_C,S_P-**93**. ^{31}P NMR studies indicated that when R_P-**93** or S_P-**93** was reacted with 3′-*O*-acetyl-*N*-benzoylcytidine (**94**) and *N*,*N*,*N*′,*N*′-tetramethylguanidine (TMG), the dinucleoside phosphotriester was formed in nearly quantitative yield with full P-stereospecificity. After subsequent sulfurization, the P-stereodefined dinucleoside phosphorothioate tri-

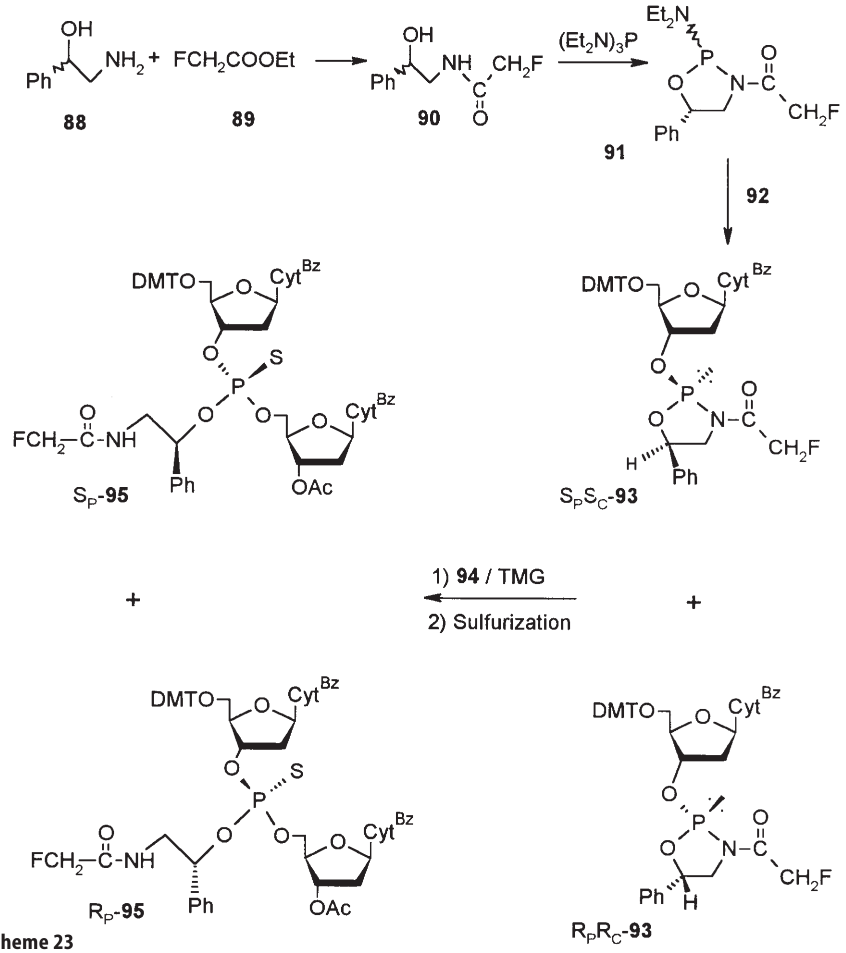

Scheme 23

esters R_P-**95** or S_P-**95** were subjected to base- and internucleotide bond deprotection under ammonia treatment.

The 2′-deoxycytidine cyclic N-acylphosphoramidite derivatives R_P-**93** and S_P-**93** were subsequently applied to the solid-phase synthesis of $[R_P, R_P]$- and $[S_P, S_P]$-tri(deoxycytidine phosphorothioate), and $[R_P, S_P, R_P]$-tetra(deoxycytidine phosphorothioate). A supplementary note provided information that the synthesis of dodeca(thymidine phosphorothioate)s with stereodefined sense of P-chirality has been accomplished. However, although further progress is expected, to our best knowledge only the oxathiaphospholane approach, presented in this account, allows for the chemical stereocontrolled synthesis of oligonucleotide analogues which, according to the requirements of antisense therapeutic strategy, have to be 16–28 base long. This methodology allowed us to synthesize PS-Oligos with a pre-determined sense of P-chirality at each internucleotide phosphorus atom. Moreover, an oxathiaphospholane approach enabled us to prepare chimeric oligonucleotides with both phosphodiester and stereodefined phosphorothioate internucleotide linkages at desired positions. As demonstrated recently, this procedure was adopted for the synthesis of isotopomeric $[PS^{18}O]$ phosphorothioates which became new and promising tools for the studies on the stereochemistry and the mechanism of action of nucleolytic enzymes. In addition, isotopomeric oligo(nucleoside $[^{18}O]$phosphate)s became available, albeit their application in mechanistic studies is still limited. The oxathiaphospholane method also appeared to be applicable to the synthesis of dinucleoside boranophosphates [78], dinucleoside N3′-O5′ phosphoramidates [75], dinucleoside phosphoroselenoates [128, 129], or dinucleoside phosphoroselenothioates [130]. The latter compounds are easily convertible to dinucleoside phosphorofluoridothioates [130]. On the other hand, *N*-oxathiaphosphorothioylation of aminoacid methyl esters allowed for the preparation of new conjugates of aminoacids with nucleoside 5′-phosphorothioates (in a few cases in stereodefined form) being considered as a potential new class of antiviral therapeutics [82]. The recent demonstration of versatility of designed methodology comes from oxathiaphosphorothioylation of polyfunctional molecules such as glycols, triols, tetraols, and polyamines, and their subsequent reactions with nucleosides, providing, among others, the new class of inhibitors of diadenosine polyphosphate hydrolases [104]. Future perspectives include application of oxathiaphospholane chemistry for phosphorothioylation of inositols, and the synthesis of polyanionic dendrimers and polymers based upon dialkylene phosphorothioates and phosphoramidothioates backbone. Their properties and application are still unpredictable, but undoubtedly the field is far from being depleted.

Acknowledgements. The authors wish to express the debt of gratitude to numerous students and coworkers, who contributed to the development of oxathiaphospholane methodology, for their hard, creative and dedicated work. Their names are listed in the references, but one has to be mentioned in particular: Andrzej Grajkowski performed the first successful synthesis and separation of nucleoside 3′-*O*-(2-thio-1,3,2-oxathiaphospholane)s and demonstrated the stereospecificity of internucleotide bond formation. Without his seminal work we would not have the honor to present our results in this book alongside the contributions of our distinguished colleagues. The financial assistance of the State Committee of Scientific Research (KBN), grant no. PBZ KBN 008/T09/98, is highly appreciated.

4
References

1. Zieliñski WS, Leśnikowski ZJ (1976) Synthesis 185
2. Lesiak K, Leśnikowski ZJ, Stec WJ, Zieliñska B (1979) Pol J Chem 53:2041
3. Zieliñski WS, Leśnikowski ZJ, Stec WJ (1976) J Chem Soc Chem Commun 772
4. Zieliñski WS, Stec WJ (1977) J Am Chem Soc 99:8365
5. Leśnikowski ZJ, Niewiarowski W, Zieliñski WS, Stec WJ (1984) Tetrahedron 40:15
6. Stec WJ (1983) Acc Chem Res 16:411
7. Baraniak J, Stec WJ (1987) J Chem Soc Perkin Trans I 1645
8. Zon G, Stec WJ (1991) Phosphorothioate oligonucleotides. In: Eckstein F (ed) Oligonucleotides and analogues: a practical approach. IRL Press, London, p 87
9. Eckstein F (2000) Antisense Nucl Acid Drug Dev 10:117
10. Stec WJ, Zon G, Egan W, Stec B (1984) J Am Chem Soc 106:6077
11. Froehler BC (1986) Tetrahedron Lett 27:5575
12. Stec WJ, Wilk A (1994) Angew Chem Int Ed Engl 33:709
13. Stec WJ, Zon G (1984) Tetrahedron Lett 25:5279
14. Hamer NK (1968) J Chem Soc Chem Commun 1399
15. Guga P, Stec WJ (1983) Tetrahedron Lett 24:3899
16. Guga P (1991) PhD thesis, CMMS PAS, Łódź
17. Okruszek A, Guga P, Stec WJ (1987) J Chem Soc Chem Commun 594
18. Stec WJ, Grajkowski A, Koziołkiewicz M, Uznañski B (1991) Nucl Acids Res 19:5885
19. Stec WJ, Grajkowski A, Karwowski B, Kobylañska A, Koziołkiewicz M, Misiura K, Okruszek A, Wilk A, Guga P, Boczkowska M (1995) J Am Chem Soc 117:12,019
20. Stec WJ, Karwowski B, Boczkowska M, Guga P, Koziołkiewicz M, Sochacki M, Wieczorek MW, Błaszczyk J (1998) J Am Chem Soc 120:7156
21. Hayashi K (1970) Macromolecules 3:5
22. Brown T, Pritchard CE, Turner G, Salisbury SA (1989) J Chem Soc Chem Commun 891
23. Karwowski B, Guga P, Kobylañska A, Stec WJ (1998) Nucleosides Nucleotides 17:1747
24. Caruthers MH (1991) Acc Chem Res 24:278
25. Koziołkiewicz M, Krakowiak A, Kwinkowski M, Boczkowska M, Stec WJ (1995) Nucl Acids Res 23:5000
26. Benimetskaya L, Tonkinson JL, Koziołkiewicz M, Karwowski B, Guga P, Zeltser R, Stec WJ, Stein CA (1995) Nucl Acids Res 23:4239
27. Koziołkiewicz M, Wójcik M, Kobylañska A, Karwowski B, Rębowska B, Guga P, Stec WJ (1997) Antisense Nucl Acid Drug Dev 7:43
28. Stec WJ, Cierniewski CS, Okruszek A, Kobylañska A, Pawłowska Z, Koziołkiewicz M, Pluskota E, Maciaszek A, Rębowska B, Stasiak M (1997) Antisense Nucl Acid Drug Dev 7:567
29. Koziołkiewicz M, Maciaszek A, Stec WJ, Semizarov D, Victorova L, Krayevsky A (1998) FEBS Lett 434:77
30. Boczkowska M, Guga P, Stec WJ (1999) J Biomol Struct Dynamics 16:1291
31. Furrer P, Billeci TM, Donati A, Kojima C, Karwowski B, Sierzchała A, Stec WJ, James TL (1999) J Mol Biol 285:1609
32. Fearon KF, Hirschbein BL, Chiu CY, Quijano MR, Zon G (1997) CIBA Foundation Symposium 209:19
33. Uznañski B, Grajkowski A, Krzyżanowska B, Kaźmierkowska A, Stec WJ, Wieczorek MW, Błaszczyk J (1992) J Am Chem Soc 114:10,197
34. Uchimaru T, Stec WJ, Tsuzuki S, Hirose T, Tanabe K, Taira K (1996) Chem Phys Lett 263:691
35. Uchimaru T, Stec WJ, Taira K (1997) J Org Chem 62:5793
36. Westheimer FH (1980) The polytopal rearrangement at phosphorus. In: Mayo E (ed) Rearrangements in ground and excited states, vol 2. Academic Press, New York, p 229
37. Eckstein F (1985) Annu Rev Biochem 54:367

38. Frey PA (1992) Nucleotidyltransferases and phosphotransferases: stereochemistry and covalent intermediates. In: Sigman DS (ed) The enzymes, vol 20, Mechanisms of catalysis. Academic Press, San Diego, p 141
39. Mizuuchi K, Nobbs TJ, Halford SE, Adzuma K, Qin J (1999) Biochemistry 38:3668
40. Guga P, Domañski K, Stec WJ (2001) Angew Chem Int Ed Engl 40:610
41. Koziołkiewicz M, Owczarek A, Guga P, Domañski K, Nowak M, Stec WJ (2001) Bioorg Med Chem 9:2403
42. Frey PA, Sammons RD (1985) Science 228:541
43. Buchwald SL, Hansen DE, Hassett A, Knowles JR (1982) Stereochemistry of selected phosphotransferases and nucleotidyltransferases. In: Purich DL (ed) Methods in enzymology, vol 87. Academic Press, New York, p 279
44. Lowe G (1983) Acc Chem Res 6:244
45. Eckstein F, Potter BVL, Uznañski B (1983) Nucl Acids Res 11:7087
46. Cepus V, Scheidig AJ, Goody RS, Gerwert K (1998) Biochemistry 37:10,263
47. Monoharan M (1993) Designer antisense oligonucletides: conjugation chemistry and fuctionality placement. In: Crooke ST, Lebleau B (eds) Antisense research and applications., CRC Press, Boca Raton, p 303
48. Kobylañska A, Okruszek A, Stec WJ (1998) Nucleosides Nucleotides 17:1977
49. Kobylañska A, Pluskota E, Świątkowska M, Wójcik M, Cierniewska-Cieślak A, Krakowiak A, Boczkowska M, Pawłowska Z, Okruszek A, Koziołkiewicz M, Cierniewski CS, Stec WJ (1999) Acta Biochim Polon 46:679
50. Pawłowska Z, Chabielska E, Kobylañska A, Maciaszek A, Świątkowska M, Buczko W, Stec WJ, Cierniewski CS (2001) Thrombosis Haemostasis 85:1086
51. Eckstein F, Gindl H (1969), FEBS Lett 2:262
52. Hacia JG, Wold BJ, Dervan PB (1994) Biochemistry 33:5367
53. Tang J, Roskey A, Li Y, Agrawal S (1995) Nucleosides Nucleotides 14:985
54. Lackey DB, Patel J (1997) Biotechnology Lett 19:475
55. Almer H, Stawinski J, Strömberg R (1994) J Chem Soc Chem Commun 1459
56. Almer H, Stawiñski J, Strömberg R (1996) Nucl Acids Res 24:3811
57. Detringer D, Behlen LS, Uhlenbeck OC (2000) Biochemistry 39:55
58. Loverix S, Winquist A, Strömberg R, Stayaert J (1998) Nature Struct Biol 5:365
59. Slim G, Gait MJ (1991) Nucl Acids Res 19:1183
60. Sierzchała A, Okruszek A, Stec WJ (1996) J Org Chem 61:6713
61. Torrence PF, Xiao W, Li G, Cramer H, Player MR, Silverman RH (1997) Antisense Nucl Acid Drug Dev 7:203
62. Sobol RW, Henderson EE, Kong N, Shao J, Hitzges P, Mordechai E, Reichenbach NL, Charubala R, Schirmeister H, Pfleiderer W, Suhadolnik RJ (1995) J Biol Chem 270:5963
63. Yang XB, Sierzchała A, Misiura K, Niewiarowski W, Sochacki M, Stec WJ, Wieczorek MW (1998) J Org Chem 63:7097
64. Sokolova NI, Dolinnaya NG, Krynetskaya NF, Shabarova ZA (1990) Nucleosides Nucleotides 9:515
65. Rosemeyer H, Seela F (1991) Helv Chim Acta 74:748
66. Yang XB, Misiura K, Sochacki M, Stec WJ (1997) Bioorg Med Chem Lett 7:2651
67. Wengel J (1999) Acc Chem Res 32:301
68. Kumar R, Singh SK, Koshkin AA, Rajwanshi VK, Meldgaard M, Wengel J (1998) Bioorg Med Chem Lett 8:2219
69. Karwowski B, Okruszek A, Wengel J, Stec WJ (2001) Bioorg Med Chem Lett 11:1001
70. Escude C, Giovannangeli C, Sun JS, Lloyd DH, Chen JK, Gryaznov SM, Garestier T, Hélène C (1996) Proc Natl Acad Sci USA 93:4365
71. Giovannangeli C, Perrouault L, Escudé C, Gryaznov SM, Hélène C (1996) J Mol Biol 261:386
72. Ding D, Gryaznov SM, Lloyd DH, Chandrasekaran S, Yao S, Ratmeyer L, Pan Y, Wilson WD (1996) Nucl Acids Res 24:354
73. Gryaznov SM, Chen JK (1994) J Am Chem Soc 116:3143

74. Nelson JS, Fearon KL, Nguyen MQ, McCurdy SN, Frediani JE, Foy MF, Hirschbein BL (1997) J Org Chem 62:7278
75. Baraniak J, Korczyñski D, Stec WJ (1999) J Org Chem 64:4533
76. Sergueev D, Shaw BR (1998) J Am Chem Soc 120:9417
77. Higson AP, Sierzchała A, Brummel H, Zhao Z, Caruthers MH (1988) Tetrahedron Lett 39:3899
78. Okruszek A, Sierzchała A, Żmudzka K, Stec WJ (2001) Nucleoside, Nucleotides Nucleic Acids (in press)
79. Jin Y, Just G (1998) Tetrahedron Lett 39:6429
80. Abraham CR, Wagner CR (1994) Nucleosides Nucleotides 13:1891
81. Wagner CR, McIntee RJ, Schinazi RF, Abraham TW (1995) Biorg Med Chem Lett 5:1819
82. Baraniak J, Kaczmarek R, Stec WJ (2000) Tetrahedron Lett 41:9139
83. Okruszek A, Sierzchała A, Sochacki M, Stec WJ (1992) Tetrahedron Lett 33:7585
84. Okruszek A, Sierzchała A, Fearon KL, Stec WJ (1995) J Org Chem 60:6998
85. Woźniak LA, Stec WJ (1999) Tetrahedron Lett 40:2637
86. Baraniak J, Kaczmarek R, Wieczorek MW (unpublished results)
87. Thompson CM, Lin J (1996) Tetrahedron Lett 37:8979
88. Baraniak J, Kaczmarek R (unpublished results)
89. Morgan BP, Holland DR, Matthews BW, Bartlett PA (1988) J Am Chem Soc 116:2923
90. Misiura K, Domañski K, Korczyñski D (unpublished results)
91. Moffat JG, Khorana HG (1961) J Am Chem Soc 83:649
92. Khorana HG (1961) Some recent developments in the chemistry of phosphate esters of biological interest. Wiley, New York, p 69
93. Misiura K (unpublished results)
94. Misiura K, Szymanowicz D, Stec WJ (1998) Chem Commun 515
95. Zamecnik PC, Stephenson ML, Janeway CM, Randerath K (1966) Biochem Biophys Res Commun 24:91
96. McLennan AG (ed) (1992) $A_{P4}A$ and other dinucleoside polyphosphates. CRC Press, Boca Raton
97. Kim BK, Zamecnik PC, Taylor G, Guo M, Blackburn GM (1992) Proc Natl Acad Sci USA 89:11,056
98. Chan SW, Gallo SJ, Kim BK, Guo ML, Blackburn GM, Zamecnik PC (1997) Proc Natl Acad Sci USA 94:4034
99. Siprashvili Z, Sozzi G, Barnes LD, McCue P, Robinson AK, Eryomin V, Sard R, Ragliabue, E, Graco A, Fusetti L, Schwartz G, Pierotti MA, Croce CM, Huebner K (1997) Proc Natl Acad Sci USA 94:11,771
100. Barnes LD, Garrison PN, Siprashvili Z, Guranowski A, Robinson AK, Ingram SW, Croce CM, Ohta M, Huebner K (1996) Biochemistry 35:11,529
101. Pace HC, Garrison PN, Robinson AK, Barnes LD, Draganescu A, Rosler A, Blackburn GM, Siprashvilli Z, Croce CM, Huebner K, Brenner C (1998) Proc Natl Acad Sci USA 95:5484
102. Druck T, Hadaczek P, Fu TB, Ohta M, Siprashvili Z, Baffa R, Negrini M, Kastury K, Veronese ML, Rosen D, Rothstein J, McCue P, Cotticelli MG, Ionue H, Croce CM, Huebner K (1997) Cancer Res 57:504
103. Liu X, Brenner C, Guranowski A, Starzyñska E, Blackburn GM (1999) Angew Chem Int Ed Engl 38:1244
104. Baraniak J, Wasilewska E, Korczyñski D, Stec WJ (1999) Tetrahedron Lett 40:8603
105. Brenner C, Varnum J (unpublished results)
106. Walkowiak B (unpublished results)
107. Marshall WS, Caruthers MH (1993) Science 259:1564
108. Okruszek A, Olesiak M, Balzarini J (1994) J Med Chem 37:3850
109. Okruszek A, Olesiak M, Krajewska D, Stec WJ (1997) J Org Chem 62:2269
110. Olesiak M, Okruszek A, Stec WJ (unpublished results)
111. Galburt EA, Chevalier B, Tang W, Jurica MS, Flick KE, Monnat RJ, Stoddart BL (1999) Nature Struct Biol 6:1096

112. Cosstick R, Vyle JS (1990) Nucl Acids Res 18:829
113. Krzyżanowska B, Stec WJ, Wieczorek MW, Błaszczyk J (1994) Heteroatom Chem 5:533
114. Błaszczyk J, Wieczorek MW, Okruszek A, Olesiak M, Karwowski B (1994) Heteroatom Chem 5:519
115. Błaszczyk J, Wieczorek MW, Okruszek A, Sierzchała A, Kobylańska A, Stec WJ (1996) J Chem Cryst 26:33
116. Błaszczyk J, Wieczorek MW, Okruszek A (1996) J Mol Struct 374:85
117. Potrzebowski MJ, Yang XB, Misiura K, Majzner WR, Wieczorek MW, Kaźmierski S, Olejniczak S, Stec WJ (2001) Eur J Org Chem, p 1491
118. Gay DC, Hamer NK (1972) J Chem Soc Perkin II 929
119. Boudjebel H, Goncalves H, Mathis F (1975) Bull Soc Chim Fr 629
120. Burgada R, Willson M, Goncalves H, Boudjebel H (1975) Bull Soc Chim Fr 2207
121. Blagoveshchenskij VS, Yakovleva OP, Borisenko AA, Zyk NV, Kisileva TS, Volfkovich SI (1976) Dokl Akad Nauk SSSR 230:845
122. Guga P, Koziołkiewicz M, Okruszek A, Stec WJ (1998) Oligo(nucleoside phosphorothioate)s. In: Stein CA, Krieg AM (eds) Applied antisense oligonucleotide technology. Wiley-Liss, New York, p 23
123. Jin Y, Just G (1998) J Org Chem 63:3647
124. Iyer RP, Guo MJ, Yu D, Agrawal S (1998) Tetrahedreon Lett 39:2491
125. Guo MJ, Yu D, Iyer RP, Agrawal S (1998) Bioorg Med Chem Lett 8 2539
126. Wang JC, Just G (1999) J Org Chem 64:8090
127. Wilk A, Grajkowski A, Phillips LR, Beaucage SL (2000) J Am Chem Soc 122:2149
128. Misiura K, Pietrasiak D, Stec WJ (1995) J Chem Soc Chem Commun 613
129. Baraniak J, Korczyński D, Kaczmarek R, Stec WJ (1999) Nucleosides Nucleotides 18:2147
130. Misiura K, Szymanowicz D, Stec WJ (1996) Collect Czech Chem Commun 61:S101

Recent Progress in Carbonylphosphonate Chemistry

Charles E. McKenna, Boris A. Kashemirov

Department of Chemistry, University of Southern California, Los Angeles, CA 90089–0744 USA. *E-mail: mckenna@usc.edu*

Carbonylphosphonates are defined for the purposes of this Review as phosphonates containing a proximal C=O function. In this review we focus on *α*-keto and *β*-ketophosphonates, including two classes of trifunctional carbonyl phosphonates, *α*-ketophosphonoglyoxylates and carbonylbisphosphonates. These compounds (and analogous derivatives) exhibit distinctive, multiple chemical properties reflecting in part the mutual intereaction of their neighboring carbonyl and phosphonate groups. In some cases, they present special problems in synthesis, and they have useful applications ranging from metal chelation to medicinal chemistry. Here they are considered from the points of view of synthesis, reactivity, value as synthons, and actual or potential bioactivity. Recent (> 1995) advances are emphasized.

Keywords. Carbonylphosphonate, Ketone, Carboxylate, Bisphosphonate, Synthesis troika acid, Phosphorylation, Monomeric metaphosphate, Nucleotide

Topics in Current Chemistry, Vol. 220

Abbreviations and Symbols

AZT	3′-azido-3′-deoxythymidine
BTMS	bromotrimethylsilane
DCC	*N*,*N*′-dicyclohexylcarbodiimide
DBU	1,8-diazabicyclo[5.4.0]undec-7-ene
DIAD	diisopropyl azodicarboscylate
DMAP	4-dimethylaminopyridine
PyBOP	(1 H-benzotriazol-1-yloscy)tripyrrolidino phosphonium hescafluorophosphate
HMPA	hexamethylphosphor amide
rt	reflux temperature
TFA	trifluoroacetic acid
THF	tetrahydrofuran
TPP	dianion of *meso*-tetraphenylporphyrin

1
Introduction

For the purposes of this Review, "carbonylphosphonates" are defined principally as phosphonates that include a C=O functionality sufficiently proximate to the P=O group that the two functional groups exert a significant influence on each other. For practical purposes, we will limit our consideration to α- and β-ketophosphonates. The chemistry of formylphosphonates, which are generally unstable compounds but have stable derivatives, has been recently reviewed [1] and will not be discussed here. The phosphonocarboxylates, a related class of compounds presenting much of interest during the past few years with respect to both chemical reactivity and biological activity, have also been excluded from systematic consideration in this Review, excepting the phosphonoglyoxylates which incorporate a ketone functionality (α-ketophosphonoacetates). We also consider carbonylbisphosphonate esters, the first examples of which were recently synthesized in our laboratory. Within the scope of these boundary conditions, we will summarize some of the advances in these areas made particularly during the five years that have elapsed since the appearance of the last major (1996) monograph on acylphosphonates [2]. Our focus will be on the synthesis, chemical properties and synthetic utility of this fascinating and versatile class of organophosphorus compounds, however we also briefly note some of their actual or potential biological applications where appropriate.

2
α-Ketophosphonates

2.1
Synthesis

α-Acyl phosphonate esters have been conventionally prepared by a Michaelis-Arbuzov reaction between a trialkyl phosphite and an acid chloride. The scope and some potential pitfalls of this classical approach have been summarized [2]. Michaelis-Arbuzov syntheses usually proceed satisfactorily when simple aroyl and alkanoyl chlorides are used, especially if purification of the product by distillation is possible. α-Acyl phosphinates are accessible by the same route, as exemplified recently in a synthesis of asymmetrical and symmetrical α-keto benzylphosphinates by Benech et al. [3] although the yield proved to be sensitive to the structure of the benzyl moiety. Similarly, bis(trimethylsilyl) phenylphosphonite reacts with trimethylacetyl chloride quantitatively to give bis(trimethylsilyl) acylphenylphosphinate [4].

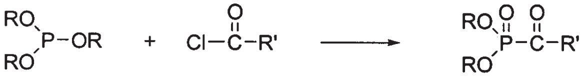

Scheme 1 R = Alk, Ar; R' = Alk, Ar

However, there has been less success in utilizing Michaelis-Arbuzov condensations for the preparation of functionalized acylphosphonates such as β,γ-unsaturated α-acylphosphonates [5, 6], epoxy acylphosphonates [7], α-ketophosphonocarboxylates [8] and α-ketobisphosphonates [9]. The latter two instances are discussed in detail in subsequent sections. In general, problems arise when the ketone group in the product becomes sufficiently activated by its neighboring P=O group(s) that it becomes susceptible to attack by the phosphite reagent, in competition with normal attack of phosphite at the acyl chloride carbonyl carbon. A similar problem of inadequate regioselectivity arises when the acyl chloride incorporates electronegative substituents proximal to the C=O group, such that the product ketone competes with unreacted acyl chloride for remaining phosphite. Attempting to solve this problem within the framework of traditional Michaelis-Arbuzov chemistry, Glabe et al. have shown that trialkyl phosphites with increased steric bulk (triisopropyl, tris(trimethylsilyl)) give acyl phosphonates which resist phosphite addition despite the presence of bromo-, tributylsilyloxy-, or *trans*-epoxide α-subsituents. However this approach was unsuccessful with acyl chlorides functionalized with *cis*- or monosubstituted epoxide groups [7].

Recently, alternative methods for preparation of acylphosphonates based on oxidation of easily prepared α-hydroxy- [10, 11] and α-diazo phosphonates [12] have been developed. A variety of oxidation methods {MnO_2, PCC (pyridinium chlorochromate), PDC (pyridinium dichromate), Pfittzner-Moffatt, Swern oxidation} have been applied to α-hydroxy phosphonate substrates [13–16].

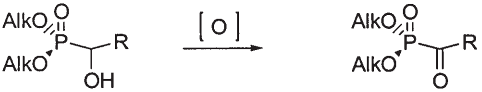

Scheme 2 R = Alk, Allyl, Ar, Heterocycle

Particularly good results have been achieved with CrO_2 in refluxing acetonitrile, a system that proved effective with a variety of structurally different α-hydroxy phosphonates [17]. Similar conversions can be carried out under surface-mediated solid-phase conditions [18], acyl phosphonates being obtained under mild reaction conditions by treatment of α-hydroxy phosphonates on alumina (neutral)-supported CrO_3 without solvent. An oxidative method proved successful in the synthesis of novel phosphonopeptides for evaluation as inhibitors of human calpain I [19].

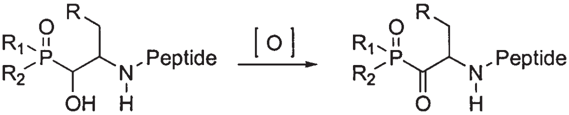

Scheme 3 R_1, R_2 = OH, OAlk, Alk, Ar; Dess-Martin oxidation in CH_2Cl_2

An alternative approach to preparation of α-ketophosphonates is indicated in a report that acylphosphonates can be obtained by heating the silyl diester of the corresponding hemiacetal above 140 °C [20]. However, the spectroscopic data presented in this paper (IR, ^{31}P-, ^{13}C-NMR) do not appear to fully support the acylphosphonate structure assigned to the reaction product.

Oxidation of α-diazo phosphonates will be considered separately with specific reference to synthesis of phosphonoglyoxylates and carbonylbisphosphonates.

2.2
Reactivity

2.2.1
Enolization

The tautomeric equilibria of α-ketophosphonates which possess a β-hydrogen are determined by the nature of the acyl moieties. It has been recently found [21] that β-aryl-α-ketophosphonates are fully enolized in solution and, at least in one case, in the solid state as well, in structures where enolization is favored by an extended conjugated π system and by the possibility of intramolecular (or intermolecular) hydrogen bonding to a P=O oxygen atom. An X-ray crystal structure determination of dimethyl β-phenyl-α-ketophosphonate revealed a hydrogen-bonded dimer in the unit cell, the enol OH of one molecule being bridged to the oxygen in the P=O function of the other.

Scheme 4

Dimethyl α-ketophosphonates may be readily converted to enols under mildly basic conditions. α-Acylphosphonate enols thus far studied stereochemically exclusively exhibit *E*-geometry, which advantageously places the two bulkiest groups substituting the C=C double bond – the alkyl R and the phosphoryl group – in a *trans* position [21].

The trapping of acylphosphonate enols by triflating agents under basic conditions has been studied recently [22]. The best results were obtained using a moderately strongly electrophilic triflating agent – nonafluorobutylsulfonyl fluoride, with DBU. The resulting α-phosphonovinyl nonaflates were successfully converted to corresponding phosphono-containing enynes and dienes via Pd-catalyzed cross-coupling reactions.

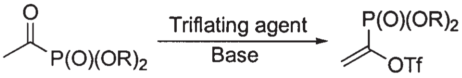

Scheme 5 R = Et, Pr-*i*

In the absence of stabilizing forces favoring the enol, the ketone form of enolizable α-ketophosphonates prevails. Thus, dimethyl 1-oxopropanephosphonate is in equilibrium with a negligible amount of its enol form in $CDCl_3$.

2.2.2
Hetero Diels-Alder and Mukaiyma-Michael Reactions, Stereoselectivity

α,β-Unsaturated acylphosphonates are effective heterodienes in reactions with heterodienophiles such as enol ethers and sulfides catalyzed by bis(oxazoline) copper (II) complexes, which can provide high diastereo- and enantioselectivity [23–25]. The enantioselective synthesis of dihydropyrans (which occur as substructures in a number of important natural products) by this method has been shown to be straightforward using 0.2 mol % of the chiral catalyst, with stereoselectivities exceeding 90% The reactions are permissive with respect to substrate structure. In particular, phenyl-, isopropyl-, and ethoxy-substituted substrates all underwent diastereoselective Diels-Alder reactions with ethyl vinyl ether to give dihydropyrans with consistently high enantioselectivities and good yields.

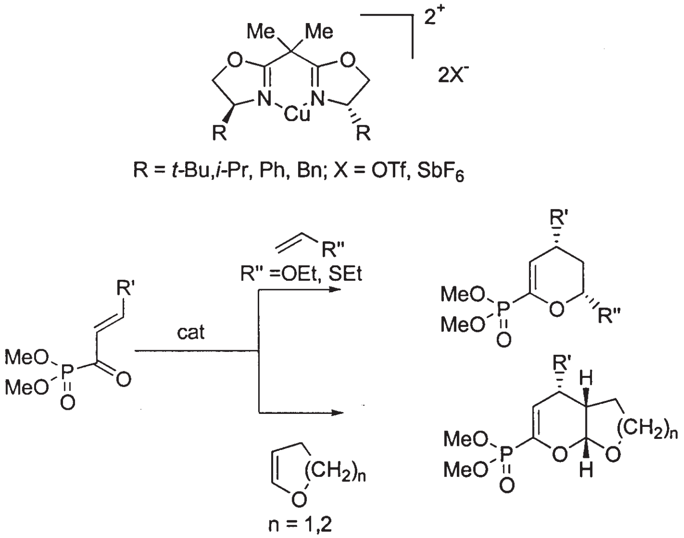

R = *t*-Bu, *i*-Pr, Ph, Bn; X = OTf, SbF_6

Scheme 6

While phenyl- and *tert*-butyl-substituted catalysts conferred similar degrees of enantioselectivity, the phenyl catalyst proved much more reactive. Interestingly, enantioselectivity reversed when the *tert*-butyl ligand replaced the phenyl ligand in the bis(oxazoline) copper (II) catalysts [23].

α-Acyl-β,γ-unsaturated phosphonates have also been explored as substrates for the Mukaiyma-Michael reaction.[26] The stereoselectivity (modest) is sensitive to the steric bulk at the Lewis acid metal center. Contrary to their earlier prediction [24], these authors did not find cycloaddition to be the most favorable pathway.

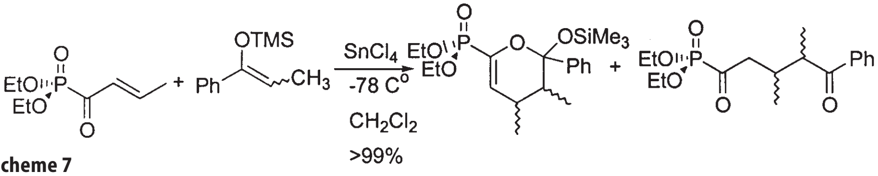

Scheme 7

2.2.3
Reduction Stereoselectivity

Over the past decade, α-hydroxy phosphonates have received increasing interest because some compounds of this type have proved to be biologically active, inhibiting renin, EPSP synthetase or HIV protease [27]. The absolute configuration of the α-hydroxy carbon is important for biological activity [27], underscoring the importance of stereoselective synthesis of these compounds. α-Hydroxy phosphonate enantiomers can be made by several methods, including stereoselective reduction of α-ketophosphonates. Reduction of diethyl α-ketophosphonates with borane and β-butyl oxazaborolidine as a catalyst has afforded (*S*)- or (*R*)-1-hydroxyalkylphosphonates in good yield and moderate to good enantiomeric excess (53–83 ee%) [28]. This method was subsequently developed and improved by Meier et al. [29–32]. Excellent enantiomeric excess (up to 99 ee%) yields in the product were achieved using catecholborane in reactions conducted at low temperatures. In studying the influence of the phosphonyl and aryl group structures on the course of these reactions, the authors concluded that modification of the phosphoryl group is chiefly important for fine-tuning the reactivity of the carbonyl group. Reduction of α-ketophosphonates by an (*S*)-oxazaborolidine catalyst led to an (*S*)-configuration at the new stereogenic center. In contrast, acetophenone derivatives and α,γ-ketophosphonates gave (*R*)-hydroxy products. These results supported a proposed reaction intermediate complex wherein the disposition of the "large/small" residues flanking the carbonyl group determines product configuration by constraining attack by the hydride of the reductant to either the re- or the si-face presented by the carbonyl group.

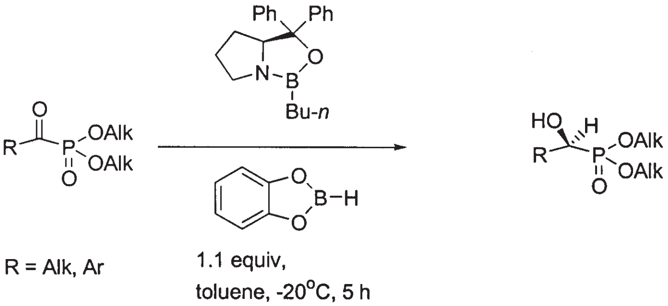

Scheme 8

An analogous approach was used in a stereoselective synthesis of β-amino-α-hydroxy phosphonates [33]. Reduction of corresponding α-keto phosphonate substrates with borane-dimethylsulfide complex aided by oxazaborolidine catalysis afforded a mixture of diastereomers, but significant diastereoselectivity was achieved using catecholborane as the reductant in toluene at –60 °C.

α-Hydroxy and α,ω-dihydroxy alkane-α,ω-bisphosphonic acids have been obtained by the reduction of the corresponding α,ω-ketones [34].

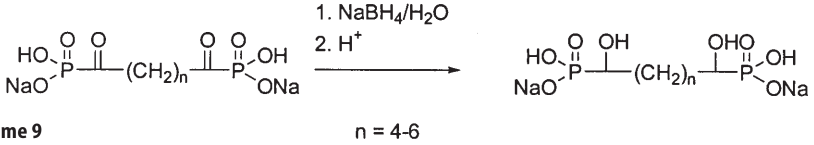

Scheme 9

2.2.4
Deoxygenation and Deoxygenative Coupling

As noted above, reactive α-ketophosphonates are susceptible to nucleophilic addition of trialkyl phosphites. The resulting anionic intermediates may be trapped by proton transfer, however if there are no protons or other electrophiles available, cleavage of the C_α-O bond can occur, as has been shown with benzoylphosphonates, where the resultant carbenelike intermediate can react either intermolecularly with trimethyl phosphite to give a phosphonate ylide or, if a suitable *ortho* substituent is present on the benzene ring, by intermolecular insertion resulting in cyclization or hydrogen abstraction from the substituent [35–37]. In all cases where cyclizations were observed, there was a marked preference for five-membered ring formation even in those cases where larger ring sizes were theoretically accessible [35]. Using a 2-phenoxymethyl substituent, where formation of a 5-membered ring system should be impossible, it was shown that the carbenoid intermediate interacts with the phenyl ring π-electrons to give a six-membered heterocyclic ring system [36]. It was also shown that with a 2-MeNH substituent, an ylide containing a P-N bond likely formed, which then underwent rearrangement to give a diphosphorus product containing a five-membered ring incorporating a P-N bond [37].

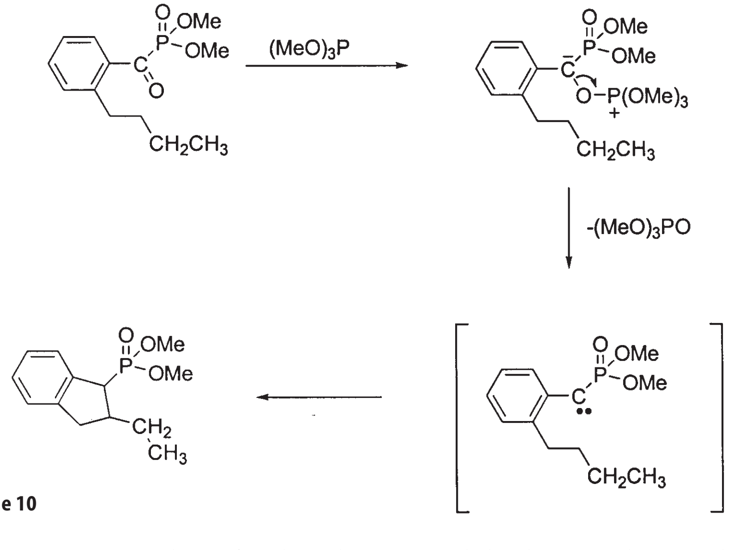

Scheme 10

Deoxygenative coupling of carbonyl compounds leading to substituted olefins is an important process in organic synthesis that can be promoted by low-valent metals. To achieve the deoxygenative coupling of ketones and aldehydes by low-valent lanthanides, Takaki et al. [38] employed an indirect approach using acylphosphonates and Sm metal or SmI_2, in which one oxygen was eliminated as a carboxylic acid and the other as a phosphate. Acylphosphonates reacted with aldehydes giving acyloxyphosphonates, and reductive elimination of carboxylic acids, followed by coupling with ketones, proceeded well. However, Horner-Emmons olefination did not proceed, and thus the overall reaction produced β-hydroxy phosphonates in good yield. The β-hydroxy phosphonates could be converted to alkenes using other bases [38].

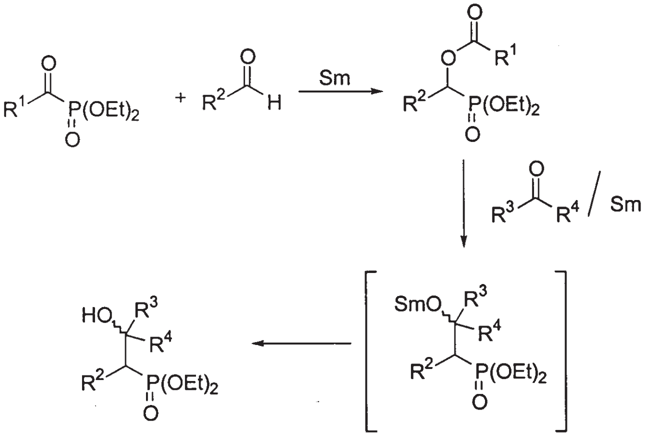

Scheme 11

2.2.5 *Halogenation*

Protein-tyrosine (PTP) inhibitors are potentially valuable pharmacological tools for studying cellular signal transduction and for therapeutic intervention. Derivatives of 1,1-difluoromethylphosphonic acid are known to be potent PTP inhibitors. An important method for synthesis of these compounds is fluorination of acyl phosphonates by diethylaminosulfur trifluoride (DAST). This method allows synthesis of *tert*-butyl-protected difluoro(aryl)- or (naphthalenyl)methylphosphonates, which under mildly acidic deprotection conditions afford desirable phosphonic acids [16, 39]. Acyl phosphonate fluorination by DAST has also been utilized for synthesis of α,α-(difluoroprop-2-ynyl)phosphonates [14].

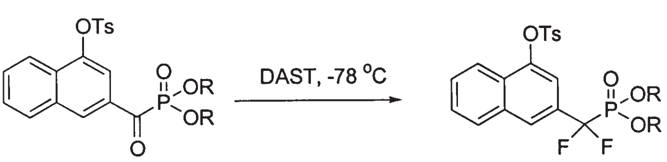

Scheme 12

R = Et, *t*-Bu

Facile acylphosphonate enolization was exploited in a synthesis of α-chlorinated fatty acids [40]. The α-chloro acylphosphonates obtained via chlorination of acylphosphonates with sulfuryl chloride were cleaved to form the target products using hydrogen peroxide-sodium bicarbonate.

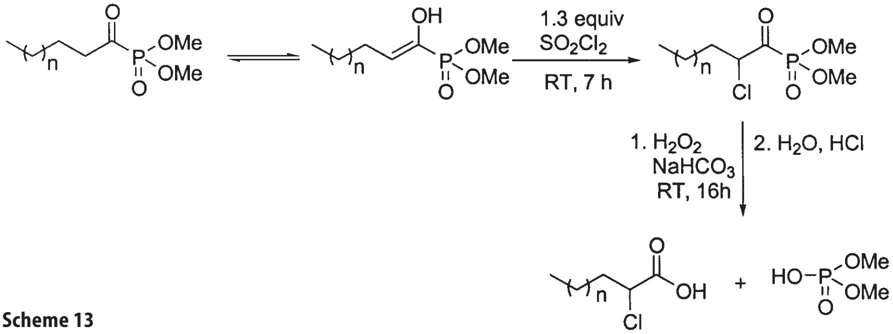

Scheme 13

2.2.6
Reactions with Nucleophiles

Acylphosphonates possess a carbonyl group which is activated to attack by oxygen or nitrogen nucleophiles such as water, alcohols, amines, and hydroxylamines, as well as by phosphites as noted above. The resulting adducts may be prone to undergo C-P bond cleavage. Breuer et al. have examined the rates and equilibria of hemiacetal formation from addition of alcohols to dimethyl acetylphosphonate and dimethyl benzoylphosphonate using ^{31}P-NMR spectrometry [41]. The equilibrium constants for the addition of various alcohols bearing electron-withdrawing substituents to dimethylacetylphosphonate were found to decrease with alcohol acidity. However, this pattern was not consistent for methanol and ethanol [41].

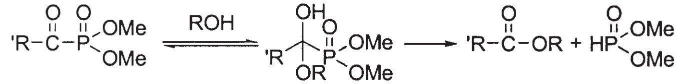

Scheme 14

An obvious synthetic application of amine addition to the α-keto group in acylphosphonates would be reductive amination. This has been demonstrated [42], and shown to be a useful route to 1-aminoalkylphosphonic acids. Thus, selected acylphosphonates were reacted with benzhydrylamine, giving after reduction of the resulting imine intermediate with triacetoxyborohydride and acid hydrolysis, satisfactory yields of the corresponding aminoalkylphosphonic acids. However, a limitation of this approach is unwanted cleavage of the phosphonate P-C bond, which was observed with other amines such as benzylamine and α-benzylmethylamine [42].

In an another interesting example of acylphosphonate amine addition [43], *para*-substituted α-aminobenzylphosphonate esters were found to add to a di-

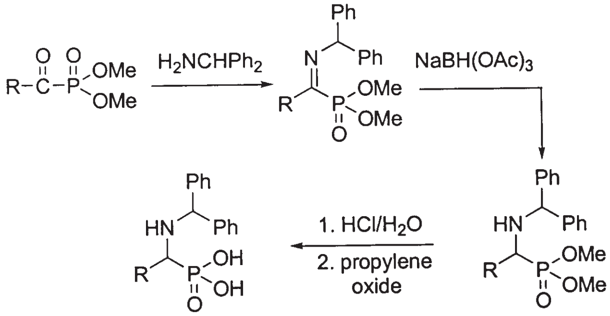

Scheme 15

alkyl benzoylphosphonate initially to yield diphosphorylated azaallyl derivatives, which when heated or subjected to basic conditions underwent a reversible 1,3-H shift in the C=N-C moiety to give an equilibrium mixture of isomers.

Reaction of α-acylphosphonate esters with Grignard or other organometallic reagents has received little attention until surprisingly recently. Maeda et al. [44] have shown that reaction between dialkyl benzoylphosphonate and PhMgBr or MeMgBr in THF at −78 °C gives the corresponding hydroxyphosphonate adducts in moderate yield. With PhLi and MeLi, tertiary alcohols were obtained in preference to hydroxyphosphonates, presumably via elimination with P-C bond cleavage, followed by further addition of carbanion to the ketone fragmentation product. Other workers have reported that dialkyl acylphosphonates react with both Grignard and Reformatsky reagents to give, instead of the expected α-hydroxy phosphonate ester, P-C bond cleavage in the initial adduct forming phosphite and a ketone: cited by Breuer, p. 685 [2].

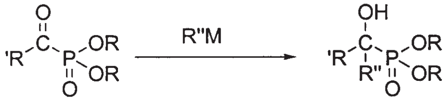

Scheme 16 R" = Me, Ph; M = MgBr, Li

Carbanions derived from isocyanoacetates formed in situ using NaH react with acylphosphonates to give 1-alkyl-2-ethoxycarbonyl-2-formylaminoeth-1-enylphosphonates [45]. Cu_2O catalysis provided stereoselectivity, giving mainly the *Z*-isomer.

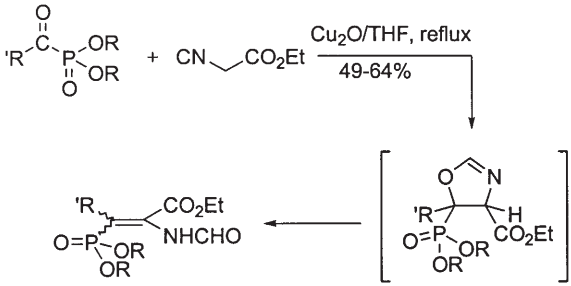

Scheme 17 R = Alk; R' = Alk, Ar

2.2.7
Reaction with Metals, Metal Complexes, Metathesis Reactions

The utility of Sm in deoxygenative coupling of carbonyl compounds has already been discussed [38]. One study has been published on the reaction of acylphosphonates with another lanthanide metal, Yb [46]. Ytterbium converted a substituted acylphosphonate under mild conditions (THF, HMPA, rt) to 1,2-diphenyl-2-oxoethyl phosphate and 1-(phosphoryloxy)-1-phenylmethylphosphonate. The reactivity of Yb was explained in terms of its oxophilicity, leading initially to an acylytterbium complex.

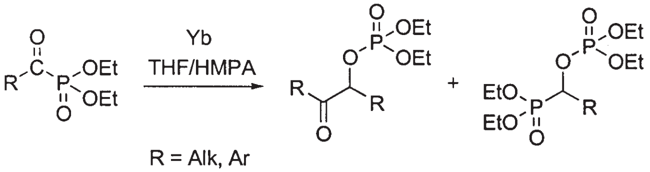

Scheme 18

Nakazawa et al. examined the action of a series of palladium complexes (PdR_2L_2, R = Me, Et; L = tertiary phosphine) on α-ketophosphonates [47]. Catalytic decarbonylation was observed, apparently via a metathesis reaction at the C-P bond.

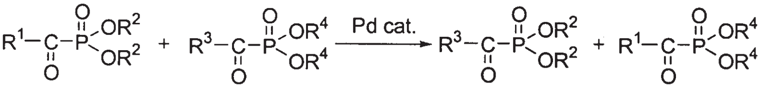

Scheme 19

2.2.8
Dealkylation, Synthesis of Acylphosphonic Acids

A number of acylphosphonic acids are of interest for their biological activity, or as intermediates in syntheses of potentially bioactive phosphonic acids [7, 34, 48–50]. In many cases, they are most conveniently prepared by hydrolysis of the corresponding esters. Due to the presence of the keto function, acid hydrolysis (heating in aqueous HCl) is generally not a practical method to achieve this. Silyldealkylation of methyl-, ethyl- or isopropyl phosphonates with BTMS, followed by very mild hydrolysis is normally compatible with acyl and other sensitive functionalities [7, 34, 48].

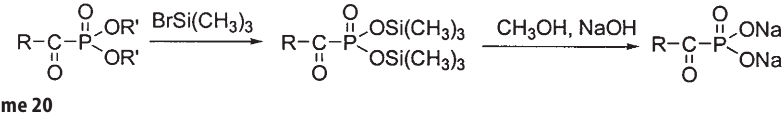

Scheme 20

Acylphosphonic acids have also been obtained by hydrolysis of di(*tert*-butyl) acylphosphonates with 85% TFA [49] or by hydrogenolysis of corresponding dibenzyl phosphonates [50]. If ionized, acylphosphonic acids are less prone to P-C bond cleavage than corresponding diesters, which in some cases can lead to better yields of desired reduction or reductive amination products [34, 50].

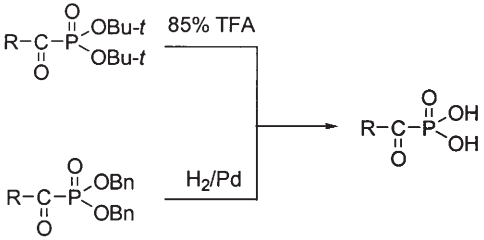

Scheme 21

3
β-Ketophosphonates

3.1
Synthesis

Several interesting approaches to the synthesis of β-ketophosphonates have recently been described. Typically, standard Arbuzov synthesis of β-ketophosphonates is unsatisfactory due to a competing Perkow reaction [51]. However, γ,δ-unsaturated β-ketophosphonates are obtained in high yield via Arbuzov reaction of triethyl phosphite with α-iodoenones, readily available from tertiary allenic alcohols [52]. Another successful example of an Arbuzov-based approach involves reaction of bromoacetylated polystyrene with triethyl phosphite, which provided immobilized β-ketophosphonate in excellent yield [53]. In another approach, the lithio derivative of dimethyl methylphosphonate was reacted with Weinreb amide to obtain the corresponding β-ketophosphonate [54]. α,α-Difluoro-α-ketophosphonates have been synthesized via a cerium-mediated route

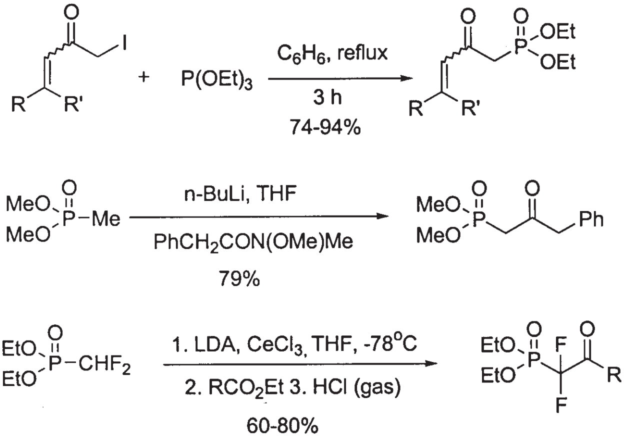

Scheme 22

[55], in which the key step is addition of dry, solid cerium (III) chloride to a solution of freshly-prepared LDA in THF at −78 °C, followed by ester electrophile addition. The acylation of organocuprates or organolithiated reagents with 2-(dialkylphosphono)alkanoyl chlorides or (dialkylphosphono)fluoroacetyl chlorides has been described as a general and efficient route to *β*-ketophosphonates [56]. Synthesis of *β*-ketophosphonates (yield, 70–90% from *tert*-butyl thioesters using the lithium anion of either methyl- or ethylphosphonate has been described [57]. Interestingly, the anion generated from dimethyl ethylphosphonate was noticeably less reactive than its diethyl counterpart.

3.2
Reactivity

β-ketophosphonates are valuable synthetic intermediates for the preparation of *α*,*β*-unsaturated carbonyl compounds via the Horner-Wadsworth-Emmons (HWE) reaction [51]. The HWE reaction has been applied to synthesis of different natural products or their precursors, including use of an intramolecular HWE in construction of a highly strained eleven-membered ring system (a potential precursor for the key biosynthetic intermediate of the protoilludane family) [58], preparation of (±)-(*E*)-*α*-atlantone [52], synthesis of C-glucosinolates [54], a halichondramide fragment [57], and synthesis of both enantiomers of the biotin vitamer 8-amino-7-oxopelargonic acid [59].

Another important application of *β*-ketophosphonates is as ligands in certain molybdenum catalysts. *β*-ketophosphonate complexes of molybdenum (VI) prepared from (*R*)- or (*S*)-camphor are highly active catalysts in the epoxidation of alkenes, polybutadienes or polyisoprenes [60, 61]. An analogous catalyst initiated the selective ring opening of (+) or (−)-limonene oxide by water to give the *trans*-diaxial diol, the *trans*-isomer being untouched [62]. Finally, the Mo(VI) complex of diethyl (2-phenyl-2-oxoethyl)phosphonate has been used in the oxidation of organic sulfides [63].

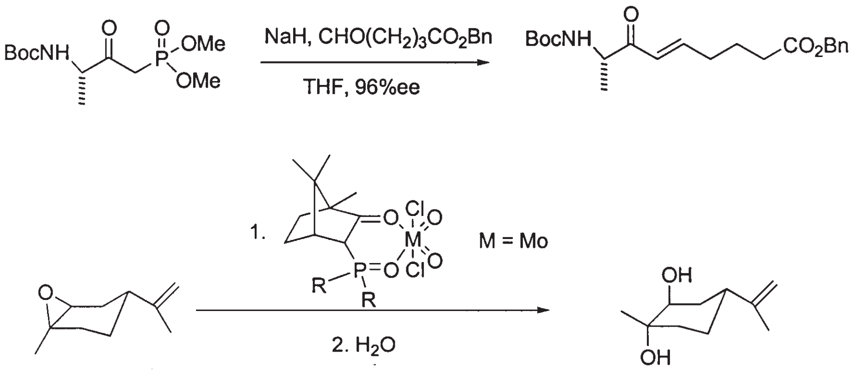

Scheme 23

4
Phosphonoglyoxylates

We originally became interested in the then unsynthesized phosphonoglyoxylate (α-oxophosphonoacetate) system as a result of structure-dependent differences in DNA polymerase activity found among phosphonoformate and phosphonoacetate analogues [64]. Beyond the replacement of the P-O-P bond in pyrophosphate by a less scissile P-C-C bond in the analogues, the phosphonoacetates in particular provided the possibility of changing their bioactivities by modification of the CH_2 group bonded to phosphorus. For example, replacement of one or both α-methylene hydrogen atoms by halogen substituents modifies basicity, steric profile and ligand properties, resulting in important changes in affinity for particular enzymes [65].

A specific application of this approach is the introduction of a *reactive* functional group at the carbon adjacent to phosphorus in a phosphonate intended to bind to a particular biochemical site. Exemplary molecules embodying this strategy are α-diazo phosphonates designed to serve as photoaffinity labels [66, 67]. It should be noted that although the α-diazo phosphonate is strikingly stabilized (less so in the monoanion and dianion) to nonphotochemical hydrolysis, practical use of these compounds for photoaffinity labeling has been limited by competing intramolecular Wolff rearrangement in the carbene photoproduct.

These considerations prompted us to investigate the synthesis and α-keto group reactivity of phosphonoglyoxylic acid. A trialkyl phosphonoglyoxylate, such as the triethyl ester, was taken as a logical precursor; this compound is also of potential value as a synthon for other interesting α-substituted phosphonoacetates that might be accessible by exploiting the versatile chemistry of the ketone function.

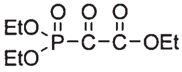

Scheme 24

4.1
Synthesis

The synthesis of triethyl phosphonoglyoxylate *via* reaction between ethyl oxalyl chloride and triethyl phosphite was claimed in the 1960s and 1970s, but no structural characterization was provided [68, 69]. A reinvestigation in our laboratory by NMR analysis showed that this reaction, and similar reactions with methyl and methyl-ethyl crossed esters of the chloride and phosphite, regardless of the addition order, give rise to complex product mixtures in which the claimed product is not observed, due to the high degree of reactivity of the newly formed ketone group although it may be formed as an intermediate (we later found that it reacts exothermically with triethyl phosphite) [8, 70].

Despite the simplicity of its structure, triethyl phosphonoglyoxylate proved to be inaccessible by a number of plausible methods based on chemical analogy with either diethyl malonate or diethyl alkylidienemalonate, evincing the striking decrease in α-C reactivity when the second RO(O)C moiety in malonate esters is replaced by a phosphono group [8,71]. Thus, N_2O_3 cleanly oxidizes diethyl malonate to diethyl oxomalonate [72], but triethyl phosphonoacetate is inert to this reagent, as well as to ruthenium tetroxide and a number of other oxidizing reagents. Although treatment of diethyl dibromomalonate with potassium acetate in ethanol gives a good yield of the oxomalonate [73], triethyl dibromophosphonoacetate is instead reduced by this reagent. A reduction also occurred when the synthesis of 2-(diethylphosphono)-2-carboxyethyldithiane was attempted. Dithianes can be converted to ketones by several different reagents under mild conditions.[74] Finally, it has been shown that dimethylsulfoxide oxidizes diethyl bromomalonate to diethyl oxomalonate [75], but triethyl monobromophosphonoacetate is unchanged by this reagent. Treatment of triethyl dichlorophosphonoacetate with aqueous potassium hydroxide, by analogy with the known conversion of tetralkyl dichloromethylenebisphosphonate to tetrasodium carbonyldiphosphonate [76] also leads to decomposition. Ozonolysis, successful with ethylidenylmalonate ester [77], did not give satisfactory results with triethyl phosphonoacrylate, which on treatment with ruthenium tetroxide, gave instead of a ketone [78], the corresponding epoxide as the major product [79].

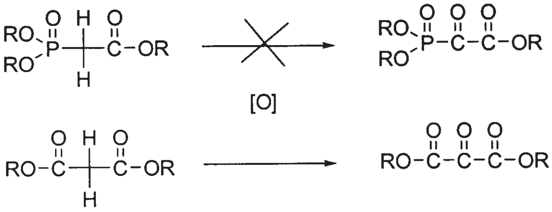

Scheme 25

Clearly in these precursors the severe electron deficiency of the methylene (or α-methylidene) carbon, flanked by two strongly electron-withdrawing groups, accounts for its resistance to oxidation and points to an 'umpolung' tactic for activation, wherein advantage might be taken of the relatively high electron density present on the carbon atom in the diazomethylene group, and the large driving force provided by elimination of N_2 in oxidation of this group. Rh(II) acetate-mediated deoxygenation of epoxides using diethyl diazomalonate was previously shown to be useful for deprotecting epoxide-protected alkenes, producing as a byproduct the oxomalonate diester [80]. Reversing the roles of product and byproduct, a similar reaction between an epoxide and a trialkyl α-diazo phosphonoacetate suggested itself as a viable route to trialkyl phosphonoglyoxylates (newer developments in Rh(II)-catalyzed oxidations of α-diazo phosphonate esters are further discussed in Sect. 5).

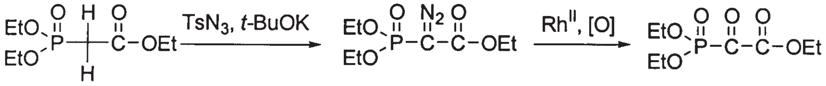

Scheme 26

Indeed, triethyl phosphonoglyoxylate was easily prepared by this approach using propylene oxide as the oxygen donor (100% by NMR, 84% isolated), with refluxing benzene (16 hr) as the solvent [79]. The course of the reaction was conveniently monitored by ^{31}P-NMR (diazo ester resonance, δ 10.8 ppm, ketone ester resonance δ -2 ppm). Workup is simple: both side products (dinitrogen and propylene) are gases at room temperature, and excess propylene oxide and solvent is removed *in vacuo*. On reuse, recovered rhodium catalyst was found to retain its activity. When 0.02 eq. (tenfold more) catalyst was used, the reaction was complete in approximately 2 h.

4.2
Reactivity

4.2.1
Physical Properties

Trialkyl phosphonoglyoxylates are brilliant emerald-yellow, mobile oils; for the ethyl ester, $\varepsilon_{400.4}$(acetonitrile) = 65.8 L/mol cm. Their visible light absorption can be rationalized on the same basis as that of carbonylbisphosphonate esters, see discussion below. Their ketone IR absorption is red-shifted (1750 (s), 1735 (vs)) relative to that of simple ketones. The phosphoryl stretching frequency is nearly identical in both triethyl α-diazophosphonoacetate and triethyl phosphonoglyoxalate; however, the ester stretching frequency is red-shifted by 35 cm^{-1} in the diazo compound. Obviously, π-delocalization lowers the C=O bond order in the diazo compounds. The ^{31}P NMR resonance and ^{13}C-NMR carbonyl resonances (δ 159.6 (d, $^2J_{PC}$ = 76 Hz, *C*=O[CO]), δ 193.6 (d, $^1J_{PC}$ = 183 Hz, *C*=O[PO])) reflect the electron deficiency at the keto carbon atom (cf. corresponding α-diazo compounds, C-P coupling 223 Hz).

4.2.2
Conversion to Acid and Salts

Trialkyl phosphonoglyoxylates are too labile to by hydrolyzed in strong aqueous acids such as HCl or HI, due to the very reactive ketone function, which, unlike that in simple acylphosphonates, can undergo reaction with BTMS. However, a method was devised to prepare the parent acid, in which the precursor diazo group does double duty as a protecting group [8]. Thus, ethyl P,P-*bis*(trimethylsilyl) α-diazophosphonoacetate was synthesized by treating the triethyl ester with BTMS, which displayed the expected regioselectivity for P vs C ester dealkylation. The mixed ester was then converted to the ketone using the Rh(II)-epoxide methodology. On contact with D_2O, the silyl ester groups instantly hydrolyzed, generating the bisphosphonic acid which, on heating to 56 °C for a day, catalyzed hydrolysis of its own C ester group. Dicyclohexylamine then afforded an analytically pure sample of the *bis*(dicyclohexylammonium) salt. The temperature is critical for the final hydrolysis step, 78 °C leading to decomposition. Phosphonoglyoxylate moderately inhibits several viral nucleic acid polymerases, the active form having been shown to be the ketone form, not the hydrate (see below) by UV and ^{31}P-NMR -pH activity profile analysis [81].

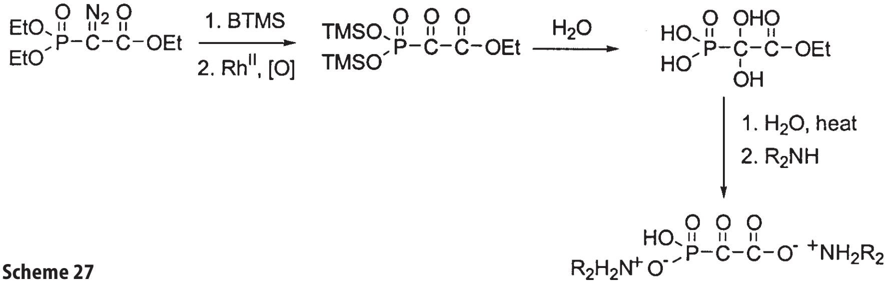

Scheme 27

4.2.3
Hydration

The ketone group in trialkyl phosphonoglyoxylates is highly electrophilic, being quantitatively converted to the hydrate by addition of one equivalent of water, and there is no evidence for rapid exchange on the NMR time scale. The hemiacetal from methanol also forms quantitatively and showed no sign of conversion to hydrate when kept 48 h in water at room temperature. However, one equivalent of a more hindered (*tert*-amyl) alcohol gave only about 5% hemiacetal.

In contrast, hydration of phosphonoglyoxylic acid is determined by the pH, and the yellow ketone form predominates above pH 7.5. Further decrease of pH shifts the equilibrium to the colorless hydrate. At the same time, a manifold of acid-base pairs for ketone and hydrate should be present. Because the hydrate and ketone do not exchange rapidly, their ^{31}P-NMR peaks are distinct, and it is possible to measure the total hydrate/ketone ratio at various pH values, and also to follow ketone to hydrate conversion by uv-visible spectroscopy. An estimation of pKa's for species in the mid-pH range gave: ketone pKa$_3$ 6.8, hydrate pKa$_3$ 7.2, pKa$_2$ 3.8. Previous work suggests that pKa measurements based on ^{31}P-NMR chemical shifts agree well with values from classical titration.

4.2.4
Oximes

Oximes derived from phosphonoglyoxylic acid possess a trifunctional array of phosphonic, iminohydroxy, and carboxylic acid groups connected to a common carbon atom, and have thus been dubbed 'troika acids' [82]. The nature of the oxime hydroxy group interaction with its neighboring groups (phosphonic or carboxylic acid group) will depend on whether the =N–OH is in an *E* or *Z* orientation, and thus the chemical behavior of troika acids will be substantially controlled by the stereochemical status of the hydroxyimino moiety.

Troika acid derivatives have been under recent investigation as phosphorylating agents and also as metal ion chelators. Both the E and Z isomers of the parent acid have been prepared in situ from the corresponding stable C-methyl precursor salts by alkaline cleavage of the carboxylate ester, and shown to undergo

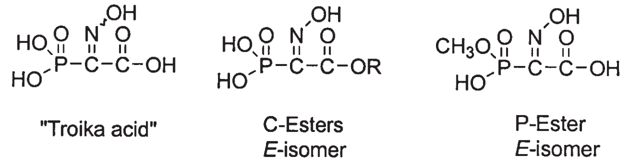

Scheme 28 R = Me, p-NO$_2$Ph, p-NO$_2$Bn

stereospecific, hydrolytic fragmentations in water near or below pH 7 at room temperature [83]. The *E* isomer cleaves at the P-C_α bond, phosphorylating the solvent to produce inorganic phosphate (in water); the *Z* isomer cleaves at the C_α-C_β bond, forming phosphorocyanidate [83]. Similar fragmentation occurs on heating the C-methyl ester *E*-isomer in alcohols, giving monoalkyl phosphates (Et, *i*-Pr, *t*-Bu). When conducted in mixture of primary and tertiary alcohol (1 : 1 EtOH-*t*-BuOH), only a twofold excess of primary alkyl phosphate was obtained (~2:1 ethyl phosphate : *tert*-butyl phosphate). Lack of selectivity in phosphorylation of a primary alcohol versus sterically hindered *t*-butyl alcohol is considered to be evidence for a dissociative (metaphosphate-like) mechanism.

Phosphorylation, the transfer of phosphoryl group (-PO_3) to a nucleophilic acceptor, is a fundamental reaction in phosphorus chemistry and is a process central to biological metabolism and biosynthesis. Monomeric metaphosphate, ($P(O)_2OH$), has frequently been postulated to exist as a highly reactive intermediate, or transition state structure, in dissociative phosphorylation mechanisms. The troika system offers interesting possibilities for introducing specific means of controlling a phosphorylation process, by taking advantage of the fact that a stable precursor, e.g., a C-monoester, can be prepared as a single geometric isomer (*E* isomer), and phosphorylation can then be made dependent on an unrelated chemical process, e.g., cleavage of the C-monoester, preferably under mild conditions, which leads to activation.

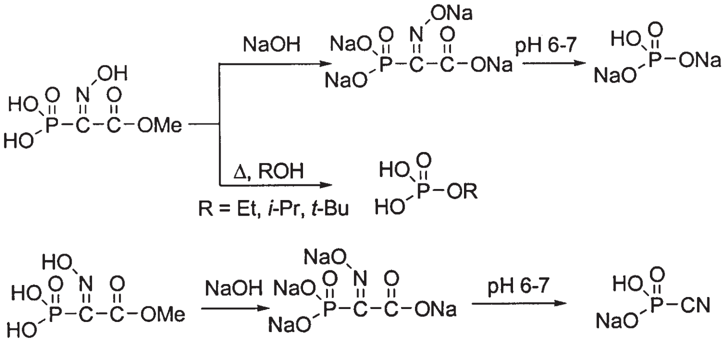

Scheme 29

Hydrolysis of troika acid C-methyl esters proceeds at pH 13–14 (the *E* isomer is much less reactive, probably owing to the proximity of the iminohydroxy anion to the carboxylate group). To explore phosphorylation from troika acid produced under milder (physiological) conditions, the C-*p*-NO_2Ph and *o*-NO_2Bn esters were synthesized and evaluated [84–86]. The rate of *p*-nitrophenoxide release from the corresponding C-ester was studied as a function of pH, temperature and added divalent metals. It was found that C-ester hydrolysis is significantly enhanced by divalent metals, especially by Ni^{2+} ions which accelerate hydrolysis at least 700 fold at neutral pH [86].

Indirect photo-induced (broad band UV, 308 nm Xe excimer laser or 355 YAG laser irradiation) phosphorylation via a C-ester caged troika acid has also been demonstrated. In alcohols or neutral aqueous buffers, irradiation of the troika acid C-*o*-NO_2Bn ester gave phosphorylation of solvent plus phosphorocyanidate, the expected *Z*-isomer product. No photoisomerization was seen in the methyl C-ester using the YAG laser 355 nm source, suggesting that oxime isomerization in C-*o*-NO_2Bn ester requires the *o*-nitrobenzyl group, possibly involving an energy- or charge transfer effect [84, 85].

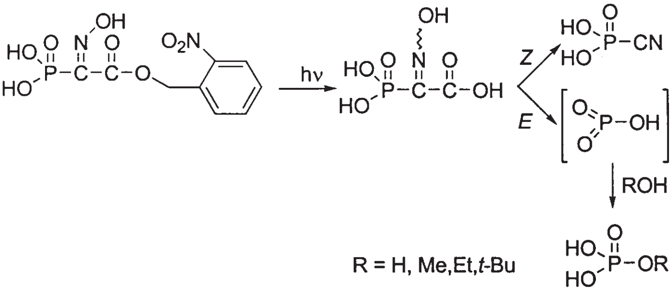

Scheme 30

In contrast to both its parent "troika" acid, and the C-Me ester which is stable in aqueous solution at both acidic and neutral pH, (*E*)-(hydroxyimino)(hydroxymethoxyphosphinyl)acetic acid (P-Me ester) was unreactive at pH 7 and 25 °C but at pH 1.5 fragmented to methyl phosphate (15%) and methyl phosphorocyanidate (85%). The predominantly non-phosphorylating fragmentation pathway, characteristic of Z-troika acid, was proposed to involve a preliminary $E \rightarrow Z$ isomerization prior to C_α-C_β cleavage [83].

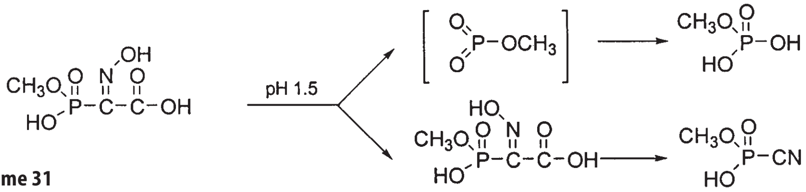

Scheme 31

Fragmentation chemistry with C-P bond cleavage has also been demonstrated in acylphosphonate oximes. *α*-Hydroxyiminobenzylphosphonates (*α*-ketophosphonate oximes) are reported to be precursors to monomeric phosphate, and can thus serve as phosphorylating agents [2]. Monomethyl hydroxyiminobenzylphosphonate fragmentation is also consistent with a dissociative mechanism [87].

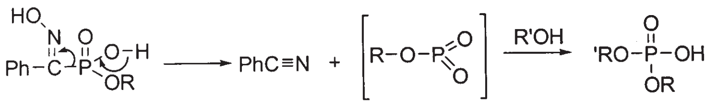

Scheme 32

Given the critical role of oxime geometry on the chemical behavior of α-ketophosphonate oximes, it is crucial to define the *E*/*Z* stereoisomerism of these compounds. X-ray crystallography, the ultimate structural method of reference, was used to identify the *E* and *Z* isomers of C-Me troika acid (as DCHA salts; in the *Z* isomer, the proximal oxime OH increases the effective second pKa of the phosphonic acid group, leading to formation of a bis-DCHA salt, whereas the E isomer only forms a mono-DCHA, facilitating isolation of both by fractional recrystallization). The ^{31}P-NMR of these compounds usually follow a pattern in which the *Z* isomer shifts more downfield, however this method requires both isomers and the shift order is not always consistent [88]. We have proposed [88] that the ^{13}C-NMR $^{1}J_{PC}$ coupling constants have more useful predictive value in determining *E* vs *Z* isomerism in phosphonoglyoxylate α-oximes and α-hydrazones, and also in distinguishing *syn* from *anti* phosphorus atoms in carbonylbisphosphonate α-hydrazones.

Comparison of NMR data for a series of such compounds with their isomer structure as determined directly or indirectly by X-ray crystallography, or other means, revealed that for the *E*-isomers, the ^{13}C-NMR $^{1}J_{PC}$ values fell within the range 171–242 Hz, whereas those for the *Z*-isomers were in the range 127–164 Hz, and thus formed two non-overlapping domains of values. Underlying this empirical correlation, we note in all the phosphonoglyoxylate oximes and hydrazones, and in a carbonylbisphosphonate hydrazone *anti*-P atom, P-C$_\alpha$-N bond angles $<120°$ (114°–117°), whereas for *Z* isomers and a hydrazone *syn*-P atom, P-C$_\alpha$-N bond angles are $>120°$ (125°–128°). We refer to this distortion from bond angle symmetry in the sp^2 hybridized α-carbon introduced by asymmetric *H*-bonding as 'canting' of the oxime or hydrazone moiety. This pattern of isomer-dependent distortion from ideal sp2 hybridization is proposed to correlate with the magnitude of $^{1}J_{PC}$ in a consistent way, such that a larger P-Cα-N angle corresponds to a smaller $^{1}J_{PC}$ value and v. v.

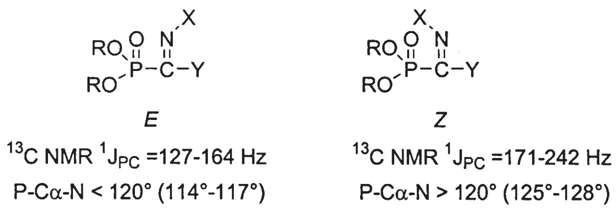

Scheme 33 R = H, Alk; X = OH, NHAr, P(O)OR'$_2$

Oximes effectively coordinate transitional metal ions, and the presence of two additional potential ligands in troika derivatives suggests evaluation of their properties as metal chelators. Recently we have been successful in immobilizing troika carboxamides on microporous polystyrene beads, and work on creating comparable macroporous bead-immobilized troika ligands is in progress.

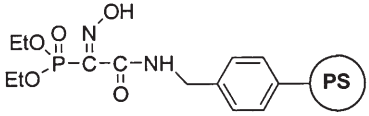

Scheme 34

In the course of this work, *N*-Benzyl (*E*)-(hydroxyimino)(diethoxyphosphinyl)acetamide was found to form an unusual neutral octahedral complex with Ni^{2+} in which three nickel atoms are disposed linearly within an enclosing structure of six of the troika ligands [89]. The ligands chelate in a tridentate fashion, the three 'teeth' being the phosphonate oxygen (P=O), the oxime nitrogen (C=N) and the deprotonated oxygen of the oxime (C=N-O-). Interestingly, the Ni atoms are in different ligand environments; the two 'outer' or flanking nickels being coordinated to three P=O oxygen atoms and three oxime nitrogen atoms, while the 'inner', central nickel is bonded to six deprotonated oxime O atoms. The structure is further stabilized by several amido NH groups via hydrogen bonding with oxime oxygens. From the top view it can be seen that the nickel atoms form a central metal core surrounded by hydrophobic benzyl groups on the periphery, which gives the impression of an insulated molecular nickel wire. However, EPR and cyclic voltammetry studies indicate that no delocalization of metal electrons occurs, as expected from the measured Ni to Ni distance.

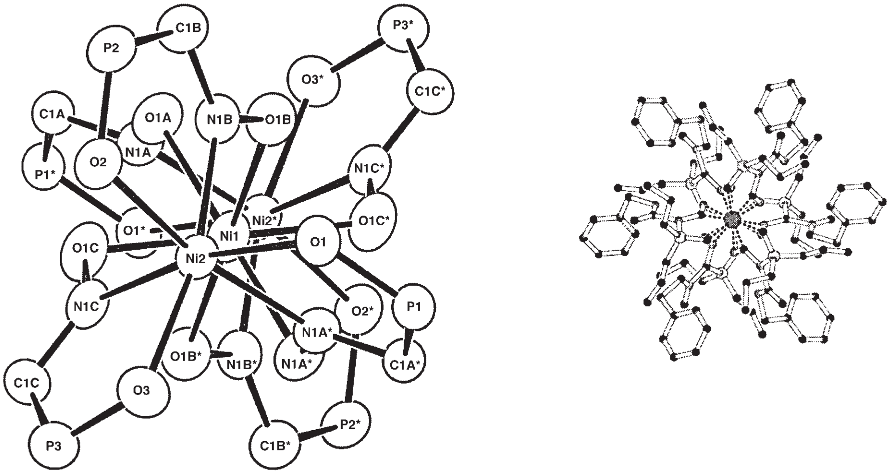

Scheme 35

4.2.5
Hydrazones

Accessible directly via the parent compound, trialkyl phosphonoglyoxylate arylhydrazones have also been conveniently prepared via reaction of trialkyl phosphonoacetate with aryl diazonium salts [90]. This route suffers from the limitation that aromatic amines which contain strongly electron-withdrawing groups, such as 2,4-dinitro aniline, give low yields of the coupling product. X-ray crystallographic analysis of the photochemically active triethyl 2-methoxy-4-nitrophenylhydrazone and of the phenylhydrazone of a phosphonoglyoxylic acid salt showed that both compounds are obtained as *E* isomers (these compounds have been studied in several different bioassays).

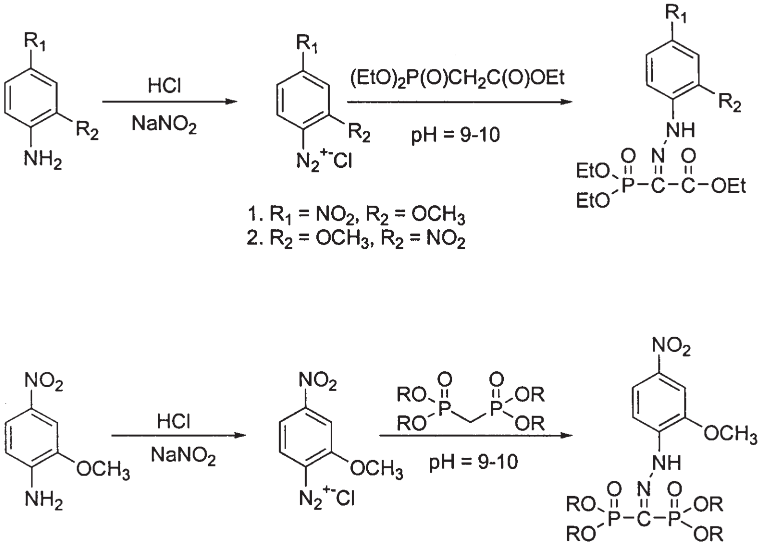

1. $R_1 = NO_2$, $R_2 = OCH_3$
2. $R_2 = OCH_3$, $R_2 = NO_2$

Scheme 36

R = Me, Et

However, when the 2-methoxy-4-nitrophenylhydrazone was heated in acetone at 78 °C for several hours, a new peak appeared in the ^{31}P-NMR spectrum of the solution, and the ^{1}H and ^{13}C-NMR spectra showed a pattern of doubled peaks, consistent with 50% conversion to the Z isomer. Attempts to isolate this isomer by preparative TLC failed due to isomerization on the silica gel [90, 91].

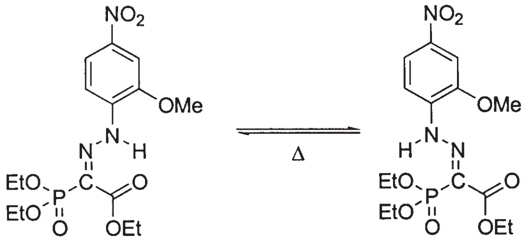

Scheme 37

5
Carbonylbisphosphonates

Bisphosphonates are analogues of pyrophosphate in which the P-O-P moiety of the latter is replaced by a (usually) less labile P-C-P group. The earliest bisphosphonates demonstrated to possess biological activity were methylenebisphosphonates bearing simple α-alkyl, α-halo or α-hydroxy substituents, with specific affinity for bone. Subsequently, structure-activity studies in several pharma laboratories have identified more active bisphosphonate drugs for treatment of osteoporosis, and there is currently growing interest in this class of compounds for cancer chemotherapy [92]. Thus, it is likely that realization of the full medical potential of bisphosphonates remains in the future, awaiting further advances in our understanding of the mechanisms of action and pharmacological properties of these compounds. Consequently, the development of new synthetic routes to specific classes of bisphosphonates is highly desirable. The synthetically versatile ketone group in carbonylbisphosphonate esters could, in principle, provide a convenient entry to an enormous range of new α-substituted pyrophosphate analogues. However, this potential has remained unevaluated due to the synthetic inaccessibility of these reactive α-ketophosphonates.

Scheme 38

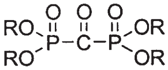

The tetrasodium salt of carbonylbisphosphonate was originally synthesized by Quimby et al. [76], using hydrolysis of a tetraalkyl dichloromethylenebisphosphonate in aqueous NaOH. In aqueous solution, the yellow ketone form reversibly converts to its colorless hydrate at acidic pH [76], a process which can be assessed by a combination of ^{31}P-NMR and uv-visible spectroscopy; at pH 7, the ketone predominates [93]. The salt moderately inhibits HIV reverse transcriptase in a p24 assay, whereas the parent methylene compound is inactive [64], displays some activity vs the pyrophosphate-dependent phosphofructose kinase of the parasite *T. gondii* [94] and has found use as a selective inhibitor of PCNA-independent DNA polymerase δ, allowing its enzyme activity to be distinguished from that of DNA polymerase α [95].

In contrast, tetraalkyl carbonylbisphosphonates have in the past proven synthetically elusive. Not only are the parent methylenebisphosphonate esters stubbornly resistant to oxidizing reagents as described above for phosphonoacetate, but even rhodium(II) acetate-mediated oxygen transfer from propylene oxide to a carbenoid derived from an α-diazo bisphosphonate ester *à la* our synthesis of phosphonoglyoxylate failed (see below). Likewise, oxidation of tetraaethyl ethylidenebisphosphonate with a number of reagents was unsatisfactory, although this compound has been oxidatively converted into both the corresponding 1,2-diol and the oxiranylidene [96]. Nevertheless, more recent work in our laboratory has been successful in creating the first practical routes to carbonylbisphosphonate esters, and to some other novel, multifunctional α-ketophosphonates. This work, and some of the chemical reactivities of carbonylbisphosphonates, will be described in the following sections.

5.1
Synthesis

5.1.1
tert-Butyl Hypochlorite Oxidations of Diazomethylenebisphosphonate Esters. The Moisture Modification

Some forty years ago, Regitz et al. reported synthesis of vicinal triketone compounds from 2-diazo 1,3-dioxo–compounds using oxygen-halogen-insertion chemistry provided by *tert*-butyl hypochlorite in formic acid. However, no analogous reaction for phosphorus compounds, in particular 2-diazo 1,3-diphosphono substrates, had been previously described.

Applying this approach, we found that tetraisopropyl and tetraethyl α-diazo methylenebisphosphonates in HCO_2H were converted by reaction with t-BuOCl to an intermediate which, on vacuum pyrolysis, provided crude samples of the corresponding esters in modest and erratic yields, always accompanied by an appreciable amount of α-,α-dichlorinated side product which proved difficult to remove, and decomposition products. The tretramethyl diazo ester produced only very low yields of the corresponding ketone, as did the unsymmetrical dimethyl diisopropyl diazo ester, probably due to the lability of the methyl ester group under the rather harsh, acidic pyrolysis conditions. Although we were afforded the first samples of carbonylbisphosphonate esters, the method was not very satisfactory due to the refractory impurities accompanying the product, and especially the exasperating capriciousness of the pyrolytic step. We were particularly mindful of the advantages of a synthesis that would proceed spontaneously at or near room temperature, and thus perhaps adaptable to combinatorial exploitation of carbonylbisphosphonate ester synthons generated in situ.

Transfer to aprotic solvent media (acetonitrile, acetone, ethyl acetate, CCl_4) was sometimes found to give trace amounts of ketone products, which appeared to increase when the solvent was not scrupulously dried, a tantalizing hint. Regitz [97] proposed that the interaction between his organic diazo substrates and *t*-butyl hypochlorite in alcohols proceeded via an intermediate α-chloro α-diazonium salt, with elimination of *tert*-butoxide, followed by proton transfer from the alcohol solvent to butoxide and nucleophilic substitution of the diazonium ion by alcoholate. *tert*-Butanol is a much more likely leaving group under the reaction conditions, and indeed much later, it was shown [98] that efficient transfer of positive chlorine from alkyl hypochlorite reagents requires at least some degree of proton transfer to the neighboring oxygen atom.

Taking into account the hint cited above, the fact that a proton donor is essential, and that the ideal final intermediate would be an unstable α-halo α-hydroxy species, H_2O would seem to be the obvious candidate combining the roles of general acid providing the proton needed to activate the *t*-butyloxy leaving group of *t*-butyl hypochlorite, and the nucleophilic oxygen source.

Indeed, we found that diazomethylenebisphosphonate esters in ethyl acetate containing a few equivalents of H_2O react at room temperature or below with *tert*-butyl hypochlorite to form the corresponding carbonylbisphosphonate es-

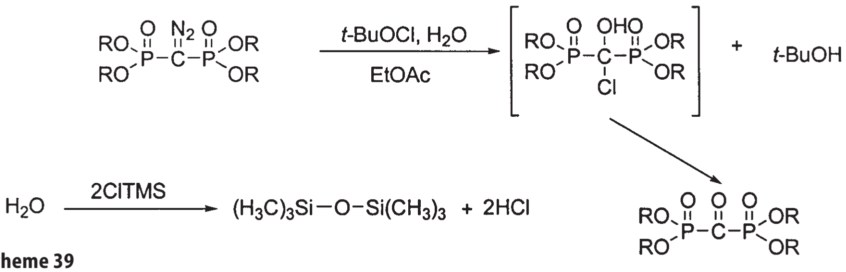

Scheme 39

ters in high yields (>90%). After a brief induction period, the reaction proceeds very rapidly with effervescence as N_2 suddenly evolves. The autocatalytic character of the reaction is rationalized on the basis that HCl is generated, which as a much stronger acid than water, protonates *tert*-butyl hypochlorite, accelerating Cl^+ transfer to the substrate. It is preferable to take advantage of the HCl thus generated in situ to adding an excess of HCl to the reaction mixture beforehand, because this will divert the chlorodiazonium intermediate to unwanted α,α-dichloro byproduct. Excess of H_2O suppresses this byproduct, but if not judiciously controlled causes conversion of the product ketone to its hydrate, which as explained in a later section can lead to decomposition products. Under the reaction conditions, hydrate formation can be virtually suppressed by quick removal of the excess H_2O as soon as ketone formation is complete (cessation of gas evolution). This can be conveniently effected by adding trimethylchlorosilane as a water "getter".

5.1.2
Rhodium(II)-Mediated Oxidations of Diazomethylenebisphosphonate Esters. Critical Roles of Metal Ligand and Epoxide Oxygen Donor

Although the hypochlorite method we previously elaborated conveniently produces carbonylbisphosphonate esters under very mild conditions, it suffers from two potential drawbacks: 1) the exothermicity and exponential increase in rate of reaction, so convenient on small scale, might pose cooling and control problems on major scale-up; 2) thus far, an efficient separation method to remove the small amount of dichlorinated side product always present, has not been found.

Diazocarboxylate esters can be transformed by transition metal catalysts such as rhodium(II) acetate into alkoxycarbonylcarbenes that undergo a wide variety of synthetically useful C-H, C-C, C-X, X-H and X-X insertion reactions (where X = heteroatom) [99]. Chemoselectivity of rhodium carbenoids derived from Rh(II) carboxylates and carboxamides has been found to exhibit striking ligand dependency, for example in work by Padwa showing that perfluorocarboxamide ligands exclusively promoted aromatic C-H insertions in Rh(II)-catalyzed decomposition of diazoamides to give oxindoles, whereas a carboxylate-based rhodium catalyst promoted other types of insertions and addition reactions [100].

As mentioned in Sect. 4, Rh(II) acetate-propene oxide smoothly converts α-diazo phosphonoacetate to the α-ketone. However, replacement of the carboxylate group in this diazo substrate by a second phosphonate moiety produces a dramatic drop in reactivity. The phosphonate group is strongly electron-withdrawing, but unlike the carboxylate substituent is unable to provide a stabilizing π-electronic interaction with the diazomethylene group as the latter begins to react with the Rh catalyst. In effect, the second phosphonate decreases electron density at the diazo carbon, rendering it less susceptible to attack by the electrophilic Rh.

Thus, we found that tetraalkyl diazobisphosphonate substrates are completely unreactive to rhodium acetate/propylene oxide, even after days of reflux in benzene which gave smooth conversion of triethyl diazophosphonoacetate to triethyl phosphonoglyoxylate in a few hours [79]. Efforts to utilize more rigorous conditions (higher boiling epoxide and solvent) with this catalyst have only confirmed the inertness of tetraisopropyl diazomethylenebisphosphonate [101]; and the corresponding tetraethyl ester was unchanged after a week in refluxing toluene containing rhodium acetate and 4-methoxyphenol [102].

Examining the role of the catalyst, it appeared reasonable to explore the effects of Rh ligands other than acetate. The effect of the Rh(II) carboxylate catalyst ligand structure on rhodium-carbenoid mediated *O*-H insertions in catalytic decomposition of various diazo compounds in the presence of hydroxylic compounds has been studied by Cox et al., who found that in this reaction, effectiveness varied with ligand, with L = $CF_3CONH > CH_3CONH > CH_3CO$, although no clear explanation of this order has been given [102]. A problem with the trifluorocetamide catalyst is that it has not been well purified or characterized, and as obtained may consist of more than one species [103]. In contrast, rhodium perfluorobutyramide [$Rh_2(NHCOC_3F_7)_4$] can be isolated as a well-defined compound [100], although it has not been used previously with diazomethylenephosphonate substrates.

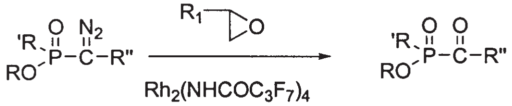

Scheme 40 R = Alk; R' =OAlk, Ph; R" = C(O)OR, $C(O)NR_2$, $P(O)(OR)_2$

Very recently, we discovered that the latter catalyst is effective in converting tetraisopropyl diazomethylenebisphosphonate to the carbonylbisphosphonate, using 1-hexene epoxide as the oxygen donor in refluxing benzene. The ketone product is obtained in high yield, and can be distilled under reduced pressure producing an analytical sample free of NMR-detectable impurities [92, 103]. This catalyst is also highly effective in the parallel synthesis of other novel trifunctional α-ketophosphonates, namely diethyl *N*,*N*-dimethyl phosphonoglyoxylamide (formed overnight at room temperature) and the mono(phenylphosphinate) analogue of tetraethyl carbonylbisphosphonate [103]. Further showing its greatly enhanced activity relative to rhodium acetate in these reactions, rhodium perfluorobutyramide is also capable of converting triethyl α-diazo phosphonoacetate in benzene to triethyl phosphonoglyoxylate at room temperature.

In addition, we now have very recent evidence that the oxygen donor – the oxirane ring – can significantly influence the overall rate of the reaction. Thus, when propylene oxide is replaced in the oxidation of diethyl *N*,*N*-dimethyl phosphonoglyoxylamide by an epoxide configured to provide stabilizing delocalization of charge developed during ring-opening – styrene oxide – the conversion, which requires overnight using propylene oxide, occurs at room temperature in less than a minute! These results demonstrate the remarkable "tunability" of the Rh(II)-epoxide route to α-ketophosphonates, which warrants further investigation. They also provide valuable tools for mechanistic studies of these reactions.

Tetraalkyl carbonylbisphosphonates and related analogues are therefore now fully available, via several routes, for further exploration of their physical properties and chemistry, and for possible exploitation as "gateway" synthons providing convenient access to a broad range of derivatives.

5.2
Reactivity

5.2.1
Physical Properties

Carbonylbisphosphonate tetraalkyl esters are bright yellow, mobile oils, in contrast to simple acylphosphonates which are typically colorless. The red shift of the carbonyl group $n \rightarrow \pi^*$ transition may be attributed to the additional stabilization of the excited state conferred by electrostatic interaction with the second phosphonate group. In the excited state, an electron is promoted from a non-bonding orbital on the carbonyl oxygen to a π^* orbital of the C=O group. As this antibonding orbital has increased electron density on the carbon atom, the excited state is stabilized by the P-O bond dipoles in the flanking phosphonate groups. Also characteristic of these compounds is their lowered carbonyl IR stretching frequencies (ν =1642–1645 cm^{-1}) compared to simple aliphatic ketones (ν = ca. 1715 cm^{-1}) Conversion of the α-diazomethylene precursor to carbonylbisphosphonate essentially reverses polarity at carbon, as reflected in the ^{31}P-NMR resonances which undergo an upfield shift of $\Delta\delta$ =17– 19 ppm (conversion to hydrate produces a downfield shift of $\Delta\delta$ = 20 ppm). Chemically, the lowered energy of the LUMO results in enhanced reactivity to nucleophiles, and stabilization of the hydrate relative to the ketone.

5.2.2
Hydration and Ketone-Hydrate Adduct Rearrangement

Hydrates of the impure bisphosphonate ketones prepared by our original *tert*-butyl hypochlorite method are readily formed (not isolated) by treatment with H_2O. However, attempts to regenerate pure ketones free of the α,α-dichloro contaminant and other impurities by evaporation of the aqueous phase (low pressure, heating) after extraction with an organic solvent lead instead to formation of an unwanted product containing both phosphonate and phosphate groups. If the water-trapping reagent in the modified method is omitted, the ketone product is also converted to its hydrate (carbonylbisphosphonate tetramethyl and tetraisopropyl esters). The hydrates are easily isolated as colorless, crystalline compounds with well defined melting points. Treatment of these pure hydrates with P_2O_5 or magnesium perchlorate in organic solvents regenerates the ketones, however a ketone-hydrate secondary reaction may occur, see below.

Tetramethyl carbonylbisphosphonate hydrate readily dissolves in H_2O, where it decomposes to dimethyl hydrogen phosphonate, a process catalyzed by base. Other hydrates are presumed to react similarly.

On heating, the hydrates produce a product, whose NMR and MS data are consistent with a novel hexaalkyl bisphosphonophosphate. This product may be formed according to the following scheme. The hydrate loses water to regenerate ketone, but also decarboxylates to form a dialkyl phosphite. The phosphite adds to the carbonyl group of the ketone, giving an unstable trisphosphono adduct which rearranges to the bisphosphonophosphate.

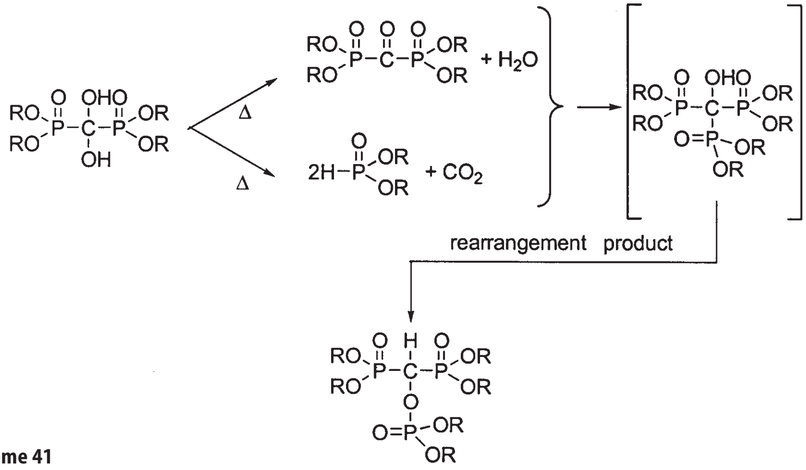

Scheme 41

To verify the proposed rearrangement mechanism, the reaction between tetraisopropyl carbonylbisphosphonate and dimethyl phosphite was investigated by ^{31}P-NMR . C → O rearrangement in the predicted triphosphono intermediate should give two different bisphosphonophosphate ester isomers, assuming that the migratory aptitudes of the dimethyloxy- and diisopropoxyphosphoryl groups are not too different. On the other hand, direct attack by the phosphite anion on the carbonyl oxygen (not shown), leading to an intermedi-

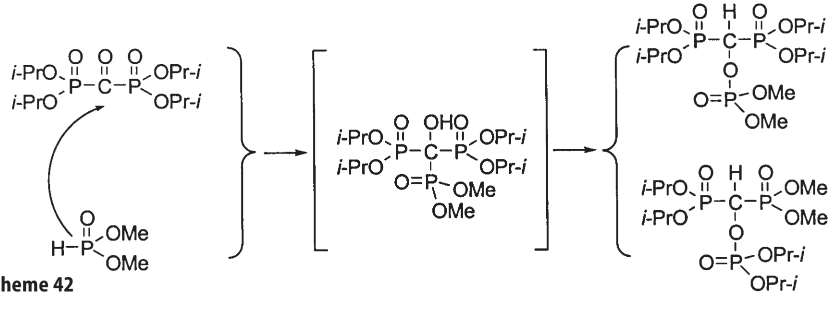

Scheme 42

ate bisphosphonophosphate carbanion, should give exclusively the dimethyl phosphate-tetraisopropyl bisphosphonate product.

Both possible products were observed, in a ratio of Me:*i*Pr = 1:0.75. This result demonstrates that the sterically congested hydroxymethylenetrisphosphonate intermediate forms but is indeed unstable to rearrangement, and indicates that the migratory aptitude of the dimethoxyphosphoryl group (after correction for a statistical factor of 2 favoring the isopropyl phosphate isomer) is about 3 times higher than that of the diisopropoxyphosphoryl group.

5.2.3
Oximes and Hydrazones

Carbonylbisphosphonate esters react smoothly with NH_2OCH_3. For example, reaction of the isopropyl ester gave the corresponding stable *O*-methyl oxime in 60% yield. The free oximes, and the corresponding oxime derivatives of acid bisphosphonates, have not yet been subjected to systematic study. However, very preliminary work indicates that the free oxime of the parent acid in aqueous solution is unstable to fragmentation with C-P bond cleavage, similar to that encountered with the troika acids.

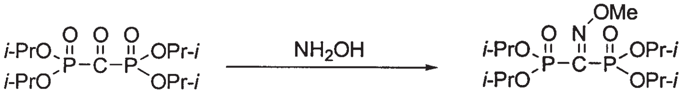

Scheme 43

The esters also react readily with aryl hydrazines to give aryl hydrazone derivatives. Examples of the latter were first synthesized (prior to the availability of tetraalkyl carbonylphosphonates) from tetraalkyl methylenebisphosphonates and aryl diazonium salts, analogously to the phosphonoglyoxylate hydrazone synthesis described in a previous section. First made as possible precursors in a ketone synthesis, several of these compounds, converted to free acid salts by treatment with BTMS followed by dicyclohexylamine in methanol, proved to have unexpected inhibitory activity vs the pyrophosphate-dependent phosphofructokinase of the parasite *T. gondii*, which causes a potentially lethal opportunistic infection in immunocompromised persons such as AIDS patients [94]. In fact, the 2,4-dinitrophenylhydrazone of carbonylbisphosphonic acid (as the tetrasodium salt) dramatically abated toxoplasmosis lesions in infected human foreskin fibroblasts [94]. Animal toxicity in this compound, probably arising from in vivo hydrolysis to the highly toxic hydrazine, precluded its future development, but the result remains an interesting lead.

Although the 2,4-dinitrohydrazone free acid is relatively stable in water, the 2-methoxy 4-nitrophenylhydrazone decomposes at acid or near neutral pH, as does the unsubstituted phenylhydrazone, to a mixture of phosphate and cyanophosphate. This can be rationalized as a fragmentation involving cleavage of both a P-C bond of the bisphosphonate and the N-N bond of the hydrazone, with an aniline as the leaving group. The basicity of the nascent amino nitrogen strongly influences the rate of the fragmentation, and phenyl ring substitution creating a significant net electron-withdrawing effect is required for stability [91].

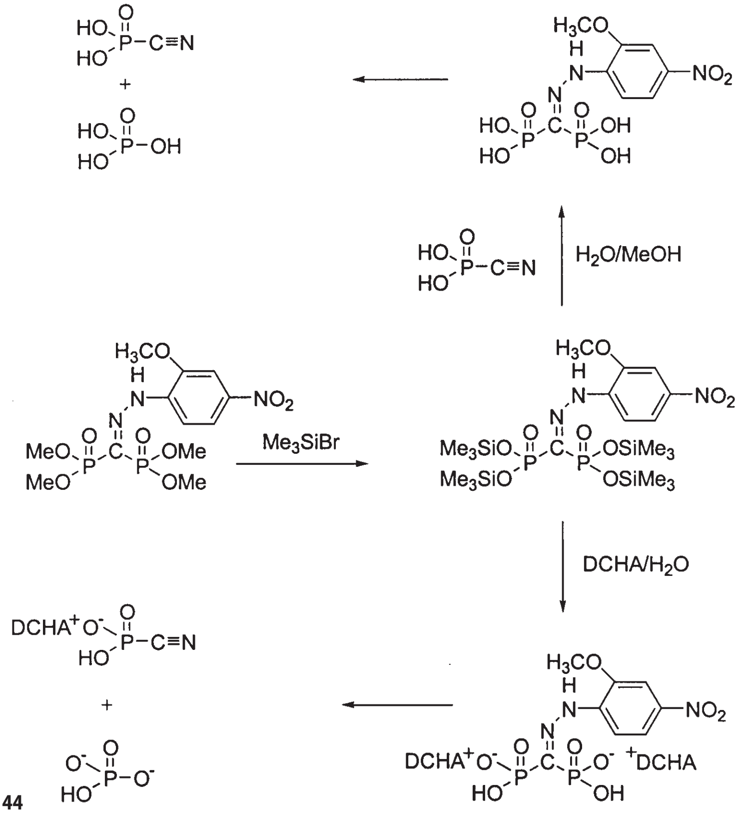

Scheme 44

An interesting regioselectivity is conferred by the presence of an hydrazone group: NaI in acetone easily monodemethylates the bisphosphonate ester, but the second, intact dimethyl group resists cleavage even after prolonged reflux. The monodealkylated product in D_2O was found by NMR to be a single isomer, indicating that strong H-bonding from the =N-NH- group to the P-O$^-$ not only 'locks in' one geometric configuration, but thereby deactivates the diester to nucleophilic attack via C-O bond breaking, by increasing electron density on α-carbon [91].

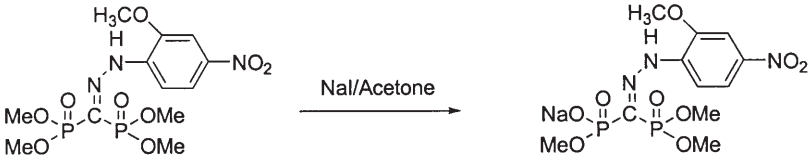

Scheme 45

Addition of alkyl and aryl amines to carbonylbisphosphonates, which could afford a new route to α-amino methylenebisphosphonates if the imine reduction proceeds normally and competing fragmentation chemistry does not pose severe problems, is currently under investigation in our laboratory.

5.2.4
Reaction with Organometallic Reagents

In principle, addition of organometallic reagents to the ketone function of carbonylbisphosphonate esters could constitute a convenient portal to a wide variety of α-substituted bisphosphonate derivatives. One aspect worth noting is the possibility of generating α-alkyl or α-aryl, α-hydroxy substituted methylenebisphosphonate esters directly by addition of an appropriate carbanion. The biological activity of bisphosphonate bone agents such as pamidronate, residronate, and their cognates, has been attributed to two structural features: 'bone hook' functionality, consisting of the two phosphonate groups and, where present, an α-hydroxy group, which together mediate primary hydroxyapatite adsorption; and the second, 'bioactive' α-substituent, which can be modified to enhance the anti-resorptive potency of the drug [104]. Addition of a carbanion to a carbonylbisphosphonate ester, assuming the adduct can be trapped by adding a proton, could simultaneously generate an α-hydroxy group with introduction of the α-R moiety.

However, as discussed in Sect. 2.2 above, reaction of carbanion nucleophiles with α-keto monophosphonate esters may lead not to (our) desired α-hydroxy α-alkylated adducts, but instead to elimination of the phosphorus-bearing moiety forming a ketone and a phosphite. Thus, with even weaker C-P bonds present, carbonylbisphosphonate reaction patterns with strongly basic carbon nucleophiles might turn out to be dominated by fragmentation: the 'carbanion conundrum'.

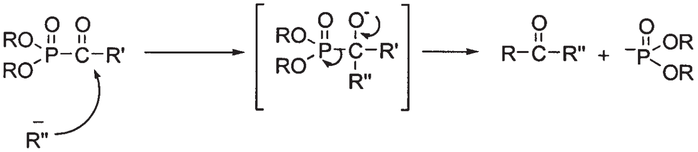

Scheme 46

Nevertheless, we discovered that tetraalkyl carbonylbisphosphonates exposed to excess Grignard reagent can be converted into the corresponding disubstituted methylenebisphosphonate esters in 40–75% yield. For example, the tetraisopropyl ester of etidronate (1-hydroxy-1,1-ethylidenebisphosphonate) was readily obtained from tetraisopropyl carbonylbisphosphonate and methyl magnesium iodide. The synthesis has been demonstrated with phenyl and benzyl Grignard reagents, and several different alkyl esters of carbonylbisphosphonate. Pending further investigation of this system, it can be speculated that the Mg^{2+} dication plays an important role in stabilizing the adduct.

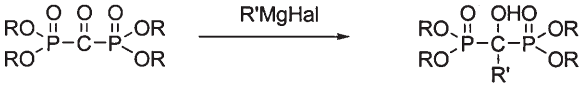

Scheme 47 R' = Me, R = Pr-*i*; R' = Ph, R = Pr-*i*; R' = Bn, R = Et

Future studies will elucidate to what extent the synthetic versatility of the ketone function can be exploited synthetically in carbonylbisphosphonate synthons.

5.2.5
Carbonylbisphosphonate Nucleotide Analogues

Phosphonate esters are widespread compounds in many biological systems. Over the two past decades chemists have paid much attention to the synthesis of phosphonic acid and their derivatives which might be considered as analogs of natural phosphate and display modified chemical and biological properties. One other interesting potential application of carbonylbisphosphonates is as pyrophosphate analogues for incorporation into nucleotides. The resulting nucleoside conjugates would resemble the well-known methylenebisphosphonate analogues, differing from them however in the important aspect that the unreactive P-CX_2-P linkage (where X = H and/or halogen, for example) is replaced by a chemically reactive ketone group, one moreover whose electrophilicity will be influenced by its local electrostatic and solvation environment. The potential lability of the P-C bond in nucleophile adducts of such conjugates must also be taken into account. Synthesis of the first example of a carbonylbisphosphonate conjugate (with AZT) was very recently achieved in our laboratory [105].

In general, phosphonate nucleotides have been made by a number of different approaches, for example:

1. Treatment of activated derivatives of phosphonates with nucleosides containing an unmasked hydroxy group [106];
2. Condensation of an activated form of the nucleoside with a phosphonic acid [107];
3. Esterification of phosphonic acids by hydroxy nucleosides using a condensing agent [108];
4. Formation of the phosphonate-nucleoside ester bond using the Mitsunobu reaction [109, 110].

To elaborate a method for coupling 5′-hydroxy nucleosides with a carbonylbisphosphonate partner or precursor, the tendency of the keto group to react with nucleophiles, possibly leading to C-P bond cleavage, has to be considered. Preliminary experiments indicated that methods 3 or 4 offered better prospects for success. We also sought a method in which the ketone functionality would be introduced into the molecule as late as possible. As our initial nucleoside partner, we selected AZT, where in addition to the possibility of creating a novel anti-viral nucleic acid polymerase inhibitor, we moderated the synthetic challenges inherent in nucleosides with reactive base substituents and/or containing a 2′-OH group requiring protection/deprotection.

We have achieved synthesis of the carbonylbisphosphonate analogue of AZT 5′-diphosphate using our newer hypochlorite route, applied to the corresponding diazomethylenebisphosphonate conjugate (itself a novel and interesting nucleotide analogue), which in turn was made by PyBOP or Mitsunobu coupling of its trimethyl ester-monosodium salt with AZT, followed by treatment with BTMS to silyldemethylate without hydrolysis. Conditions were found permitting chemoselective oxidation of the diazo function in the tris(trimethylsilyl) ester of the conjugate, followed by deprotection under extremely mild conditions (exposure to neutral water).

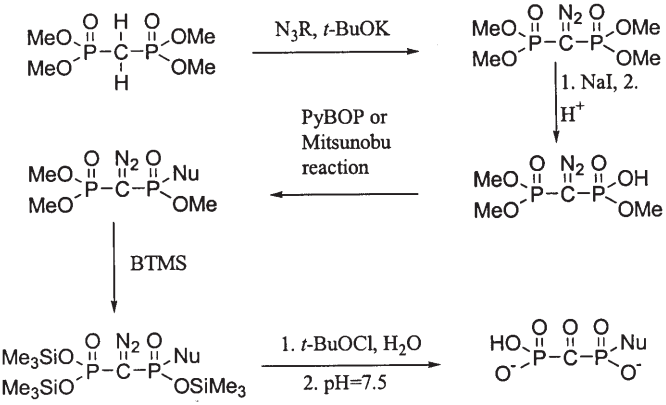

Scheme 48

PyBOP, proceeding through a presumed benzotriazolyl ester intermediate, was more effective than alternative coupling agents such as DCC, DCC/DMAP, DCC/1-hydroxybenztriazole, and bromotris(dimethylamino)phosphonium hexafluorophosphate.

The Mitsunobu reaction has been used previously to prepare 5′-*O*-acylnucleosides and nucleoside 5′-phosphates [111, 112]. With purine nucleosides, the approach failed (< 1% yields) in the preparation of 5′-phosphates, the main product being N^3,5″-cyclonucleosides resulting from an intramolecular nucleophilic attack by a purine ring nitrogen atom on the 5′-carbon atom. The predominant formation of the purine cyclonucleosides was attributed to electrostatic interactions between the phosphorus cation and the purine base which brought the reaction sites (5′ and 3-N) close enough to favor cyclization [113].

It was found recently that 2′,3′-*O*,*O*-protected adenosine and similar derivatives could be efficiently phosphorylated under Mitsunobu conditions when the reaction was carried out in anhydrous pyridine. Less nucleophilic phosphonates also reacted, but gave lower yields [114]. The use of nucleosides non-protected at the 2′ and 3′ positions led to the formation of by-products, and 5′-phosphorylated adenosine or derivatives could not be isolated satisfactorily.

The mechanism of the Mitsunobu reaction of alcohols with phosphonic acids has been recently studied [109]. A typical Mitsunobu coupling reaction proceeds via Path A and it is generally recognized that the rate-determining step is the reaction of alcohol with the protonated betaine to generate an alkoxyphosphonium salt, which then readily cascades to product. Path B is accessed only when there is no acidic component present to protonate betain.

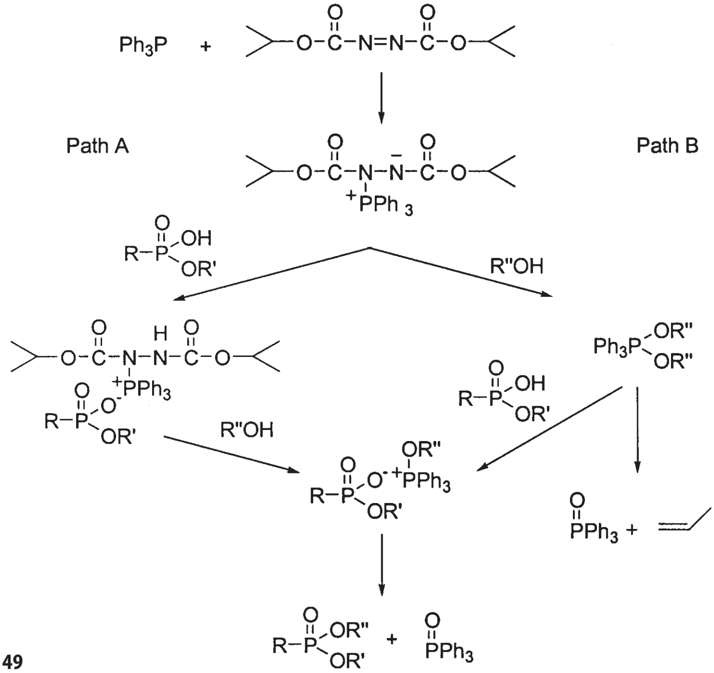

Scheme 49

If equimolar excesses of phosphonic acid, triphenylphosphine, and DIAD relative to the alcohol are used, the protonated betaine is formed and reacts slowly with the alcohol to form the alkoxyphosphonium salt. When a slight excess of unprotonated betaine is present, formation of the phosphonium salt via general base catalysis is facilitated. However, with a greater excess of unprotonated betaine, path B may be accessed resulting in formation of a dialkoxyphosphorane which can then undergo E_2 elimination, leading to unwanted side products. These mechanistic considerations were taken carefully into account in planning our Mitsunobu-based synthetic approach to the carbonylbisphosphonate nucleotide analogue.

The tetramethyl ester of diazomethylenebisphosphonate [12] was chosen for its ease of monodemethylation (NaI in acetone, added stepwise to abate formation of unwanted *P*,*P′*-didemethylated product).

Condensation of the diazo monosalt with AZT using PyBOP was carried out under conditions considered to be optimal [108], however the yield of the conjugate intermediate was below 50%, possibly due to the recognized moderate sensitivity of PyBOP-promoted monophosphonic acid condensations to steric hindrance.

In contrast, our Mitsunobu condensation chemistry proceeded nearly quantitatively after 4 hr at rt (by ^{31}P-NMR ; isolated yield >80%) when conducted in dry dioxane using 1.5 equiv of AZT, TPP and DIAD.

The sequence of steps and reaction conditions in the remainder of the synthesis is also critical. The diazo conjugate must be oxidized with *t*-BuOCl after chemoselective tridemethylation with BTMS in CH_2Cl_2 at rt. The oxidation with *t*-BuOCl was also carried out (EtOAc) at room temperature, rapidly (5 min) with only a fourfold excess of H_2O, immediately followed by rapid solvent removal in vacuo and pH adjustment (in water) to 7.5. The product, which was purified by gradient HPLC on a C-18 column was characterized by ^{31}P-, ^{1}H-, and ^{13}C-NMR, and by high resolution mass-spectrometry. Its chemical properties and biological activity are currently undergoing evaluation, and synthesis of further examples of carbonylbisphosphonate nucleotide analogues is under study.

Acknowledgements. The corresponding author most gratefully acknowledges financial support from the National Institutes of Health, the Electric Power Research Institute, and Biokeys Pharmaceuticals, Inc.

6
References

1. Iorga B, Eymery F, Mouries V, Savignac P (1998) Tetrahedron 54:14637
2. Breuer E (1996) In: Hartley FR (ed) The Chemistry of Organophosphorus Compounds, vol 4. John Wiley & Sons, New York p 653
3. Benech JM, Coindet M, El Manouni D, Leroux Y (1997) Phosphorus Sulfur Silicon Relat. Elem. 123:377
4. Boyd EA, Boyd MEK, Loh VM (1996) Tetrahedron Lett. 37:1651
5. Winkler T, Bencze WL (1980) Helv. Chim. Acta 63
6. Szpala A, Tebby JC (1981) J. Chem. Soc.-Perkin Trans. 1:1363
7. Glabe AR, Sturgeon KL, Ghizzoni SB, Musker WK, Takahashi JN (1996) J. Org. Chem. 61:7212
8. McKenna CE, Levy JN (1989) J. Chem. Soc., Chem. Comm.: 246
9. McKenna CE, Kashemirov BA (2000) US Patent 6, 147, 245
10. Texier-Boullet F, Foucaud A (1982) Synthesis: 916
11. Baraldi PG, Guarneri M, Moroder F, Pollini GP, Simoni D (1982) Synthesis: 653
12. Khare AB, McKenna CE (1991) Synthesis: 405
13. Burke TR, Smyth MS, Nomizu M, Otaka A, Roller PP (1993) J. Org. Chem. 58:1336
14. Benayoud F, Hammond GB (1996) Chem. Commun.: 1447
15. Burke TR, Smyth MS, Otaka A, Roller PP (1993) Tetrahedron Lett. 34:4125
16. Yao ZJ, Ye B, Wu XW, Wang SM, Wu L, Zhang ZY, Burke TR (1998) Bioorg. Med. Chem. 6:1799
17. Liao YH, Shabany H, Spilling CD (1998) Tetrahedron Lett. 39:8389
18. Kaboudin B (2000) Tetrahedron Lett. 41:3169
19. Tao M, Bihovsky R, Wells GJ, Mallamo JP (1998) J. Med. Chem. 41:3912
20. Ismailov VM, Aydin A, Guseynov F (1999) Tetrahedron 55:8423
21. Afarinkia K, Echenique J, Nyburg SC (1997) Tetrahedron Lett. 38:1663
22. Okauchi T, Yano T, Fukamachi T, Ichikawa J, Minami T (1999) Tetrahedron Lett. 40:5337
23. Evans DA, Johnson JS, Burgey CS, Campos KR (1999) Tetrahedron Lett. 40:2879
24. Evans DA, Johnson JS, Olhava EJ (2000) J. Am. Chem. Soc. 122:1635
25. Evans DA, Johnson JS (1998) J. Am. Chem. Soc. 120:6197
26. Telan LA, Poon CD, Evans SA (1996) J. Org. Chem. 61:7455
27. Kafarski P, Lejczak B (1991) Phosphorus Sulfur Silicon Relat. Elem. 63:193
28. Gajda T (1994) Tetrahedron: Asymmetry 5:1965
29. Meier C, Laux WHG (1995) Tetrahedron: Asymmetry 6:1089
30. Meier C, Laux WHG (1996) Tetrahedron: Asymmetry 7:89

31. Meier C, Laux WHG (1996) Tetrahedron 52:589
32. Meier C, Laux WHG, Bats JW (1995) Liebigs Ann.: 1963
33. Barco A, Benetti S, Bergamini P, De Risi C, Marchetti P, Pollini GP, Zanirato V (1999) Tetrahedron Lett. 40:7705
34. Chen R, Breuer E (1998) J. Org. Chem. 63:5107
35. Griffiths DV, Griffiths PA, Karim K, Whitehead BJ (1996) J. Chem. Res.-S: 176
36. Griffiths DV, Griffiths PA, Karim K, Whitehead BJ (1996) J. Chem. Soc.-Perkin Trans. 1: 555
37. Griffiths DV, Harris JE, Whitehead BJ (1997) J. Chem. Soc.-Perkin Trans. 1:2545
38. Takaki K, Itono Y, Nagafuji A, Naito Y, Shishido T, Takehira K, Makioka Y, Taniguchi Y, Fujiwara Y (2000) J. Org. Chem. 65:475
39. Ye B, Burke TR (1996) Tetrahedron 52:9963
40. Stevens C, De Buyck L, De Kimpe N (1998) Tetrahedron Lett. 39:8739
41. Katzhendler J, Ringel I, Karaman R, Zaher H, Breuer E (1997) J. Chem. Soc.-Perkin Trans. 2:341
42. Ryglowski A, Kafarski P (1996) Tetrahedron 52:10685
43. Onys'ko PP, Kim TV, Kiseleva EI, Prokopenko VP, Sinitsa AD (1994) Russian Journal of General Chemistry 64:1549
44. Maeda H, Takahashi K, Ohmori H (1998) Tetrahedron 54:12233
45. Huang WS, Zhang YX, Yuan CY (1997) Synthesis: 162
46. Taniguchi Y, Fujii N, Takaki K, Fujiwara Y (1995) J. Organomet. Chem. 491:173
47. Nakazawa H, Matsuoka Y, Nakagawa I, Miyoshi K (1992) Organometallics 11:1385
48. Salomon CJ, Breuer E (1995) Tetrahedron Lett. 36:6759
49. Ganzhorn AJ, Hoflack J, Pelton PD, Strasser F, Chanal MC, Piettre SR (1998) Bioorg. Med. Chem. 6:1865
50. Khomutov AR, Osipova TI, Khurs EN, Alferov KV, Khomutov RM (1996) Russ. Chem. Bull. 45:1961
51. Maryanoff BE, Reitz AB (1989) Chem. Rev. 89:863
52. Friesen RW, Blouin M (1996) J. Org. Chem. 61:7202
53. Alexandratos SD, Hussain LA (1998) Macromolecules 31:3235
54. Aucagne V, Gueyrard D, Tatibouet A, Quinsac A, Rollin P (2000) Tetrahedron 56:2647
55. Blades K, Lequeux TP, Percy JM (1997) Tetrahedron 53:10623
56. Coutrot P, Grison C, Lachgar M, Ghribi A (1995) Bull. Soc. Chim. Fr. 132:925
57. Hulme AN, Howells GE, Walker RH (1998) Synlett: 828
58. Elliott MR, Dhimane AL, Hamon L, Malacria M (2000) Eur. J. Org. Chem.: 155
59. Lucet D, LeGall T, Mioskowski C, Ploux O, Marquet A (1996) Tetrahedron: Asymmetry 7:985
60. Clarke R, Gahagan M, Mackie RK, Foster DF, Cole-Hamilton DJ, Nicol M, Montford AW (1995) J. Chem. Soc.-Dalton Trans.: 1221
61. Nicol M, Cole-Hamilton DJ (1998) J. Mater. Chem. 8:1511
62. Salles L, Nixon AF, Russell NC, Clarke R, Pogorzelec P, Cole-Hamilton DJ (1999) Tetrahedron: Asymmetry 10:1471
63. Miggins M, Kakarla UK, Knight DA, Fettinger JC (1996) An. Quim. 92:59
64. McKenna CE, Levy JN, Khawli LA, Harutunian V, Ye TG, Starnes MC, Bapat A, Cheng YC (1989) Acs Symposium Series 401:1
65. McKenna CE, Khawli LA, Levy JN, Harutunian V, Ye T-G, Bapat A, Starnes MC, Cheng Y-C (1989) In: Martin JC (ed) Nucleotide analogues as antiviral agents (ACS Symposium Series), vol 401. American Chemical Society, Washington, D.C. p 1
66. Bartlett PA, Carruthers NI, Winter BM, Long KP (1982) J. Org. Chem. 47:1284
67. Goldstein JA, McKenna CE, Westheimer FH (1976) J. Am. Chem. Soc. 98:7327
68. Bewart W, Gerd W, Heinrich A (1972)., Germany
69. Kreutzkamp N, Mengel W (1967) Arch. Pharm. 300:389
70. McKenna CE, al. e In: unpublished results. See also: Levy J, Ph.D. Thesis (1989), Univ. of Southern California. The reaction product structures speculatively proposed in the latter document were not confirmed by later work in our laboratory. (ed).
71. Levy JN (1989), Ph. D., University of Southern California
72. Dox AW (1944) Org. Syn., Coll Vol 1:266

73. Pardo SN, Salomon GJ (1981) J. Org. Chem. 46:2958
74. Seebach D Synthesis 1:17
75. Hunsberger IM, Tien JM (1959) Chem. Ind.: 88
76. Quimby OT, Prentice JB, Nicholson DA (1967) J. Org. Chem. 32:4111
77. Jung ME, Shishido K, Davis LH (1982) J. Org. Chem. 47:891
78. Courtney JL (1987) In: Mijs WJ, de Jonge CR (eds) Organic Syntheses by Oxidation with Metal Compounds. Plenum Press, New York p 445
79. Levy JN, McKenna CE (1993) Phosphorus Sulfur 85:1
80. Martin MG, Ganem B (1984) Tetrahedron Lett. 25:251
81. McKenna CE, Khare A, Ju J-Y, Li Z-M, Duncan G, Cheng Y-C, Kilkuskie R (1993) Phosphorus Sulfur 76:139
82. Kashemirov BA, McKenna CE, Ju J-Y, Bau R (1995) J. Am. Chem. Soc. 117:7285
83. Kashemirov BA, Fujimoto M, McKenna CE (1995) Tetrahedron Lett. 36:9437
84. Carrick JM, Kashemirov BA, McKenna CE (2000) Tetrahedron 56:2391
85. Carrick JM, Kashemirov BA, McKenna CE (1999) Phosphorus, Sulfur Silicon Relat. Elem. 147:656
86. Kashemirov BA, Fujimoto-Posner M, McKenna CE (1999) Phosphorus, Sulfur Silicon Relat. Elem. 147:153
87. Katzhendler J, Breuer E et al. (2000) J. Chem. Soc. 111:777
88. McKenna CE, Kashemirov BA, Ju JY (1994) J. Chem. Soc.-Chem. Commun.: 1211
89. Kashemirov BA, Carrick JM, Bau R, McKenna CE (2001) Phosphorus Sulfur Silicon Relat. Elem. submitted
90. Ju J-Y, Heagy M, Khare A, Yi EH-C, Bau R, McKenna CE (2001) to be submitted
91. Ju JY (1993), Ph.D. Thesis, University of Southern Calif.
92. McKenna CE (2001) Phosphorus, Sulfur Silicon Relat. Elem. submitted
93. McKenna CE, Levy JN unpublished results
94. Peng Z-Y, Mansour JM, Araujo F, Ju J-Y, McKenna CE, Mansour TE (1995) Biochem. Pharm. 49:105
95. Talanian RV, Brown NC, McKenna CE, Ye TG, Levy JN, Wright GE (1989) Biochemistry 28:8270
96. Duncan GD, Khare AB, Li Z-M, McKenna CE (1995) J. Org. Chem 60:7080
97. Regitz M, et al. (1969) Berichte Chem. 666:777
98. Tassignon T, et al. (1995) Tetrahedron 121:343
99. Shapiro EA, Dyatkin AB, Nefedov OM (1993) Russian Chemical Reviews 62:485
100. Brown DS, Elliott MC, Moody CJ, Mowlem TJ, Marino Jr. JP, Padwa A (1993) J. Org. Chem 59:2447
101. Li ZM, E. MC In: unpublished. (ed).
102. Cox GG, Miller DJ, Moody CJ, Sie E-RHB, Kulagowski JJ (1994) Tetrahedron 50:3195
103. Bonaz-Krause PI, Kashemirov BA, McKenna CE (2001) Phosphorus, Sulfur Silicon Relat. Elem. submitted
104. Ebetino FH, al. e (1999) Phosphorus Sulfur Silicon Relat. Elem. 198:199
105. Kashemirov BA, Rozé CN, McKenna CE (2001) Phosphorus, Sulfur Silicon Relat. Elem. submitted
106. Rosowsky A, Fu HN, Pai N, Mellors J, Richman DD, Hostetler KY (1997) J. Med. Chem. 40:2482
107. Davisson VJ, Davis DR, Dixit VM, Poulter CD (1987) J. Org. Chem. 52:1794
108. Campagne JM, Coste J, Jouin P (1995) J. Org. Chem. 60:5214
109. Campbell DA, Bermak JC (1994) J. Org. Chem. 59:658
110. Campbell DA (1992) J. Org. Chem. 57:6331
111. Shimokawa S, Kimura J, Mitsunobu O (1976) Bulletin of the Chemical Society of Japan 49:3357
112. Kimura J, Fujisawa Y, Yoshizava T, Fucuda K, Mitsunobu O (1979) Bulletin of the Chemical Society of Japan 52:1191
113. Kurihara T, Nakajima Y, Mitsunobu O (1976) Tetrahedron Lett. 17:2455
114. Saady M, Lebeau L, Mioskowski C (1995) Synlett: 643

Author Index Volume 201–220

Author Index Vols. 26–50 *see Vol.* 50
Author Index Vols. 51–100 *see Vol.* 100
Author Index Vols. 101–150 *see Vol.* 150
Author Index Vols. 151–200 *see Vol.* 200

The volume numbers are printed in italics